HYDRO-ECONOMIC MODELING OF MULTI-OBJECTIVE RESERVOIR OPERATIONS UNDER SEASONAL FLOW VARIABILITY

(Application to Omo-Gibe River Basin)

PhD Dissertation

By

Bahru Mekuria Gebeyehu

October 2023

Addis Ababa Institute of Technology

School of Civil and Environmental Engineering

HYDRO-ECONOMIC MODELING OF MULTI-OBJECTIVE RESERVOIR OPERATIONS UNDER SEASONAL FLOW VARIABILITY

By

Bahru Mekuria Gebeyehu

A Dissertation Submitted to Graduate School of Addis Ababa University, Addis Ababa Institute of Technology, School of Civil and Environmental Engineering in partial fulfilment of the requirement for the degree of

DOCTOR OF PHILOSOPHY

In

CIVIL ENGINEERING

Under the supervision of:

Dr. Asie Kemal

Assistant Professor, School of Civil and Environmental Engineering, Addis Ababa Institute of Technology, AAU, Ethiopia

Dr. Getachew Tegegne

Associate Professor, Department of Civil Engineering, Sustainable Energy Centre of Excellence, Addis Ababa Science and Technology University, Ethiopia

Professor Assefa M. Melesse

Department of Earth and Environmental, Institute of Environment, Florida International University, USA

October 2023

Addis Ababa, Ethiopia

Dissertation Approval Sheet

The Addis Ababa University (AAU) thesis committee of the Addis Ababa Institute of Technology (AAIT) certifies that this is the authorized version of the following thesis.

HYDRO-ECONOMIC MODELING OF MULTI-OBJECTIVE RESERVOIR OPERATIONS UNDER SEASONAL FLOW VARIABILITY

By:

Bahru Mekuria Gebeyehu — Date

APPROVED BY

BOARD OF EXAMINWES:

Advisor: Asie Kemal (Assis. Prof.) — 25/10/2023 — Date

Co-Advisor: Assefa M. Melesse (Prof.) — 25/10/2023 — Date

Co-Advisor: Getachew Tegegne (Asso. Prof.) — 25/10/2023 — Date

External Examiner 1: Prof. Seifu Tilahun — 02/02/24 — Date

External Examiner 2: Dr. Semu Moges — 02 23 2024 — Date

Internal Examiner: Dr. Dereje Hailu — 02 02 24 — Date

Chairperson: Dr. Abrham Gebre — Date

DECLARATION

I certify that I wrote this PhD dissertation entirely on my own, with the help of only the sources, support, and advises who were properly acknowledged and cited in this paper. The usage of any materials or findings in this work that are not its own has been duly-accommodated and cited.

_____ _____

Bahru Mekuria Gebeyehu Date

DEDICATION

I dedicate this dissertation to my family, next to the Almighty God, the Virgin Mary, and the Holly Sprits, without whom I could not have written this chapter of my life.

ABSTRACT

Effective river basin management is challenging due to competing demands and environmental constraints. Understanding current reservoir operations is critical for developing alternative policies. This study applies a reservoir operation simulation-optimization technique to identify the best policies by utilizing economical approaches that balance competing objectives and system uncertainty.

It may not accurately reflect a hydrologic model's genuine simulation capability to evaluate its performance just in terms of a formal simulation method. Hence, this study examined the effect of subbasin spatial scale on the hydrological model prediction uncertainty for different flow quantiles within the Omo Gibe River basin's sub-basins: Abelti, Wabi, and Gecha watersheds, from 1989 to 2020. The study found that the SWAT model accurately reproduced the observed hydrograph with over 85% accuracy for the Abelti watershed, over 82% accuracy for the Wabi watershed, and over 73% accuracy for the Gecha watershed. The subbasin spatial scale impacted the reproduction of flow quantiles, and the best scales for peak and low flows were found to be 79-98% and 29-42%, respectively. The study highlights the importance of investigating proper subbasin spatial scales for sustainable management of floods and drought. Furthermore, it suggests an improvement over the existing method of evaluating hydrological models and emphasizes the need to account for hydrologic model uncertainty for a good assessment.

This study also addresses the challenge of estimating water resources in ungauged catchments, such as the Omo-Gibe River basin in Ethiopia, which is ungauged in about 70% of its area. The Reliability-weighted (RB) approach, a new method that combines three commonly used parameter transfer techniques (Global mean, Physical similarity, and Spatial proximity), was introduced to predict runoff in regions with unreliable data. The weights are computed using the donor catchment's hydrological model's reliability value during the calibration and validation periods. The RB method outperformed all three regionalization approaches by about 30% for the test catchments, and the proposed strategy's regionalization performance had a metric Nash-Sutcliffe efficiency greater than 0.50 approximately 85% of the time. The study shows that the RB approach is a useful tool for assessing available water resources in ungauged catchments.

The Omo Gibe cascade reservoir operations problem was examined and solved using a cutting-edge evolutionary optimization method (Borg MOEA). The Omo Gibe River Basin system faces competing sectoral needs for hydropower generation, flood management, public and private irrigation, flood recession farming, and environmental flows. The results of the model showed reliable and robust optimal solutions, enabling the evaluation of the tradeoffs between revenue generation, minimum environmental flow provision, and reservoir storage conditions. Under the existing scenario, the hydropower can produce up to 4.6 billion ETB, while the irrigation revenue is 720 million, which is expected to increase faster than hydropower revenue in the near-future scenario, up to 9 billion, whereas hydropower revenue will produce 10 billion, creating more competition, higher water usage, and necessitate better resource management. In addition, the renovated Gibe III Power Station's hydropower production can increase by approximately 65% in 2019 compared to the actual hydropower production. The evolutionary algorithm models used for reservoir operations are outstanding. Employing these advanced optimization models with more data can lead to a better understanding and improved reservoir operations.

ACKNOWLEDGEMENTS

First and foremost, I want to thank God the Father, God the Son, and God the Holy Spirit for their love, grace, and unity throughout my life, which has enabled me to fulfil the objectives I established. I'd also like to thank Saint Merry, Holy Angels, Saints, and monks for their assistance throughout my life and for providing me with the fortitude, resources, and blessings I needed to finish my Ph.D. dissertation.

I am grateful to all of my family members: my parents, brothers and sisters, and family members for their never-ending motivation and magnificent blessings. My sister, Menbere Mekuria, has always been a devoted and spirited supporter of mine. Her unwavering and true dedication to my cause is beyond words. I'm thrilled to be a member of such a lovely family.

I sincerely appreciate the inspiration, knowledgeable direction, patience, and support provided by my supervisors: Dr.-Ing. Asie Kemal, Dr. Getachew Tegegne, and Professor Assefa M. Melesse as I prepared this dissertation. I owe a huge debt of gratitude to Dr. Getachew, who insisted that I concentrate on publishing.

I want to express my sincere gratitude to the civil and environmental engineering faculty and staff of AAiT, Addis Ababa University, for their seamless support of my Ph.D. works throughout my study term. I would also want to express my gratitude to the Ethiopian National Meteorological Agency, the Ethiopian Ministry of Water and Energy, and the Ethiopian Electric Power Cooperation for their kind assistance during my research and for providing me with the essential input data.

Last but not least, I'd like to take this opportunity to thank everyone who helped me finish this Ph.D. thesis. Throughout my schooling process, I appreciated their aspirational thoughts, invaluable constructive criticism, and cordial advice. I genuinely appreciate their open and

informative perspectives on a variety of project-related difficulties. I'd like to thank my friends Dr. Fikru, Abebe Arega, and others not mentioned here in particular for their unwavering support and inspiration.

PREFACE

The current thesis, " Hydro-Economic Modelling of Multi-Objective Cascade Reservoir Operations under Seasonal Streamflow Variability" was submitted and successfully defended as one of the requirements for the Ph.D. Degree at the School of Civil and Environmental Engineering (Addis Ababa Institute of Technology) under the mentorship of Dr.-Ing Asie Kemal, Dr. Getachew Tegegne, and Professor Assefa M. Melesse. From December 2018 to July 2023, the Ph.D. project was sponsored by the Ethiopian Ministry of Education.

The Ph.D. dissertation's substance is based on four papers released in scholarly journals. The appendix number, written in Geez numbers, is used to designate the papers in the text.

፩. Bahru M. Gebeyehu, Asie K. Jabir, Getachew Tegegne, and Assefa M. Melesse (2023). Choosing an interpolation approach to cover deficient Climate data: A case study of sparsely gauged Omo-Gibe River Basin, Ethiopia. 2023 International Conference on Nile Basin and the Sudd Wetlands: Climate Change Adaptability and Suitability presented on March 20-21, 2023 at Florida International University, USA.

፪. Bahru M. Gebeyehu, Asie K. Jabir, Getachew Tegegne, and Assefa M. Melesse (2023). Subbasin Spatial Scale Effects on Hydrological Model Prediction Uncertainty of Extreme Stream Flows in the Omo Gibe River Basin, Ethiopia. Remote Sensing, MDPI. DOI: 10.3390/rs15030611.

፫. Bahru M. Gebeyehu, Asie K. Jabir, Getachew Tegegne, and Assefa M. Melesse (2023). Reliability-weighted Approach for Streamflow Prediction at Ungauged Catchments. Journal of Hydrology, Elsevier. DOI: 10.1016/j.jhydrol.2023.129935

፱. Bahru M. Gebeyehu, Asie K. Jabir, Getachew Tegegne, and Assefa M. Melesse (2023). Multi-Objective Cascade Reservoir Operations Under Seasonal Streamflow Variability: A Hydro-Economic Model.

“የሰው ልጅ እግዚአብሔርን በዘነጋ ጊዜ የጥፋት ውሃ ታዘዘበት ፤

የኖህ መርከብ ኢትዮጵያ ሆይ ፣ እጅችሽን ወደ እግዚአብሔር ዘርጊ።”

TABLE OF CONTENT

LIST OF TABLES

LIST OF FIGURES

LIST OF ACRONYMS

ANN	Artificial Neural Network
BMC	Billion Meter Cube
DEM	Digital Elevation Model
EMODPS	Evolutional Multi-Objective Direct Policy Search
ESO	Explicit Stochastic Optimization
FDRE	Federal Democratic Republic of Ethiopia
GIS	Geographic Information System
GM	Global Mean
GTP I	Growth and Transformation Plan I
IDW	Inverse Distance Weighting
ISO	Implicit Stochastic Optimization
LOOCV	Leave One Out Cross Validation
LULC	Land Use Land Cover
MOEA	Multi-Objective Evolutionary Algorithm
NSE	Nash-Sutcliff Efficiency
OGRB	Omo Gibe River Basin
OK	Ordinary Kriging
OCK	Ordinary Co-kriging
OSeMOSYS	Open-Source energy Modeling System
PS	Physical Similarity
RB	Reliability-weighted
RBFs	Radial Basis Functions

RMSE	Root Mean Square Error
SP	Spatial Proximity
SWAT	Soil and Water Assessment Tool
SWIM	Soil and Water Integrated Model
Topkapi	TOPopographic Kinematic wave APproximation and Integration
UBNRB	Upper Blue Nile River Basin

1. INTRODUCTION

1.1. Background of the Study

River basin management has historically faced difficulties from a range of conflicting water demands, including hydropower production, flood control, and the supply of water for domestic and agricultural usage. Water institutions are very unlikely to change their current procedures in the absence of a serious failure or water conflict due to the rigidity of water legislation (Sheer, 2010). Though water managers must deal with rising water demands and more changeable hydrologic regimes, there is no guarantee that previous management strategies will not fail in the future (Milly et al., 2008). Therefore, comprehending the consequences of our current reservoir operations and formulating alternative strategies that more effectively balance competing objectives and performance uncertainties is essential.

Ethiopia, a water tower in Africa, has the largest surface and subsurface water resources in the region. However, only a small fraction of this potential is utilized to accomplish the national economic and social development goals of the country (Gebresenbet, 2016). The national economic and social development plan had been hampered owing to very few efforts that had been applied in developing the country's water resources as engines to propel. However, due to increasing demands for electricity and rapid regional growth (Sundin, 2017), the government is currently committed to increasing the utilization of these surface water resources by constructing dams and reservoirs in different river basins for hydropower energy generation, agriculture, water supply, flood control, and environmental protection. To maximize the net benefit of these developments, an economic examination of the resource trade-offs is needed. Furthermore, such integrated water resource management might address the issue of hydrological variability (Meredith and Givental, 2016).

Reservoirs are critical for managing the variability of river basin water resources (Quentin Grafton et al., 2016). Reservoir operations are a fundamental water management strategy humans can modify in response to observable environmental effects. However, the depiction of reservoir operations in hydrological models such as SWAT 2012, for example, is limited and simple. Users can input measured daily or monthly releases in the current reservoir module if historical data are available, but this does not allow users to estimate how reservoirs could perform in the future (Wu et al., 2020). Users can easily establish an average daily water discharge rate for small uncontrolled reservoirs. In contrast, many agricultural systems across the world are supplied by massive surface reservoirs with more variable activity. These include mega-dams in the American West, as well as modern hydropower buildings in Asia, Latin America, and Africa aimed at increasing electrification through hydropower generation while also providing irrigation (Zhang et al., 2018).

Reservoir managers are becoming more open to adopting more complex, adaptive rules into operations, although many reservoirs follow fundamental principles (Jasperse et al., 2020; Talbot and Pathak, 2020). Thanks to recent advancements in multiobjective optimal control methods, more complex reservoir operating rules that can better balance competing socioecological outcomes, adapt to system variability, or mitigate the effects of streamflow variability have been discovered (Giuliani et al., 2021; Zaniolo et al., 2021). Therefore, for an appropriate exploitation and distribution of these resources, models for the management of water resources are required.

On the other hand, technical developments have led to an increase in global electricity consumption, notably in Africa. This is why hydropower provides for the great majority of energy generation in Ethiopia's energy sector. But hydropower energy generation is strongly dependent on streamflow and proper reservoir management. These reservoirs could supply water for irrigation, energy, flood control, and environmental protection, among other things.

Alternatively, despite its inherent multisectoral potential, reservoir operations are still a popular academic topic due to its computational requirements and mathematical problems (Salazar et al., 2017). Emerging computer platforms have the potential to improve reservoir management by reducing the level of simplification and approximation that has previously made high-fidelity simulation models difficult to use (Giuliani et al., 2015a). Recent water resources literature studies (Alba et al., 2013; Maier et al., 2014; Nicklow et al., 2010) show how meta-heuristics and parallel computing platforms are expanding the possible applications of simulation-optimization frameworks.

Cascade reservoirs in the Omo Gibe River basin, like many other water resource projects, face complex reservoir operation challenges, especially due to competing objectives that raise different concerns while attempting to maximize benefits, necessitating an advanced competitive scenario for the river basin's utilization and sustainability.

1.2. Statement of the problem

Water resources in the Omo Gibe River basin remain underutilized and are not distributed as effectively as they could be. Furthermore, insufficient research has been undertaken to evaluate the master plan established utilizing the most recent modeling approaches for water distribution or other goals. Aside from the inherent uncertainties in hydrological model simulation, the river basin is known as a data-scarce zone. On top of that, due to the hydrological variability, the lack of water causes power plants in this region to run at a lower efficiency. Conversely, the abnormally extended and widespread rains that began in June 2006 affected over 500,000 people; more than 600 people died as a result of the flash floods. Pastoralists also lost their cattle as a result of floods and other innumerable damages (EEPCO, 2009; Ocha, 2010; Woldegebrael et al., 2022). Recently (2019), a similar water scarcity and flooding sequentially occurred in the river basin, resulting in

the loss of many lives and substantial destruction. Aside from this, local farmers in the lower Omo region rely on floods coming from the upstream. Therefore, these conflicting issues require an advancing technique for better usage, sustainability, and operational challenges of the reservoir system.

Water is often available at average flows to serve various needs. When dealing with low-flow scenarios, it is vital to create a balance between various operating objectives while minimizing negative repercussions. Sometimes achieving one aim requires sacrificing another. To correctly balance these opposing goals, we must use a unique, practical, and multifunctional optimization approach that allows us to investigate many objectives at the same time.

1.3. Objectives

The fundamental goal of this dissertation is to provide hydroeconomic modeling of multiobjective reservoir operation under seasonal flow variability conditions of the Omo Gibe River cascade reservoir operation using cutting-edge multiobjective optimization.

The specific objectives of the proposed study are as follows:

- To select a robust rainfall interpolation method in a data-scarce region
- To investigate subbasin spatial scale effects on the hydrological model prediction uncertainty of extreme streamflow.
- To propose a reliability-weighted approach for streamflow prediction in ungauged catchments
- To investigate economic trade-offs between competing water needs for existing and near-future scenarios utilizing the hydro-economic model of a cutting-edge optimizer, Borg MOEA.

1.4. Research Questions

In pursuit of the aforementioned study objectives, the following research questions can be addressed:

I. Which resilient rainfall interpolation algorithm(s) produces lower uncertainty in climate prediction in a data-scarce region?

II. How does subbasin spatial scale variation influence overall flow simulation results and/or flow quantile reproduction in hydrological model simulations?

III. What is the performance of the newly proposed reliability-weighted (RB) method in comparison to the three widely applied regionalization approaches?

IV. How does a hydroeconomic model based on a recently developed state-of-the-art multiobjective optimization algorithm (Borg MOEA) handle the Omo Gibe River cascade reservoir operational challenge, making it easier to deliver timely feedback to decision-makers and resulting in a decision-making revolution?

1.5. Expected research outputs

The results of the investigation will have ramifications for both theory and practice. The theoretical significance of this study is that it sheds light on the trade-offs between the competing demands for water from various reservoirs, as well as how to address the challenges associated with operating these reservoirs under flow variability conditions while maintaining the stability of their water supply.

Employing the best trade-offs between competing water users, especially under drought situations of low streamflow with high seasonal flow variability, and enhancing socioeconomic advantages and sustainability are other ways to put practical touch into practice in reservoir operating firms.

It is also possible to reduce flooding and its consequences, which are currently a major problem in Ethiopia's various river basins.

The study will not only solve the research gaps mentioned above but also provide a more comprehensive understanding of competing water uses in reservoir operation using an advanced multiobjective optimization evolutionary algorithm (Borg MOEA) and hydroeconomic models.

1.6. Scope of the study

The study focuses on the challenges of water allocation and utilization in the Omo Gibe River basin. The Omo Gibe River basin is one of the data-sparse regions, with a shortage of adequate data. Dealing with such constraints to do a hydrological model simulation and then quantify hydrological model uncertainty, specifically subbasin spatial scale effects. The study also looks at regionalization as a means of transferring flow parameters from gauged to ungauged catchments. Furthermore, economic tradeoffs between various conflicting water demands will be sought to improve reservoir operation as a final target under current and near-future circumstances.

1.7. Research Methodology and Dissertation Structure

Simulation-based research is being conducted to achieve these objectives. In the current work, a modeling chain is used to perform reservoir operation challenges through a hydroeconomic modeling of the Omo Gibe River basin (Fig. 1-1). Following data quality evaluation and testing, a hydrological model is used to simulate streamflow in the project region over a historical period. The model has been properly calibrated to produce a variety of parameter settings. This study also tests the impact of subbasin spatial scale effects to assess the performance of the hydrological model. Furthermore, obtaining streamflow time series at the proper site is a substantial hurdle to water resource development, particularly in developing nations such as Ethiopia. As a result, a new regionalization strategy is created in this study to address this challenge. The reservoir

operation optimization is then computed using a computational technique to assist decision-makers in making informed decisions.

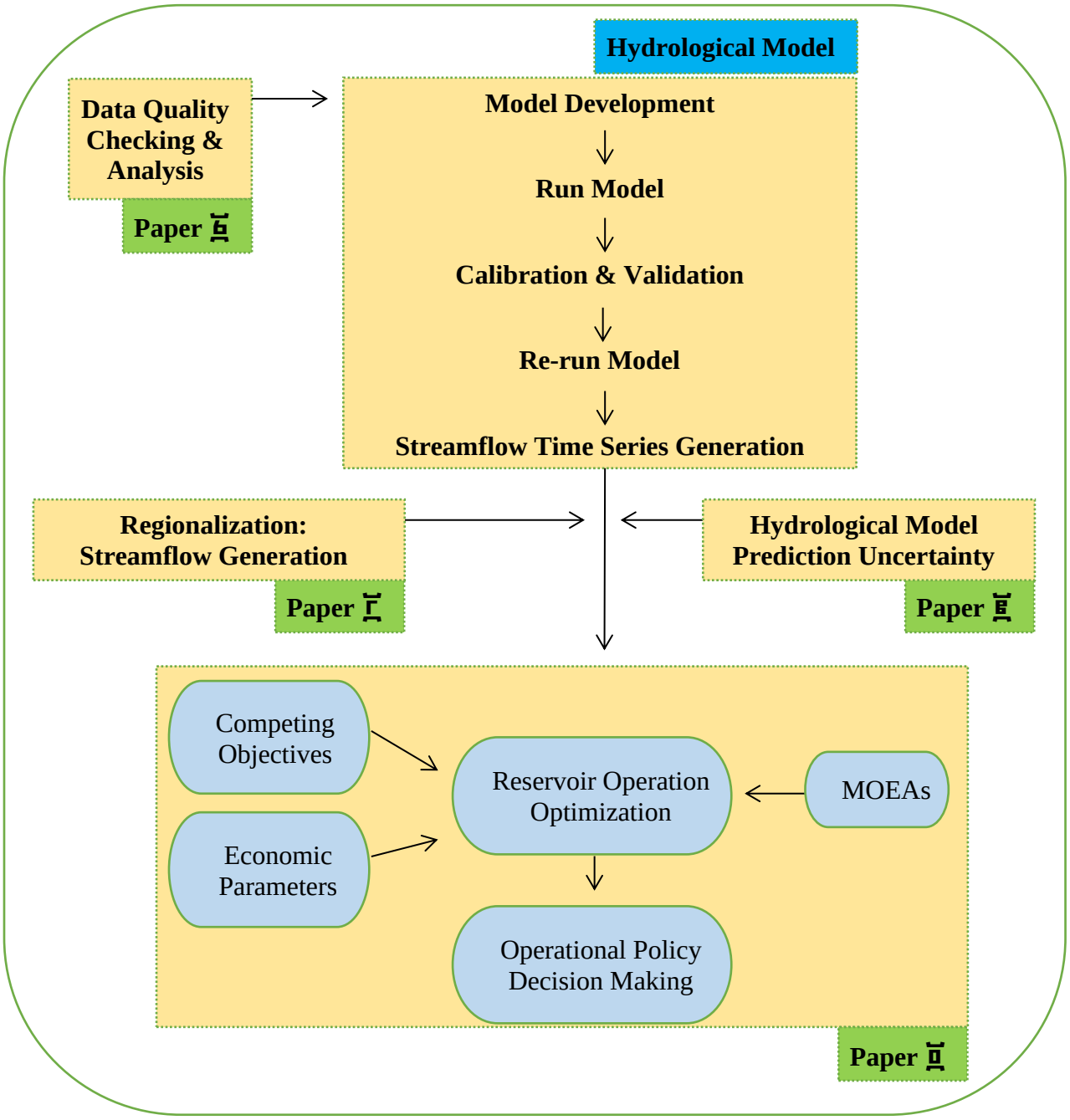

Figure 1.1. Dissertation Conceptual framework

A compilation of peer-reviewed publications makes up the thesis. Two of the research studies have been peer-reviewed and published; the third is a conference paper that was delivered at an international conference; and the fourth is ready for submission.

This thesis consists of eight chapters. The first is this Introduction chapter, while the concluding chapter comes last. A general flow that parallels the research process connects the thesis's introduction, main body, and conclusion. Each chapter includes techniques, analysis, and results, with the exception of chapter two, which stands alone as a state-of-the-art literature review. Furthermore, each chapter has its own concluding remarks.

Chapter 1. Introduction: This section covers reservoir operation challenges in the Omo Gibe River basin, including the problem description, research objectives, questions, expected output, work scope, research methods, and dissertation structure.

Chapter 2. State-of-the-art literature review: This chapter begins with a basic introduction and goes on to examine hydrological modeling aspects, seasonal flow variability, hydroeconomic modeling, multiobjective reservoir operation, optimization approaches, objective functions, research gaps identified, and a concluding remark.

Chapter 3. Description of the study area, data, and quality analysis: This chapter provides a description of the research region's topography, land use and land cover, soil, and climate. In addition, the data quality is examined and assessed.

Chapter 4. Choosing an interpolation approach to cover deficient climate data in the sparsely gauged Omo Gibe River basin, Ethiopia: In this chapter, the best interpolation method for the study region is determined after a thorough review and analysis of rainfall interpolation algorithms. The testing and analysis of data quality is an extension that is described and reviewed in Chapter 3.

Chapter 5. Subbasin Spatial Scale Effects on Hydrological Model Prediction Uncertainty of Extreme Stream Flows in the Omo Gibe River Basin, Ethiopia: In this work, the Omo Gibe River basin's three chosen catchments are used to explore the impact of subbasin spatial scale on hydrologic model prediction uncertainty for various flow quantiles. The findings demonstrated that SWAT could replicate the observed hydrograph with accuracies greater than 85%, 82%, and 73% for the catchments. Additionally, the majority of the data were covered by the coarser subbasin spatial scale, while the finer subbasin spatial scale offered the most accurate simulation that was closest to the observed streamflow pattern. Furthermore, it was discovered that 79-98% and 29-42% were the optimal subbasin spatial scales for peak and low flows, respectively.

Chapter 6. Reliability-weighted Approach for Streamflow Prediction at Ungauged Catchments: This chapter aimed to present a dependable technique for accurately determining surface water resources in ungauged catchments. It combines the advantages of three commonly used parameter transfer methods: global mean, physical similarity, and spatial proximity through weighted averaging. The suitability of the proposed scheme was checked in the Omo Gibe and Upper Blue Nile River basins in Ethiopia. The reliability-weighted method outperformed all three regionalization approaches by 30% and had a metric Nash-Sutcliffe efficiency greater than 0.50 in approximately 85% of the test catchments. Additionally, the runoff prediction performance of the proposed approach was comparable to that of the on-site calibrated model. Finally, the uncertainty in runoff prediction was reduced by combining the strengths of parameter transfer strategies relying on their reliability at test gauging stations.

Chapter 7. Multi-Objective Cascade Reservoir Operations Under Seasonal Streamflow Variability: A Hydro-Economic Model: This chapter presents and evaluates the effectiveness of the autoadaptive Borg Multi Objective Evolutionary Algorithm (MOEA) to support evolutionary

many-objective direct policy search (EMODPS). The Omo Gibe River Basin system faces competing sectoral needs for hydropower generation, public and private irrigated farmland, flood recession farming, and environmental flows. The results show that it is possible to stabilize hydropower generation, reservoir storage, and release under two scenarios of economic tradeoffs between competing needs, emphasizing the importance of using such advancing evolutionary algorithm models.

Chapter 8 concludes with a summary of the dissertation's main findings and recommendations for further basin study.

2. STATE OF THE ART LITERATURE REVIEW

2.1. Introduction

The development of water resource infrastructure consists primarily of reservoirs. A reservoir can be either man-made (such as water kept behind dams) or natural (such as water stored in lakes). Reservoirs, which can also have several uses, are used to store water for later use. Operating reservoirs must balance competing demands from downstream water users, irrigation, electricity, and flood management (van der Vat, 2015). Determining the most promising approach in a multiobjective situation with multiple stakeholders is thus crucial. Furthermore, to maximize the long-term benefits for all water users, the connections between these water consumers must be addressed. Implementing a set of allocation measures, such as priority setting and subsidies, could lead to increased water use efficiency. To better understand these conflicting issues between different stakeholders, many conceptual modeling approaches are being used in integrated water resource management. As a result, many new modeling tools are being developed, some of which have novel methodologies and notable benefits.

The administration and operation of a system in charge of storing a valuable commodity will always be a subject of inquiry and potential development due to the dynamic nature of hydrology. The emphasis is now on improving the operational efficacy and efficiency of current reservoir systems to maximize their beneficial uses. Hence, this dissertation offers state-of-the-art hydroeconomic optimization for multiple reservoir operations, with the purpose of assisting decision-making in water resource management.

2.2.Previous Works and Research Gaps

2.2.1. Previous Works

The Omo Gibe River basin in southwest Ethiopia drains the humid Shewan highlands into the hot and dry Lower Omo Valley, where it forms a biodiverse delta and flows into Lake Turkana on the Ethiopia-Kenya border. The Omo Gibe River basin has traditionally been a pastoral area where nomadic indigenous tribes move on a regular basis in response to the availability of water and food, which is regulated by the river's monsoonal flows. Seasonal climate fluctuations are linked to the oscillation of the Intertropical Convergence Zone (ITCZ), a low-pressure convergence zone. The main rainy season begins when southwesterly winds flow across Ethiopia's southwest highlands. From September to November, the ITCZ passes through southern Ethiopia in a northerly direction and in a southerly direction from March to May. However, the installation of dams for hydropower generation and the expansion of irrigable agriculture in the basin are altering the historical flow pattern generated by these monsoonal rains (Woodroofe, 1996).

In this river basin, Sundin (2017) examines the relationship between water and energy. Two hydrological (Topkapi) and energy (OSeMOSYS) modeling approaches were combined in the study. Even though the connection was successful, there was a mismatch in the hydrological response, which showed that the model did not accurately reflect the reservoir volume.

Earlier studies of hydropower reservoir operation in the Omo Gibe River Basin used HEC-ResSim (Daniel, 2011; Gebresenbet, 2016). According to Daniel (2011), the Gibe III power plant simulation produced an average of 6,488 GWh/year of energy and 758.94 MW of power. The maximum amount of firm energy and power that could be guaranteed 90% of the time were 5885 GWh/year and 679.725 MW, respectively. The Gibe III power plant was also built to accommodate three different future irrigation scenarios (Phase 1 covers 20,670 hectares, Phase 2 covers 54,600

hectares, and Phase 3 covers 142,900 hectares). Gebresenbet (2016) presented new reservoir operating regulations and power guidance curves to improve cascade reservoir operation and minimize some of the challenges associated with floods in the lower Omo River plain. The author also provided new operational rules for estimating future water levels and making release decisions, as well as a tractable model that could deliver daily power output and improve it up to a maximum of 28% for practical consideration over the next two decades. Despite the relevance of the produced findings, tradeoffs between conflicting goals were not considered in each study, and the problem of flooding and power outages persists.

A study by Tedla et al. (2015) briefly investigated the optimization of electricity production associated reservoir operation of cascade hydropower facilities in the Omo-Gibe River basin. In the study, they combined Climate-Hydro-Energy Modeling with RiverWare, a generic tool for complex reservoir system modeling, and extensively investigated the influence of climate change-induced hydrological variability on hydroenergy generation capacity across the Omo-Gibe River basin.

2.2.2. Research Gaps

Several studies have attempted to assess the effects of spatial discretization on the outputs of hydrological models (Blöschl and Sivapalan, 1995; Craig et al., 2020; Kling and Gupta, 2009; Tan et al., 2020; Tegegne et al., 2019; Wood et al., 1988), but the results are typically equivocal. For example, Mamillapalli et al. (1996) discovered that increasing the number of subbasins enhanced the SWAT model's accuracy. However, according to Bingner et al. (1997), the size and number of subbasins are not important variables when estimating runoff in SWAT. The majority of past studies have explored how subbasin spatial scale impacts the replication of the full observed

hydrograph, but they have not examined how subbasin spatial scale affects the replication of the various flow quantiles.

The majority of river basin development studies in Ethiopia, notably in the Omo Gibe River basin, appear to ignore this subbasin spatial scale influence. This could be one of the reasons why the region has recently witnessed the two extreme hydrological phenomena of power outages and flooding. Therefore, it is vital to investigate the subbasin spatial scale to replicate the peak and low flows for the proper subbasin spatial scales in replicating various flow quantiles for long-term flood and drought control.

It was also proven by Cibin et al. (2010) that the hydrological modeling software SWAT is more sensitive to particular parameters under different flow regimes (low, medium, and high flow). For a better understanding of the model outputs and decision-making processes, uncertainty analysis in such models may therefore merit additional research.

Better management of the available water resources depends on an understanding of the hydrological processes and the assessment of the frequencies and magnitudes of streamflow. The availability of data for hydrologic modeling is a major barrier to effectively estimating the water resources of a basin. For example, the Omo-Gibe River basin, which is seeing tremendous socioeconomic growth, including the establishment of cascade hydropower generation, is ungauged in approximately 70% of its area. As a result, regionalization remains a critical difficulty in creating solid projections in these ungauged catchments.

Many approaches for modeling ungauged basins using gauging station data have been developed (Arsenault et al., 2019; Blöschl and Sivapalan, 1995; Choubin et al., 2019; Ditthakit et al., 2021; Oudin et al., 2008). These approaches are used by hydrologists to detect patterns and trends from gauged to ungauged basins for hydrologic modeling studies. Streamflow in such ungauged basins

is often estimated from donor-gauged catchment/s utilizing single (Flatley and Rutherfurd, 2022; Oudin et al., 2008; Samuel et al., 2011; Yilmaz and Onoz, 2020) and combination parameter transfer system outputs (Merz and Blöschl, 2004; Nester et al., 2011; Sellami et al., 2014; Zhang et al., 2015).

Furthermore, researchers have attempted to extend the effect of regional links to estimates for ungauged watersheds to account for the inherent unpredictability of the projected model outcome. Zhang et al. (2015) and Merz and Blöschl (2004), for example, demonstrated how output averaging can help minimize uncertainty in ungauged watershed runoff predictions. To achieve the lowest possible uncertainty in the predicted outcome, the intended watershed is simulated using inputs from multiple contributors rather than just one, and the runoff estimate is obtained by averaging the modeling outputs using various sets of data from multiple donors.

Thus, using a novel reliability-weighted (RB) strategy that combines the advantages of the global mean, physical similarity, and spatial proximity parameter transfer approaches, this study provides a reliable method for precisely forecasting surface water supplies in ungauged catchments. Once streamflow at ungauged locations is acquired, reservoir system optimization using an appropriate optimization tool will be closer to the probable solution in such a sparsely gauged river basin.

Apart from this, Tedla et al. (2015) attributed reservoir system improvement to their investigation of the Omo Gibe River basin's cascade reservoir to increase the river basin's efficacy. To optimize the river basin's net benefit, however, a comprehensive approach is needed. This plan should incorporate all ongoing commercial and existing irrigation, flood recession water demands, hydropower, flood control, environmental flows, and other restrictive aspects in the river system to avoid serious resource allocation challenges.

Similarly, Jillo et al. (2017) used the Water Evaluation and Planning System (WEAP) tool to analyze the performance of the Omo-Gibe River basin under several scenarios. The authors attempted to establish whether or not the river basin's infrastructure upgrades, which mostly entail irrigation and hydropower, will result in adequate flow. The authors concluded that the river basin would have an adequate supply of water for both the present and the future based on the scenarios they considered.

Furthermore, the economic trade-offs between all competing water demands must be quantified using a robust optimization model for higher precision in decision making when the quantity of water is reduced and becomes more unpredictable due to seasonal variability. As a result, using a coupled hydroeconomic model to analyze the functioning of the Omo Gibe cascade reservoir will improve the basin's overall profitability and sustainability.

Abera et al. (2018) published a study on the operation of the Tekeze hydropower reservoir, Eastern Nile, Ethiopia. Despite the fact that the study did not include a hydroeconomic model in its analysis, the authors encouraged more research employing a hydroeconomic model in such reservoir operating systems. Mulat (2015) also recommended a thorough examination of reservoir system operations to gain a proper understanding of competing water resource systems through a tradeoff analysis that was conducted to quantify the likely impacts and benefits of current and future development options in the Blue Nile basin using a simulation approach. Hence, a thorough investigation would offer the engineer and operator additional knowledge, making decision-making easier.

Therefore, a complete strategy for reservoir optimization that takes into account all conflicting water demands over the Omo Gibe cascade reservoir needs to be researched further. Thus, the coupling of a hydroeconomic model with a recently designed state-of-the-art multiobjective

optimization algorithm (Borg MOEA) is proposed in this study. In addition, the Borg MOEA, an advanced multiobjective evolutionary technique, has yet to be tested in Ethiopia.

2.3. Hydrologic Modeling

The primary goal of hydrologic models, which are conceived as simplified representations of one particular aspect of the hydrological cycle, is to illustrate the physical mechanisms that drive the conversion of precipitation to runoff. Today, there are various hydrologic models accessible, each with its own structural design. Many scholars have classified these models based on their perspectives and purposes (Chow, 1971; Jajarmizadeh et al., 2012; Shaw et al., 2010).

There are several models for modeling and simulating stream flows in river systems, ranging from the hydrological model for rainfall runoff to the high computational hydraulic model for flow allocation and routing of river flows. Due to the lack of readily available pertinent data and information, hydrological models are typically only applicable to semiarid and arid regions. The primary contributing factors to this are that many river basins are not gauged and that some crucial data for hydrological processes were overlooked. To name a few of these data are soil properties, land use land cover, and weather data for the basins, all of which have a high spatial resolution. Furthermore, in gauged river basins, certain physical parametric data from the watershed are difficult to quantify yet critical to understanding hydrological processes (Blöschl, 2006; Moradkhani and Sorooshian, 2008; Singh, 1988). In such cases, hydrological models provide appropriate alternatives that can be utilized to more correctly forecast river stream flows.

With regard to evapotranspiration, stream flow, recharge to subsurface storage, and other aspects of the hydrological cycle, hydrological models can be useful tools for better understanding how changes in climate and land use affect these elements. Having a better understanding of the hydrologic processes in a watershed is helpful for the proper management and integration of

concerns around water resources in the management plans of irrigation, hydropower, health, and other sectors (Gebresenbet, 2016). These hydrologic processes must be represented with the appropriate hydrological models because many of the basins contain only a few observation points for a few parameters (Mengistu, 2019).

2.3.1. Hydrological Water Balance

The Soil and Water Assessment Tool (SWAT) is a continuous, long-term distributed parameter model that can simulate the surface and subsurface flow of watersheds (Arnold et al., 1998). It is used worldwide to examine the distribution of the watershed's water balance and climate change. The model's key advantage is that it can be used to examine how land management techniques affect the water and sediment yields of the watershed. The key characteristics of the watershed were analyzed by SWAT using the hydrological water balance, which serves as the foundation for all hydrology studies (Neitsch et al., 2011). Figure 2.1 depicts a schematic representation of hydrological dynamics in the SWAT model. The simulation of a watershed's hydrology falls into two main, discrete categories that can each be handled separately. The main channel in each subbasin might receive different loadings of water, sediment, nutrients, and pesticides depending on the hydrologic cycle's land phase, which is the first process category. The second process category works in the hydrologic cycle's water or routing phase and directs water, sediments, and other materials through the watershed's network of channels to the outflow. To produce stream flow to the watershed exit, flow directed from each HRU is added. The water balance at the land phase is estimated by changes in soil water storage for each day based on the computation of the relevant processes. The primary source of water is precipitation. When solving the water balance equation, essential processes such as evaporation, runoff, soil water percolation, and groundwater movement are included. Following the completion of the water balance computation, the subbasins

are linked in the water phase, and the water is then directed via the subbasins (Pfannerstill et al., 2014; Van Griensven et al., 2012).

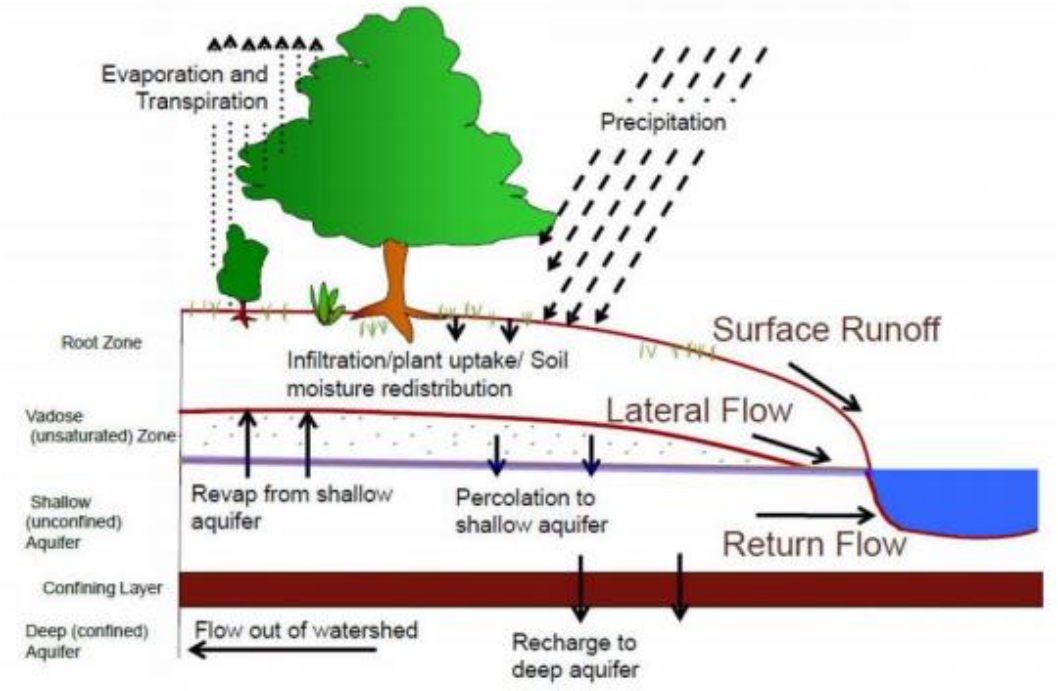

Figure 2.1. Schematic representations of the hydrological cycle (Neitsch et al., 2011).

2.3.2. Hydrologic Model Parameter Calibration and Validation

When the river flow regime must be accurately replicated, the hydrologic model assessment utilizing one or more indicators is stated in the literature to be insufficient (Chilkoti et al., 2018). The use of hydrologic models to evaluate the impacts of anthropogenic changes, such as land use and climate change, on water quality and quantity is growing. To reduce the uncertainty of future predictions, it is critical to create highly calibrated models given the expanding scientific work on the assessment of these changes for future scenarios (Peel and Blöschl, 2011). Successful model calibration is the cornerstone of any positive scientific finding (Van Griensven et al., 2012). The calibration process is typically not very difficult for conceptual hydrologic models with few

parameters. However, the calibration process becomes increasingly challenging as model complexity increases (Chilkoti et al., 2018; Gebresenbet, 2016).

For SWAT and other comparable watershed models, Abbaspour et al. (2007) state that there are frequently hundreds of modeling units for a single watershed and dozens of model parameters used to characterize features within the model. Calibrating these model parameters so that the output of the model matches empirical data, such as streamflow observations gathered inside the watershed, is one of the modeler's most crucial and challenging responsibilities. For calibrating SWAT models, numerous algorithms and techniques have been created and put to use. In the SWAT community, SWAT-CUP is frequently used to apply calibration methods to SWAT models. Different calibration procedures are included in SWAT-CUP, along with routines for SWAT model sensitivity analysis, validation, and uncertainty analysis (Abbaspour et al., 2007). SWAT modelers could benefit from additional processes and algorithms that have been developed in the scientific community for calibration but have not yet been incorporated into SWATCUP. For instance, neither multiobjective calibration approaches nor genetic algorithm calibration approaches are included in SWATCUP (Abbaspour, 2015). However, SWAT modelers might benefit from these calibration techniques, particularly for sizable watersheds with a wealth of available streamflow measurements (Arnold et al., 2012; Bekele and Nicklow, 2007; Ercan and Goodall, 2016). Multiple-objective calibration, as opposed to the more popular single-objective calibration algorithms now available to SWAT users in tools such as SWAT-CUP, better constrains the calibration process, resulting in a calibrated model that is more closely aligned with the physical conditions within the watershed (Chilkoti et al., 2018). According to Cibin et al. (2010), to offer a more accurate representation of the various watershed processes, the parameters affecting the runoff generation process must be identified and included in the calibration process.

Various approaches to SWAT model calibration are described in the literature (Abbaspour et al., 2007; Arnold et al., 2012; Cibin et al., 2010). The majority of research relies on a single objective function optimized by error statistics, such as the Nash-Sutcliffe efficiency (NSE). The major disadvantages of using a single objective function as goodness of fit are as follows: (a) a single measure is used to judge simulation performance (Pfannerstill et al., 2014); (b) squared errors are frequently used but have been shown to be biased toward high flow (Shafii and De Smedt, 2009); and (c) one objective function may not be adequate to incorporate the effect of several parameters under calibration, especially for complex models (Madsen, 2000).

2.3.3. Subbasin Spatial Scale Effects on the Hydrological Model Prediction Uncertainty of Extreme Stream Flows

Planning for water resources and flood prevention are the two main applications of hydrological prediction (Kibuye et al., 2020). Furthermore, studying low flows is necessary to comprehend water quality, which influences stream flow, chemical concentrations, and the distribution of habitats and animals. Additionally, it is crucial for those involved in the construction of infrastructure to analyze extreme flows (high and low flows). Therefore, it is crucial to pay closer attention to the prediction and replication of flow quantiles (such as high, moist, mid-range, dry, and low flows). To simulate hydrological processes and water quality, numerous studies have developed various types of hydrological models (Arnold et al., 2012; Butts et al., 2004; Devia et al., 2015; Pandi et al., 2021).

Unlike lumped models, fully distributed and semidistributed models discretize catchments into numerous homogeneous units to account for the heterogeneity of a watershed (Dal Molin et al., 2020; Veettil et al., 2021). However, compared to the framework for semidistributed hydrological modeling, fully distributed models are more data-intensive and have higher processing needs.

Many researchers in this field favor the semidistributed hydrological model for assessing water resources because of this benefit. The discretization of the basin into many subbasins is a crucial component of semidistributed hydrological models. A basin is discretized into smaller subwatersheds in the Soil and Water Assessment Tool (SWAT) modeling process based on classifications of the land use, soil, and slope. Each of these subwatersheds is then further subdivided into smaller hydrological response units (HRUs). Therefore, the method used to identify homogenous units as subbasins or HRUs may have an effect on how well hydrological models can reproduce the frequency and spatial distribution of the information presented. Default discretization is widely used in SWAT hydrological modeling approaches; nevertheless, doing so may make the simulation more uncertain (Tegegne et al., 2019). Hydrological forecast uncertainty must be examined to make educated judgments about water resource management. One of the most important sources of uncertainty in hydrological predictions is measurement errors in the model's inputs, along with the model's parameters, organizations, and other components (Abbaspour et al., 2015; Beven, 1993). The primary source of uncertainty in hydrological models is the input data (Butts et al., 2004; Faramarzi et al., 2013; Rozos et al., 2021), and many studies have focused on estimating these uncertainties (Abdar et al., 2021; McMillan et al., 2018). Relatively few studies, however, have reproduced the various flow quantiles while taking into account the shortcomings of the hydrological model due to the spatial scale of the model subbasins.

The effects of spatial discretization on the results of hydrological models have been investigated in a number of studies (Blöschl and Sivapalan, 1995; Kling and Gupta, 2009; Tan et al., 2020; Tegegne et al., 2019; Wood et al., 1988), although the results are frequently inconsistent. For instance, Mamillapalli et al. (1996) found that increasing the number of subbasins increased the accuracy of the SWAT model. However, Bingner et al. (1997) claims that the size and quantity of

subbasins are not important factors when determining runoff in SWAT. Most earlier studies have focused on how subbasin size impacts the replication of the total observed hydrograph, but they have not looked at how subbasin spatial scale influences the replication of different flow quantiles. It is vital to explore how the subbasin division level affects the creation of the hydrograph's various flow quantiles to acquire a better understanding of low and high flow behavior. Furthermore, the uncertainty associated with the subbasin spatial scale in reproducing the observed hydrograph may impede hydrological modeling prediction.

2.3.4. Streamflow Prediction at Ungauged Catchments

Planning and management of water resources are nearly exclusively based on time-series data of unbroken streamflow (Niu and Feng, 2021). Since most basins lack observational data, hydrologists have encountered challenges in gathering river flow observations within the study area. There are many unmeasured basins worldwide, especially in developing nations, because there are not enough hydrological and meteorological observations globally. The key factors influencing this are the various concomitant and/or individual constraints of socioeconomic and geographic feature circumstances. A basin that lacks streamflow observational data is said to be ungauged. Runoff models are also crucial for risk management, water resource management, and aquatic environment preservation. Therefore, hydrologists face a significant challenge when simulating runoff at a place of interest when little to no such measurement data are available for the study of the proposed project.

The International Association for Hydrological Sciences (IAHS) released predictions for the Ungauged Basin (PUB) during the 23rd International Union of Geophysics and Geodesy in 2003 for the following ten years (2003–2012). It aims to significantly advance catchments that are not taken into account in hydrologic forecasts. The implementation of the project has promoted the

development of parameterized regionalization plans for ungauged catchments. Despite the fact that PUB was terminated in 2012, work on regionalization techniques that permit streamflow modeling in ungauged watersheds has persisted ever since (Oudin et al., 2008; Zhu et al., 2021).

According to numerous studies (Arsenault et al., 2019; Blöschl and Sivapalan, 1995; Choubin et al., 2019; Ditthakit et al., 2021; Oudin et al., 2008), gauging station data have been utilized to mimic ungauged basins. Hydrologists employ these techniques to identify patterns and trends in gauged and ungauged basins for hydrologic modeling studies. Some of the frequently used information transfer (regionalization) methodologies in earlier research include the global mean (GM), spatial proximity (SP), regression-based (Rb), and physical similarity (PS) methods (Flatley and Rutherfurd, 2022; Oudin et al., 2008; Samuel et al., 2011; Sellami et al., 2014; Yilmaz and Onoz, 2020; Zamoum and Souag-Gamane, 2019). The spatial proximity strategy provides the best regionalization option when there is a higher concentration of monitoring stations, whereas the regression model produces the least acceptable results, and the physical similarity approach is in the middle, according to Oudin et al. (2008) who used 913 gauged catchments in France to compare the regionalization strategies of Rb, PS, and SP. Additionally, they claimed that in regions with a larger density of streamflow gauging stations, the spatial proximity technique outperformed the similarity strategy.

For a more thorough regionalization perspective, it is commonly expected to estimate streamflow in ungauged basins using the combined outputs of the parameter transfer system (Merz and Blöschl, 2004; Nester et al., 2011; Sellami et al., 2014; Zhang et al., 2015). Similarly, multimodel averaging is extensively utilized in a number of hydrological sectors (Arsenault and Brissette, 2016; Arsenault and Brissette, 2014; Razavi and Coulibaly, 2016). To obtain the anticipated outcome with the least amount of uncertainty, the planned watershed is explicitly modelled once

more using inputs from multiple donors rather than just one. The estimated runoff is then calculated by averaging the simulation outcomes using different sets of data from different contributors. Despite this, not all experts believe that a specific technique is particularly useful for gauging streamflow in unmeasured catchments. Therefore, additional research into these hydrological processes may lead to a better regionalization strategy than what is currently being used.

2.4. Seasonal Flow Variability

The efficient management of a multipurpose reservoir necessitates knowledge of high and low flows (Su et al., 2020; Tegegne et al., 2019). Many studies in river flow analysis are dedicated toward an investigation of changes in streamflow, including wet and dry season flows, and the attribution of these to a changing climate.

In many cases, studies of inflows for high and low flows are performed independently. However, Su et al. (2020) used empirical analyses and Bayesian models to relate climate indices and preseason flow regimes to the prediction of low flow period attributes, with an interesting application of determining how the operation of the Three Gorges Dam (TGD) may have altered the flow regime in the dry season in terms of the 7-day low flow attribute.

A recent research investigation (Kuriqi et al., 2020) provides a better understanding of intra/interannual streamflow variability and trends, allowing for more effective water resource planning and management for both short-term and long-term demands. It is actually highly challenging to provide a trustworthy prediction of the discharge (Q) for a certain river at a given moment since river discharge depends on numerous stochastic processes and has a high degree of variability among years (Abrahamsson and Håkanson, 1998). A common practice is to measure river discharge over an extended period of time (decades), after which a statistical estimate of the likelihood that Q will fall within a specific range at a particular time is provided. If a sufficiently

extensive and trustworthy set of empirical data is available, this method can be used for a variety of applications (Chow, 1971).

Engineers, water managers, policymakers, and other stakeholders must be aware of seasonal shifts and streamflow variability trends to take proactive structural and nonstructural measures to prevent basin or regional water scarcity issues while also promoting aquatic ecosystem preservation (Kuriqi et al., 2020). The management of water resources is further impacted by climatic variations due to the lengths, timing, rates, and intensities of precipitation (Azmat et al., 2015). As a result, precipitation anomalies, such as droughts and floods, can negatively impact the ecological balance (Zhang et al., 2013b). For effective water management, especially in light of impending challenges brought on by population increase and global warming, trends and variations in climatological variables such as temperature and precipitation are crucial (Cannarozzo et al., 2006).

In water resource management, synthetic streamflow generations are being used to account for streamflow variability. By generating synthetic streamflow, it is possible to evaluate different management plans under stochastic realizations that are not present in the historical record. These realizations can be produced using stationary or nonstationary models. Some recent works (Quinn et al., 2017; Giuliani et al., 2017; Zatarain Salazar et al., 2017) have utilized the methods introduced by Kirsch et al. (2013) and Nowak et al. (2010) to build stationary streamflow ensembles.

2.5. Water resource development projects in the Omo Gibe River basin

In the last 20 years, the Omo Gibe River basin has seen the development of three power facilities: Gibe I, II, and III; a fourth, Koysha, is currently under construction. Gibe I is a modest dam with a power plant, but Gibe II is only a power plant connected by an approximately 26-kilometer-long tunnel just downstream from Gibe I. In comparison, Koysha and Gibe III are massive dams and

power plants. The creation of the Koysha and Gibe III mega dams in the basin has tremendously improved economic growth. Ethiopia plans to produce enough power for its own needs, supply electricity to everyone, and then export energy to other countries by 2025 (Asress et al., 2013; Panos et al., 2016; Woodroofe, 1996). As of 2016, a majority of the people were without electricity, mostly in rural regions such as the Omo Gibe River basin, while Ethiopia's national electrification rate was only 25% (Panos et al., 2016; Zaniolo et al., 2021a). Omo-Gibe hydropower facilities are being expanded to achieve the nation's ambitious targets. The large reservoirs behind the dams also make more consistent electricity output possible in this dry geographic area, where most of the yearly flow (90%) happens in only four months of the year (Sundin, 2017).

Due to storage reservoirs, large irrigated agricultural areas can now be cultivated (Avery and Eng, 2012). The Kuraz Sugar Plantation, which will eventually span 175,000 hectares downstream of the Koysha dam, is being developed by the state-owned Ethiopian Sugar Corporation (ESC). ESC's goal is to become a top-10 sugar exporter (Jordan et al., 2022). In the area's south, foreign and private investors have obtained leases for the Kuraz Sugar Development Project from the Ethiopian Ministry of Agriculture and Natural Resources (Horne et al., 2011). According to Carr (2017a), the site will mostly be used for cotton crops. Given the great aridity of the area, these projects reroute water from the main canal, allowing crops to flourish (Human-Rights-Watch, 2017).

Furthermore, in the Omo Gibe River Basin (Woodroofe, 1996), flood recession is identified as a land use type associated with the river delta and happening in limited bands along the banks of the Lower Omo Valley. Although the exact area of the flood recession region is difficult to define due to changes in flood size over time, it is estimated that 100,000 people rely on the system (Woodroofe, 1996).

The entire area under flood recession, according to Nederveen et al. (2011), is 11,037 hectares, however, this includes bare soil, open bushland, and riverine woods. When the annual flood recedes, the principal crops grown in the lowlands along the Omo River's riverbanks are millet, maize, and sorghum (Nederveen et al., 2011). Once the flood recedes, agropastoral inhabitants in the lowlands, particularly in the lower Omo, cultivate crops on riverbanks with a traditional hoe (Eyasu et al., 2015).

2.6. Socioeconomic and Environment

Water resource development to generate power, irrigate land, minimize floods, and so on may harm the environment and the socioeconomic level of individuals over a vast geographic area. The most efficient and cost-effective technique for preserving the environment, mitigating the negative socioeconomic effects of the affected area, and promoting sustainable development is to assess and resolve environmental and social issues as soon as possible (EEPCO, 2004).

The majority livelihood strategy used by the people in the woredas and communities impacted by the project is mixed farming, which combines the production of crops and the rearing of livestock. The prevalence of mixed farming should not, however, be used as a cover for the variety, complexity, subtleties, and diversity of livelihood choices, as well as the corresponding agroecological variances in those regions (EEPCO, 2016).

Alternatively, around 200,000 indigenous people use flood recession farming as a main nutrition source for their livestock in the lower Omo-Gibe River. Because the dry environment of the Lower Omo Gibe is insufficient to sustain rain-fed crops, this method employs the yearly inundations created by the Omo-Gibe River's late summer flood surge as a form of irrigation (Carr, 2017a). The river's banks are the primary food supply for the locals, as they may cultivate maize and

sorghum there after the floodwaters recede. After rising in the Omo Valley in July, the Omo-Gibe River floods the plain with silt in August and September (Carr, 2017a; Jordan et al., 2022). According to certain studies, the development of the basin's water infrastructure could result in a food shortage for the indigenous people (Carr, 2017a; Human-Rights-Watch, 2017). This would slow the flood wave and lessen the chances of not having enough land to raise crops in any given year. However, the exceptionally severe and sustained rains that began in June 2006 harmed over 500,000 people, with flash floods killing over 600 people. Pastoralists lost their cattle as a result of floods and other natural disasters (EEPCO (2009), Ocha (2010), and Woldegebrael et al. (2022)).

2.7. Hydroeconomic Modeling in reservoir operation

2.7.1. Introduction

Hydroeconomic modeling provides data on the economic returns from alternative activities and institutional setups that influence decisions about how to use water, which helps us better understand the systems of water resources (Hafi, 2006). The analysis of challenges related to water scarcity, drought, and climate change can be performed effectively using hydroeconomic modeling. All significant hydrologic and engineering components of the investigated river basin are represented by these models, which are spatially distributed. Additionally, hydroeconomic models make it possible to accurately capture the results of interactions between the hydrologic and economic systems, guaranteeing that the best economic outcomes take into consideration the spatial distribution of water resources (Kim et al., 2019).

Table 2-1 outlines typical hydroeconomic modeling research studies undertaken globally. Distinctions in spatial and temporal scales, resolution techniques, and models sometimes obstruct the connection between economic and hydrologic models (Harou et al., 2009). A different strategy

is to combine historical information provided by water authorities with simulated information and network topology from preexisting hydrologic models.

Table 2-1. Papers Reviewed addressing hydroeconomic modeling

Item	Type of Model Used	Objective Function	Location	Reference
1.	Holistic, ESO, Stochastic Dual Dynamic Programming	Irrigation and hydropower	Euphrates, Turkey and Syria	Tilmant et al. (2008)
2.	Holistic, nonstochastic, deterministic, nonlinear programming	Irrigation, hydropower and environmental flow	Maipo River, Chili	Cai et al. (2003)
3.	Holistic, nonstochastic, deterministic, nonlinear programming	Irrigation and hydropower	Nile, Ethiopia, Egypt and Sudan	Whittington et al. (2005)
4.	Holistic approach	Irrigation, public water supply, flood protection and environmental flows	Florida, USA	Mirchi et al. (2015)
5.	Holistic, nonstochastic, nonlinear optimization	Irrigation and hydropower	Blue Nile, South Sudan	Satti et al. (2015)
6.	Holistic, non-linear programming, IHEOM-LMRB optimization algorithm	Irrigation, hydropower and fishery	China, Myanmar, Lao PDR, Thailand, Cambodia and Vietnam	Do et al. (2020)
7.	Dynamic programming, linear programming, nonlinear programming	Urban water supply, industrial activities and rice irrigation	Brazil	Dalcin and Fernandes Marques (2020)

This technique can be used to quickly and accurately create a reduced form hydrological model of the river basin under investigation (Cai et al., 2003).

A modular or compartmental method and a holistic approach are the two primary types of modeling approaches (Brouwer and Hofkes, 2008; Harou et al., 2009). Table 2-2 shows representative instances of each strategy along with their benefits and drawbacks. According to Harou et al. (2009), hydroeconomic models describe regional-scale hydrologic, engineering, environmental, and financial aspects of water resource structures within a logical framework.

Hydroeconomic models, which combine the concepts of economics and engineering, translate the idea of fixed demand into the economic worth of water, which is defined by water rights, priority, and future forecasts (Harou et al., 2009; Lund and Ferreira, 1996). In their article, Harou et al. (2009) conducted a review of the literature and noted the key steps in model design as well as the various issues, formulations, levels of integration, spatial and temporal scales, and techniques for problem solving that were addressed and used by more than 80 hydroeconomic modeling efforts from 23 countries over the course of 45 years. Through the use of water allocation and the proper operation of the present demand-supply chain, the concept of economic demand for water is optimized to maximize the net benefit. However, water managers do not typically adopt the suggestions of this hydroeconomic model in regard to optimizing the operation of reservoirs (Harou et al., 2009; Labadie, 2004). These researchers proposed collaborating with water management and enhancing integration into existing or trustworthy simulation models as a potential remedy to the existing deficiencies.

Table 2-2. Advantages (+) and disadvantages (-) of holistic programming and modular heuristic approaches to hydroeconomic reservoir optimization (van der Vat, 2015).

Holistic programming	Modular heuristic	Source
Can deal explicitly with the stochastic characteristics of model input (+)	Stochastic inputs are considered implicitly and only as far as included in the time series of the model input (-)	(Labadie, 2004; Rani and Moreira, 2010)
Able to identify unique global optimal solution (+)	Approximation of the optimal solution only with risk of identifying a local optimum (-)	Labadie (2004)
Optimization of release flows only, operation rules have to be derived (-)	Optimization of any simulation model input, also possible directly on operation rules (+)	(Labadie, 2004; Rani and Moreira, 2010)
Requires recoding and simplification to model the water resources and economic systems (-)	Can be constructed around existing and accepted simulation models (+)	(Harou et al., 2009; Labadie, 2004; Rani and Moreira, 2010)

According to the hydroeconomic modeling for reservoir optimization shown above, there are essentially two opposed strategies with a few potential hybrid forms in between (van der Vat, 2015):

- *Implementation of a case-specific mathematical program using a holistic, ISO, or ESO optimization model (sometimes referred to as holistic programming).*
- *Creation of a modular, deterministic, ISO simulation-optimization model using a combination of an evolutionary algorithm, economic valuation, and preexisting simulation models (also known as a modular heuristic).*

Earlier studies (e.g., Abera et al., 2018; Annys et al., 2020; Gebresenbet, 2016; Tedla et al., 2015) did not include economic penalties or value functions. This is true for the Omo Gibe River basin as well as other Ethiopian river basins. As a result, the effectiveness of each model run can only be measured by how well the output matches the matching output, rather than by economic performance. Since improvements cannot always be seen in time series plots and mean square difference values for the various model outputs at some stage in the fine-tuning of the model, the exclusion of economic functions from the analysis of a basin's reservoir may hinder the improvement of the release rules. The consideration of trade-offs between competing goals in the pursuit of maximum net benefit is also quite challenging. Hydroeconomic models, on the other hand, have the ability to change the idea of fixed demand into the economic worth of water as determined by water rights, priority, and long-term projections (Harou et al., 2009; Lund and Ferreira, 1996). Thus, by incorporating hydroeconomic analysis into reservoir management challenges, especially when reservoir operations involve several stakeholders with conflicting objectives, the performance and sustainability of a river basin can be enhanced.

2.7.2. Multiobjective Reservoir Operation

The abundance of literature on multipurpose reservoir operating scenarios in integrated river basin management has grown in recent years. Many researchers, including Stretch and Adeyemo (2018), Ahmad et al. (2014), Horne et al. (2016), Labadie (2004), and Rozos (2019), have investigated the state of the art in reservoir operation optimization. To effectively manage a reservoir, it is necessary to develop a collection of guidelines, policies, schedules, procedures, and strategies that best address certain goals. Usually, decisions on releases are guided by reservoir operating standards. Decisions about how to distribute water releases and storage capacity among reservoirs and uses over varying time periods are operational (Daniel, 2011). The optimization of water uses in

connection to economic objective traits is a major theme in many of the publications that have been studied (see Table 2-1).

The four kinds of optimization methodologies are linear programming, nonlinear programming, dynamic programming, and computational intelligence (Ahmad et al., 2014; Rani and Moreira, 2010). The first three approaches, which have been used in numerous studies such as the ones mentioned above, demand reformulating the problem using a full mathematical program. Only dynamic programming allows for ESO or explicit stochastic optimization. Although ESO is the conceptually most appealing strategy, Rani and Moreira (2010) say that it suffers greatly from computing issues, significantly limiting model construction.

Optimization techniques such as evolutionary algorithms, artificial neural networks, and fuzzy modeling are examples of optimization approaches that include computational intelligence, often known as (meta-)heuristics. Their application in water resource management has been investigated (Maier et al., 2014). A metaheuristic approach is a trial-and-error strategy that mixes user techniques into a more effective or dependable method for solving a class of computing problems. Only hydropower optimization was considered in the earlier operation of the Omo Gibe cascade reservoir (Gebresenbet, 2016; Tedla et al., 2015). In reality, irrigation of the river basin is taken into account in another study (Daniel, 2011; Jillo et al., 2017); however, the authors try to demonstrate the state of the river basin under various scenarios of model simulation rather than the optimization of these competing purposes. Other large irrigation projects, however, are now under development and will soon be connected to the system. This will result in a war for water distribution between multiple sectors, including agriculture, hydropower, and the environment. Therefore, the study should be broadened to a more comprehensive plan that considers irrigation water demand as a system constraint to avoid problems with resource allocation. To create a

decision-support system, it is also crucial to study the trade-offs between these conflicting demands, particularly in light of the fact that the availability of water is declining and becoming more unpredictable owing to external factors such as climate change (Tedla et al., 2015). As a result, for the river basin to have better control over its water resources, advanced tools that can manage such competing goals are needed.

2.7.3. Optimization algorithms and objective functions

2.7.3.1. Introduction

There are two types of optimization algorithms: single-objective algorithms and many-objective algorithms. A single objective optimization method will maximize only one objective function; however, a multiobjective optimization algorithm will often optimize two or more objective functions.

In the first category, the multiobjective problem is first reduced to a single-objective optimization problem using conversion techniques (such as the weighting method, constraint method, and penalty factor) and then solved using linear programming and dynamic programming, among other traditional mathematical techniques (Tomlinson et al., 2020). In their study Feng et al. (2017), the weighting coefficient is utilized in conjunction with linear programming to allocate the quarter-hourly generation of hydrothermal-nuclear plants among different power grids. Hu et al. (2014) incorporated the benefits of statistical water quality models, multiobjective reservoir operations, and a self-adaptive evolutionary algorithm (based on differential evolution and utility function) in a separate study. Despite the fact that the first group can often decrease optimization difficulties well, it is frequently influenced by erroneous conversion coefficients and cannot provide sufficient information on the optimal trade-off front (Zheng and Zecchin, 2014).

The second group of multiobjective evolutionary algorithms (MOEAs) such as multiobjective particle swarm optimization (MOPSO), multiobjective differential evolution, and nondominated sorting genetic algorithm-II (NSGA-II) frequently address all objectives simultaneously (Zhang et al., 2013a). MOEAs have no tight limitations on the mathematical features of optimization problems and can provide a set of nondominated solutions in a single run, which has captured the interest of academics (Niu et al., 2018). Borg MOEA, a high-performing MOEA that can strongly support many-objective water resource applications (Reed et al., 2013), is one of the state-of-the-art MOEAs that outperforms many multiobjective algorithms.

MOEAs and other metaheuristic algorithms, as well as their applications, are described in detail in (Coello et al., 2007; Zhou et al., 2011). By utilizing -NSGA-II, MOEA/D, Borg MOEA, and NSGA-III to optimize reservoir management strategies based on multidisciplinary objectives such as flood control, hydropower generation, and water supply, Hurford et al. (2014) and others (Al-Jawad and Tanyimboh, 2017; Dai et al., 2017; Hadjimichael et al., 2020; Qi et al., 2016; Salazar et al., 2017) are examples of using these techniques to solve water resource management problems. The reservoir operation policy's purpose was to meet downstream water needs during a drought while guaranteeing that there was enough water in the reservoir to last the following year. Al-Jawad and Tanyimboh (2017) evaluated Borg MOEA's performance using a multipurpose reservoir. According to the conclusions of their analysis, the reservoir's performance was improved by 14.83 million m^3 of additional maximum reservoir capacity. Furthermore, under the simulated low flow scenario, sustainable water storage in the reservoir was achieved, while the overall annual imbalance between monthly reservoir releases and water needs was reduced by 64.7%. Furthermore, because of its higher reliability compared to a number of powerful, well-established

algorithms, the Borg MOEA has been widely employed by researchers (Giuliani, 2014; Giuliani et al., 2021; Rangarajan et al., 2022; Woodruff et al., 2012; Y. Al-Jawad and M. Kalin, 2019).

2.7.3.2. Multiobjective evolutionary algorithm (MOEA)

A multiobjective problem is generally formulated as follows:

$$\text{Minimize } F(x) = (f1\ (x), f2\ (x), \ldots. fP\ (x))\ x \in S$$

$$\text{subject to } ci\ (x) = 0, \forall i \in \vartheta$$

$$cj\ (x) \leq 0, \forall j \in \varphi$$

where *fi (x)* is the objective function to be minimized, x is the set of decision variables, S is the decision space, and ci and cj are the constraints within sets ϑ and φ (Deb, 2011).

Many MOEAs, notably NSGA-II, have been used in hydrologic models (Bekele and Nicklow, 2007; Ercan and Goodall, 2016). According to Reed et al. (2013), the Borg MOEA is a top-performing MOEA that might effectively support numerous applications involving water resources. Of the ten algorithms examined across the issue set, it had the best consistency. It combines ϵ-dominance, a measure of convergence speed named ϵ- progress, randomized restarts, and autoadaptive multioperator recombination into a unified optimization framework (Hadka and Reed, 2013; Reed et al., 2013). Borg is a member of the group of evolutionary algorithms that develop solutions based on genetic operators, producing a set of Pareto-optimal solutions. The technique uses six operators in the recombination process to speed up the search process, and it stores all of the nondominated solutions in a dominance archive.

To preserve diversity, the objective space is divided into hyperboxes whose dimensions are all equal, as shown in Figure 2-3. Thus, the ϵ-box index vector is used to find the dominant solutions instead of the objective function values. The algorithm calculates this index by dividing the

objective function value by ϵ and then sets the result as the succeeding integer value. If two or more solutions are in the same box, the dominant solution is the one that is nearest to the lower-left corner of the ε-box in the case of a minimization problem. Graphical representation of the ϵ-progress concept in a minimization problem with two objectives. Solutions (1) and (2) are new solutions in unoccupied boxes and thus represent improvements. Solution (3) is not considered an improvement because it resides in a previously occupied box. The shaded boxes were previously occupied while the unshaded boxes were not previously occupied (Al-Jawad and Tanyimboh, 2017; Hadka and Reed, 2013).

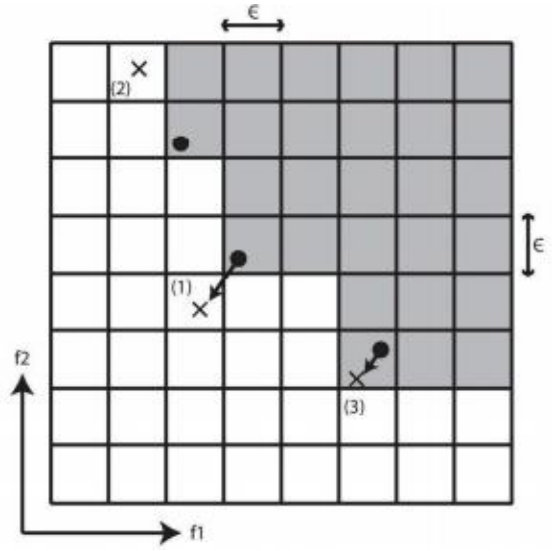

Figure 2.2. 2D representation depicting the ϵ-progress concept (Hadka and Reed, 2013).

During the evolutionary process, new solutions are formed from two parent solutions. One of the parent solutions is taken from the elite archive, and the other is chosen from the population via tournament selection, which generates selection pressure by staging a competition among individuals from the population. The tournament winner is the one with the highest fitness as assessed by the objective function (Mitchell, 1998; Sivanandam et al., 2008). It would be determined by supremacy in Borg MOEA. If one solution in the competition dominates the other, it advances; if they are both nondominated, one will be chosen at random. To maintain selection

pressure, Borg employs variable tournament sizing. By increasing the tournament size as the population develops, the likelihood of a nondominated solution from the population being selected to participate in the tournament does not decrease as much as it would otherwise (Hadka and Reed, 2013). After determining the parent solutions, their genes are joined to generate a new solution. For stagnation measurement, ε-progress was introduced (Hadka and Reed, 2013), which measures the improvement while searching for new solutions. If the algorithm finds new solutions in a new unoccupied ε-box, then there is progress and the algorithm is allowed to continue (Figure 2-3). On the other hand, if there is no improvement based on ε-progress for a certain number of evaluations, a revival process is triggered to escape from any local optima.

The method employs numerous recombination operators to produce offspring. When selecting the recombination operators within the framework provided by Borg MOEA, the dynamic properties of the optimization problem's objective and solution spaces, including the composition and diversity of the candidate solutions and the landscape of the objectives, are taken into account. When compared to six cutting-edge MOEAs on a range of test issues, Hadka and Reed (2013) found that Borg performed as well as or better than the other MOEAs on the majority of the tests. The recombination operators of the Borg MOEA are as follows:

- Simulated binary crossover (SBX) (Deb and Agrawal, 1995);
- Differential evolution (DE) (Storn and Price, 1997);
- Parent centric crossover (PCX) (Deb et al., 2002);
- Unimodal normal distribution crossover (UNDX) (Kita et al., 2000);
- Simplex crossover (SPX) (Tsutsui et al., 1999); and
- Uniform Mutation (UM) (Michalewicz et al., 1994).

Furthermore, with the exception of UM, all operators apply polynomial mutation (PM) (Deb and Agrawal, 1995) to the progeny they generate. A particular operator's ability to contribute nondominated solutions to the dominance archive determines how likely it will be selected to

produce offspring when compared to the other recombination operators; as a result, operator selection probabilities are proportional to each operator's efficiency and individual contributions. The values of the decision variables in the offspring produced are contained by their upper and lower bounds. The summary of the algorithm's coefficients and parameters can be found in Table 2-3 (Hadka and Reed, 2013), where L stands for the number of decision variables, is the dimension of the hyperbox in the objective space, and $\sigma_\eta, \sigma_\epsilon,$ and σ_ζ are the variance parameters that regulate the spatial distribution of the offspring produced by the PCX and UNDX operators.

Table 2-3. Default values of the parameters used in Borg MOEA (Hadka and Reed, 2013)

Parameter	Value	Parameter	Value
Initial population size	100	*SPX parents*	10
Tournament selection size	2	*SPX offspring*	2
Epsilon, ϵ	0.01	*SPX epsilon*	2.0
SBX rate	1.0	*UNDX parents*	10
SBX distribution index	15.0	*UNDX offspring*	2
DE crossover rate	1.0	*UNDX* σ_ξ	0.5
DE step size	3.0	*UNDX* σ_η	$0.35\sqrt{L}$
PCX parents	10	*UM rate*	1/L
PCX offspring	2	*PM rate*	1/L
PCX σ_η	0.1	*PM distribution index*	20
PCX σ_ζ	0.1		

Based on how many solutions made using each recombination operator have been uploaded to the elite archive, the chance of any recombination operator being chosen is updated throughout the run (Hadka and Reed, 2013).

Generally speaking, any optimization problems mainly have two parts, objective and constraint functions. The objective and constraint functions might be either explicit or implicit, linear or non-linear. When a response function is evaluated, for instance, through a numerical simulation,

implicit functions are frequently present. Using this method has the benefit of needing fewer trials to determine the actual optimal response compared to the simulation approach or the one-variable-at-a-time method. However, this method has a downside in that the consecutive vertices of the procedure must be chosen based on a set of rules. Additionally, a comprehensive knowledge of mathematics is required to use this technique (Mythili et al., 2013; Venter, 2010).

2.8. Concluding Remark

According to van der Vat (2015), operating reservoirs must strike a balance between competing needs from downstream water consumers, agriculture, energy, and flood management. It is therefore critical to identify the most promising strategy in a situation with various stakeholders and multiple objectives. To better understand the demands between different stakeholders, many conceptual modeling approaches are being used in integrated water resource management. However, due to the dynamic nature of hydrology, the administration and management of a system in charge of storing a valuable commodity will always be a subject of research and possible progress. As a result, hydrological modeling of a river basin, as well as the compilation of the relevant data, are required to better manipulate the output of the basin to facilitate decision-making about water resource management. However, the presence of various parties in a river basin with competing objectives adds extra problems that may hinder the most beneficial solutions.

To solve the multiobjective dilemma, the literature study in this chapter has focused mainly on hydrological modeling together with various hydroeconomic models. Hydrological models attempt to simulate and estimate streamflow at a desired location using appropriate methodologies. Hydroeconomic models, on the other hand, convert the idea of fixed demand into the economic worth of water as determined by water rights by fusing engineering and economic principles. Despite a thorough investigation of economic valuations being completed, management strategies

and policy knowledge are unfortunately less likely to be easily described by a hydroeconomic objective function. Collectively, these studies show how, as an alternative to the traditional hydroeconomic model, it is imperative to explicitly apply the priority set by the policy on water resource distribution. As a result, incorporating the cutting-edge multiobjective evolutionary algorithm (Borg MOEA) technique into the hydroeconomic model can result in a more reliable, easy, and intelligible means of achieving transparent water distribution based on policy knowledge.

Previous studies were unable to model the Omo Gibe River basin's water management challenges in depth to tackle the freshwater scarcity problem. Several studies in this basin are mainly concerned with boosting the output of cascade hydropower (Elias et al., 2015; Gebresenbet, 2016; Mengistu, 2019). The availability of sustainable water in this river basin will be extensively investigated in the current investigation in light of the issues associated with water scarcity. When considering the development of the basin, it is crucial to acknowledge the opposing goals that must be reconciled. Moreover, the variations in streamflow that transpire throughout the year in the research area will be factored into the decision-making process. The competing water necessities, such as producing hydroelectric power, controlling flood hazards, facilitating farming and business irrigation, and ensuring ecological preservation, will be scrutinized to determine the optimal compromises.

3. Description of Study Area, Data and Quality Analysis

3.1. Introduction

The Omo Gibe River Basin has the third-highest potential for runoff volume (16.6 km^3) in the nation, after the Abbay (54.8 km^3) and Baro-Akobo (23.6 km^3) River Basins (Awulachew et al., 2007). This basin, which ranks second only to Abbay in terms of hydropower development potential, accounts for the majority of Ethiopia's current hydropower-generating expansion. The basin in southwest Ethiopia lies between $4^0$30' to $9^0$00' N latitude and $35^0$00' to $38^0$00'E longitude (Figure 3-1) and drains the humid Shewan highlands into the hot and dry Lower Omo Valley, where it forms a biodiverse delta and flows into Lake Turkana on the Ethiopia-Kenya border. The Omo Gibe River basin has traditionally been a pastoral area where nomadic indigenous tribes move on a regular basis in response to the availability of water and food, which is regulated by the river's monsoonal flows. Seasonal climate fluctuations are linked to the oscillation of the Intertropical Convergence Zone (ITCZ), a low-pressure convergence zone. The main rainy season begins when southwesterly winds flow across Ethiopia's southwest highlands. From September to November, the ITCZ passes through southern Ethiopia in a northerly direction and in a southerly direction from March to May. However, the installation of dams for hydropower generation and the expansion of irrigable agriculture in the basin are altering the historical flow pattern generated by these monsoonal rains (Woodroofe, 1996).

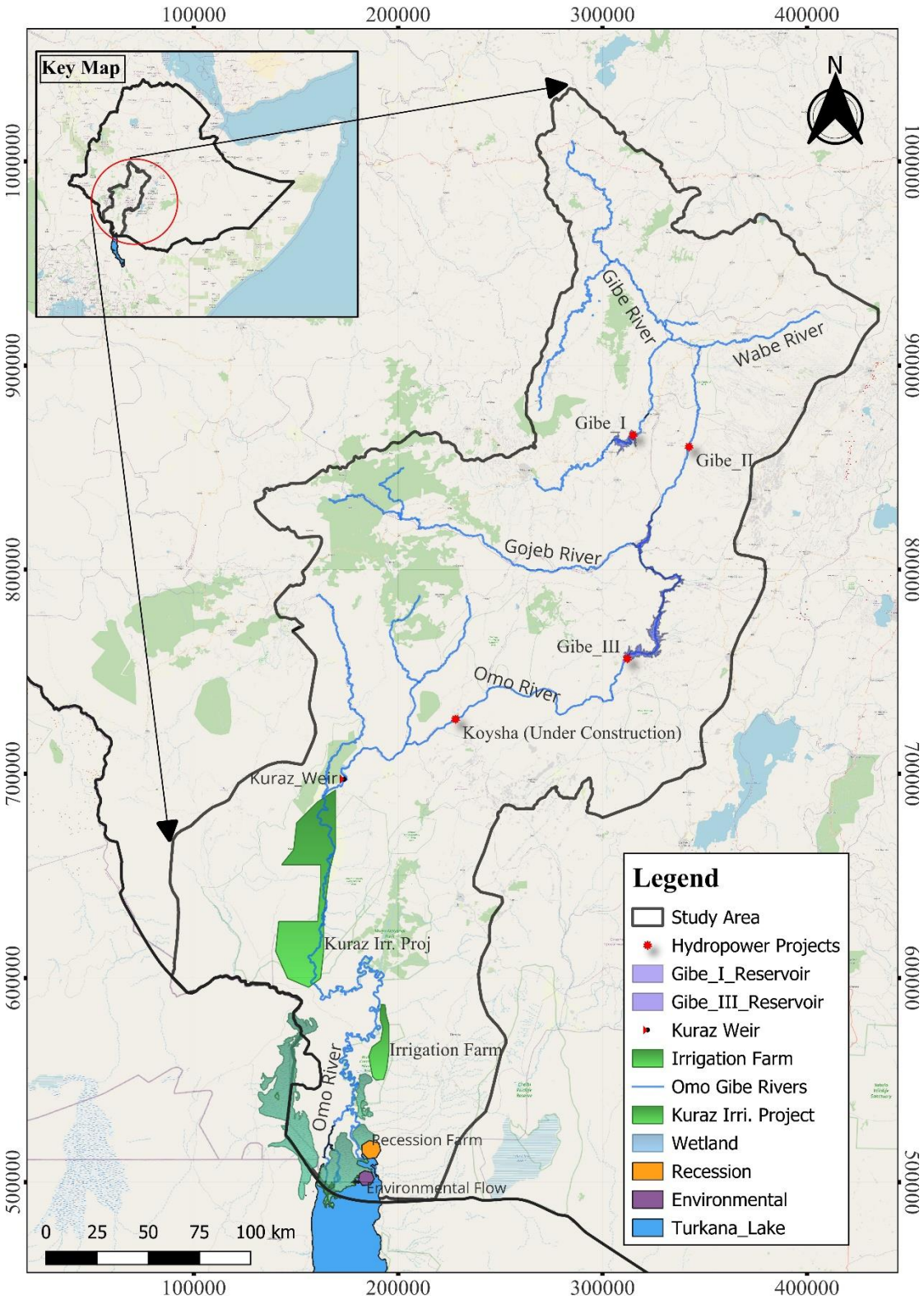

Figure 3.1. Study area location together with its major socioeconomic developments: the Omo-Gibe River Basin, Ethiopia.

3.2. Topography

The basin is roughly divided into two halves: highlands in the north and lowlands in the south. Almost every other element of the basin reflects this divide. The northern highlands are profoundly cut and drained by the Gibe and Gojeb river systems, which merge to produce the Omo in a deep valley. The highlands have steep slopes with dissected hills, while the lowlands have generally mild and undulating slopes. The highland portions of Mount Ghuge have an elevation of 3625 m asl, while the lowland regions have an elevation of up to 235 m asl. Figure 3 -2 illustrates the topography of the Omo Gibe River basin and the main river. However, the elevation range from the DEM is 3844 – 305 m. The discrepancy in elevation could be due to datum and resolution discrepancies between the former and the latter referred DEM. The Ethiopian Ministry of Water and Energy is the source of 30x30 m resolution DEM. The highlands have steep slopes and dissected hills, as opposed to the lowlands, which have gentler and more undulating slopes. Additionally, the Omo Gibe River has a total length of approximately 1,200 km, with an average slope of 3.1 m/km (Woodroofe, 1996).

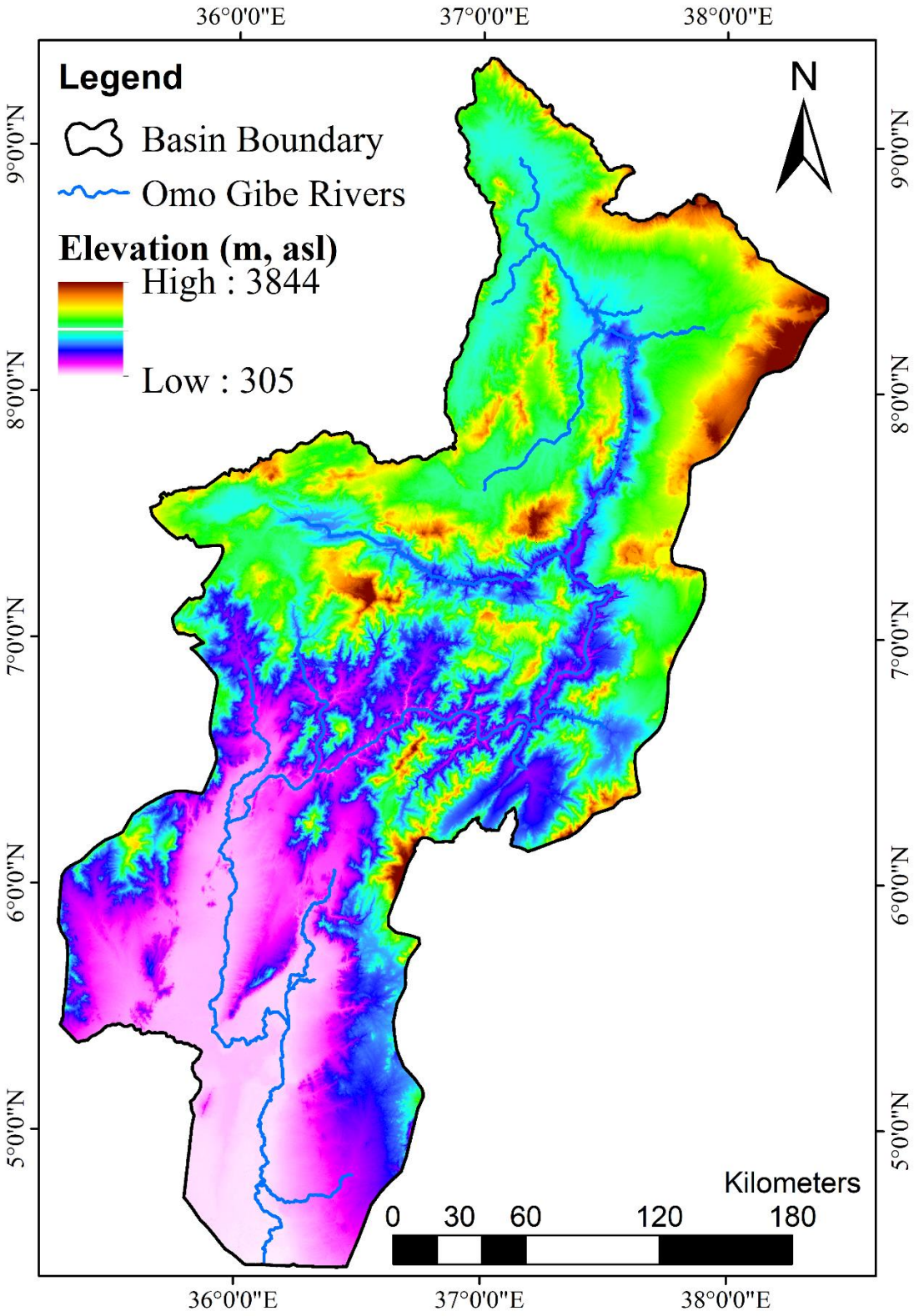

Figure 3.2. The topography of the Omo Gibe River basin and main river representation

3.3. Land Use/Land Cover

In the Omo-Gibe Basin, the majority of the northern catchments are heavily cultivated and under rising land pressure. The only remaining deforested regions are those that are too steep and difficult to farm. The flatter, worse-drained bottom lands of the northern catchments are typically not farmed but instead are used for eucalyptus tree plantations and dry-season grazing. While the eastern portion of the basin contains some of the most densely populated and intensively farmed areas in the nation, the main gorges of the basin are relatively unpopulated and support a cover of open woodland and bushland with grasses. The human density is lower and the amount of natural vegetation is higher in the south of the basin (Daniel, 2011; Woodroofe, 1996).

The distribution of land use land cover (LULC) and the types, SWAT codes, and area coverage of LULC taken into consideration in the current study of the Omo Gibe River basin are shown in Figure 3-3 and Table 3-1, respectively. The Water and Land Resources Centre at Addis Ababa University is the source of 30x30 m resolution LULC data.

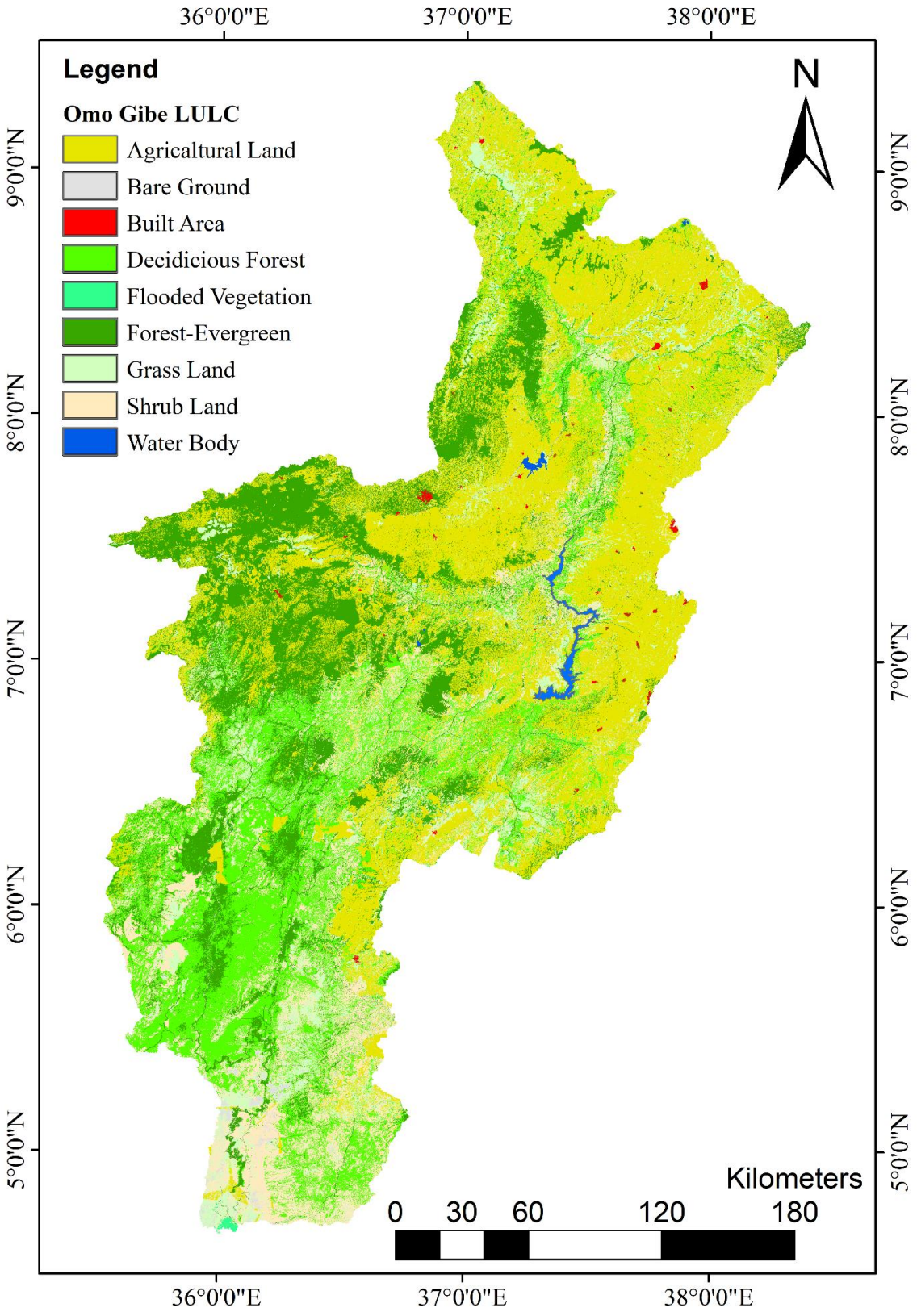

Figure 3.3. Land use land cover distribution of the Omo Gibe River basin

Table 3-1. Characteristics of the Omo Gibe River Basin Land Use Land Cover.

S.No.	LULC Type	SWAT Code	Area (Km^2)	Area (%)
1	Forest-Evergreen	FRSE	14059.55	19.64
2	Decidicious Forest	FRST	14317.29	20.00
3	Shrub Land	RNGB	9961.07	13.92
4	Agricaltural Land	AGRL	26124.28	36.50
5	Grass Land	RNGE	6182.08	8.64
6	Bare Ground	BARR	660.75	0.92
7	Flooded Vegetation	WETL	54.33	0.08
8	Water Body	WATR	80.82	0.11
9	Built Area	URBN	129.24	0.18

3.4. Soils

The deep to extremely deep red and reddish-brown clay loam overlying clays are the predominant soil types in the highland regions, and they are well drained. In contrast, the valley bottoms have less permeable soils with poor drainage. Humic nitisol (27.4%) and humic alisol (18.1%) are the two most common soil types in the basin. The deep, very variable soils of the basin are variable both laterally and vertically. Sandy soils that range from shallow to deep and are infertile predominate at higher elevations to the east (Woodroofe, 1996).

Soil textural and physicochemical properties such as bulk density, organic carbon content, hydraulic conductivity, soil texture, and soil texture for unique strata of each type of soil are included in the soil data. The majority of the soil data utilized in this study to investigate the hydrological modeling of the Omo Gibe River basin were extracted from the United Nations Food

and Agriculture Organization, FAO Digital Map of the World (https://data.apps.fao.org/map/catalog/srv/eng/catalog.search#/home, accessed on 21 May 2022) (Nachtergaele et al., 2010).

The distribution of soil and the types, SWAT codes, and area coverage of soil taken into consideration in the current study of the Omo Gibe River basin are shown in Figure 3-4 and Table 3-2, respectively.

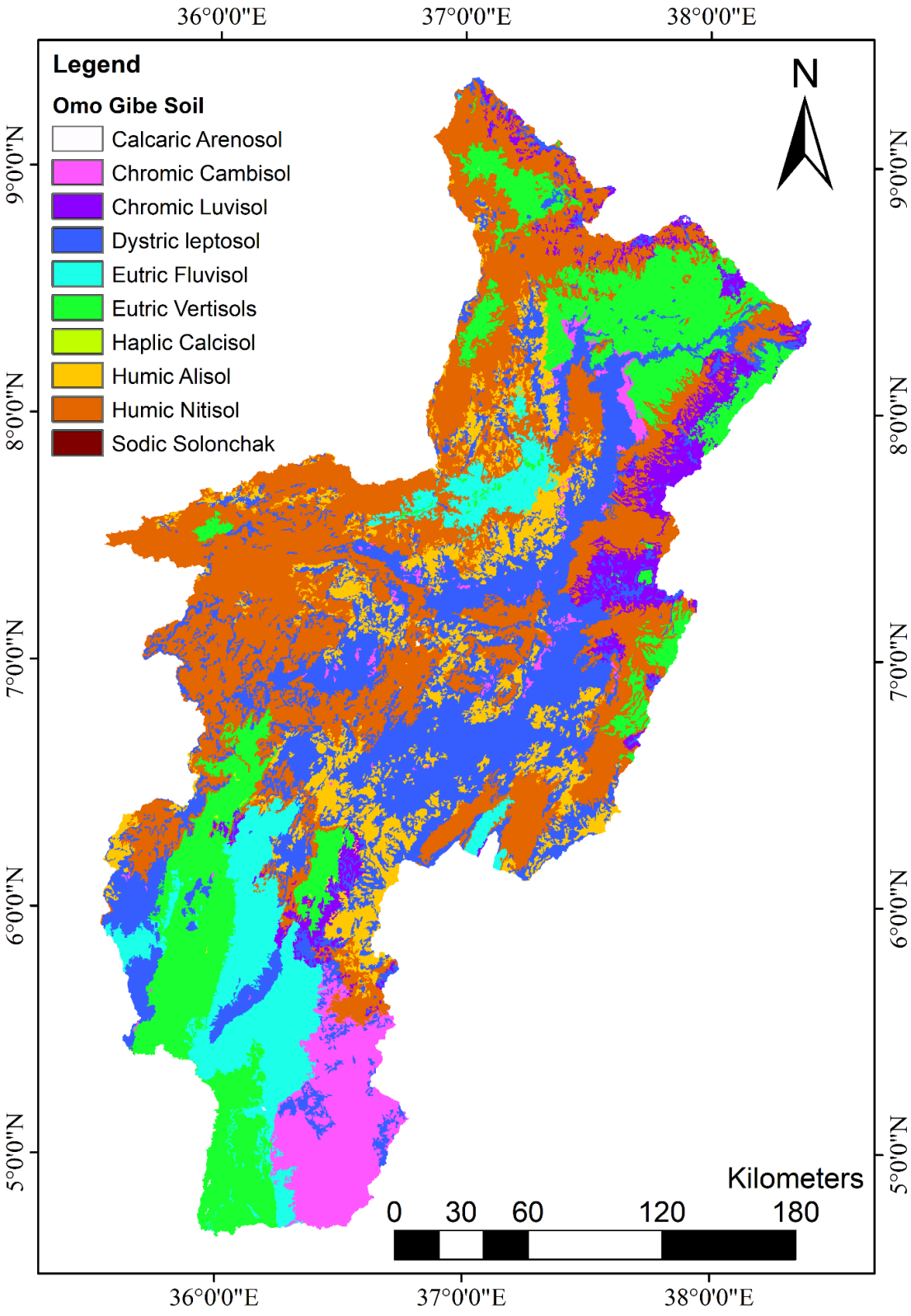

Figure 3.4. Soil type distribution of the Omo Gibe River basin

Table 3-2. Soil Characteristics of the Omo Gibe River Basin.

S.No.	Soil Type	SWAT Code	Area (Km^2)	Area (%)
1	Eutric Fluvisol	FLe	6005.57	8.39
2	Eutric Vertisols	VRe	11817.26	16.51
3	Humic Nitisol	NTu	23310.23	32.58
4	Chromic Cambisol	CMx	3967.62	5.54
5	Humic Alisol	ALu	6017.08	8.41
6	Chromic Luvisol	LVx	3048.93	4.26
7	Calcaric Arenosol	ARc	5.22	0.01
8	Sodic Solonchak	SCm	0.51	0.00
9	Dystric Leptosol	LPd	17362.97	24.26
10	Haplic Calcisol	FRh	22.12	0.03

3.5. Climate

The Omo Gibe River Basin is divided into three distinct climate zones that correspond to the country's classification of climate zones: Kolla (hot zone), Weyna-Dega (temperate zone), and Dega (cool zone). The hills surrounding Jima, as well as the headwaters of the Gojeb River, have a tropical humid climate. This is correct because the majority of the watershed is classified as tropical subhumid - a climate classification that lies midway between tropical humid and hot. The remainder of the floodplain's southernmost part, which faces Lake Turkana, has a hot, arid climate. Seasonal fluctuations in climate are caused by the Intertropical Convergence Zone (ITCZ) oscillation. When the ITCZ flows over southern Ethiopia from September to November in one

direction and southward from March to May in the other, a wet season (from June to September) and a dry season (from December to April) alternate each year. During the rainy season, strong precipitation is produced in the area by the action of Atlantic equatorial westerlies and southerly winds from the Indian Ocean, owing mostly to the Atlantic moisture component. During the dry season, moist air from the Gulf of Aden and the Indian Ocean blows in, causing light rainfall. Because the Atlantic Ocean is the main source of moist air from the southwest, the eastern parts of the highlands are rain shadowed. The highest rainfall occurs to the northwest of Jima (outside of the Omo Gibe River Basin). Rainfall falls precipitously in the basin's lowest southern reaches (Gebresenbet, 2016; Mohammed, 2014; Woodroofe, 1996).

As one moves south through the lowland plains of the Omo River to an elevation as low as 300 m asl near Lake Turkana, the temperature rises and the amount of rainfall decreases. The average daily temperatures in the delta region, where the majority of recession farming is practiced, hover at approximately 30 °C, with summertime maximums exceeding 40 °C (EEPCO, 2009). Figure 3-5 displays the location of the gauging stations for both climate and streamflow of the study area.

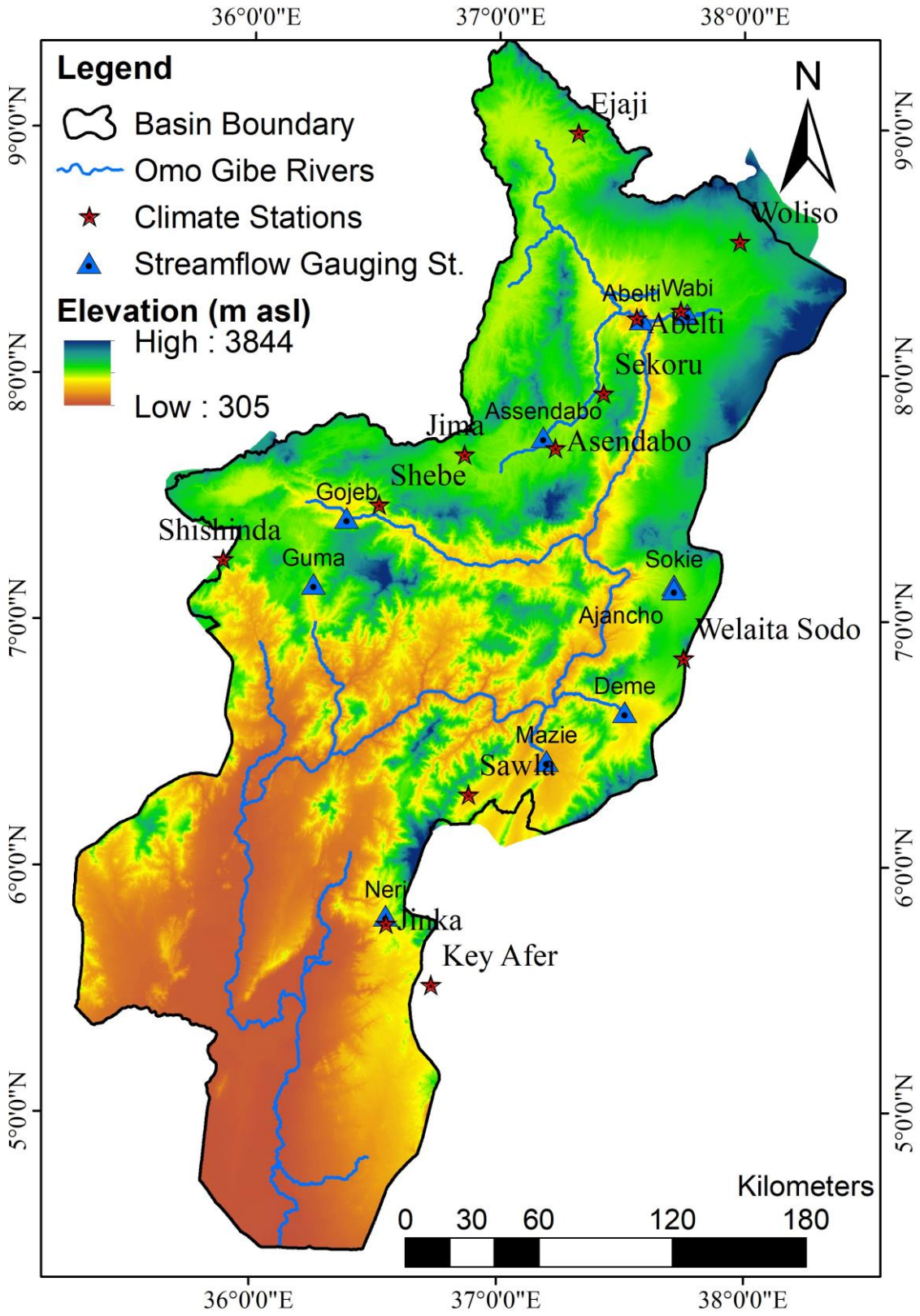

Figure 3.5. Locations of climate and streamflow gauging stations

3.6. Rainfall

The Omo-Gibe Basin experiences a dry season from October to May and a wet season from June to September. January has the least amount of rainfall (Worku et al., 2014). The basin is divided into three separate rainfall regimes based on rainfall distribution patterns. The middle eastern region experiences bimodal rainfall, the northeastern region has asymmetric bimodal rainfall, and the western mountain slopes experience a substantially flattened unimodal profile (Awulachew et al., 2007).

The annual rainfall within the Omo Gibe catchment decreases from north to south and with its decrease in elevation. As seen from Figure 3-6, it varies from a minimum of 1,200 mm in the lowlands to a maximum of approximately 1,900 mm in the highland areas (EEPCO, 2009). The average annual rainfall calculated over the entire basin is 1,426 mm, with a mean annual temperature of 20.4 °C. Seventy-five to 80% of the annual rainfall occurs during a five-month period from May to September (EEPCO, 2009). In the current study, out of the analysed rainfall over the years (1989-2020), the mean yearly precipitation ranges from approximately 1700 mm (Shebe Station) in the basin's northern and western regions to approximately 1400 mm (Sawula Station) below its lower middle. Furthermore, in another study, the mean annual rainfall decreased rapidly southward to less than 300 mm toward Lake Turkana (Woodroofe, 1996).

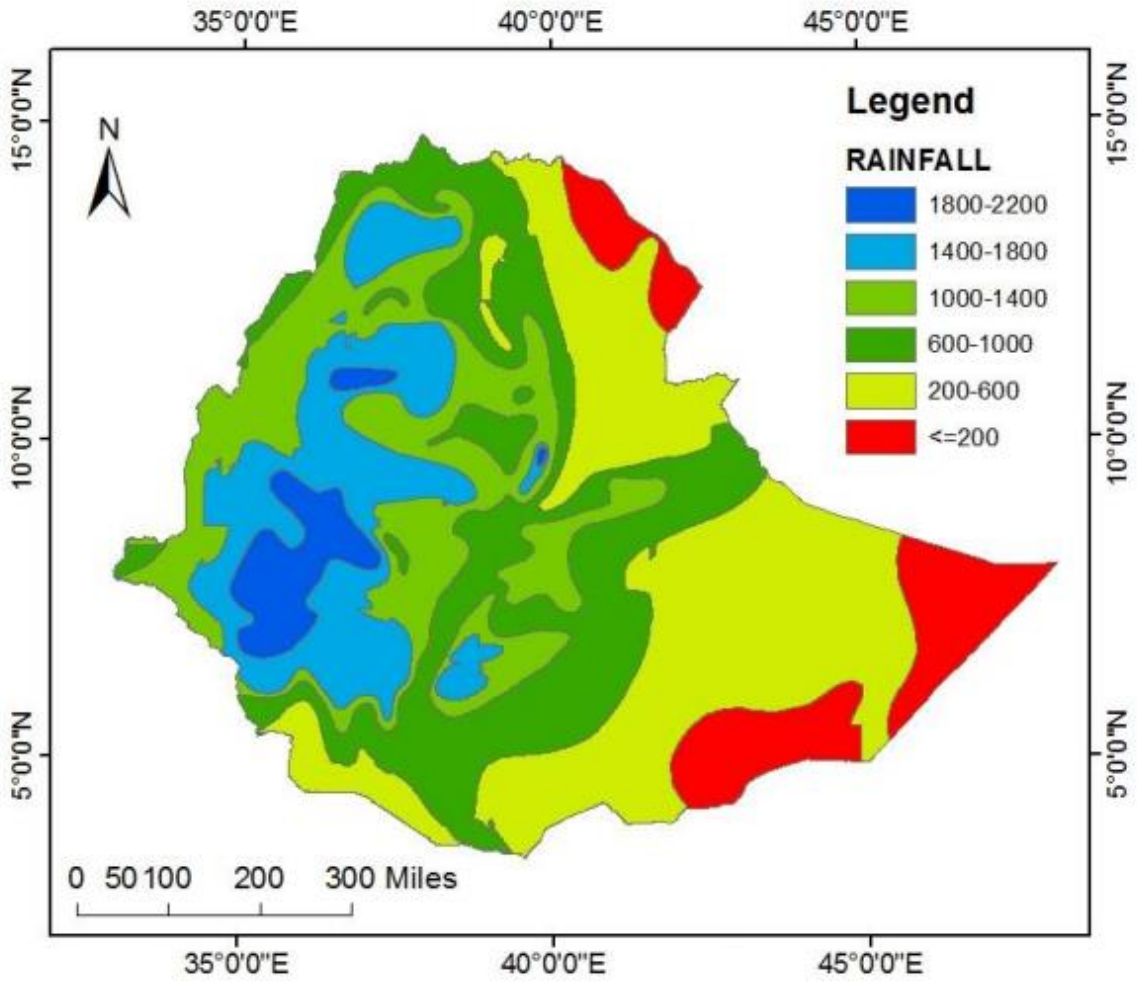

Figure 3.6. Rainfall distribution in Ethiopia (EEPCO, 2009).

3.7. Data Description and Quality Analysis

3.7.1. Data description

Before beginning any research project or data processing, it is necessary to perform a thorough search for the data. As a result, the primary goal of the study was to gather appropriate information and data on the subject. This section defines and discusses the many types of data needed for the study, as well as their sources and analysis. Furthermore, before beginning the analysis and modeling of hydrological and meteorological data, it is necessary to ensure that the data are homogeneous, correct, sufficient, and complete, with no missing data. Data mistakes produced by

poor recording, station relocation, and processing are problematic because they create confusing and unclear results that may contradict the reality of the simulated outcome.

Hence, for the modeling process and the evaluation of the basin's water resources, two types of data are necessary. These are physical and spatial data. DEMs, land use/cover maps, soil maps, and watershed area maps are examples of spatial data that can be displayed in GIS. Hydrological (streamflow) data, meteorological (rainfall, temperature, relative humidity, wind, and solar radiation), land use/cover, and soil-specific data comprise physical information. The SWAT model requires rainfall, temperature, relative humidity, wind, and solar radiation at the daily time step as input variables. The flow data used for calibration and validation at each subbasin outlet, on the other hand, can be daily, monthly, or yearly.

3.7.2. Meteorological Data

The meteorological record durations used in this study range from 29 to 37 years (see Table A-1 in Appendix A). In the upper portion of the basin, in particular, there are a number of operational rainfall stations with reasonably long time series data. Only the stations specified in Table A-1 that are relevant to this investigation are gathered and examined. The National Meteorological Service Agency contributed meteorological data for this study, as well as a description of the selected stations.

3.7.2.1. Missing data filling

For a variety of reasons, climate monitoring stations may have partial records; as a result, the gaps should be filled systematically. To fill in the missing precipitation data, the kriging technique, a cutting-edge technology that leverages data from multiple nearby stations, was applied. These adjacent stations are located nearby and evenly spaced around the spot where the missing data are

requested. A more detailed description and analysis can be found in the following chapter (Chapter 4).

Figure 3.7 depicts the average monthly precipitation for a few selected river basin sites. The graphic demonstrates that the basin has three distinct rainfall patterns, which are supported by previous research (Awulachew et al., 2007; Mohammed, 2014; Woodroofe, 1996). The first category contains Ejiji and Woliso, which are located to the north and northeast of the basin, respectively, where rainfall is substantial and seasonal, with particularly high amounts in July and August, indicating a unimodal distribution. Shishinda and Wolaita Sodo are in the second group, where the seasonal influence is less pronounced and rainfall is more or less continuous from April to September, generating a trapezoidal pattern. The third group, which includes Jinka and Key Afer, is located near the basin's southern end and has a bimodal rainfall pattern, with a high rainfall in April and a low rainfall in October. The shift of the ITCZ is responsible for this variation.

The artificial neural network (ANN) approach, a cutting-edge technology that uses data from a station's historical data via a train-test split method, was utilized to fill in the missing temperature data. The prophet model, an additive forecasting model for univariate time series datasets that uses the ANN technique, is implemented in Python code. After systematic visual inspection and elimination of any potential outliers, the model runs. The concerned station is then populated at the appointed time and location. (*Note: In this situation, stations with up to 20% missing hydro-climate data are chosen and passed through the missing data filling process within the study region*). Appendix A provides a more detailed explanation and analysis.

Figure 3-8 depicts the monthly mean maximum (average daily maximum) and minimum (average of daily minima) values of the basin's representative stations in the upper, middle, and lower parts. The minimum temperature (approximately 13 °C most of the year) varies little, except for Key

Afer which is (approximately 17 °C most of the year), but the maximum temperature decreases dramatically in the upper section of the basin between July and August. The mean annual temperature in the basin likewise varies from approximately 16 °C in the highlands to the north to more than 23 °C in the south, following the temperature-elevation relationship.

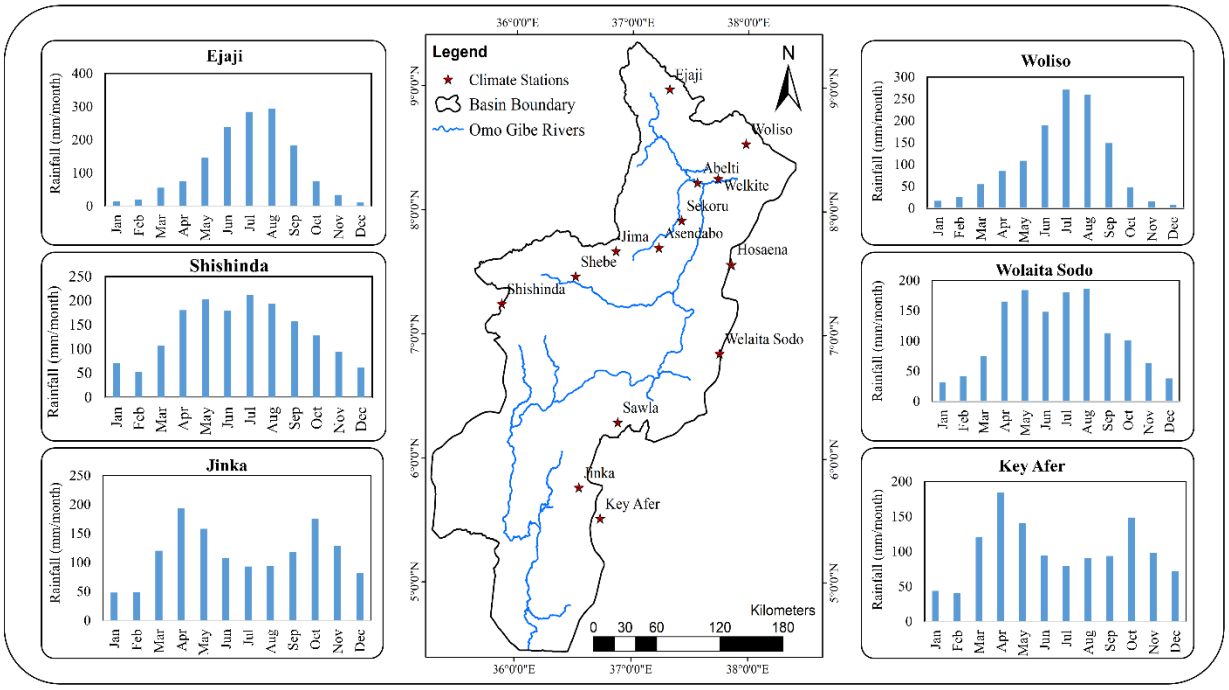

Figure 3.7. The upper, middle, and lower regions of the Omo Gibe River basin's mean monthly rainfall histogram (1989-2020) for typical meteorological stations.

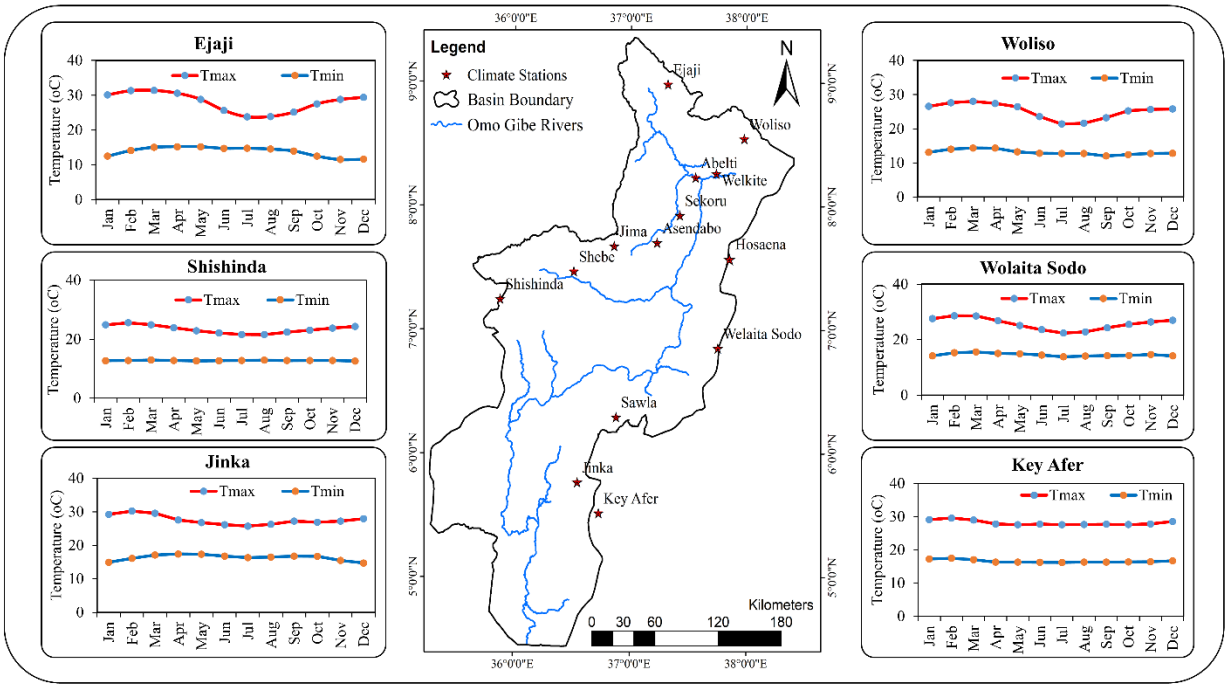

Figure 3.8. The upper, middle, and lower regions of the Omo Gibe River basin's mean monthly maximum and minimum temperature plots (1989-2020) for typical meteorological stations.

3.7.2.2. Consistency and homogeneity check

Inconsistencies in rainfall data from the station might appear if the conditions pertinent to its recording had changed significantly over the course of the recording period. This disagreement would become obvious as soon as the significant change was implemented (Gao et al., 2017). The double mass curve method is used to check a record for consistency. The technique is used to update records to adjust for nonrepresentative variables such as geographical changes or rain gauge exposure. The gauge in question's cumulative total is compared to a typical cumulative total sample of nearby gauges. If there is a clear shift in the curve's regime, it must be corrected. The current study needed no extra changes because the research sites remained consistent throughout.

3.7.3. Hydrological (Streamflow) Data

The Hydrology Department of the Ministry of Water and Energy analyses and archives data from gauge stations in the Omo Gibe River basin. The hydrological station records lengths considered

in this study range from 15 to 45 years (see Table B-1 in Appendix B). The Abelti station on the Gibe River has the longest record, dating back to 1963.

A similar notion, the prophet model, was also implemented in Python programming to fill in the gaps in a streamflow's missing data. Following a comprehensive visual inspection and the removal of any potential outliers, the model is performed. The suspected station is then filled at the specified time and location. (*Note: In this situation, stations with up to 20% missing hydro-climate data are chosen and passed through the missing data filling process within the study region*).

Figure 3-9 depicts the seasonal variation of daily raw streamflow data at the Abelti gauging station in comparison with model-predicted values. As seen in the graphic, the model captures the majority of the data distribution while predicting its prediction estimations. Appendix B contains a more detailed justification and analysis.

However, the majority of the river basin's streamflow measuring stations are located far from the Omo Gibe River. Only the Abelti streamflow gauging station has a long-term record in the basin, and it also covers a greater drainage area (15,764 km^2 out of 79,000 km^2). Furthermore, no data beyond 2008 are available for this station. The remaining streamflow monitoring sites have short streamflow records and cover a relatively small catchment area. In addition, the recorded data at these stations are inconsistent and these streamflow measuring sites are dispersed across the river basin (see Figure 3-5). Because water resource development is based on streamflow potential in a river basin, a thorough understanding of these stream flows can provide a broader perspective on the sustainability of infrastructure that may be established there. As a result, current infrastructure developments in this river basin are mainly dependent on regionalization approaches, particularly the catchments of Abelti, Wabi, and Gojeb. These catchments, in fact, cover only approximately 27% of the Omo Gibe River basin. This is due to the basin's lack of reliable recorded streamflow

data. The potential of the regionalization approach in creating streamflow at a specific site is significant for such poorly gauged data. A comprehensive overview and analysis of cutting-edge regionalization strategies are provided in Chapter 5. Furthermore, the current research proposes a novel reliability-weighted regionalization strategy that surpasses the three most generally used regionalization techniques.

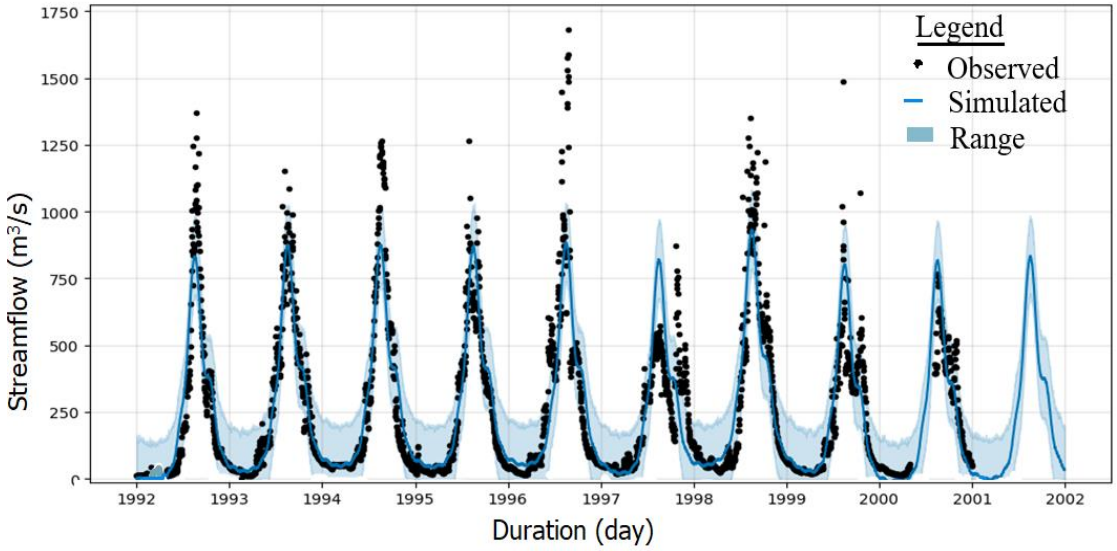

Figure 3.9. Seasonal variation of raw streamflow data with forecasted values at the Abelti gauging station

4. Choosing an interpolation approach to cover deficient climate data in the sparsely gauged Omo-Gibe River Basin, Ethiopia[ፎ]

Abstract

The management of water resources in a region, basin, and subbasin is strongly reliant on the collection of climate data. Rainfall is prominent climatic data, yet it is not found where it is needed for a variety of reasons. It's crucial to find suitable rainfall interpolation algorithms (RIAs) to reduce hydrological prediction uncertainty. However, the selection of a reliable RIA in areas with limited data is not well-researched. This study compares deterministic (inverse distance weighting) and geostatistical (ordinary kriging and ordinary co-kriging) techniques in the data-scarce Omo-Gibe River Basin, Ethiopia. The basin has significant political, economic, ecological, and hydrological importance for Ethiopia and Kenya. Four well-known error statistics, the Pearson correlation coefficient, and the cross-validation method were used to evaluate the candidate algorithms' prediction performance. The results show that for the spatial interpolation of rainfall, geostatistical approaches performed better than deterministic methods. The study recommends using ordinary kriging to estimate rainfall distribution within the Omo-Gibe River basin. This method has the lowest prediction error when compared to observed and estimated monthly rainfall and reduces uncertainty in input data for hydrological predictions in areas with limited data.

Keywords: Rainfall; Uncertainty; Inverse Distance Weighting; Ordinary Kriging; Co-Kriging, Cross-Validation.

ፎ

Bahru M. Gebeyehu, Asie K. Jabir, Getachew Tegegne, and Assefa M. Melesse (2023). Choosing an interpolation approach to cover deficient climate data in the sparsely gauged Omo-Gibe River Basin, Ethiopia. 2023 International Conference on Nile Basin and the Sudd Wetlands: Climate Change Adaptability and Suitability presented on March 20-21, 2023 at Florida International University, USA.

4.1. Introduction

Precipitation is one of the most essential climate variables. It is generally known that hydrological forecasting is highly dependent on precipitation. However, precipitation statistics are typically only accessible at specific sites, which may not accurately represent the spatial variability of a study region. Furthermore, acquiring spatially continuous data for a wide range of locations, such as mountainous and deep coastal regions, is difficult and expensive, especially in data-scarce regions. Thus, spatial interpolation techniques are required to generate a continuous (or predictive) surface from sampled point values (Wang et al., 2014). As a result, the accurate estimation of precipitation in ungauged/sparsely gauged areas using existing rainfall station data is critical for a range of applications such as natural resource management, agriculture management, ecosystem modelling, and hydrological modelling (Ashiq et al., 2010). Several rainfall interpolation algorithms (RIAs) have been created and used in climate studies over the last several decades (Aalijahan and Khosravichenar, 2021; Ashiq et al., 2010; Hu et al., 2019; Ly et al., 2013; Makhmudova and Makhmudov, 2021; Zhang et al., 2014), and finding the most suitable precipitation interpolation method remains a search objective for many places (Ly et al., 2011; Matos et al., 2014; Zhang et al., 2014).

Several studies have been conducted to compare the commonly used RIAs in various places throughout the world to reduce the hydrological prediction uncertainty associated with the input data. For example, among the extensively utilized methodologies in Iran, Zeinivand (2015) offered the Thiessen polygons method for precipitation interpolation: Thiessen polygons, inverse distance weighting (IDW), and universal kriging. İçağa and Emin (2018) evaluated three spatial interpolation approaches for monthly precipitation prediction in Turkey: inverse distance weighting, simple kriging (SK), and co-kriging (CK); their results revealed that SK outperformed

the other two methods. Furthermore, Adhikary et al. (2016) found that the ordinary kriging (OK) approach with genetic programming outperformed the artificial neural network (ANN) in capturing precipitation spatial variability in their investigation in Victoria, Australia. In addition, Wang et al. (2014) investigated the robust interpolation algorithm among IDW, radial basis functions (RBF), global polynomial interpolation (GPI), OK, local polynomial interpolation (LPI), and universal kriging (UK) to generate a spatial distribution of annual precipitation in Ontario, Canada, and recommended the LPI for the region.

According to the literature, the effectiveness of various interpolation methods in predicting precipitation vary greatly depending on the research region, underscoring the need to individually test such methods for different regions. Furthermore, little study has been conducted on RIA identification in data-scarce regions. It is crucial to recognize that there is no consensus on the best approach for interpolating precipitation, and the only way to determine which method is optimal for a given situation is to compare the accuracy of their predictions (da Silva et al., 2019; Hofstra et al., 2008; Kurniawan et al., 2019; Ly et al., 2013; Sun et al., 2009). Additionally, it is crucial to look at the more suitable RIA in areas with a lack of data, such as Ethiopia's Omo-Gibe basin, to increase the quality of the input data used for the hydrological forecast. To our knowledge, however, no prior study has examined the robust spatial RIA in the study region. Therefore, in order to close this gap, this study tested one deterministic and two geostatistical RIAs to determine which interpolation technique was optimal for adding missing precipitation to the study region.

4.2. Materials and Methods

4.2.1. Study Area and Data Description

The Omo-Gibe River basin is one of Ethiopia's most important river basins, with three hydroelectric dams—Gibe I, Gibe II, and Gibe III—as well as a portion of the irrigation project

developed. Furthermore, a potential additional dam project for the area downstream of Koysha is being investigated, which is currently being constructed as a fourth dam in the river basin in addition to the Kuraz irrigation project, which might further improve Ethiopia's socioeconomic activity. Because a thorough description can be found in Chapter 3, this section has been deleted for brevity and to eliminate redundancy.

4.2.2. Methods

This study investigated three distinct interpolation strategies to represent the spatial variability of rainfall in the Omo-Gibe River Basin. Two forms of RIAs are used: deterministic models (inverse distance weighting) and geostatistical models (ordinary kriging and ordinary co-kriging). The data are processed using 'Spatial Analyst' (Geo-statistical Analyst Tool, ArcGIS version 10.4), an ArcGIS component.

4.2.2.1. Inverse distance weighting (IDW)

In the IDW approach, the value of one point is more closely correlated with neighbouring points than with points further away (Chang, 2006). The general equation of the approach is addressed in Equation (4.1) below:

$$Z_0 = \frac{\sum_{i=1}^{n} Z_i \frac{1}{d_i^k}}{\sum_{i=1}^{n} \frac{1}{d_i^k}} \quad (4.1)$$

where the parameters are described as

Z_o = estimated value at point o,

Z_i = value of Z at point i,

d_i = distance between points i and o,

n = number of points used in the estimate, and

k = specified power that controls the degree of local impact.

4.2.2.2. Kriging Method

Kriging is a robust statistical interpolation technique that, unlike deterministic approaches, can offer unbiased forecasts with little fluctuation while taking spatial and statistical correlations between observed sites into account (Oliver and Webster, 2014; Wang et al., 2014). Kriging is distinct from other interpolation techniques in that it can quantify the degree of inaccuracy that occurs during value prediction. It may generate a variety of output surfaces, such as probabilities, forecasts, and predictions with standard errors (Johnston et al., 2001). The kriging method employs a semivariogram to measure the spatially linked component or spatial self-correlation. The kriging equation (Bhattacharjee et al., 2013) is expressed in Equation (4.2) below:

$$\hat{Z}(x_o) - \mu = \sum_{i=1}^{N} \omega_i [Z(x_i) - \mu(x_o)] \quad (4.2)$$

The parameters in Equation (4.2) are described as follows:

$\hat{Z}(x_0)$ = estimated random field value at point x_0,

μ = mean value treated as constant over the entire region of interest,

ω_i = weight assigned to the ith interpolating point, and

$Z(x_i)$ = measured attribute value at a point (x_i)

If the dataset has a spatial dependence, the points of contact closest to one another must have a smaller semivariance than more distant locations. OK, UK, and SK are the Kriging methods that are built-in functions within the ArcGIS Geostatistical Wizard. The difference between OK and SK is that the assumption of stationarity, which expects the mean and distribution to stay constant throughout the region. SK makes use of this assumption, while OK does not, and rather recalculates the suggest throughout the modelled vicinity through a transferring search radius. However, the mean of some spatial data cannot be assumed to be constant generally but varies, since it also absolutely depends on the location of the sample. On the other hand, the UK is a multivariate

extension of OK with a trend (Hengl, 2009), and it makes use of a linear or higher deterministic fashion characteristic $\mu(x_i)$ instead of a regular trend μ. In this study, OK is going to be used due to its acceptance and widespread usage of the method. For the utilization of these kriging techniques, the dataset should be normalized, or it should be nearly normally distributed so that this strategy can give the best estimate with the lowest error coefficient (Aalijahan and Khosravichenar, 2021).

4.2.2.3. Co-kriging Method

Co-kriging is a multivariate version of kriging that estimates the main variable using the spatial correlation between the primary variable (precipitation) and an auxiliary variable (here the heights of the gauging stations). To reduce prediction variance, this cokriging technique employs a record of one or more secondary variables in addition to the main variable (Giraldo et al., 2020). In this study, the ordinary cokriging (OCK) approach is utilized, which is similar to the Kriging method. In cokriging, in addition to generating the semi-variograms of the primary and secondary variables, the cross semivariogram, which expresses the spatial correlation between those two variables, must be calculated. The cokriging equation (İmamoğlu and Sertel, 2016) (Equation (4.3)) is as follows:

$$Z*(x_i) = \sum_{i=1}^{N} \lambda_i Z(x_i) \sum_{k=1}^{N} \lambda_k U(x_k) \quad (4.3)$$

Definitions of the parameters in equation (4.3) are:

λ_i = weight of the primary Z variable at x_i,

λ_k = weight of the U auxiliary variable at x_k, and

$U(x_k)$ = observed value of the x_k auxiliary variable.

4.2.2.4. Cross-validation of the candidate interpolation algorithms

The performances of the candidate RIAs are investigated using cross-validation approaches (Deutsch and Journel, 1992; Haylock et al., 2008; Refaeilzadeh et al., 2009) through the following procedure: 1) the rainfall amount is estimated for every observation point using each candidate

interpolation algorithm, 2) the estimated value is compared with the observed value, and 3) finally, the model with the least error is regarded as the superior model. In cross-validation, each measured point is sequentially omitted, and therefore the value is anticipated by way of the usage of the remainder of the dataset. The difference between each measurement and the respective predicted value is the error. Cross-validation can also be used to select the simplest possible modelling settings for the respective method (e.g., search radius, power option, kernel parameter) (Ohmer et al., 2017). There are various ways to compare estimated and observed values, and the most important ones include the mean error (ME), mean square error (MSE), root mean square error (RMSE), and root mean square standardized error (RMSSE) (Deutsch and Journel, 1992; Goovaerts, 2000; Sun et al., 2009). The equations to calculate ME (Equation (4.4)), MSE (Equation (4.5)), RMSE (Equation (4.6)), and RMSSE (Equation (4.7)) are given below:

$$ME = \frac{1}{n}\sum_{i=1}^{n}\left(z(x_i) - \hat{z}(x_i)\right) \tag{4.4}$$

$$MSE = \frac{1}{n}\sum_{i=1}^{n}\left(z(x_i) - \hat{z}(x_i)\right)^2 \tag{4.5}$$

$$RMSE = \sqrt{\frac{1}{n}\sum_{i=1}^{n}\left(z(x_i) - \hat{z}(x_i)\right)^2} \tag{4.6}$$

$$RMSSE = \sqrt{\frac{1}{n}\sum_{i=1}^{n}\left(\frac{z(x_i) - \hat{z}(x_i)}{\sigma_i}\right)^2} \tag{4.7}$$

Definitions of the parameters in Equation (4.4) – Equation (4.7) are:
$z(x_i)$ = observed value,
$\hat{z}(x_i)$ = estimated value, and
n = number of sites.

To assess the success of these error statistic measures, ME, MSE, and RMSE values close to 0, and RMSSE values close to 1 imply higher interpolation performance (Johnston et al., 2001). As a result, for ME, MSE, and RMSE error statistic measures, the lower the value with respect to each

interpolation method will be taken into account in the analysis. The same is true for RMSSE, however, the one that approaches 1 is considered to have better interpolation performance.

4.3. Results

4.3.1. Performance of Interpolation Methods

The performance results of the candidate RIAs are presented in Table 4-1. IDW, OK, and OCK all have MEs of 25%, 42%, and 33%, respectively. Conversely, the RMSEs of 8%, 58%, and 34% are found with IDW, OK, and OCK respectively. The performance comparison based on Pearson's correlation coefficient, R resulted in 17%, 50%, and 33% of IDW, OK, and OCK, respectively. In addition, the two statistical measurement errors, mean square error (MSE) and root mean square standardized error (RMSSE) also produced 58% and 42%, and 67% and 33% of OK and OCK, respectively. The distribution of error statistics along with adopted interpolation methods are shown in Figure 4-1 (A - E). The graphs in the figure show the plots of error statistic methods and values of the selected RIAs with the corresponding months. It is proven in Figure 4-1 (A) that in most months, IDW results in higher values of ME, whereas OK and OCK have seemingly similar trends together with lower error values. In terms of RMSE, Figure 4-1 (B), IDW scores higher values in the months between the 5^{th} and 9^{th} while outside this range all show some lower values and have most likely have the same trend. Graphs in Figure 4-1 (C and D) compare RMSE and MSE measurement error statistics of the two geostatistical RIAs of OK and OCK. As demonstrated in Figure 4-1 (C), most of the time OK performs better regarding RMSE than OCK. In this respect, the better the performance with respect to RMSE between the two methods is the one that approaches to 1 more from both sides. In another instance, the measure of the performance against MSE in Figure 4-1 (D) revealed that OCK slightly outperformed OK on average over time. The last statistical error measurement parameter of this study is R. Figure 4-1 (E) depicts the

distribution of performance measures against R. Except for February and March, IDW perform poorly compared to the other two methods.

Table 4-1: Interpolation Methods: inverse distance weighting (IDW); ordinary kriging; ordinary cokriging; and validation Methods: mean error (ME); root mean standard error (RMSE); mean standard error (MSE), root mean square standardized error (RMSSE), and Pearson's Coefficient (R) per month.

Month	ME			RMSE			MSE			RMSSE			R		
	IDW	OK	OCK	IDW	OK	OCK	IDW	OK	OCK	IDW	OK	OCK	IDW	OK	OCK
1	4.138	1.553	**0.295**	35.810	**31.197**	38.397	-	0.041	**0.014**	-	**0.940**	1.077	0.238	0.501	**0.777**
2	1.914	0.514	**0.366**	**17.958**	18.285	19.072	-	0.022	**0.012**	-	**0.988**	1.058	**0.397**	0.301	0.225
3	2.598	**0.264**	0.341	30.166	29.205	**27.351**	-	**0.005**	**0.005**	-	1.097	**1.039**	**0.254**	0.224	0.136
4	9.412	**2.878**	3.143	64.088	**59.592**	64.850	-	0.024	**0.026**	-	0.910	**0.956**	0.649	**0.699**	0.630
5	1.803	1.831	**0.797**	62.006	**61.635**	62.551	-	0.018	**0.007**	-	**0.941**	0.851	0.677	**0.682**	0.673
6	0.955	**0.419**	3.860	65.488	61.040	**58.160**	-	**0.005**	0.052	-	**0.868**	0.785	0.685	0.733	**0.770**
7	0.586	**0.277**	0.485	68.089	62.399	**58.568**	-	**0.002**	0.005	-	**0.998**	1.060	0.683	0.739	**0.776**
8	**1.229**	3.046	2.093	78.685	**72.947**	73.866	-	0.032	**0.030**	-	**0.933**	1.103	0.739	**0.780**	0.777
9	3.218	**0.506**	0.906	51.858	**50.901**	51.289	-	**0.010**	0.011	-	1.040	**1.003**	0.612	**0.631**	0.625
10	0.532	0.906	**0.040**	36.209	35.429	**34.384**	-	0.024	**0.001**	-	**0.939**	0.907	0.153	0.189	**0.309**
11	3.414	**0.311**	0.673	42.472	**39.170**	41.814	-	**0.007**	0.014	-	0.880	**1.031**	0.721	**0.767**	0.733
12	**0.158**	0.259	0.350	22.668	**22.130**	22.345	-	**0.005**	0.009	-	**1.022**	0.951	0.697	**0.714**	0.708

Note: Numbers with bold and underlined are the lowest in terms of measurement statistical errors, whereas with respect to Pearson's correlation coefficient, R the highest value of each month.

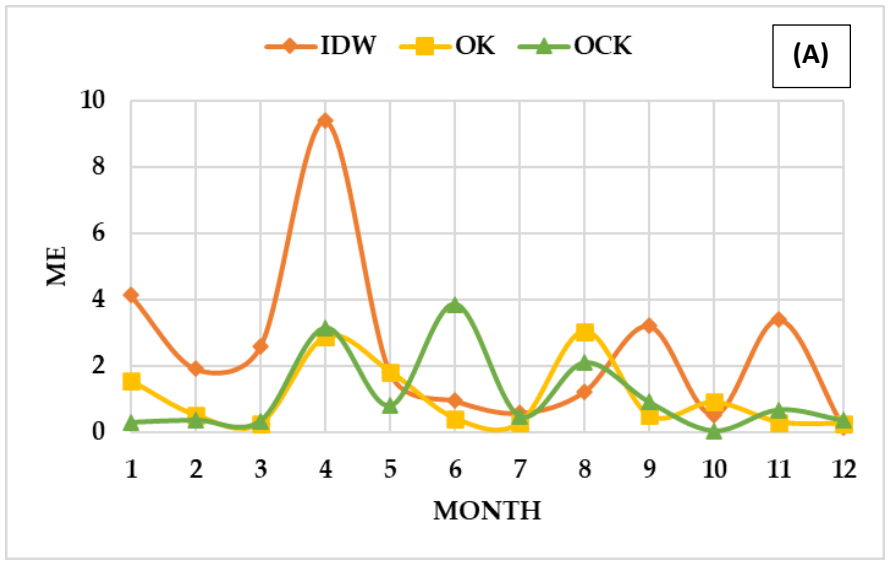
IDW
OK
OCK
(A)
ME
MONTH
0
2
4
6
8
10
1 2 3 4 5 6 7 8 9 10 11 12

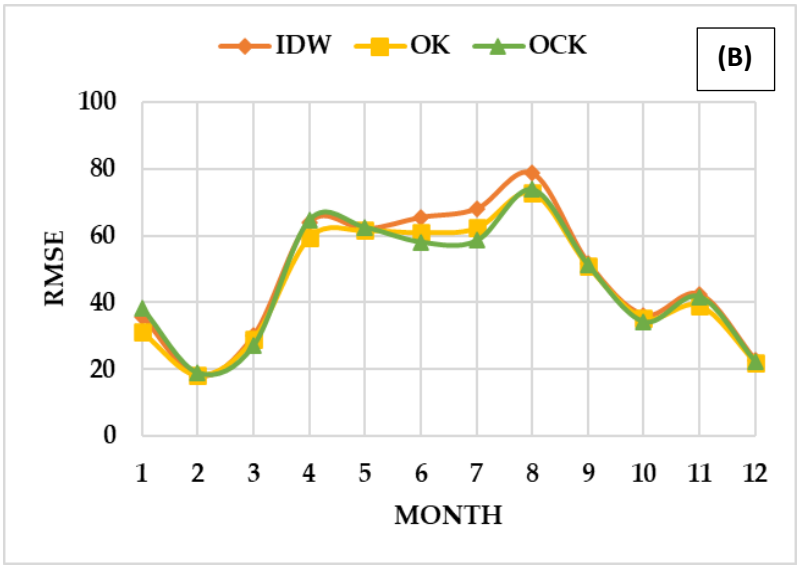
IDW
OK
OCK
(B)
RMSE
MONTH
0
20
40
60
80
100
1 2 3 4 5 6 7 8 9 10 11 12

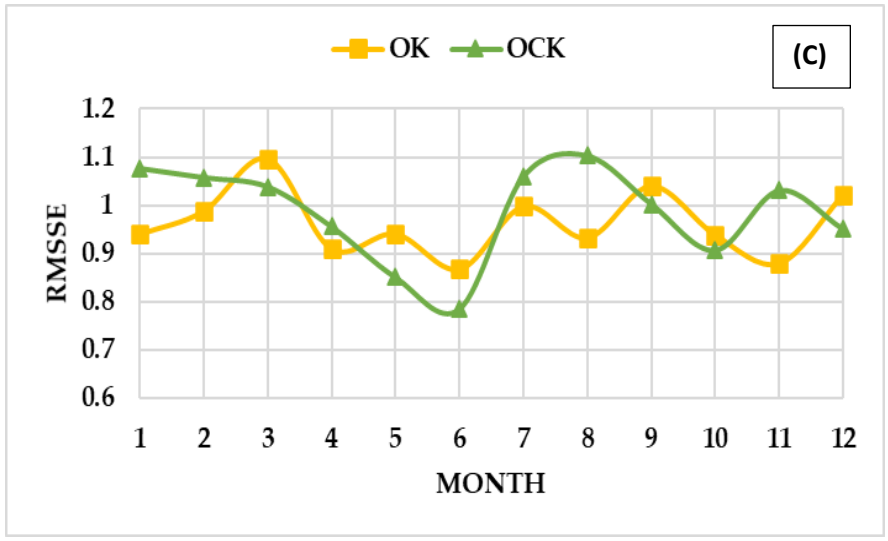
OK
OCK
(C)
RMSSE
MONTH
0.6
0.7
0.8
0.9
1
1.1
1.2
1 2 3 4 5 6 7 8 9 10 11 12

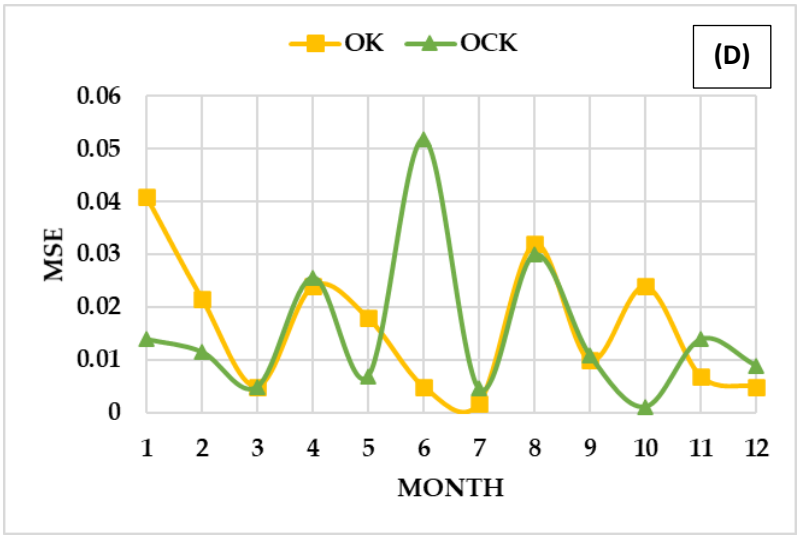
OK
OCK
(D)
MSE
MONTH
0
0.01
0.02
0.03
0.04
0.05
0.06
1 2 3 4 5 6 7 8 9 10 11 12

Continued…

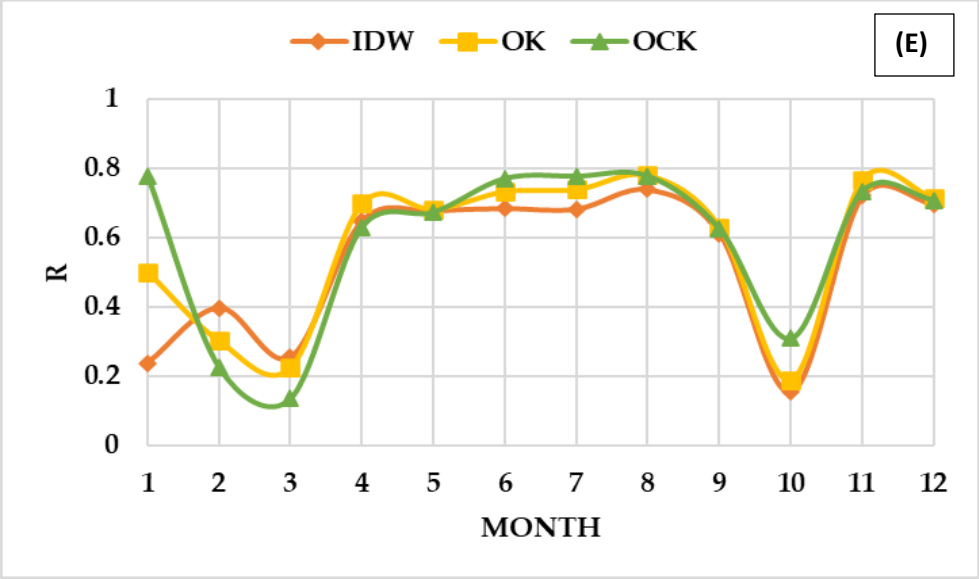

Figure 4.1. The distribution of error statistics: (A), mean error (ME); (B), root mean standard error (RMSE); (C), root mean square standardized error (RMSSE), (D), mean standard error (MSE), and (E), Pearson's Correlation Coefficient (R) per selected month a year with respect to Interpolation Methods: inverse distance weighting (IDW); ordinary kriging (OK); ordinary cokriging (OCK).

However, OCK seemingly has higher R values most of the time. The plot of OK on the other hand demonstrates average values between the two methods except for April and November under which it outperforms the other.

4.3.2. Cross-validation results

This study used ME, RMSE, MSE, and RMSSE to find the optimal interpolation method among the aforementioned approaches with common measurement error. Table 4-1 displays the cross-validation findings for all methods based on measurement error and Pearson's correlation coefficient, R values. In the table, the mean prediction error is as close to 0 as feasible, and the standard errors are correct, as evidenced by a root-mean-square standardized prediction error close to 1 (Adhikary et al., 2016; Johnston et al., 2001). The same holds true for larger magnitude R

values, which perform better. Hence, OK produces the best results for interpolating monthly precipitation in the research area (see Table 4-1 and Figure 4-1).

4.3.3. Rainfall Spatial Variability

Figure 4-2 displays the spatially interpolated monthly precipitation in the research region for selected months of the year. Based on long-term monthly average values, the basin's precipitation distribution is divided into three areas: northern and north west, which has a high rainfall magnitude reaching a yearly average of 1900 mm, southern lowland which has an average annual rainfall of 400 mm, and the north-east and along the western part of the basin which falls between the two extremes. The three-rainfall area covering the basin has distinct characteristics. As it progresses from north to south, the rainfall distribution displays unimodal (Wolkite), trapezoidal (Bonga), and bimodal (Jinka) patterns. Rainfall usually begins in March and lasts until October for those with unimodal and trapezoidal patterns. The peak of the trapezoidal rainfall distribution occurs from April to September, whereas the peak of the unimodal rainfall distribution occurs in August. Those with a bimodal pattern, on the other hand, have their greatest value between April and October. This outcome is also consistent with past research findings (EEPCO, 2009; Woodroofe, 1996).

Figure 4-2 (A, B, and C) depicts the rainfall distribution chosen for the comparison scenarios of the three interpolation algorithms for April 2004 spatial data points in the river basin. Similarly, Figure 4-2 (D) displays the rainfall distribution for August 2004 using the best-performing ordinary kriging model.

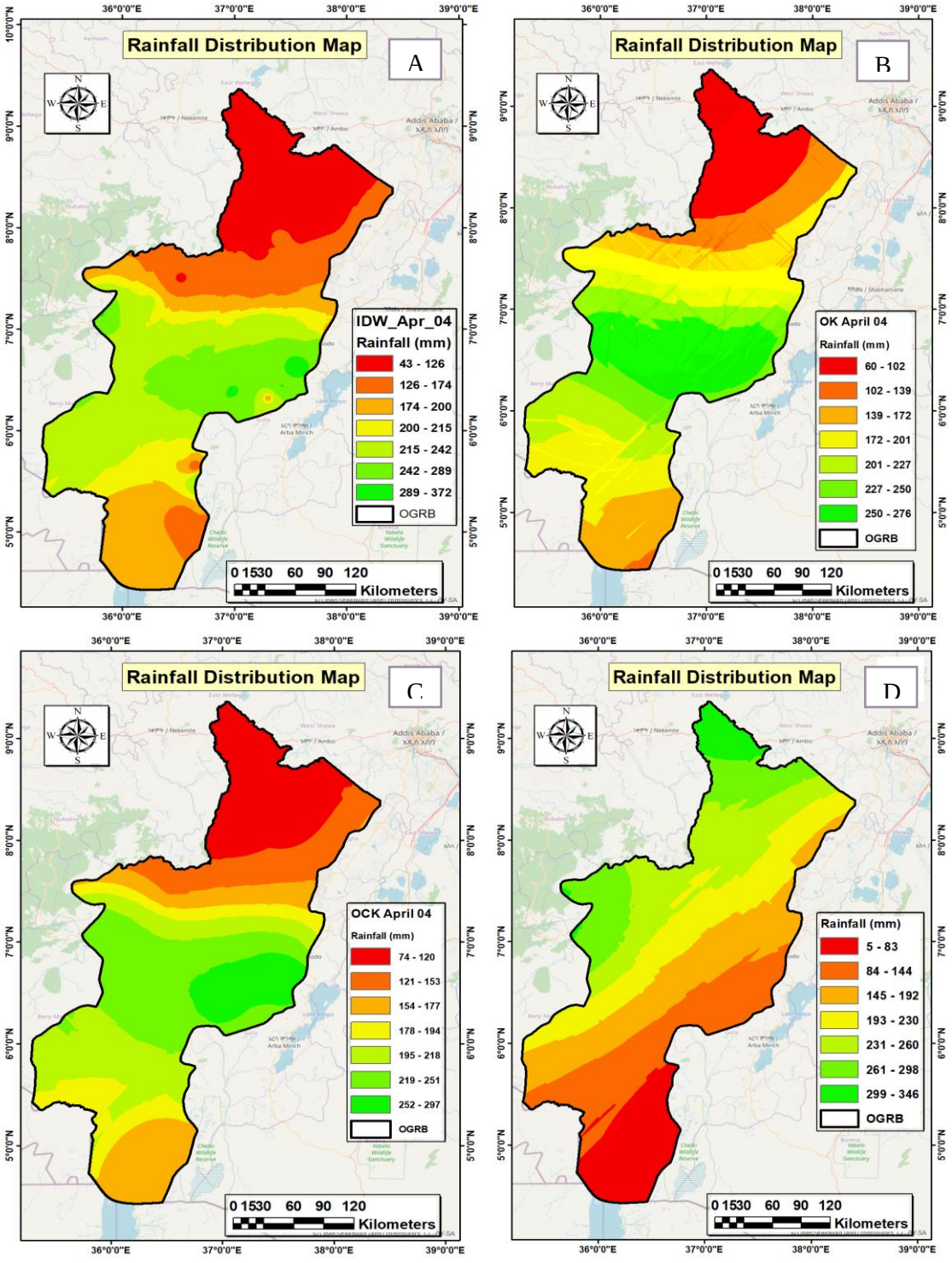

Figure 4.2. Samples of Spatial Rainfall Distribution Maps of IDW, OK, and OCK (Figures A, B, and C) for April 2004 and the best-performed interpolation method of OK (Figure D) for August 2004 of the river basin.

A time series graph of the observed (raw) and estimated (filled) values for the dry and wet seasons (January and August) at Sawula station is given in Figure 4-3.

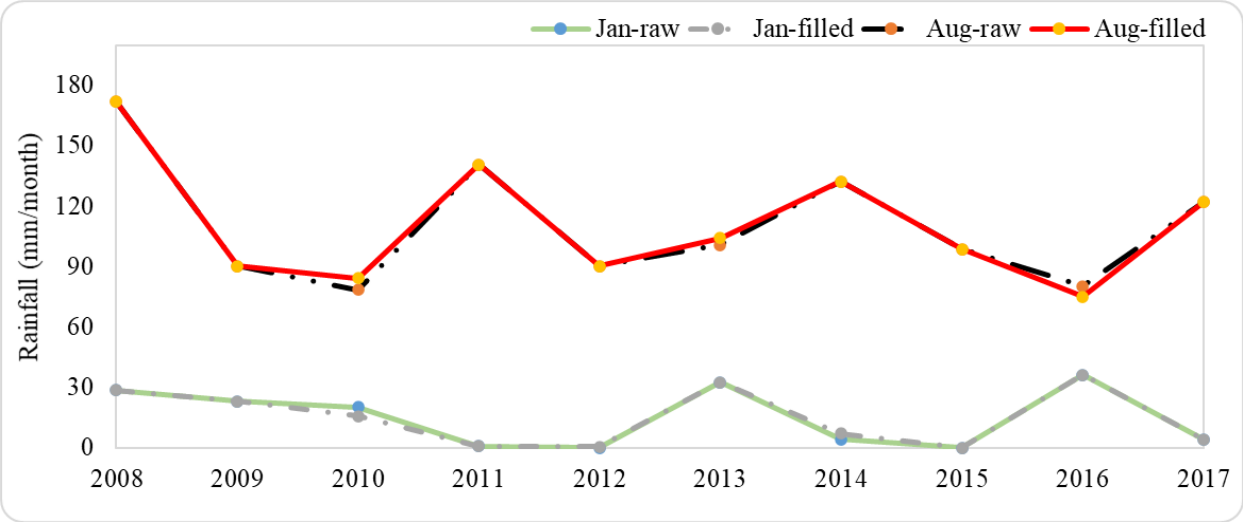

Figure 4.3. Time series graph of Sawula station's observed and estimated values for January and August months (dry and wet seasons, respectively).

4.4. Discussion

Table 4-1 compares the findings of the analysis for the three analysed spatial interpolation methods. Ordinary kriging had the lowest errors with ME and MSE of 42% and 58%, respectively, and the highest R-value of 50%, and overall, with an average measurement error value of ranked first of all methods, it delivered the most correct interpolation findings for the Omo-Gibe River Basin.

In general, kriging and cokriging produced more accurate results than the other techniques in most regions, as there is no model that can be definitively picked as the best one for all regions. Despite some research describing IDW as the quality approach (Blanco et al., 2017; Hodam et al., 2017), many researchers emphasize the high accuracy of geostatistical methods (Kriging and Co-Kriging) for precipitation estimation, with cokriging often showing the best possible accuracy (Ohmer et al., 2017). Although it was discovered in this study that ordinary kriging outperforms the other two

methods, IDW and OCK, which may be due to the sparsity of spatial data points in the area, other data sources, such as remotely sensed data, can be included in addition to the one used in this study, for further interpolation accuracy and interpretation of the analysed data.

The monthly precipitation map obtained via ordinary kriging in the Omo-Gibe River Basin suggests that the best month-to-month precipitation is concentrated in the mountainous north-western middle and southern parts depending on the mode of distribution pattern, and vice versa for the lowest precipitation amounts. In general, finding an appropriate method for interpolating and estimating precipitation in a given area can have a wide range of applications, mostly due to unique characteristics. On the one hand, accurate precipitation interpolation can be of great assistance to land-use planners in allocating suitable hydropower, agricultural, industrial, tourist, residential, and other uses. On the other hand, accurate precipitation estimates can be very useful and effective in controlling and managing natural and environmental disasters such as floods, droughts, landslides, desertification, and deforestation, which are directly and indirectly related to the amount of precipitation in the region. As a result, precise precipitation interpolation in a region gives decision-makers a complete picture of precipitation circumstances that may be used to successfully develop and manage water resources. Therefore, developing an adequate model for the accurate spatial estimation of precipitation in locations with diverse local weather requirements, such as this study area, which is always in precipitation crisis, is a major issue.

4.5. Conclusions

For problems and research involving water resources, such as hydrological analysis, disaster management, hydropower operation, and agricultural management, the precipitation maps are the most important database. Therefore, developing a reliable interpolation technique to calculate precipitation distribution in areas devoid of synoptic and rain gauge stations is a critical challenge.

To the best of our knowledge, the Omo-Gibe River Basin specifically and all of Ethiopia in general have not yet been tested using any of the three frequently used and popular methods we compared in this work. This study found that of the IDW, OK, and OCK approaches, using the OK methodology to create precipitation interpolation would provide an important foundation for future regional planning and policymaking related to water supply in the Omo-Gibe River Basin. Other locations with comparable hydro-climatological settings can benefit from the robust interpolation method used in this research region.

5. Subbasin Spatial Scale Effects on Hydrological Model Prediction Uncertainty of Extreme Stream Flows in the Omo Gibe River Basin, Ethiopia

Abstract

Quantification of hydrologic model prediction uncertainty for various flow quantiles is of great importance for water resource planning and management. Thus, this study is designed to assess the effect of subbasin spatial scale on the hydrological model prediction uncertainty for different flow quantiles. The Soil Water Assessment Tool (SWAT), a geographic information system (GIS) interfaced hydrological model, was used in this study. Here, the spatial variations within the subbasins of the Omo Gibe River basin in Ethiopia: Abelti, Wabi, and Gecha watersheds from 1989 to 2020 were examined. The results revealed that (1) for the Abelti, Wabi, and Gecha watersheds, SWAT was able to reproduce the observed hydrograph with more than 85%, 82%, and 73% accuracy in terms of the Nash-Sutcliffe efficiency coefficient (NSE), respectively; (2) the variation in the spatial size of the subbasin had no effect on the overall flow simulations. However, the reproduction of the flow quantiles was considerably influenced by the subbasin spatial scales; (3) The coarser subbasin spatial scale resulted in the coverage of most of the observations. However, the finer subbasin spatial scale provided the best simulation closer to the observed stream flow pattern;

Bahru M. Gebeyehu, Asie K. Jabir, Getachew Tegegne, and Assefa M. Melesse (2023). Subbasin Spatial Scale Effects on Hydrological Model Prediction Uncertainty of Extreme Stream Flows in the Omo Gibe River Basin, Ethiopia. Remote Sensing, MDPI. DOI: 10.3390/rs15030611.

(4) the SWAT model performed much better in recreating moist, high, and very-high flows than it did in replicating dry, low, and very-low flows in the studied watersheds; (5) a smaller subbasin spatial scale (towards a distributed model) may better replicate low flows, while a larger subbasin spatial scale (towards a lumped model) enhances high flow replication precision. Thus, it is crucial to investigate the subbasin spatial scale to reproduce the peak and low flows, (6) In this study, the best subbasin spatial scales for peak and low flows were found to be 79–98% and 29–42%, respectively. Hence, it is worthwhile to investigate the proper subbasin spatial scales in reproducing various flow quantiles toward sustainable management of floods and drought.

Keywords: subbasin spatial scale; GIS; parameter uncertainty; flow quantiles; watershed management; parameter sampling distribution; sensitivity rank variation

5.1. Introduction

Hydrological prediction is primarily useful for flood protection and water resource planning (Kibuye et al., 2020). Moreover, understanding water quality, which affects stream flow, chemical concentrations, and the distribution of habitats and animals, necessitates an examination of low flows. Furthermore, the analysis of extreme flows (high and low flows) is of great importance for infrastructure development. As a result, it is critical to pay more attention to the prediction and reproduction of flow quantiles (e.g., high, moist, mid-range, dry, and low flows). Several studies have been developing several types of hydrological models to mimic hydrological processes and water quality (Arnold et al., 2012; Butts et al., 2004; Devia et al., 2015; Gao et al., 2010; Pandi et al., 2021; Refsgaard, 1997).

Both the fully distributed and semidistributed models are able to account for the heterogeneity of a watershed by discretizing catchments into many homogenous units as opposed to lumped models (Carpenter and Georgakakos, 2006; Dal Molin et al., 2020; Veettil et al., 2021). However, fully

distributed models are more data-intensive and have greater processing requirements than the framework for semidistributed hydrological modelling. Due to this advantage, the semidistributed hydrological model is preferred by many researchers in this field for evaluating water resources. A key feature of semidistributed hydrological models is the discretization of the basin into several subbasins. In Soil and Water Assessment Tool (SWAT) modelling, a basin is discretized into smaller subwatersheds based on land use, soil, and slope categorization, and each of these subwatersheds is then further divided into finer hydrological response units (HRUs). The approach used to designate homogeneous units as subbasins or HRUs may thus have an impact on hydrological models' capacity to replicate the frequency and geographical distribution of the information provided. Approaches to SWAT hydrological modelling frequently employ default discretization; however, doing so may make the modelling more uncertain (Tegegne et al., 2019). To make informed decisions about water resource management, hydrological prediction uncertainty must be quantified. Measurement errors in the model's inputs, together with the model's parameters, organizations, and other elements, are among the most significant causes of uncertainty in hydrological predictions (Abbaspour, 2015; Beven, 1993). The input data used in hydrological models are the main source of uncertainties (Butts et al., 2004; Faramarzi et al., 2013; Rozos et al., 2021), and numerous studies have concentrated on quantifying these uncertainties (Abdar et al., 2021; McMillan et al., 2018). However, due to the spatial scale of the model subbasins, relatively few studies have taken into consideration the flaws in the hydrological model while reproducing the various flow quantiles. The SWAT model integrates input variables at the subbasin and HRU levels to estimate basin responses using regionally distributed inputs. As a result, the geographic area throughout which the input data are integrated to form parameters may have an effect on the model output. Temperature and rainfall measurements, both of which contain

equivalent quantities of subbasin-level meteorological data, are examples of data at the subbasin level. When aggregating geographical data at finer resolutions, it is necessary to represent geographic features at the right subbasin sizes, which reduces the number of data units needed to describe the original spatial data by the same number of spaces. Based on the data, it appears that this division has a lower spatial resolution. As the subbasin increases in size, streamflow prediction may be less responsive to variations in rainfall measured at specific stations. Because the aggregation procedure may change the geographical and statistical aspects of the input data, the framework for hydrological modelling obtains a new source of uncertainty. Thus, depending on the geographical subbasin sizes of the input data, the hydrological model's output may differ. The causes of variability in the subbasin are also intimately linked to the geographic size of the subbasin, according to (Arnold et al., 1998). The model's forecast may be exceedingly inaccurate since the magnitude of the subbasin contributes to an anomaly in addition to the measurement error already present in the input data. As a result, it is critical to discretize watersheds in a way that takes into account the variety of soil and land uses, together with the spatial variation in both temperature and rainfall measurements. When subbasin partitioning has properly reflected the variety of the basin, in terms of input data, it is believed that the model predictions will not differ considerably after a specific number of subbasins.

Several studies have attempted to determine the impacts of spatial discretization on the outputs of hydrological models (Blöschl and Sivapalan, 1995; Craig et al., 2020; Kling and Gupta, 2009; Tan et al., 2020; Tegegne et al., 2019; Wood et al., 1988), but the findings are often inconclusive. For instance, Mamillapalli et al. (1996) observed that adding more subbasins improved the SWAT model's accuracy. However, according to Bingner et al. (1997), the size and number of subbasins are not key considerations for calculating runoff in SWAT. The majority of prior investigations

have analysed how subbasin size affects the replication of the entire observed hydrograph, but they have not examined how subbasin spatial scale affects the reproduction of the various flow quantiles. To gain a better understanding of low and high flow behaviour, it is critical to investigate how the subbasin division level influences the formation of the hydrograph's various flow quantiles. Moreover, hydrological modelling prediction may be hampered by the uncertainty related to the subbasin spatial scale in recreating the observed hydrograph. Regarding this, some studies have shown how the spatial scale of a subbasin affects parameter uncertainty (Kumar and Merwade, 2009; Tianqi et al., 2003). When compared to marginally significant parameters, meaningful parameters, for instance, have a very tight range of uncertainty about a variety of watershed configurations, which implies the use of parameter sensitivity analysis to identify the dominant parameters that best capture the system's hydrological response (Kumar and Merwade, 2009). Hence, the level of model uncertainty must be minimized by a thorough analysis of parameter sensitivity (Hamby, 1994; Tegegne and Kim, 2018).

Several methods have been suggested by previous studies to quantify hydrologic model parameter uncertainty (Abbaspour et al., 2007; Coxon et al., 2015; Dwelle et al., 2019; Fan, 2019; Mannina and Viviani, 2010; Smith, 2013; Tegegne and Kim, 2018; Uniyal et al., 2015; Valdez et al., 2022; Wang et al., 2016; Wang et al., 2017). The most commonly used approaches to quantify hydrologic model parameter uncertainty include sequential uncertainty fitting version 2 (SUFI-2) (Abbaspour et al., 2004), generalized likelihood uncertainty estimation (GLUE) (Beven and Binley, 1992), Bayesian recursive estimation technique (Sorenson and Alspach, 1971), generalized polynomial chaos expansion (Xiu and Karniadakis, 2003), shuffled complex evolution metropolis algorithm (Vrugt et al., 2003), and maximum likelihood Bay (Vrugt et al., 2005). SUFI-2 is the most frequently used method for daily and monthly calibration and validation of hydrological

parameters, sensitivity analysis, and uncertainty analysis (Abbaspour et al., 2007). It is straightforward to complete the calibration process within the time limits that can be achieved with SUFI-2's semiautomated design (Uniyal et al., 2015). As a result, this work uses the SUFI-2 method to examine the parameter uncertainty in the hydrological modelling of various flow phases. This study will also assess the uncertainty in hydrological modelling at the subbasin spatial scale for various flow phases. It is well known that the precision of the physical and climatological input data, the state of watershed management, and spatial representation have an impact on the uncertainty of hydrological modelling. This study takes into account three unique watersheds with various spatial sizes to address this issue. However, model uncertainties between the three watersheds are assumed to be constant. Moges et al. (2020) explore this type of model uncertainty in their work.

The organization of this chapter's research is as follows. Section 5.2 describes the Materials and Methods. Sections 5.2.1 and 5.2.2 introduce the research area and data description, respectively. Section 5.2.3 describes the methods employed in the study. Section 5.3 presents the findings of the investigation, while Section 5.4 discusses them. Section 5.5 contains conclusions.

5.2. Materials and Methods

5.2.1. Study Area and Data Description

The Omo Gibe River Basin has the third-highest potential for runoff volume (16.6 km^3) in the nation, after the Abbay (54.8 km^3) and Baro-Akobo (23.6 km^3) River Basins (Awulachew et al., 2007). This basin, which is second only to Abbay in terms of potential for hydropower development, accounts for the majority of the country's current hydropower-generating growth. This section has been deleted for brevity and to prevent repetition because Chapter 3 has more

information. As a result, only a small portion of it—which is pertinent to the topic—is included in this section.

The Abelti, Wabi, and Gecha watersheds, on the other hand, were specifically selected as subbasins of this river basin to explore the change in hydrological modelling parameter uncertainty with watershed management and the validity of input data. The Gecha watershed is located in the basin's reach's southwest corner, although the Abelti and Wabi watersheds are found in the basin's higher reaches (Figure 5-1).

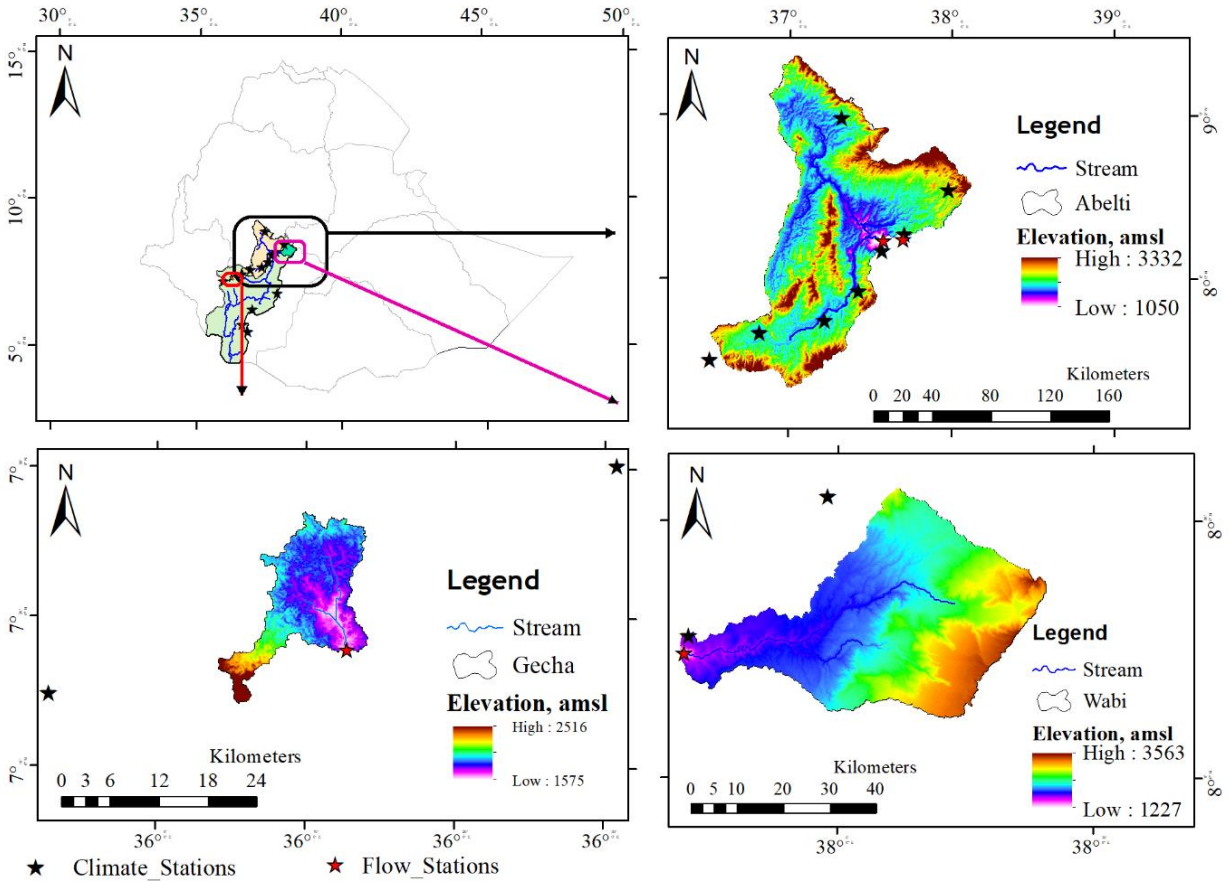

Figure 5.1. The Abelti, Wabi and Gecha watershed's location in the Omo-Gibe River Basin.

5.2.2. Data Description

ArcSWAT requires the following input data: digital elevation model (DEM), land use land cover (LULC), soil map, and weather data. The hydrological department of Ethiopia's Ministry of Water

and Energy provided a 30 m resolution DEM and measured flows of the study watersheds. The Water and Land Resources Centre at Addis Ababa University provided the LULC data. The soil map was created using the United Nations Food and Agricultural Organization's (FAO) Digital Map of the World (https://data.apps.fao.org/map/catalog/srv/eng/catalog.search#/home, accessed on 21 May 2022) and meteorological data received from the Ethiopian meteorological institute. As can be found from their web address, field surveys, remote sensing and other natural data, professional judgement, and laboratory research were used to develop the soil data and its maps. The Abelti watershed (15,746 km^2), the largest gauged subbasin of the Omo Gibe River Basin, has 60.76% agricultural land and a distribution of 9.28% range grass, 3.83% scrub/shrub, 24.67% wooded area, and 3.83% scrub/shrub. Urban space, undeveloped land, and wetlands make up the remaining 1.46%. In this basin's 1866 km^2 Wabi watershed, there are 17.75% wooded regions, 59.26% agricultural areas, 4.34% scrub/shrub areas, 17.39% range grass areas, and other places, including urban areas and barren lands, accounting for 1.28%. Moreover, the Gecha watershed (175 km^2) has 2.64% range grass, 39.82% farms, and 57.60% wood. The Abelti watershed's seven monitoring stations and data from observations made from 1989 to 2020 reveal that the region's yearly mean temperature is 19.98 °C and its yearly average rainfall is 1417 mm, with the summer months experiencing the region's largest rainfall events (June–August). The 15,746 km^2 drainage basin of the Abelti stream gauging station was where the daily streamflow data were collected. Notably, 1050 to 3563 m above the mean sea level is within the research area. Seven, two, and two weather stations were employed for the Abelti, Wabi, and Gecha subbasins, respectively, to collect observed daily weather data during a record period of 32 years (1989–2020). In the Abelti, Wabi, and Gecha subbasins, one weather station corresponds to approximately 2249, 933, and 87 km^2, respectively. Compared to their distributions within themselves, meteorological stations are rather

few in number in the studied area. Additionally, the hydrological studies in the three chosen basins provide essential details on the variations in hydrological processes in basins with a predominance of agricultural use (such as Abelti and Wabi) and forest use (such as Gecha).

5.2.3. Methods

5.2.3.1. The SWAT Model

The uncertainty of the hydrological modelling parameter in the research basin was evaluated using the SWAT model (Arnold et al., 1998; Neitsch et al., 2011). This model was selected to satisfy the study goals due to its broad use and effective execution (Chaemiso et al., 2016; Devia et al., 2015; Hussainzada and Lee, 2021; Jiang et al., 2021; Nguyen et al., 2022; Tegegne et al., 2019; Ullrich and Volk, 2009). The applicability of the SWAT model in the upper Omo Gibe basins, which also include the Abelti and Wabi watersheds in our research, was reported more recently (Nesru et al., 2020). SWAT modelling divides the Abelti, Wabi, and Gecha watersheds into a number of subbasins, which are then discretized into smaller HRUs with a variety of land use, soil, and slope characteristics. Each subsurface basin's runoff is individually calculated and routed to determine the total surface runoff of the drainage basins. The SWAT model requires the following input data types to represent the features of the study basin: meteorological data (i.e., solar radiation, rainfall, wind speed, relative humidity, and temperature), land use, soil, and DEM. Using the equation indicated below, the water balance is computed (Neitsch et al., 2011):

$$SW_t = SW_o + \sum_{i=1}^{t} (R_{day} - Q_{surf} - E_a - W_{seep} - Q_{gw})_i \qquad (5.1)$$

where *SWt* is the final soil water content (in millimetres of water), SW_0 is the soil water content at the start of day *i* (in millimetres of water), and t is the time (in days); R_{day} is the amount of rainfall in millimetres of water for day *i*, Q_{surf} is the amount of surface runoff in millimetres of water for

day *i*, evapotranspiration (E_a) is the quantity of water lost by evaporation throughout day *i*, W_{seep} is the quantity of water, expressed in millimetres of water per day *i*, that enters the vadose zone from the soil profile, and Q_{gw} is the amount of return flow in millimetres of water for day *i* (mm water).

The flow through the channel was routed using the variable storage coefficient approach, and the potential evapotranspiration was calculated using the Penman–Monteith method. The Thiessen polygon method was used to determine the mean area rainfall in the watersheds of Abelti, Wabi, and Gecha. The surface runoff volume was calculated using the modified Soil Conservation Service runoff curve number (SCS-CN). The SCS-CN depends on the permeability of the soil, the type of land use, and the preexisting soil water conditions. In-depth information about the SWAT model is provided by (Neitsch et al., 2011).

5.2.3.2. Parameter Sensitivity

Overparameterization in distributed hydrological models is a well-known and prevalent problem (Beven, 1989; Pokhrel et al., 2008; Seibert et al., 2019). Sensitivity analysis approaches are frequently employed to reduce the number of parameters that must be fitted to input–output data (Malik et al., 2022; Song et al., 2015; Yang et al., 2019). In addition, (Tegegne and Kim, 2018; Tegegne et al., 2019) reported that a particular subset of the original parameters had an effect on streamflow generation using the SWAT model in the Yongdam and Gilgel Abay water-sheds (South Korea and Ethiopia, respectively), indicating the requirement of implementing sensitivity analysis of parameters during calibration. Sensitivity studies are commonly described using the words “local” and “global”. While a global analysis provides sensitivity with respect to a parameter’s whole distribution, a local analysis establishes sensitivity with respect to parameter point estimates. The latter has the benefit that the results from global sensitivity analysis are more

reliable (Abbaspour et al., 2017). The parameters that affect streamflow simulation using SWAT were therefore identified using the global sensitivity analysis approach, which was used in this study's model parameter sensitivity analysis. Therefore, before SWAT model calibration, global sensitivity analysis is conducted to identify the most sensitive parameters. It is based on how each parameter's target function alters on average, as all other parameters do (Tegegne and Kim, 2018). The global sensitivity analysis uses multiple regression to determine each parameter's sensitivity (Abbaspour et al., 2017):

$$g = \alpha + \sum_{i=1}^{n} \beta_i b_i \tag{5.2}$$

where g represents the value of the objective function, α is the regression constant, and β is the parameter coefficient. The statistical properties of t-stat and p value are then used to quantify the relative significance of each parameter b; a higher absolute value of t-stat and a lower p value denotes a more sensitive parameter. The statistics of the parameter sensitivity are obtained using multiple regression. When using the *t*-test, the accuracy with which the regression coefficient is measured is expressed as *t*, where *t* is the coefficient of a parameter divided by its standard error. When a parameter's coefficient is large in relation to its standard error, that parameter may be regarded as sensitive to the simulation. A parameter's t-statistic and the values in the student's t-distribution table can be compared to obtain the *p*-value (available in most statistical handbooks). Each term's *p* value evaluates whether the coefficient is equal to zero, the null hypothesis (no effect). The null hypothesis can be disproved if the *p* value is low (0.05). As a result of the relationship between changes in the predictor value and changes in the response variable, a predictor with a low *p*-value is therefore likely to be a useful addition to the model. On the other hand, a higher *p* value indicates that the predictor is not related to changes in the response, showing that the parameter is not particularly sensitive. A thorough literature search was conducted to determine the 17 (Table 5-1) crucial SWAT model parameters that have the greatest impact on estimates of streamflow in the study area (Cibin et al., 2010;

Dakhlalla and Parajuli, 2019; Narsimlu et al., 2015; Neitsch et al., 2011; Spruill et al., 2000; Tegegne and Kim, 2018; Tegegne et al., 2019).

Table 5-1. SWAT model flow parameters used in the study basin.

Parameter Name with Their Extension	Parameter Descriptions	Unit	Valid Ranges
ALPHA_BF.gw	Baseflow alpha factor	(days)	0–1
ALPHA_BNK.rte	Baseflow alpha factor for bank storage	(-)	0–1
CH_K2.rte	Effective hydraulic conductivity in main channel	(mm/h)	−0.01–500
CH_N2.rte	Manning's "n" value for the main channel	(-)	−0.01–0.3
CN2.mgt (r)	SCS runoff curve number	(-)	−0.2–0.2
ESCO.hru	Soil evaporation compensation factor	(-)	0–1
GW_DELAY.gw	Groundwater delay time	(days)	0–500
GW_REVAP.gw	Groundwater "revap" coefficient	(-)	0.02–0.2
GWQMN.gw	Threshold depth of water in the shallow aquifer	(mmH_2O)	0–500
HRU_SLP.hru	Average slope steepness	(-)	0–1
OV_N.hru	Manning's "n" value for overland flow	(-)	0.01–30
REVAPMN.gw	Threshold depth of water	(mm)	0–500
SLSUBBSN.hru	Average slope length	(-)	10–150
SOL_AWC (..).sol (r)	Available water capacity of the soil layer	(mmH_2O/mm soil)	0–1
SOL_BD (..).sol (r)	Moist bulk density	(g/cm^3)	0.9–2.5
SOL_K (..).sol (r)	Saturated hydraulic conductivity	(mm/h)	0–2000
SURLAG.bsn	Surface runoff lag time	(days)	0.05–24

Note: Parameter names with (r) indicate relative change, whereas the rest of the parameters are replaceable. During the calibration process, parameter limits for each study watershed are maintained.

5.2.3.3. Hydrologic Model Calibration and Validation

To capture the hydrologic phenomenon, the hydrological modelling technique necessitates various working procedures. In this study, the Abelti, Wabi, and Gecha watersheds will be analysed using the SWAT model for the period of 1989 to 2020. Furthermore, to achieve a better hydrologic prediction performance, the observed runoff data of each watershed will be divided into three

distinct parts with different purposes: (1) warmup, (2) calibration, and (3) validation. The values of the parameters in the performed hydrologic simulation will then be determined and validated using these observed runoff data.

For the uncertainty analysis, the SUFI-2 approach (Abbaspour et al., 2007) is employed. It is an inverse optimization tool that uses a global search algorithm and the Latin hypercube sampling methodology to assess the activities of objective functions. Because it allows for variable objective functions while producing appropriate model calibration results, it is a superior modular calibration strategy. This method is connected to the SWAT-CUP calibration package. The model's effectiveness is assessed using Nash-Sutcliffe efficiency (NSE), the most well-liked likelihood function for SUFI-2 in the literature (Gupta et al., 2009; Hosseini and Khaleghi, 2020; Khalid et al., 2016; Malik et al., 2022; Nash and Sutcliffe, 1970).

$$NSE = 1 - \frac{\sum_{i=1}^{n}(O_i - P_i)^2}{\sum_{i=1}^{n}(O_i - \bar{O})^2} \tag{5.3}$$

where P_i, O_i, and $\bar{O}$ represent the simulated, measured, and average values, respectively.

The statistical distribution ranges of the output variables obtained using Latin hypercube sampling for parametric uncertainty replication are set at 2.5% and 97.5%, excluding the worst 5% of calculations (Abbaspour et al., 2015). In this study, we evaluated the agreement between simulation and observational results using the percentage of measurements falling inside the 95% prediction uncertainty (95PPU), the *P*-factor, and the relative width of a 95% probability band, the *R*-factor. Notably, 1 for the *P*-factor and 0 for the *R*-factor are used to describe a simulation that perfectly matches the measured data. According to the literature, *P*- and *R*-factors should be equivalent to and/or greater than 0.7 and less than 1.2, respectively (Abbaspour et al., 2015). The calculations of the *P*- and *R*-factors are presented as follows:

$$P = \sum_{t=1}^{T} \frac{Z_t}{T} x\ 100, \tag{5.4}$$

$$Z_t = \begin{cases} 1\ if\ Q_t^o \in \left(Q_{t,2.5\%}^s, Q_{t,97.5\%}^s\right) \\ 0\ otherwise \end{cases} \tag{5.5}$$

$$R = 1/T \sum_{t=1}^{T} \frac{Q_{t,97.5\%}^s - Q_{t,2.5\%}^s}{\sigma_{obs}} \tag{5.6}$$

where T represents all of the time steps in the collected data, the model's time step is given by t, and the observed discharge must fall within the 95 PPU range for Z_t to equal 1. At time step t, Q_t^o represents the observed data; S designates the simulated data, O denotes the observed data, σ_{obs} denotes the standard deviation of the measured data, $Q_{t,97.5\%}^s$ and $Q_{t,2.5\%}^s$ represent, respectively, the simulated upper and lower limits at time t (the cumulative distribution level at 97.5% and 2.5%).

5.2.3.4. Spatial Scales of the Subbasin for Modelling High and Low Flows

To examine the impacts of the subbasin spatial scale on distinct flow regimes, quantile curve analysis was carried out to identify phases that might serve as generic signals of river flows. The quantile curve intervals for this instance were based on the work of (Kannan and Jeong, 2011; Pfannerstill et al., 2014; Tegegne et al., 2019; Yilmaz et al., 2008). Various flow phases have been developed by many researchers. For example, Kannan and Jeong (2011) and Tegegne et al. (2019) categorize it as five and seven, respectively. In this investigation, we followed the quantile curve categorization by (Tegegne et al., 2019), which is described as very-high-flow (0–5%), high-flow (5–10%), moist-flow (10–40%), mid-range-flow (40–60%), dry-flow (60–90%), low-flow (90–95%), and very-low-flow (95–100%). Hence, this study examined how the subbasin spatial scale affected these seven different categories of "flow phases". To more accurately estimate flood damage and water quality, it may be helpful to analyse the high and low flows at the proper spatial scale for a subbasin.

Of the two alternatives available in SWAT for stream definition, in this study, the stream network density and subbasin count were varied using the DEM-based stream definition. After calculating the flow direction and accumulation, a threshold area that determines the drainage area needed to create a stream's beginning is identified. The essential stream area threshold, which is used to establish the characteristics of the stream network, may be used to determine the size and overall number of created subbasins. Figure 5.2 depicts three independent but consecutive study watersheds (2%, 10%, and 20%), which were utilized to specify the stream network and subbasin configuration to specify a minimum threshold area. In fact, 2% of the watershed area is very similar to the default minimum threshold value in ArcSWAT. For each subbasin discretization scenario in the Abelti, Wabi, and Gecha watersheds, a comparable minimal threshold drainage area that is necessary to produce a stream's origin was employed. As a result, this percentage drainage area is used to construct several subbasins in each of the watershed scenarios, yielding subbasin subdivision levels of 30, 8, and 4 for the Abelti watershed, 27, 3, and 3 for the Wabi watershed, and 23, 3 and 3 for the Gecha watershed.

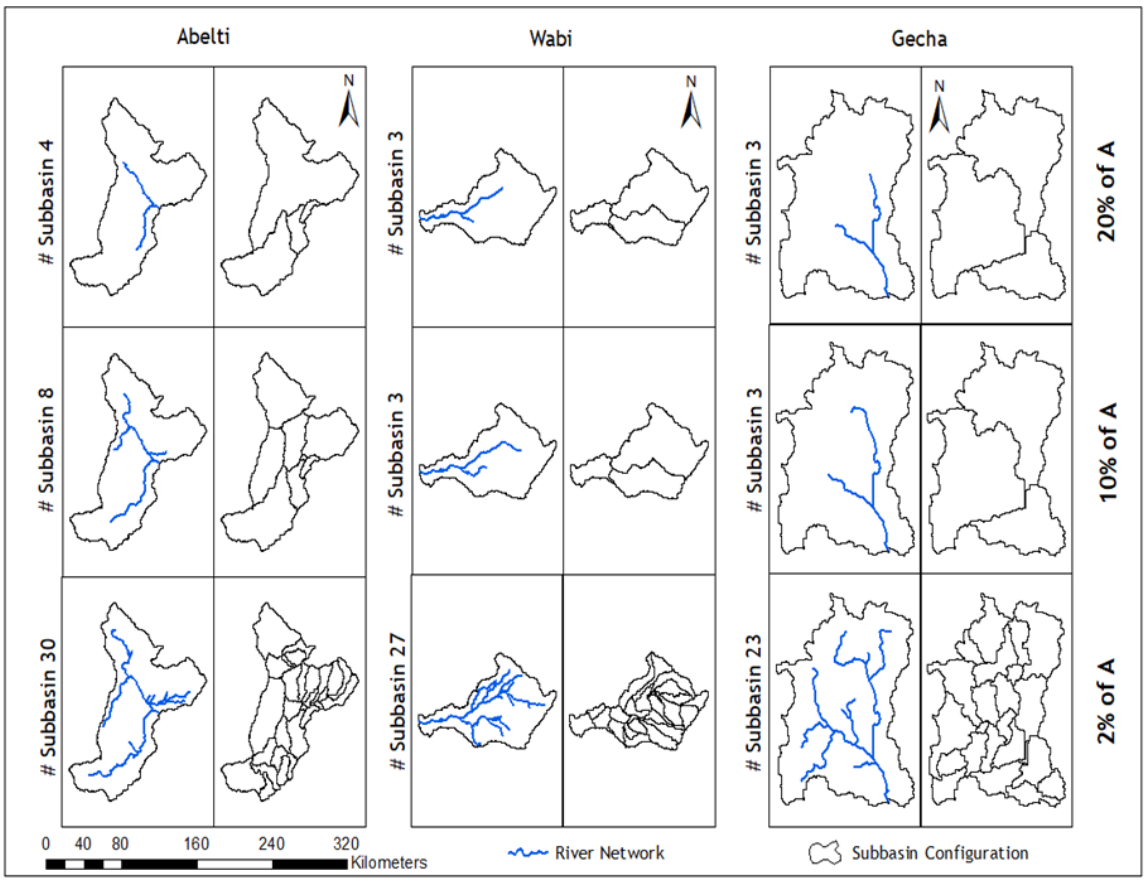

Figure 5.2. Three subbasin subdivision levels for the study area (Abelti, Gecha and Wabi watersheds). (Note: A = watershed area).

SWAT allows the user to specify the number of HRUs for each subbasin discretization scenario by specifying land use, soil type, and slope class thresholds as a percentage of the entire area of the subbasin or as a specific region. For example, if a subbasin has a land use threshold of 10%, it means that the subbasin's utilization area which is less than 10% of the entire land use area gets eliminated and the remaining land use area is reapportioned so that 100% of the land use area in the subbasin is modelled. The quantity of HRUs inside a given subbasin may change when the discretization level varies. It is crucial to understand that the catchment's land use and soil characteristics may have a significant impact on the curve number parameter (CN2) of the SWAT model. Therefore, as CN2 is frequently the most sensitive parameter in SWAT modelling studies,

subbasin discretization may also have an impact on its sensitivity (Cibin et al., 2010; Tegegne and Kim, 2018; Tegegne et al., 2019). In this study, a default threshold value of 20% land use, 10% soil type, and 20% slope was employed for the HRU definition for each subbasin discretization level.

Using the minimal drainage area necessary to create a stream's origin as a guide, Figure 5-3 depicts how, at each degree of subbasin division, the fractional order subbasin area varies. The area of the subbasin subdivision level shrinks as the number of subbasins increases. The outcome of this investigation is compatible with that of the study of (Tegegne et al., 2019). Here, in this study, sequential percent area (2%, 10%, and 20% of the watersheds) is considered rather than distinct subbasin numbers.

The SWAT model's comparative effectiveness was evaluated to determine if reductions in root-mean-square error (RMSE) for recreating the various stages of the actual flow duration curve occurred when the subbasin discretization level was raised. The frequency content of the actual and simulated streamflow was compared using the RMSE performance metric. In their study, Pfannerstill et al. (2014) asserts that analysis of observed and simulated flow duration curve (FDC) segments can be performed using the RMSE performance metric. The usage of RMSE in the framework of FDC data analysis is justified by the fact that it is used to assess the complete water cycle without taking the timing of outflow incidents into consideration (Pfannerstill et al., 2014).

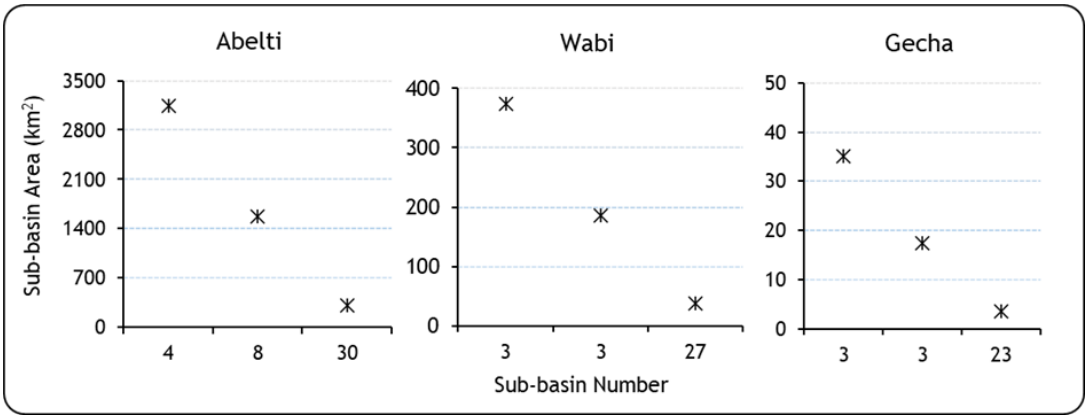

Figure 5.3. Variations in subbasin area and its subdivisions within the studied area.

Using Equation (5.7), one can determine the improved RMSE for the target subbasin.

$$RMSE_{Sub_i}^{IMP}Q_i = [RMSE_{Sub_i}^{Q_i} - RMSE_{BESTSub}^{Q_i})/RMSE_{Sub_i}^{Q_i}] \quad (5.7)$$

where Q_i is quantile level i; Sub_i is subbasin i; $RMSE_{Sub_i}^{Q_i}$ is the *RMSE* of subbasin i at Q_i, and $RMSE_{BESTSub}^{Q_i}$ is the best subbasin in terms of the *RMSE* for Q_i.

5.3. Results

5.3.1. Hydrological Model Performance and Subbasin Discretization

The findings of the sensitivity analysis indicated (Figure 5-4 and Table 5-2) that the parameters ALPHA BNK, CN2, and GW DELAY were the most significant parameters in terms of the sensitivity levels in the majority of the discretization of each subbasin, Abelti, Wabi, and Gecha, respectively. Furthermore, CN2 is among the three most sensitive parameters in all the study watersheds. Because the parameter CN2 is crucial in determining how much runoff is generated from a hydrological response unit, the three watersheds' streamflow models' sensitivity to the parameter was anticipated (Cibin et al., 2010; Tegegne and Kim, 2018).

Streamflow data for Abelti and Wabi (1992–2007), and Gecha (1996–2012) were used to assess the model's simulation capabilities. The watershed calibration periods for Abelti, Wabi, and Gecha

are (1992–2002), (1992–2001), and (1996–2009), respectively. Their separate validation periods were (2003–2007), (2002–2007), and (2010–2012). The values of the objective function (NSE) in Table 5-2 show how sensitive the model's performance corresponds to the number of subbasin divisions and are used to replicate the observed hydrograph. The model's parameters were adjusted for every discretization level of the subbasin in each watershed to assess how sensitive they were in the model. The Abelti watershed, the Wabi watershed, and the Gecha watershed all had subbasin subdivisions of 30, 3, and 3, respectively, which led to the best simulation results for the overall observed flow hydrograph. The coarser subdivision model typically performed poorly in the watersheds compared to its performance at a finer subbasin spatial scale. The implication of this finding is that data sets with spatial clarity are more reliable.

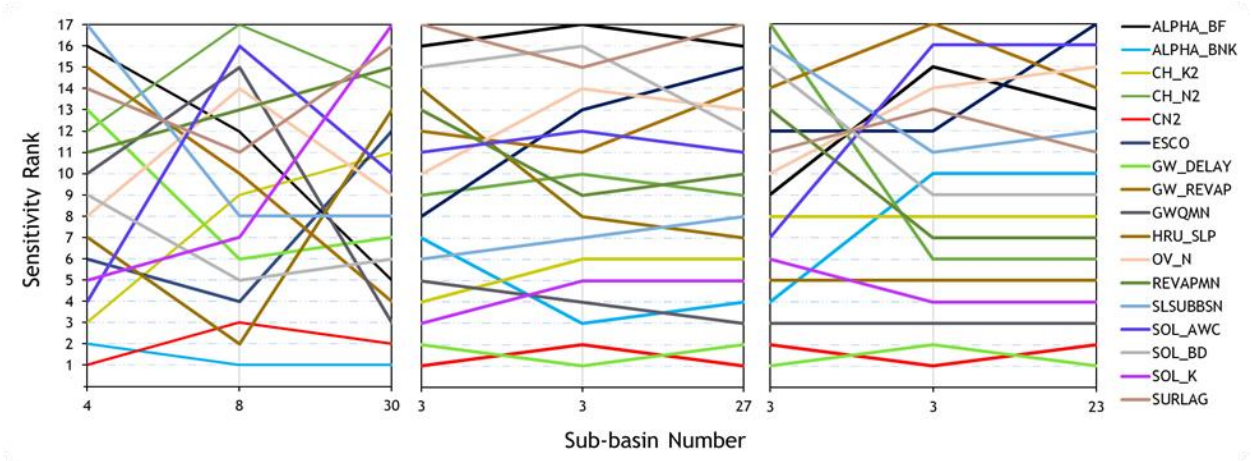

Figure 5.4. Sensitivity rank variation of the SWAT model's flow parameters for the three subbasins of Abelti, Wabi, and Gecha, as determined by the t statistic, are shown on the left, centre, and right, respectively.

Table 5-2. SWAT model metric valuation over the calibration and validation phases.

Watershed	No. of Subbasins	No. of HRUs	P-Factor		R-Factor		NSE	
			Calibration	Validation	Calibration	Validation	Calibration	Validation
	4	36	0.71	0.70	0.85	1.14	0.85	0.74
Abelti	8	62	0.71	0.72	**0.69**	**0.84**	0.88	**0.88**
	30	172	**0.82**	**0.77**	0.92	1.16	**0.89**	0.86
	3	26	0.79	0.76	**0.67**	0.90	0.82	0.77
Wabi	3	26	**0.84**	**0.81**	0.73	1.06	**0.85**	**0.82**
	27	170	0.81	0.79	0.81	**0.76**	0.84	0.80
	3	12	0.74	**0.78**	**0.82**	**0.89**	0.73	**0.83**
Gecha	3	12	**0.76**	0.72	0.84	0.90	**0.74**	0.81
	23	80	0.74	0.75	0.88	0.99	0.73	0.82

Note: best values are shown in bold for each subdivision.

5.3.2. Impacts of Parameter Sampling Distribution on Subbasin Spatial Scale

The SUFI2 simulation employed 500 samples for sensitivity analysis. The first three most sensitive factors in each watershed's subbasin spatial level are shown in scatter plots (Figures 5-5 – 5-7). These examples correspond to well-known features. Figures 5-5 – 5-7 provide dotty plots for the Abelti, Gecha, and Wabi watersheds at each subbasin spatial scale. The consequences of parameter ALPHA BNK are more noticeable in the Abelti watershed at all subbasin division stages, whereas GW DELAY and CN2 are more noticeable in the Gecha and Wabi watersheds, respectively. Additionally, high-density sample areas are shown on dotty plots with a density distribution. High- and relatively low-parameter sampling zones are shown by dark and light blue dotty plots, respectively, while individual observations are indicated by yellow symbols. The parameter samples are therefore somewhat concentrated mostly around the peak value across all watersheds for those subbasin subdivision levels, as evidenced by the dotty plots.

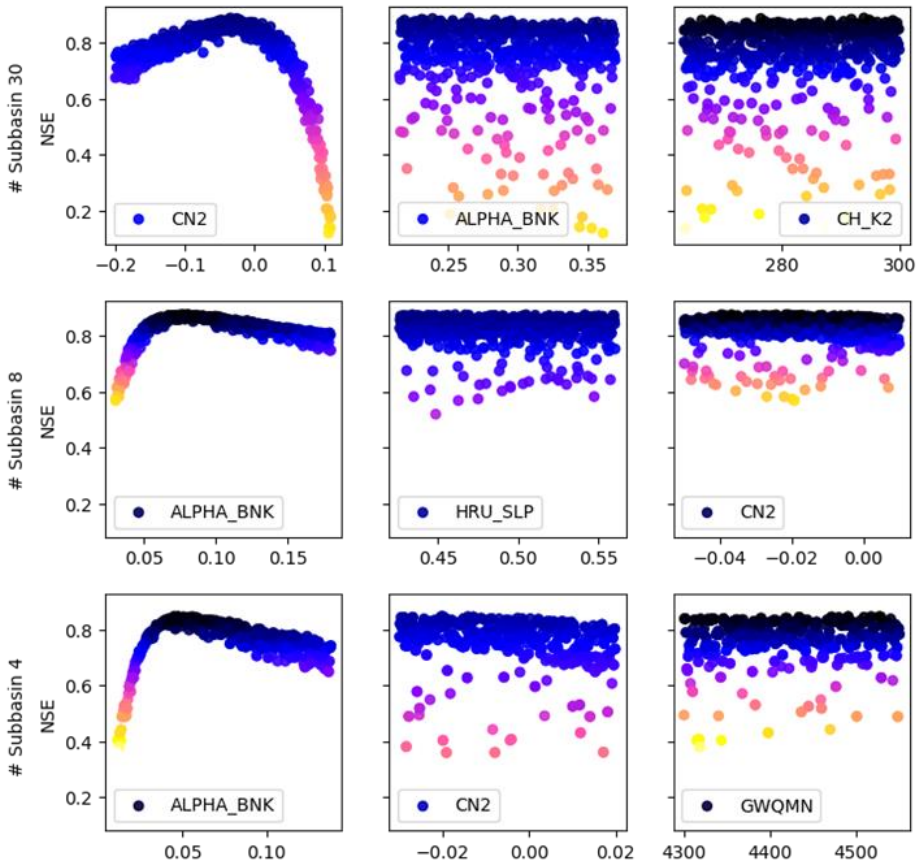

Figure 5.5. Dotty plots of the coefficient of NSE against SWAT parameters (left columns represent the most sensitive) using SUFI2 based on 500 samples from the Abelti watershed. (Note that # Subbasins 30, 8, and 4 account for 2%, 10%, and 20% of the Abelti watershed area, respectively).

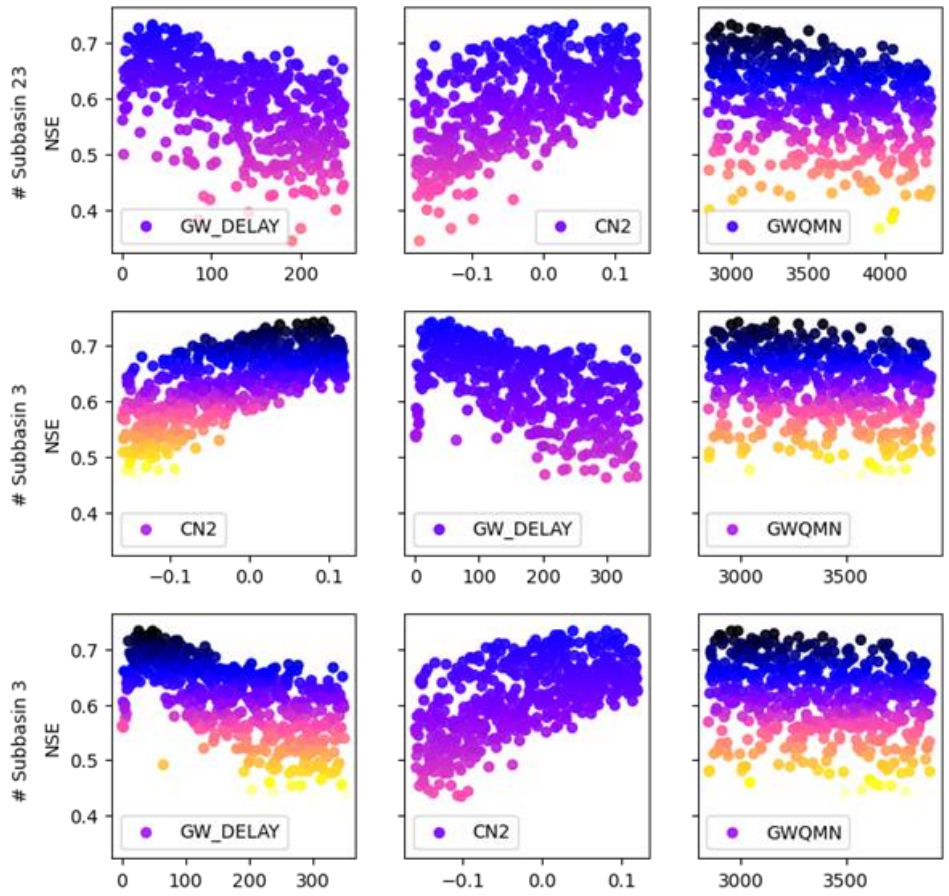

Figure 5.6. Dotty plots of the coefficient of NSE against SWAT parameters (left columns represent the most sensitive) using SUFI2 based on 500 samples from the Gecha watershed. (Note that # Subbasins 23, 3, and 3 account for 2%, 10%, and 20% of the Gecha watershed area, respectively).

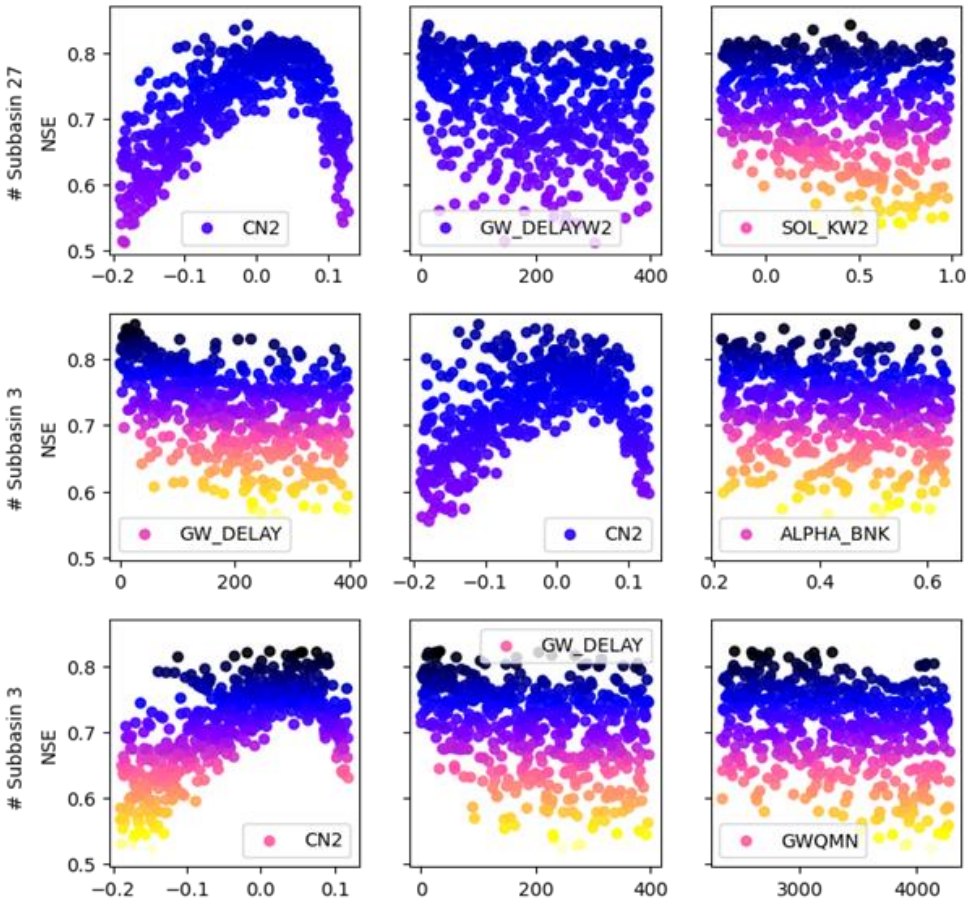

Figure 5.7. Dotty plots of the coefficient of NSE against SWAT parameters (left columns represent the most sensitive) using SUFI2 based on 500 samples from the Wabi watershed. (Note that # Subbasins 27, 3, and 3 account for 2%, 10%, and 20% of the Wabi watershed area, respectively).

5.3.3. Parameter Uncertainty in Hydrological Modelling across Various Subbasin Spatial Scales

The 95PPU was calculated using the SUFI2 approach. Figures 5-8 – 5-10 depict the measured and well-simulated streamflow patterns, as well as the 95PPU band. The P- and R-factors served as the model's performance measures and were used to compute uncertainty. Hence, in this study, the metrics were determined using the uncertainty results for the Abelti watershed's subbasin subdivision scales of 4, 8, and 30, the Gecha watershed's subbasin subdivision scales of 3, 3, and

23, and the Wabi watershed's subbasin subdivision scales of 3, 3, and 27. After employing the P-to-R-factor ratio (P/R), it was discovered that the parameter uncertainty results obtained using the SUFI2 approach for the Abelti, Gecha, and Wabi watersheds performed outstandingly at subbasin partition sizes of 8, 3, and 3, respectively (Abbaspour, 2015). Out of the whole basin area, the mean subbasin division that yields the lowest amount of uncertainty in the study is determined to be between 11% and 27%. The mean subbasin division for the optimal reproduced SWAT model's simulated flow, on the other hand, was determined to be 2% to 10% of the entire drainage system for the watersheds.

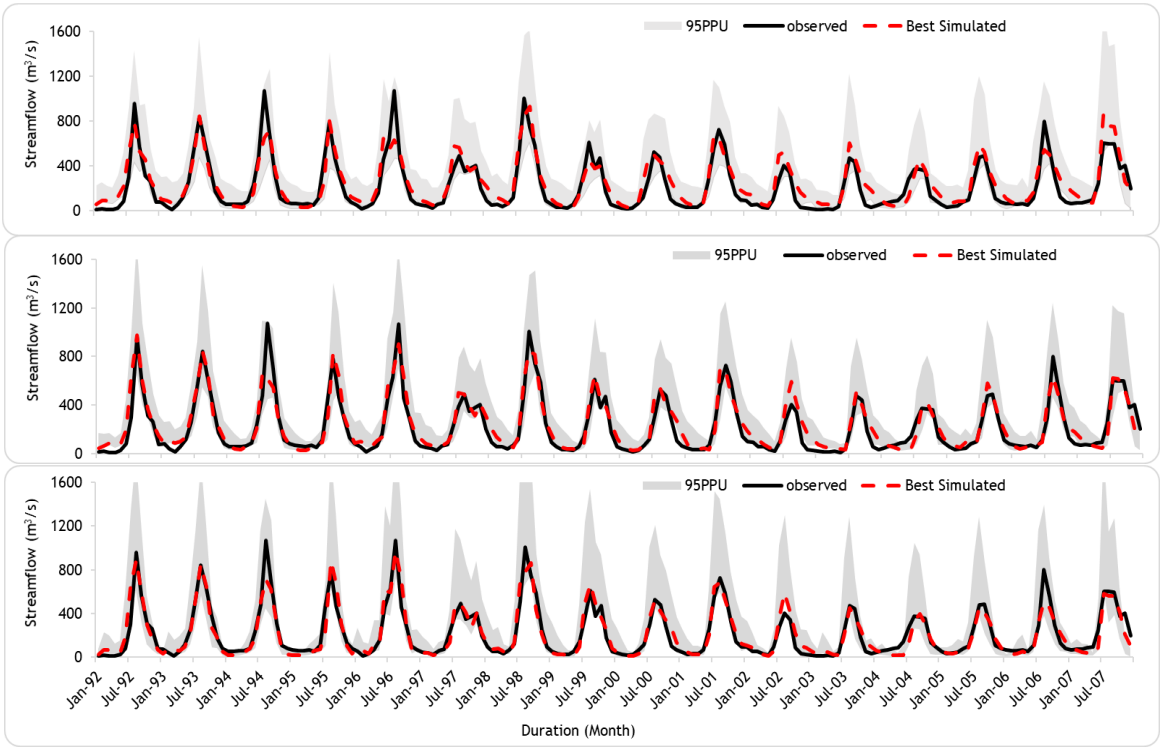

Figure 5.8. Top-down orientation of observed and best-simulated flows with their 95% confidence level of subbasin segmentations of 4, 8, and 30 at the Abelti watershed.

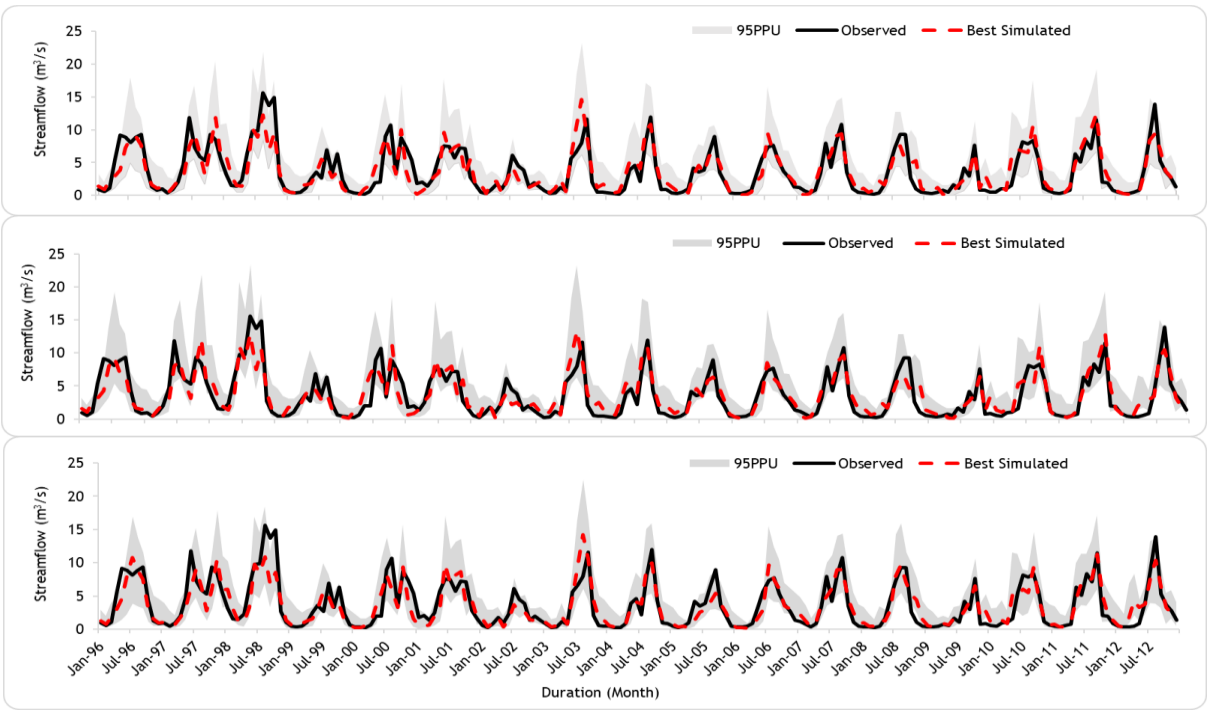

Figure 5.9. Top-down orientation of observed and best-simulated flows with their 95% confidence level of subbasin segmentations of 3, 3, and 23 at the Gecha watershed.

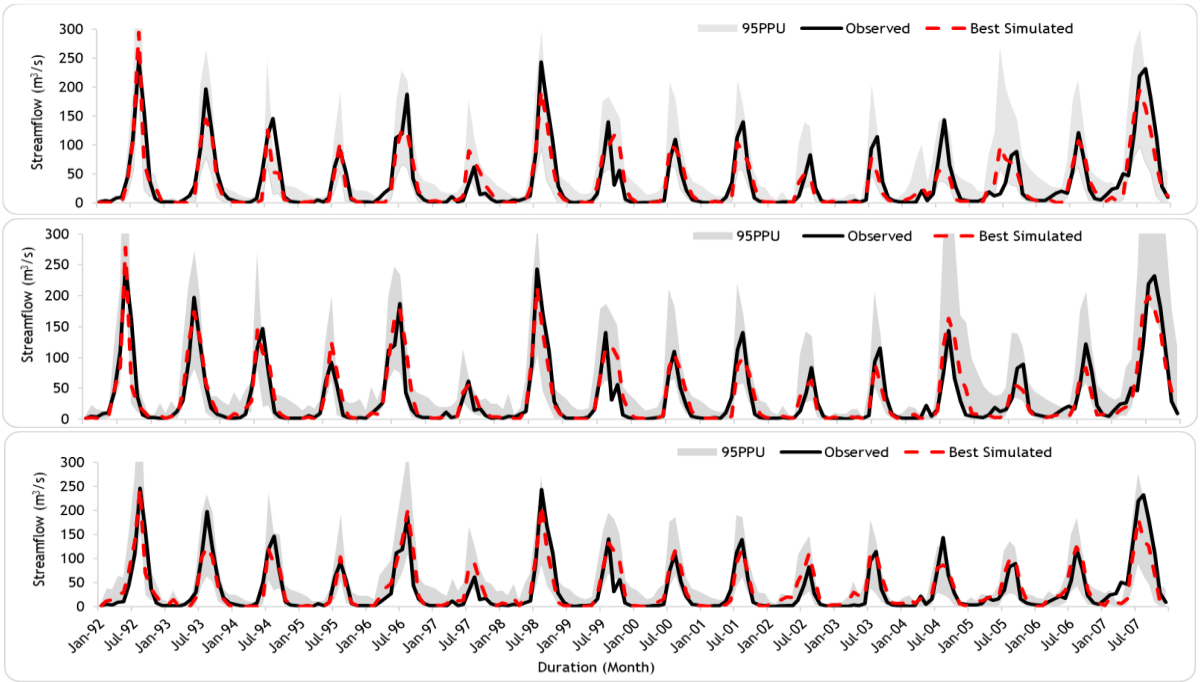

Figure 5.10. Top-down orientation of observed and best-simulated flows with their 95% confidence level of subbasin segmentations 3, 3, and 27 in the Wabi watershed.

5.3.4. Impact of Subbasin Spatial Scales on the Reproduction of Various Flow Phases

The varied hydrograph phases must be accurately replicated for more efficient water management and planning. Different flow quantiles may be described using the flow duration curve (FDC). To more precisely determine the appropriate subbasin number of various views for each hydrograph plot in the study basins, the FDCs were then divided into seven quantiles. Figure 5-11 displays, for the Abelti, Wabi, and Gecha watersheds, the 95PPU plots of the best-estimated flows at various subbasin geographical sizes.

Performance varied slightly across the board since the simulation used varied subbasin geographic sizes. The modelling of these different flow phases also exhibits performance variances in the study case (see Figure 5-11).

The analysis shows that the absurdly inflated estimates of very-low, low, dry, and midrange flows were made at the lower subbasin partition scale for the Abelti catchment scenario. On the other hand, at the upper subbasin divisional levels, the extremely high flow was underestimated. The remaining high and moist flows, despite their appearing to be overstated, are actually fairly minor (see Figure 5-11). The SWAT model performed poorly in replicating the Abelti watershed's dry and low flows throughout all subbasin spatial scales (see Figure 5-11). The simulated flow variation, on the other hand, was extremely close to the observations, and it reproduced the moist, high, and very-high flows with good precision. Apart from the very high flows, the Abelti watershed SWAT model performance was found to reflect almost every flow regime across subbasin subdivisions 8 and 30. The findings could be explained by CN2's low and high responsiveness at coarser and finer subbasin levels, respectively, because it has been demonstrated that CN2 has a considerable influence on the SWAT model (Wu et al., 2022).

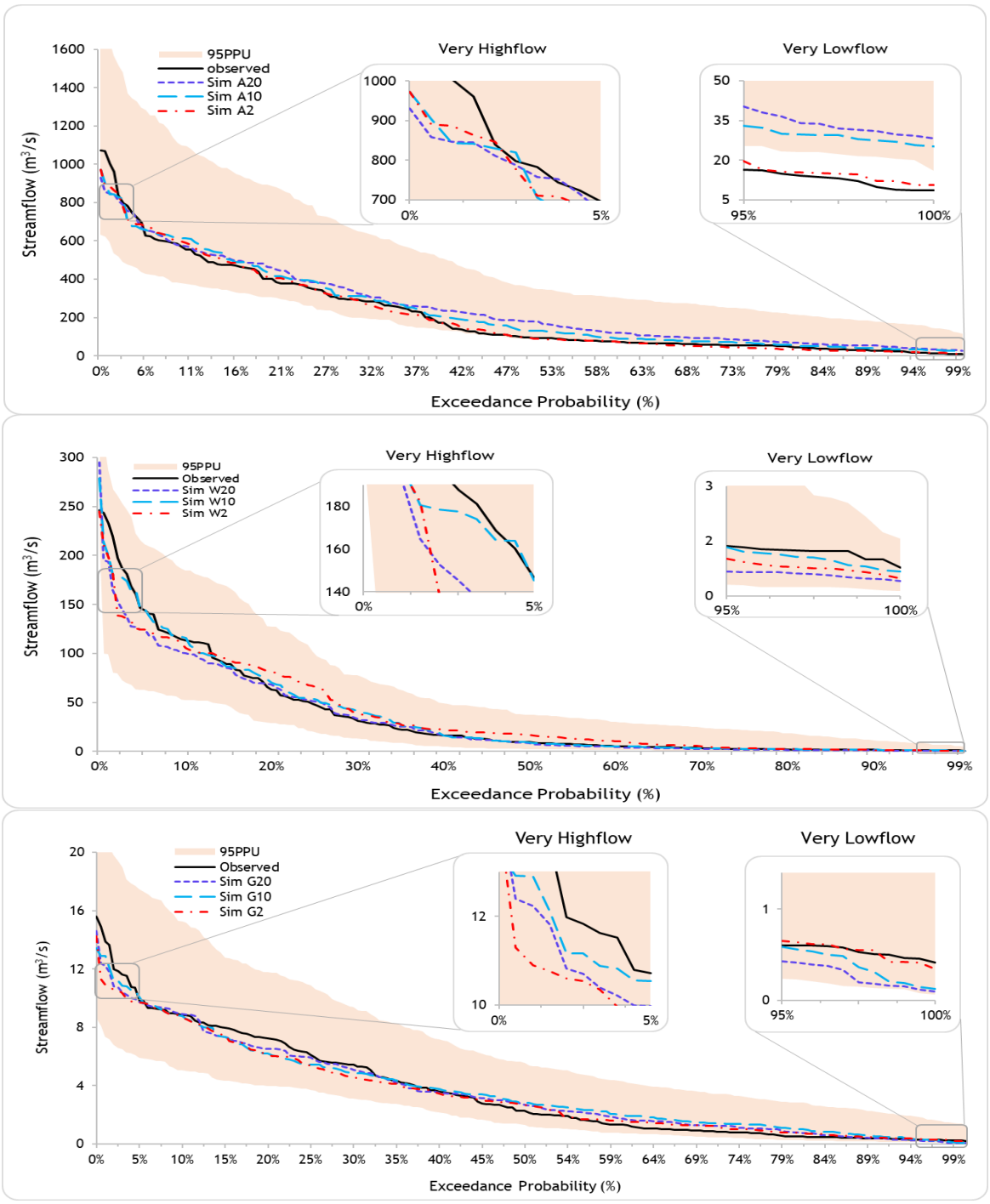

Figure 5.11. Observed and best-simulated flow for the two extreme (0–5 and 95–100%) flow phases based on the 95PPU plot and several subbasin spatial scales of the Abelti, Wabi, and Gecha catchments (top-down, respectively). (Note that A = Abelti, G = Gecha, and W = Wabi together with their 2, 10, and 20 as percentages of the total area to obtain different subbasin numbers).

Figure 12 depicts the improvements in RMSE for modelling the various flow phases in the analysed watersheds over the periods of calibration and validation. The calibration phase had average RMSE advancements of 58%, 68%, and 63%, whereas its validation period showed average RMSE improvements of 56%, 71%, and 63%, respectively, at the Abelti, Gecha, and Wabi catchments' different flow phases by using an appropriate subbasin geographic level.

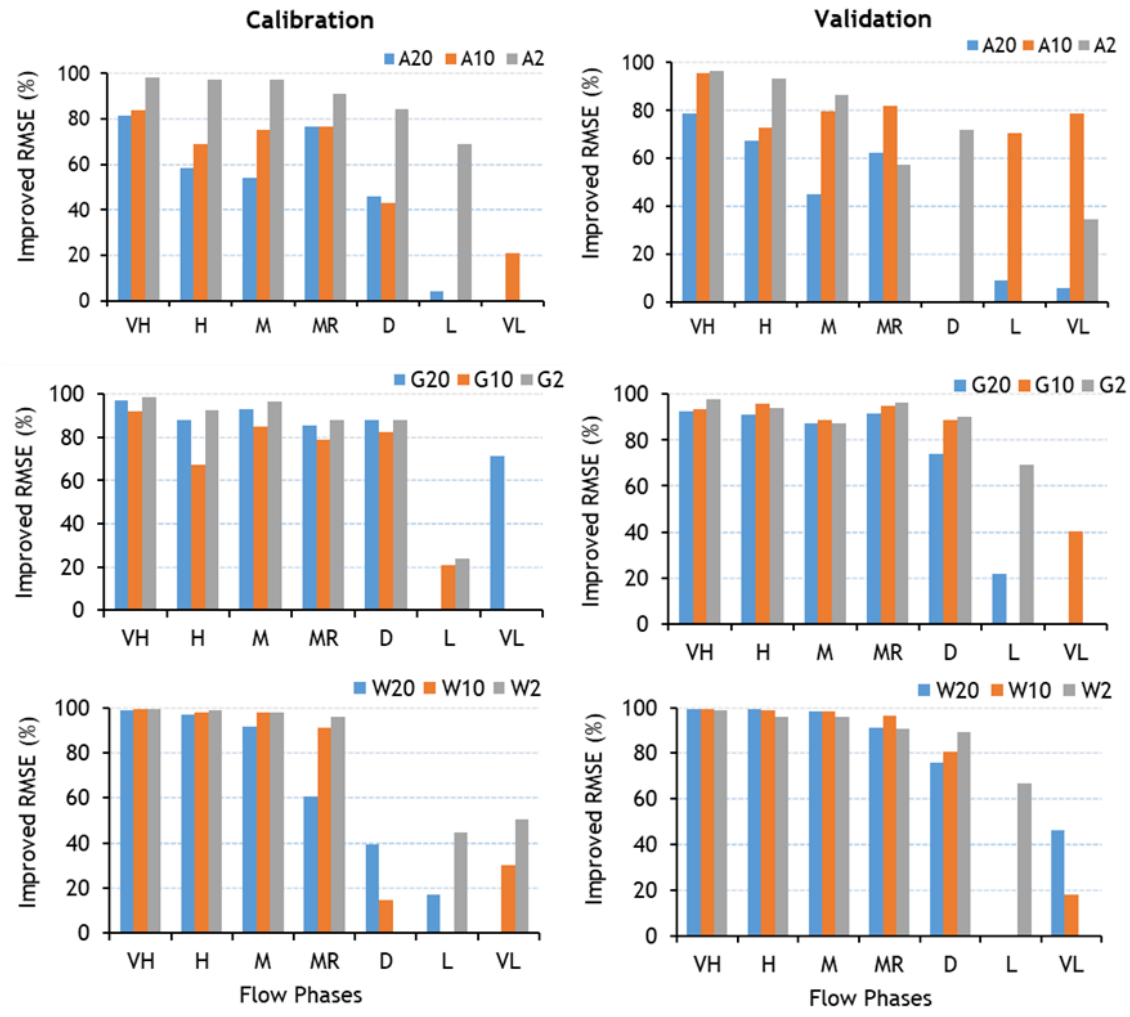

Figure 5.12. Variations in the improved RMSE (%) at various flow phases for calibration and validation conditions (top-down orientation Abelti, Gecha and Wabi watersheds). Note: A = Abelti, G = Gecha, and W = Wabi watersheds 2, 10 and 20 = Percentage of total area for each watershed to obtain various subbasin divisions VL, L, D, MR, M, H, and VH represent very low, low, dry, midrange, moist, high, and very high, respectively.

5.4. Discussion

This study examines the impact of subbasin spatial scale on the hydrological model prediction uncertainty of exceptional stream flows. Thus, for the results of a specific basin to be valid, a hydrological model must operate successfully in line with the necessary statistical criteria.

A good estimate and knowledge of the behaviour of the basin's many runoff components are just as critical as a good overall model. In general, regardless of the degree of spatial discretization, the SWAT model captures the hydrological processes of the research basin utilizing the output of simulated hydrographs and obtained goodness-of-fit values (Caldeira et al., 2019). However, the spatial discretization of subbasins is critical in recreating various simulated flow phases for the different quantile flows.

Similar to the work of (Singh and Jha, 2021), our results demonstrate that catchment size has no discernible influence on the sensitivity of a number of factors, such as CN2 and AL-PHA_BNK. Another study, however, discovered that CN2 affects subbasin discretization, demonstrating that when subbasin discretization rises, CN2's sensitivity rank also rises (Tegegne et al., 2019). It is true that the classification underlying soil and land use usage for every subbasin may vary when the subbasin subdivision level changes, which may therefore have an impact on CN2. The outcome matches the results of (Gassman et al., 2007; Tegegne et al., 2019), who both concluded that CN2 is a crucial variable affecting hydrological simulations in all model applications. The largest source of uncertainty in streamflow simulations, according to some studies, was CN2 (Eckhardt and Arnold, 2001; Guo and Su, 2019). The fact that the relevance of the SWAT model parameters changed with the number of subbasins demonstrated the influence of subbasin partitioning on parameter responsiveness.

These results are in line with those reported by (Haverkamp et al., 2002; Mamillapalli et al., 1996), who discovered that increasing the amount of subbasin discretization boosted simulation accuracy. The precision of the model plateaus at the subdivision level of the subbasin correlates to the highest accuracy. The 30 (Abelti), 3 (Wabi), and 3 (Gecha) subbasin subdivision schemes accurately reflect the spatial variations in spatio-climatic conditions, which might provide an explanation for the performance variance as being linked to CN2's sensitivity to the subbasin spatial scale. The overall flow domain simulation experiments for each level of subbasin segmentation were good, as stated by (Moriasi et al., 2007), with an NSE value above 0.65.

It is crucial to bear in mind that when the NSE value is more than 0.5, the scores of the flow simulation of the hydrological model are acceptable (Moriasi et al., 2007). Figures 5-5 through 5-7 show that the NSE values for the majority of sampling locations in the study watersheds were more than 0.5. Contrary to Figure 5-7, which displays all sample locations in the Wabi watershed with NSE values above 0.5, the scatter diagrams for the Abelti and Gecha watersheds also include some sampling frequencies with NSE values less than 0.5.

Information on measured flow and precipitation data may be the main issue in the Abelti and Gecha basins, respectively. Data on rainfall from the watershed's insufficient geographic coverage might possibly be a factor. Aside from the fact that the parameter sampling in all three catchments was insufficient, the results demonstrate that larger sampling sets would be better for locations with limited data to increase the replicability of the sample points.

Our findings show that subbasin geographic size has little influence on the evaluation of uncertainty in hydrological model parameters, with the fairly coarse subbasin spatial scale having the lowest uncertainty compared to the smaller subbasin division levels. It thus demonstrates how combining meteorological and physical variables at a finer geographical dimension might help to

reduce uncertainty in hydrological model parameters related to watershed data quality. The conclusions of this study agree with those of (Tegegne et al., 2019). The main challenge in the Abelti and Gecha basins may be connected to the recorded flow and precipitation data. Precipitation data from the watershed's limited geographic coverage might be a concern. Aside from the fact that parameter sampling was insufficient in all three catchments, the results demonstrate that larger sampling sets would be better for areas with low data to increase the reliability and accuracy of the sample points.

The 95PPU contained more than 70% of the observations in the lower subbasin subdivision levels 4 and 8 of the Abelti watershed, as well as the entire subbasin division units in the Gecha and Wabi watersheds. However, as the quantity of drainage basins grew, so did the relative thickness of the 95PPU. The fact that all the P- and R-factor values were within acceptable ranges suggests that all the parameter uncertainties were maintained within acceptable limitations. As a result, the 95PPU bracketed the lion's share of the observed values, confirming SWAT's ability to model flow dynamics within the watershed under discussion. It was discovered that the Abelti and Gecha watersheds have wider relative 95PPUs than the Wabi watershed. This may be because the precision with which the injected values with the watersheds of Abelti and Gecha strongly influence the quality of hydrological model simulation, creating a high degree of uncertainty in the results. The Abelti and Gecha watersheds have few and erratically placed weather gauging stations. Despite being recreated with more accuracy at smaller subdivisions, the best-simulated low flow response on the larger subbasin spatial scale deviated significantly from the real values (Figures 5-8 and 5-10). The Gecha watershed's data quality may be a contributing factor in the absence of solid evidence for spatial diversity impacts (Figure 5-9).

Replicating very low and low flows across the Wabi watershed fared better at smaller to intermediate subbasin sizes (subbasin divisions of 3 and 27). However, at a modest to wider spatial scale, the SWAT output recreated the features of the very high, high, moist, and dry observed flows quite consistently. The model effectively duplicated the bulk of the flows on a medium spatial scale.

In certain circumstances, the mid-range and dry flow exceed the expected flow at smaller spatial scales. However, other components present throughout the model simulation process might be the source of the variance. The Gecha watershed's very low, low, dry, and midrange flows might be more properly approximated at a reduced geographical scale. However, the model's output at a broader geographical scale accurately represented the response variables of very high, high, and moist observed flows. As a consequence, the results show that improved replication of the low flow unique phases should be attainable with a chance of 40–100% utilizing lower geographical scales, which increase the number of drainage basins identified during the definition of the SWAT watershed. This conclusion is consistent with the findings of comparable studies, including (e.g., (Tegegne et al., 2019)). As a result, the findings of this study may be beneficial for distributed model water quality and quantity modelling at an appropriate subbasin spatial scale.

Figure 11 clearly shows that the 95PPU comparative ranges for very high flows are narrower than those for low flows. Given that the majority of hydrological models are designed to replicate peak flows and that the NSE performance metric was used to fine-tune the model's parameters, which obviously favour the replication of high flows, this conclusion is unsurprising. The 95PPU covered the observations in the high-flow region with a coverage of 100% compared to the low flow ranges. It is obvious that the strategy employed in this work, which comprises looking at the correct subbasin varied sizes to every flow stage of the FDC, appears to be well adapted to decreasing the

discrepancy between hydrological model findings and observations. More study is suggested to increase the precision of the low-flow hydrological model parameters.

The contrast in the spatial scale of the subbasin is noticeable when compared to the reproduction of the individual flow phases throughout the whole recorded hydrograph. With more subbasin subdivisions, there is less variation in the produced outcomes, and the conclusions may be more consistent. Figure 5-11 depicts in great detail how the spatial presentations of the model's physical and meteorological inputs, as well as the circumstances for watershed management, all have an effect on the disparities in the modelling output processes. The simulation's inaccuracy was nearly twice as high in the Abelti and Gecha watersheds, as it was notable in low flow regimes in the Wabi watershed.

The improvement of RMSE for investigating the optimal subbasin spatial scale throughout the calibration period was 81% when simulating mid-range flow in the Abelti watershed, 86% when modelling dry flow in the Gecha watershed, and 27% when simulating very low flow in the Wabi watershed. During the validation period, the Abelti watershed's very low flow was recreated with a 40% accuracy gain, the Gecha watershed's dry flow with an 84% accuracy gain, and the Wabi watershed's dry flow with an 81% accuracy gain. This is obvious from the approach of the study, which was demonstrated to be an effective strategy for minimizing SWAT simulation error while simulating low flows.

5.5. Conclusions

The primary sources of error in hydrologic simulation are closely associated with physical data input, model parameters, and the structure of the model. In this work, SUFI2 was applied to characterize parameter uncertainty using SWAT modelling. Moreover, the subbasin spatial scale effects on the SWAT modelling prediction uncertainty were investigated. To replicate various flow

phases of the FDC for the Abelti, Gecha, and Wabi watersheds in the Omo-Gibe River Basin, Ethiopia, the uncertainty of the hydrological modelling parameter was assessed. The Wabi watershed seems to have a reasonable spatial inclusiveness of meteorological and physical data input, in contrast to the Abelti and Gecha watersheds, which have rather poor spatial representations of these inputs to the hydrological model. Thus, this study also considered how the precision of the data input and the conditions for watershed management affect the variability in the uncertainty in the hydrological modelling parameters. The analysis revealed that the subbasin spatial scale substantially affected the reproduction of various flow phases but only slightly affected the overall flow simulations.

The 95PPU covered the majority of the observed hydrograph with the coarser geographic scale of the subbasin. Moreover, the coarser subbasin geographic size resulted in a smaller 95PPU proportional width. The key findings of the study are summarized as follows: (1) for the Abelti, Gecha, and Wabi watersheds, SWAT was able to reproduce the observed hydrograph with more than 85%, 73%, and 82% accuracy in terms of NSE, respectively; (2) the SWAT model performed much better in recreating moist, high, and very-high flows than it did in replicating dry, low, and very-low flows in the watersheds. This outcome is in line with previous studies (e.g., Tegegne et al. (2019)). Moreover, with low flows compared to high flows, the relative uncertainty range widens; (3) the establishment of proper subbasin spatial scale considerably improved hydrologic modelling accuracy in mimicking the FDC's various flow phases. As a result, in order to better understand the severity and frequency of these diverse phases of flow behaviour, a variety of relevant subbasin spatial scales may be required (e.g., for flood damage estimates and water quality models); (4) in the Abelti, Gecha, and Wabi watersheds, the mean RMSE improvements in subbasin spatial scales for high flows varied by 79%, 91%, and 98%, respectively, whereas those

for low flows varied similarly by 29%, 42%, and 32%. Consequently, a smaller subbasin spatial scale (towards to distributed model) may better replicate low flows, while a larger sub-basin spatial scale (towards to lumped model) enhances high flow replication precision. The subbasin spatial scales used in this study may have adequately captured the spatial variability in the physical and climatic aspects of the watersheds. It is critical to remember that the physical and climatic parameters of the watershed analysed may change spatially, which may have an impact on the conclusions made. Hence, further investigation on similar subbasin spatial scales across other watersheds is needed.

Given the nature of the study, combining morphological and meteorological inputs at a larger spatial scale within a subbasin can often lower the uncertainty of the hydrological model parameters. However, compared to the larger subbasin spatial scales, the simulation's best results were produced at the smaller subbasin spatial scale and were more consistent with the data that had actually been observed. Most of the observed high flows were contained by the 95PPU, but a large percentage of the recorded low flows were not. Therefore, more work must be put into lowering the parameter uncertainty in low-flow hydrologic modelling.

Finally, the research significantly increased the hydrological model's accuracy in simulating the different flow phases by using a reasonable subbasin spatial scale; for the Abelti, Gecha, and Wabi watersheds, the overall average simulation errors were decreased by approximately 82, 79, and 77%, respectively. Therefore, the suggested method could help us better comprehend the frequency and size of the various flow quantiles for a reasonable assessment of high flows (for example, reducing flood risks) and low flows (for example, modelling water quality).

6. Reliability-weighted Approach for Streamflow Prediction at Ungauged Catchments[1]

Abstract

Understanding the hydrological processes and the determination of the frequencies and magnitudes of streamflow are crucial for better oversight of available water resources. A significant obstacle to accurately assessing the water resources of a basin is the accessibility of data for hydrologic modelling. For example, the Omo-Gibe River basin, which is seeing tremendous socioeconomic growth, including the establishment of cascade hydropower generation, is ungauged in approximately 70% of its area. As a result, regionalization remains a critical difficulty in creating solid projections in these ungauged catchments. Thus, this study aimed to provide a dependable technique for accurately determining surface water resources in ungauged catchments. To accomplish this, a new approach called reliability-weighted (RB) has been introduced to predict runoff in regions with unreliable data. This method combines the advantages of three commonly used parameter transfer methods: global mean, physical similarity, and spatial proximity through weighted averaging. The weights are computed using the reliability-weighted values of each parameter transfer strategy, which are also computed using the donor catchment's hydrological model's reliability value during the calibration and validation periods. The suitability of the proposed scheme was checked in the Omo Gibe and Upper Blue Nile River basins in Ethiopia.

[1]

Bahru M. Gebeyehu, Asie K. Jabir, Getachew Tegegne, and Assefa M. Melesse (2023). Reliability-weighted Approach for Streamflow Prediction at Ungauged Catchments. Journal of Hydrology, Elsevier. DOI: 10.1016/j.jhydrol.2023.129935

After analysing parameter transfer techniques using the jackknife algorithm at several target-gauging stations, it was found that the reliability-weighted method outperforms all three regionalization approaches by approximately 30% for the test catchments. In addition, approximately 85% of the time, the proposed strategy's regionalization performance has a metric Nash-Sutcliffe efficiency greater than 0.50. Alternatively, according to the median efficiency of the Nash-Sutcliffe model, the newly proposed strategy reduces the spatial and temporal losses by approximately 0.01 and 0.02, respectively, when compared to the second-best performing option. Furthermore, the performance of the presented approach's runoff prediction at the test gauged catchments was very comparable to the performance of the on-site calibrated model. The newly proposed approach therefore proved to be a useful tool for assessing the potential of available water resources in ungauged catchments. Finally, the uncertainty in runoff prediction at ungauged basins was reduced by combining the strengths of parameter transfer strategies relying on their reliability at test gauging stations.

Keywords: Omo Gibe River basin; Upper Blue Nile River basin; Parameter transfer; Surface water assessment; Ungauged catchment, Reliability weighting.

6.1. Introduction

Water resource management and planning rely almost entirely on uninterrupted streamflow time-series data (Niu and Feng, 2021). Hydrologists have had difficulty obtaining river flow observations within the area of investigation since the majority of basins lack observational records. Many ungauged basins exist around the world, particularly in developing regions, because there are not enough meteorological and hydrological observations on a worldwide basis. This is mainly related to the different combinations and/or individual constraints of socioeconomic and geographic feature conditions. Alternatively, ungauged basins are those with no streamflow

observational data. Furthermore, runoff models are essential in managing risk, management of water resources and aquatic environment conservation. Therefore, simulating runoff in a place of interest when little or no such measurement data are available for analysis of the proposed project provides a substantial problem for hydrologists.

Predictions in Ungauged Basin (PUB) for the subsequent ten years (2003-2012) were issued in 2003 by the International Association for Hydrological Sciences (IAHS) during the 23rd International Union of Geophysics and Geodesy. It attempts to considerably advance catchments that are not gauged in hydrologic predictions. The project's deployment has encouraged the creation of parameterized regionalization strategies for ungauged catchments. Although PUB ended in 2012, work on regionalization strategies that allow for streamflow modelling in ungauged watersheds has continued since then (Oudin et al., 2008; Zhu et al., 2021).

Many methodologies have been used to simulate ungauged basins using data from gauging stations (Arsenault et al., 2019; Blöschl and Sivapalan, 1995; Choubin et al., 2019; Ditthakit et al., 2021; Oudin et al., 2008). These strategies are used by hydrologists to find patterns and trends from gauged to ungauged basins for hydrologic modelling studies. Global mean (GM), spatial proximity (SP), regression-based (Rb), and physical similarity (PS) methods are some of the frequently employed information transfer (regionalization) methodologies in previous research (Flatley and Rutherfurd, 2022; Oudin et al., 2008; Samuel et al., 2011; Yilmaz and Onoz, 2020; Zamoum and Souag-Gamane, 2019). When 913 gauged catchments in France were used to compare the regionalization strategies of Rb, PS, and SP, Oudin et al. (2008) claim that if a greater concentration of monitoring stations is present, the spatial proximity strategy delivers the optimum regionalization option, whereas the regression model yields the worst acceptable outcomes, and the physical similarity approach is intermediate. Furthermore, they stated that the spatial proximity

technique outperformed the similarity strategy in areas with a higher density of streamflow gauging stations.

For a fuller regionalization viewpoint, it is usually assumed to estimate streamflow in ungauged basins using the combined outputs of the parameter transfer system (Merz and Blöschl, 2004; Nester et al., 2011; Sellami et al., 2014; Zhang et al., 2015). Multimodel averaging is commonly employed in various hydrological domains (Arsenault and Brissette, 2016; Arsenault and Brissette, 2014; Razavi and Coulibaly, 2016). Depending on the literature, the combined output of several hydrological processes produces more accurate research results than a single model. The SP strategy exceeds the PS methodology, which takes the donor catchment with the highest similarity, according to Li and Zhang (2017), and the comprehensive similarity technique, which further integrates the PS and SP methods, slightly surpasses the SP strategy.

Arsenault and Brissette (2014) developed the regression augmented (RA) regionalization method, which successfully integrates the multilinear regression methodology with the PS and SP methods. In 268 Canadian catchments, they discovered that RA outperformed overall PS and SP regionalization techniques. Narbondo et al. (2020) used an updated viewpoint of physical similarity to improve predictions of runoff in basins that are ungauged. The findings demonstrated remarkably good runoff prediction in scarcely and/or ungauged watersheds. In a further study, Arsenault et al. (2019) predicted runoff in Mexico's unmeasured watersheds using six regionalization strategies (PS, SP, PS IDW RA, SP IDW RA, PS IDW, and SP IDW) based on three hydrologic models. The research revealed that the SP and SP IDW RA strategies outperformed the other methodologies utilized in the study basin.

Researchers have attempted to extend the effect of regional linkages to estimates for ungauged watersheds to take into consideration the inherent unpredictability with the expected model

outcome. Zhang et al. (2015) and Merz and Blöschl (2004), for example, have demonstrated how output averaging may minimize uncertainty in ungauged catchment runoff estimates. In this way, the intended watershed is simulated using inputs from multiple contributors rather than just one, and the runoff estimate is obtained by averaging the outputs of the modelling using various sets of data from multiple donors to achieve the lowest possible uncertainty in the predicted outcome. An alternative strategy is to combine the strengths of the parameter schemes based on their reliability at the test catchments.

Thus, the key objective of this study is to suggest a reliable technique for accurately forecasting surface water resources in ungauged catchments. To anticipate runoff in unmeasured catchments, this work suggests the reliability-weighted (RB) strategy, which combines the benefits of the global mean, physical similarity, and spatial proximity parameter transfer approaches. The accuracy at gauged catchments that were previously thought to be ungauged is taken into consideration while determining each regionalized model's weight, which is done to determine how effective the suggested parameter transfer technique is. Cross-validation is then undertaken using the leave-one-out or jack-knife technique, and each catchment is first regarded as ungauged. The particular flows are then utilized to judge how effectively the flow prediction algorithms for each catchment performed. Then, statistical tests are utilized to assess the accuracy of flow estimation in “pseudo” ungauged basins (Kanishka and Eldho, 2020; Swain and Patra, 2017).

6.2. Material and Methods

6.2.1. Study area

This section has been removed for brevity and to avoid repetition because chapter 3 contains more details on the subject. As a result, only a small portion of it—which is pertinent to the topic—is included in this section. Figure 6-1, depicts seven catchments (five from the Omo Gibe River Basin

(OGRB) and two from the Upper Blue Nile (Abbay) River Basin (UBNB), that were employed to achieve the stated target.

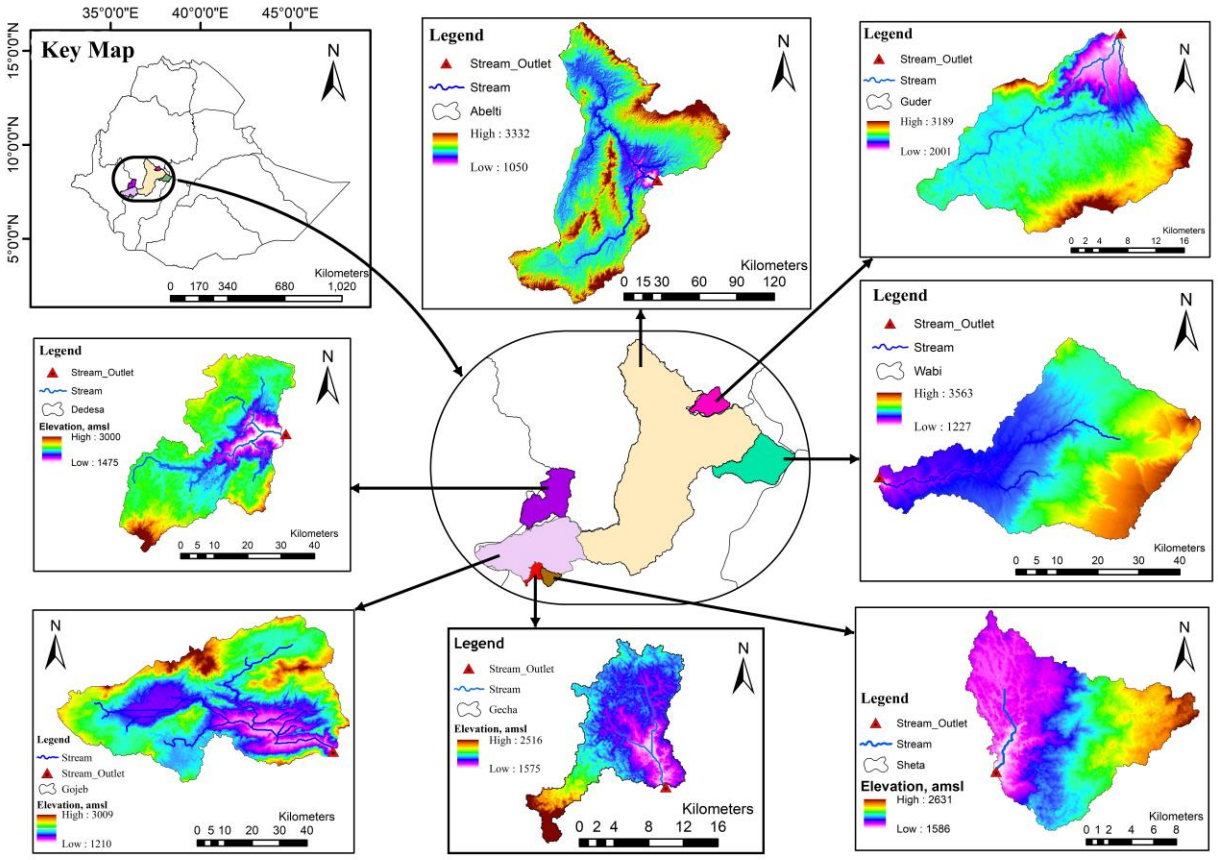

Figure 6.1. Study catchment locations: five catchments (Abelti, Wabi, Gojeb, Sheta, and Gecha) in the OGRB and two nearby catchments (Dedesa and Guder) in the UBNRB, Ethiopia.

6.2.2. Data description

Digital elevation models (DEMs), land use and land cover (LULC), soil maps, and meteorological information are required for ArcSWAT. A 30 m resolution DEM and flow measurements for the study watersheds were provided by the hydrological division of Ethiopia's Ministry of Water and Energy. The LULC data were provided by the Water and Land Resources Centre at Addis Ababa University. The Digital Map of the World (DMW) from the Food and Agricultural Organization (FAO) of the United Nations was used to construct the soil map. The daily weather observations

are gathered from 15 weather gauging stations, including Asendabo, Wolkite, Woliso, Ejiji, Kachis, Bonga, Jima Sawula, Jinka, Key Afer, Hosaena, Wolaita, Nekemte, Sokoru, and Shishinda. The Soil and Water Assessment Tool (SWAT) is used for simulation using meteorological data via these weather stations. In fact, the Ethiopian Meteorological Institute and the Ethiopian Ministry of Water and Energy provided meteorological data from fifteen stations and streamflow data from seven stations (Abelti, Wabi, Gojeb, Gecha, Sheta, Guder, and Dedesa).

6.2.3. Methods

6.2.3.1. Hydrologic model

SWAT (Arnold et al., 1998), a semidistributed model, was utilized for the OGRB's five gauged watersheds (i.e., Abelti, Wabi, Gojeb, Sheta, and Gecha) and the UBNRB's two gauged watersheds (i.e., Guder and Dedesa). Orkodjo et al. (2022) and Mengistu et al. (2021) recently employed the SWAT model efficiently in the Omo Gibe and Abbay river basins, respectively. SWAT was designed as a physically, continuous time-based hydrologic model to anticipate ramifications of land use planning methods on sediment, water, and Agri-based chemical outputs over a long time span in enormous, complicated catchments with a diversity of soil, land use, and management variables (Wen et al., 2020). Based on SWAT, a basin is split into several subregions, each of which is then divided into units with distinct land use and soil distinguishing features termed hydrological response units (HRUs). Its outflow is simulated individually on every subwatershed and routed to determine the basin's aggregate surface runoff. Several types of input data, such as DEM, soil, land use and land cover, and meteorological data (i.e., rainfall, temperature, solar, wind speed, and relative humidity), are required for this model to effectively portray the characteristics of the basin (Neitsch et al., 2011).

One uses Equation 6.1 to calculate the hydrologic balance:

$$SW_t = SW_o + \sum_{i=1}^{t}\left(R_{day} - Q_{surf} - E_a - W_{seep} - Q_{gw}\right)_i \quad (6.1)$$

where SW_o represents the soil's initial water content on day i, SW_t represents the final water content, and t indicates the time step. R_{day} is the rainfall quantity on day i. E_a is the measure of evaporation on day i. Q_{surf} is the runoff quantity on day i. Q_{gw} is the quantity of groundwater flow on day i, and W_{seep} is the volume of water from the soil profile that entered the vadose zone on day i. Except for t, which has a unit of day, the other scales have a unit of mm.

SWAT provides three unique choices for predicting potential evapotranspiration based on the availability of data: the Priestley-Taylor, Penman–Monteith, and Hargreaves approaches (Neitsch et al., 2011). The potential soil-water-evaporation is determined as a function of the leaf area index and potential evapotranspiration. Actual soil water evaporation is approximated by applying nonlinear relationships between water content and soil depth. Root depth, potential evapotranspiration, and leaf area index are used to mimic plant water evaporation, which may be constrained by the soil water content. A detailed SWAT description is given in the work of Neitsch et al. (2011). The modified soil conservation service runoff curve number (SCS-CN) was chosen to compute the surface runoff volume. To calculate flow across the channel, a variable storage coefficient approach is used, and the Penman Monteith approach is applied to determine potential evapotranspiration.

6.2.3.2. Parameter sensitivity analysis

Parameter sensitivity analysis must be performed before model calibration to discover important flow parameters in each test catchment. It is possible to utilize sensitivity analysis to reduce the quantity of parameters that need to be fitted to the input-output data that, in turn, reduce the hydrologic modelling output uncertainty. Depending on the characteristics of the data set being studied, sensitivity analyses are frequently referred to by the terms "local" or "global" analyses. In

this study, a global sampling method is considered, which arbitrarily or methodically scans the whole spectrum of feasible parameter values and groupings. The statistical indicators t test and p values are employed to calculate the sensitivity and relevance of every parameter estimate. The SWAT flow metrics employed in this research are identified by performing a thorough literature study (Abbaspour, 2015; Gebeyehu et al., 2023; Neitsch et al., 2011; Orkodjo et al., 2022; Tegegne et al., 2019; Upadhyay et al., 2022).

6.2.3.3. Parameter calibration and validation

The construction of water resource projects in the OGRB and UBNRB has hampered numerous hydrological processes. As a result, a number of areas where fundamental streamflow data cannot simply be produced for predictions applying hydrological processes. For this, seven gauged stations (Abelti, Wabi, Gojeb, Sheta, Dedesa, Gecha, and Guder) are considered, and the recorded flow periods included to operate the SWAT were (1992-2007) for the Abelti, Wabi, Gojeb, and Guder catchments, (1996-2012) for the Gecha catchment, (1998-2012) for the Sheta catchment, and (1991-2006) for the Dedesa catchment. With the exception of Dedesa, where two years are utilized instead, the very first 3 years are employed as the warm-up period in the model calibration procedure for each gauged catchment of the OGRB and UBNRB. To calibrate the SWAT flow parameters, the SWAT Calibration and Uncertainty Programs (SWAT-CUPs)' Sequential Uncertainty Fitting (SUFI2) (Abbaspour et al., 2004) program was utilized. The Nash Sutcliffe efficiency (NSE) approach, developed by Nash and Sutcliffe (1970), is the objective function used for the estimate of flow parameters for SWAT:

$$NSE = 1 - \frac{\sum_{i=1}^{N}(O_i - P_i)^2}{\sum_{i=1}^{N}(O_i - \bar{O})^2} \tag{6.2}$$

where P_i represents an estimated value, O_i represents an observed value, and $\bar{O}$ represents a mean observed value.

6.2.3.4. Parameter transfer schemes for ungauged subbasins

The physical similarity (PS) technique employs some catchment physical attributes to group the similarity of catchments. In other words, this technique identifies a donor catchment that is analogous to the target ungauged catchment. The donor parameter is then fully transferred to the relevant ungauged catchment for hydrologic modelling. The primary benefit of the PS strategy over the regression method is that it employs physical attributes but does not require the linearity assumption (Arsenault et al., 2019). The attributes selected for catchment similarity will determine if this approach is successful. Geomorphological attributes (i.e., basin mean elevation and land use) and climate attributes (such as yearly mean precipitation, yearly mean temperature, aridity index, and average potential evapotranspiration) were used to determine homogeneous regions in the study basin. The k-means and principal component analysis (PCA) techniques are used to discover the homogeneous regions. The spatial proximity (SP) used a spatial distance interpolation technique to estimate model parameters at ungauged catchments. This method implies that all catchments within a given radius are comparable. This study identified similar regions by using the inverse distance weighting (IDW) approach. For estimating flow in ungauged basins, one might anticipate that catchment features would offer useful hydrological information (Razavi and Coulibaly, 2013); however, under the spatial proximity concept, these factors are not taken into account. The global mean (GM) technique computed every modelled variable for all the ungauged watersheds as the average values of each variable from all calibrated values at the gauged catchment areas. As a result, the model parameters are identical throughout all catchments of ungauged areas. This technique is predicated on the assumption that all catchments in the study region have equal hydrological features and that any variations in model parameters are caused by random variables (Guo et al., 2021).

6.2.3.5. Reliability-weighted (RB) approach

An alternative strategy is to combine the strengths of the parameter schemes based on their reliability at the test catchments. The weighted multimodel averaging technique has indeed been successfully used for the other subsections of hydrology (e.g., Arsenault and Brissette (2016); Arsenault et al. (2015); Diks and Vrugt (2010); Tegegne et al. (2020); Wan et al. (2021)). Previous studies concluded that the combined output of multiple hydrological models provides better results than individual models. Hence, this study also applied the weighted averaging concept combining the advantages of the three parameter transfer schemes (PS, SP, and GM). The weight of each regionalized model is determined based on its reliability at the gauged catchments that were originally considered ungauged to test the performance of the parameter transfer approaches.

The reliability-based skill score employed in this study is the mean square error (MSE). The general steps to compute the reliability-weighted skill score are summarized as follows:

1) Consider the output patterns of the regionalized model j be $S_{j,i,t}$ in each gauging site i and time step t, the corresponding observed streamflow pattern at each gauging site be $O_{i,t}$ and the mean of the observed streamflow be $\bar{O}_i$ at site i. The $MSE(S, \rightleftarrows O)_{j,i}$ and $MSE(\bar{O}, \rightleftarrows O)_i$ can be defined as follows:

$$MSE(S,O)_{j,i} = \frac{1}{T}\sum_{t=1}^{T}\left(S_{j,i,t} - O_{i,t}\right)^2 \tag{6.3}$$

$$MSE(\bar{O},O)_{i} = \frac{1}{T}\sum_{t=1}^{T}\left(\bar{O}_{i} - O_{i,t}\right)^2 \tag{6.4}$$

where *t*, is the time step for each gauging site *i*.

2) The $MSE(S, \rightleftarrows O)_{j,i}$ can be decomposed in to the mean error and pattern error (Murphy, 1988) as follows:

$$MSE(S,O)_{j,i} = \left(\bar{S}_{j,i} - \bar{O}_i\right)^2 + \sigma^2_{s_{j,i}} + \sigma^2_{o_i} - 2\sigma_{so_{j,i}} \quad (6.5)$$

where $\sigma_{so_{j,i}} = \frac{1}{T}\sum_{t=1}^{T}\left(S_{j,i,t} - \bar{S}_j\right)\left(O_{i,t} - \bar{O}_i\right)$ is the sample covariance of the simulation and observation,

$\sigma_s^2 = \frac{1}{T}\sum_{t=1}^{T}(S_i - \bar{S})^2$ presents the sample variance of the simulation using the regionalized model.

$\sigma_o^2 = \frac{1}{T}\sum_{t=1}^{T}(O_i - \bar{O})^2$ presents the sample variance of the observation,

3) Transform the $MSE(S, \rightleftarrows O)_i$ performance term into a dimensionless skill score by normalizing using the term $MSE(\bar{O}, \rightleftarrows O)_i$ as follows:

$$R_{j,i} = 1 - \frac{MSE(S,O)_{j,i}}{MSE(\bar{O},O)_{j,i}} \quad (6.6)$$

It should be noted that the model's reliability ($R_{j,i}$) varies from 0 (unreliable) to 1 (reliable).

4) Compute the skill score $R_{j,i}$ for the calibration $R_{j,i}^{cal}$ and validation $R_{j,i}^{val}$ period of the hydrologic simulation at each site.

5) The weight $W_{j,i}$ for the j^{th} model is derived by multiplying two aspects: 1) the model's ability to simulate runoff throughout the period of calibration $R_{j,i}^{cal}$ and 2) how well the model's performance of replicating the runoff throughout the period of validation $R_{j,i}^{val}$. Compute the reliability-weighted skill score ($W_{j,i}$) of each parameter transfer scheme j for each gauging site as follows:

$$(W_{j,i}) = (R_{j,i}^{cal})^m (R_{j,i}^{val})^n \quad (6.7)$$

where m and n represent the weighting factors for each criterion. In this study, both parameters are fixed at one, but one can determine the sensitivity of the parameters on the weight performance.

6) The computed weights ($W_{j,i}$) for each model and site are transposed to the ungauged sites based on the notion of the inverse distance weighted (IDW) approach. The reliability-weight estimation of each parameter transfer scheme based on the IDW approach could be useful even to give more weight to values closest to the ungauged catchment centroid. The underlined assumption here is that the parameter transfer scheme performance has a local influence that diminishes with distance. The reliability-weighted value of the parameter transfer scheme j at the ungauged site $\hat{\imath}$ ($\widehat{W}_{j,\hat{\imath}}$) can be calculated as follows:

$$\widehat{W}_{j,\hat{\imath}} = \frac{\sum_{i=1}^{n}\left[\left(W_{j,i}\right)\left(\frac{1}{d_i^p}\right)\right]}{\sum_{i=1}^{n}\left(\frac{1}{d_i^p}\right)} \tag{6.8}$$

where d denotes the distance between the midpoint of gauged site i and ungauged site $\hat{\imath}$, p is a power parameter in the IDW, and the quantity n represents the number of donor catchments to model the ungauged catchments. The reliability-weighted value for ungauged catchment-4 shown in Figure 6-2 can be computed with the following procedure. Let j = 1, 2, 3 for the GM, SP, and PS approaches, respectively. The reliability-weighted values of the GM and SP approaches from each gauged catchment in the study region are considered in the IDW average computation for the ungauged catchment since there is no catchment attribute required to transfer the

information in these two parameter transfer approaches. Hence, the IDW average value for the GM and SP approach at catchment-4 can be computed as follows:

$$\widehat{W}_{1,4} = \frac{\sum_{i=1}^{3}\left[\left(\frac{W_{1,1}}{d_{1,4}} + \frac{W_{1,2}}{d_{24}} + \frac{W_{1,3}}{d_{3,4}}\right)\right]}{\sum_{i=1}^{3}\left(\frac{1}{d_{1,4}} + \frac{1}{d_{2,4}} + \frac{1}{d_{3,4}}\right)} \tag{6.9}$$

$$\widehat{W}_{2,4} = \frac{\sum_{i=1}^{3}\left[\left(\frac{W_{2,1}}{d_{1,4}} + \frac{W_{2,2}}{d_{24}} + \frac{W_{2,3}}{d_{3,4}}\right)\right]}{\sum_{i=1}^{3}\left(\frac{1}{d_{1,4}} + \frac{1}{d_{2,4}} + \frac{1}{d_{3,4}}\right)} \tag{6.10}$$

The reliability-weighted value of the PS approach of all the gauged catchments is only considered in the computation where there is physical similarity between catchment-4 and all gauged catchments. Otherwise, the reliability-weighted values of the PS at the catchments that have physical similarity with the ungauged catchment are considered in the computation. Let the ungauged catchment-4 be physically similar to only the gauged catchment-1 and catchment-3, and therefore, the IDW reliability-weighted value at catchment-4 can be computed by

$$\widehat{W}_{3,4} = \frac{\sum_{i=1}^{2}\left[\left(\frac{W_{2,1}}{d_{1,4}} + \frac{W_{2,3}}{d_{3,4}}\right)\right]}{\sum_{i=1}^{3}\left(\frac{1}{d_{1,4}} + \frac{1}{d_{3,4}}\right)} \tag{6.11}$$

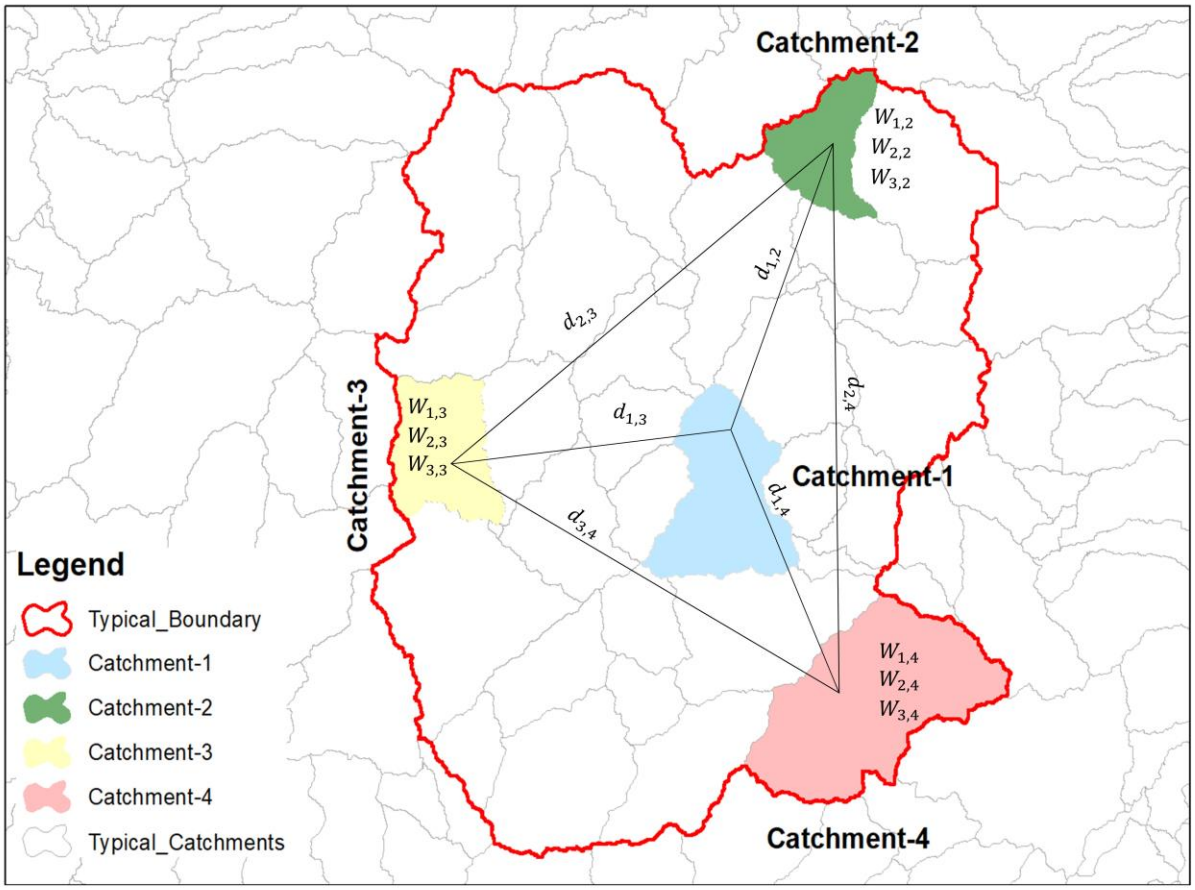

Figure 6.2. Spatial configurations of idealized catchments for the proposed reliability-weighted regionalization approach (*Note: $d_{i,j}$ = distance between the considered catchments, $W_{i,j}$ = reliability weights of each catchment*)

7) Finally, the simulated value by each parameter transfer approach at the ungauged sites can be weighted averaged as follows:

$$\hat{S}_{\hat{\imath}} = \frac{\sum_{j=1}^{J}\left[\left(\widehat{W}_{j,\hat{\imath}}\right)\left(S_{j,\hat{\imath}}\right)\right]}{\sum_{j=1}^{J}\left(\widehat{W}_{j,\rightleftarrows\hat{\imath}}\right)} \tag{6.12}$$

where $S_{j,\hat{\imath}}$ is the simulated flow output of parameter transfer scheme j at ungauged site $\hat{\imath}$, $\hat{S}_{\hat{\imath}}$ is the weighted averaged simulated flow output of all parameter transfer approaches at ungauged site $\hat{\imath}$, and j is the number of parameter transfer approaches

considered. Alternatively, one can weight average the regionalized model parameters of each parameter transfer scheme at the ungauged site.

It is significant to highlight that the functionality of the weighting approach is successively evaluated at each test catchment with the jackknife approach by comparing the performance of the weighted averaged simulated flow and the effectiveness of each individual parameter transfer strategy. The primary concept behind weighing the simulated flow outputs of each parameter transfer approach is to incorporate diverse information. This should reduce the runoff prediction uncertainty in the ungauged catchments of the study basin, in which the sporadic and systematic flaws of the SWAT results for the individual parameter transfer schemes are almost certain to be neutralized collectively.

6.2.3.6. Validation of the parameter transfer approach

The success of the parameter transfer approach should be evaluated by comparing the estimated and measured response characteristics for gauging station test watersheds. A leave-one-out evaluation technique is used to help validate the proposed approach because the number of gauged catchments in this study is limited to seven. For each test catchment, the runoff produced from the simulation using the best calibrated parameter and regionalized parameter is contrasted and evaluated to complete the validity of the suggested strategy.

6.2.3.7. Uncertainty analysis of the hydrological model

Hydrologic model calibration is useless and imprecise in the absence of uncertainty (Abbaspour, 2015; Moges et al., 2021). To anticipate hydrologic conditions in gauged and ungauged catchments, a calibrated and regionalized model should account for parameter uncertainty. The SUFI-2 tool (Abbaspour et al., 2004) is employed to estimate the hydrologic model predictive uncertainty. SUFI-2 uses the Latin hypercube sampling procedure to sample from the parameter

intervals, and the initial parameter ranges are updated at each iteration until a narrower parameter uncertainty range is obtained. It is evaluated based on the closeness of the percentage of observations covered by the 95% prediction uncertainty (p-factor) to 100% and the relative width of a 95% probability band (r-factor) to zero (Abbaspour et al., 2004). A 100% p-factor and 0 r-factor represent a simulation that exactly corresponds to the observed data. Most of the observations can be covered by the 95% interval (p-factor) at a large parameter range (r-factor). Therefore, the two indicators must be used to evaluate the model uncertainty results. The objective function and the range of physically suitable parameters are specified in the SUFI-2 phases. The 95PPU is calculated and evaluated based on the two performance measures (p-factor and r-factor). It has been claimed that an effective simulation requires a p-factor of greater than 70% and an r-factor of less than 1.2 (Abbaspour et al., 2015). The following equation can be used to calculate the p-factor and r-factor:

$$p-\text{factor}=\frac{\sum_{t=1}^{T}Z_t}{T}\times 100, Z_t=\begin{cases}1, if\, Q_t^O\in\left(Q_{t,2.5\%}^S, Q_{t,97.5\%}^S\right)\rightleftarrows\\ 0, \quad otherwise\end{cases} \tag{6.13}$$

$$r-factor=\frac{\frac{1}{T}\sum_{t=1}^{T}\left(Q_{t,97.5\%}^S-Q_{t,2.5\%}^S\right)}{\sigma_{obs}} \tag{6.14}$$

where $Q_{t,\rightleftarrows 97.5\%}^S$ and $Q_{t,\rightleftarrows 2.5\%}^S$ denote the upper and lower simulated boundaries at time *t*, respectively. The higher boundary is determined at the cumulative distribution's 97.5% level, while the lower boundary is calculated at the cumulative distribution's 2.5% level, *T* represents the observed data's time step number, *S stands for "simulated," O for "observed," t for "simulation time step"*, σ_{obs} represents the observed data's standard deviation, Q_t^O represents the observational values at time step *t*, and Z_t equals 1 when the observed discharge falls inside the 95PPU region.

6.3. Results and Discussion

6.3.1. Model parameter estimation in gauged catchments

The most sensitive flow parameters for the OGRB and UBNRB are determined to be nine (i.e., CN2, ALPHA_BNK, GW_DELAY, ESCO, HRU_SLP, GW_REVAP, SOL_AWC, SOL_K, and OV_N) and six (i.e., CN2, ALPHA_BNK, GW_DELAY, GWQMN, OV_N, SOL_K), respectively, both of which have p values under 0.01. Figure 6-3 shows the variability of the study flow parameters' p values, from low to zero. Based on the average p value of all stations, CN2 was characterized as the most delicate variable (see Fig. 6-3).

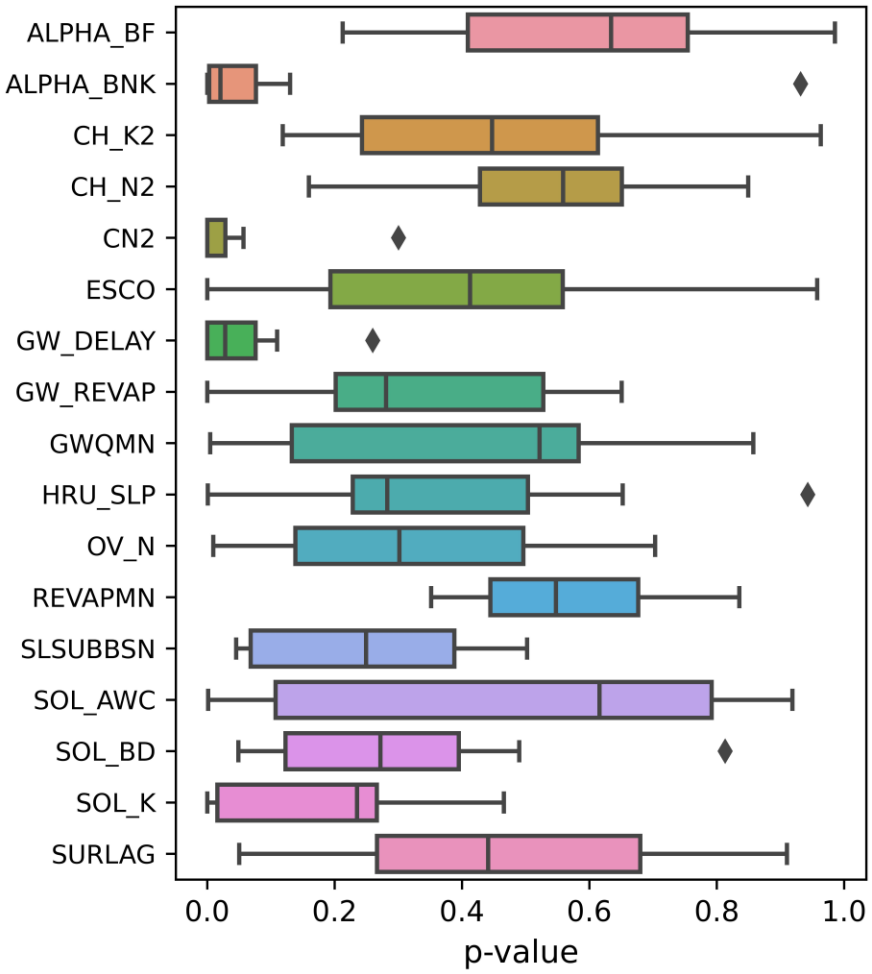

Figure 6.3. Variations in p value for the flow parameters of the SWAT model in the study area

Figures 6-4 and 6-5 display the measured streamflow, best-simulated streamflow, and 95% prediction uncertainty (which incorporates all model uncertainties) for the gauged catchments in the study basins. As noted earlier, we used the proportion of data falling within the 95% probability bound (95PPU) (p-factor) and the proportional width of the 95% probability band (r-factor) as performance indicators for the model to calculate the uncertainty.

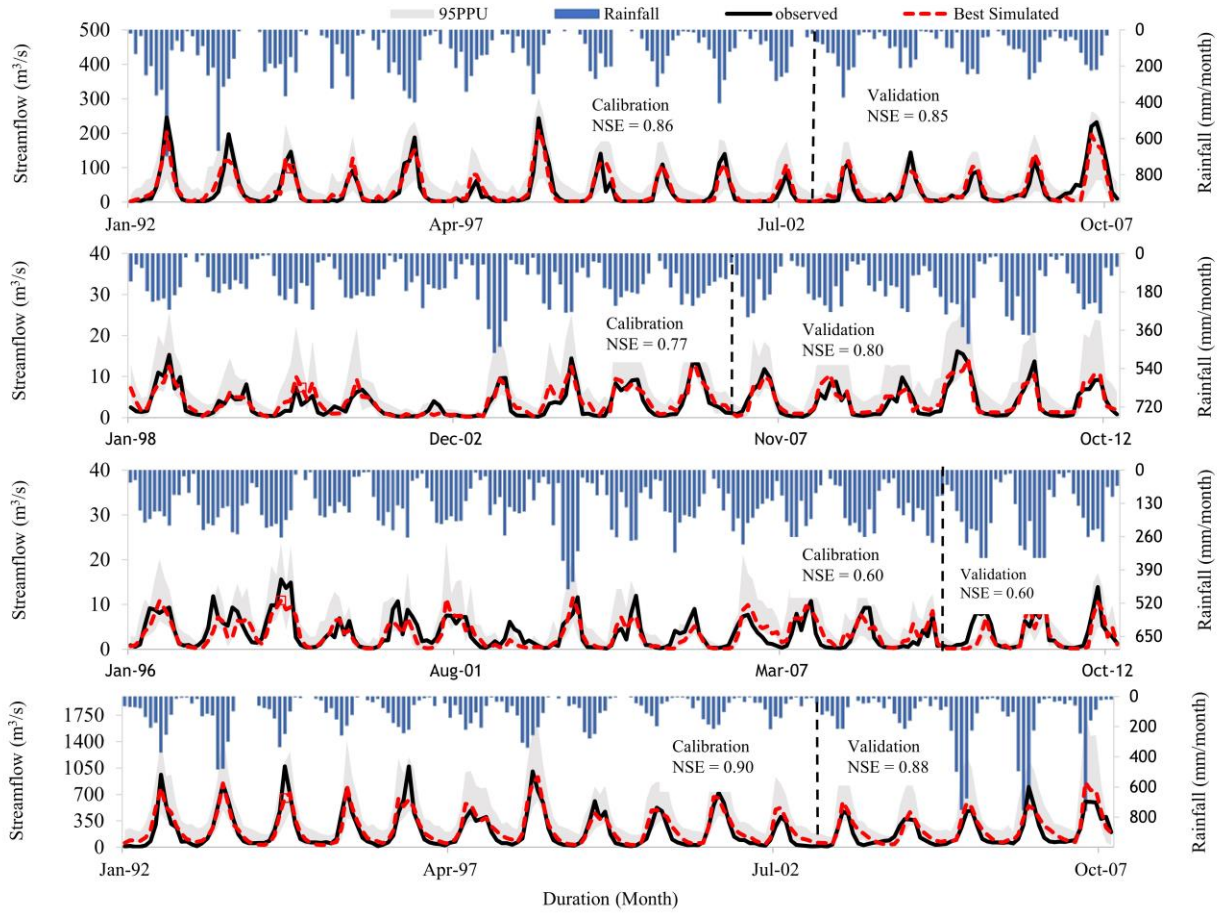

Figure 6.4. Model simulation with 95% prediction uncertainty (top-down: Gojeb, Sheta, Gecha, and Abelti watersheds in the OGRB)

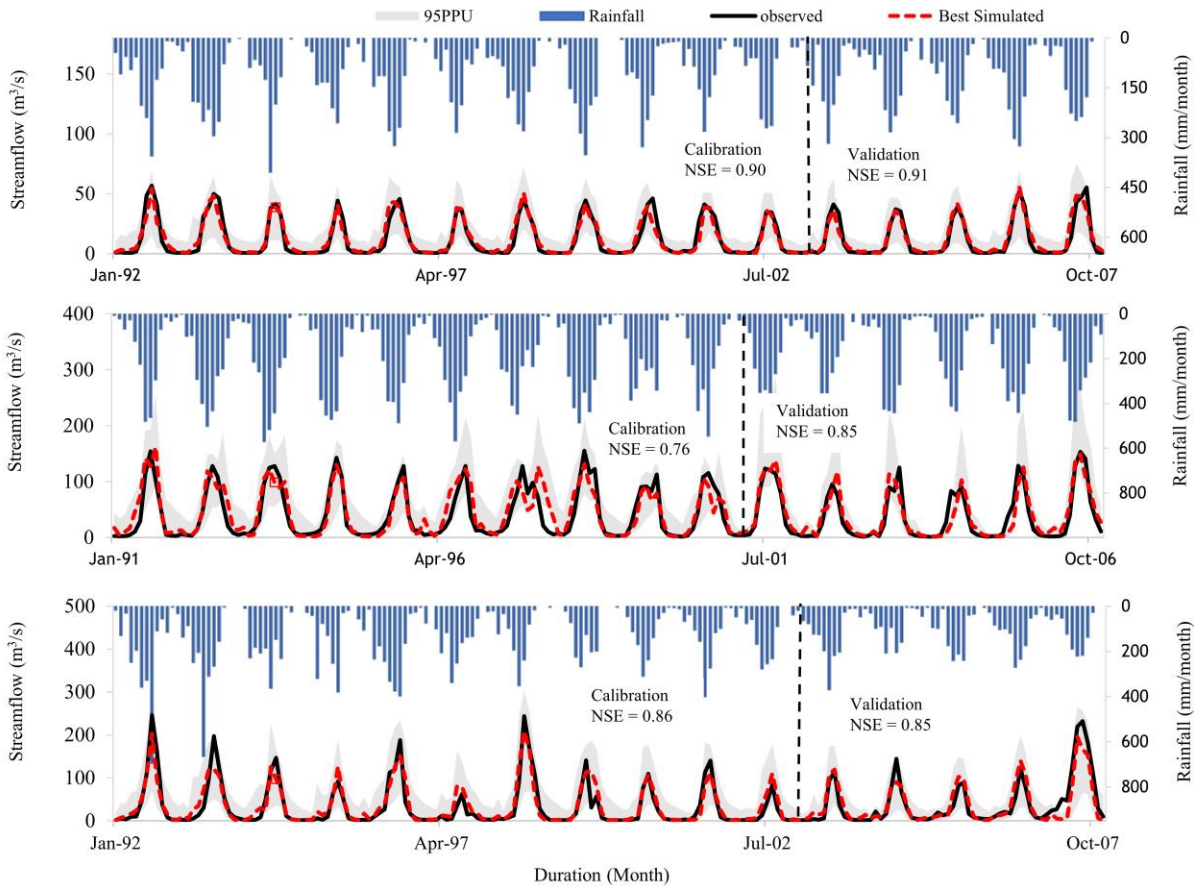

Figure 6.5. Model simulation with 95% prediction uncertainty (top-down: Guder and Dedesa (both watersheds in the UBNRB) and Wabi watershed (in the OGRB))

Furthermore, the uncertainty range in the case of the OGRB is relatively higher than the uncertainty of the UBNRB (see Figs. 6-4 & 6-5). Figure 6-4 shows p-factors of 0.75, 0.88, 0.71, and 0.76 and r-factors of 1.00, 1.15, 1.00, and 0.85 for the Gojeb, Gecha, Sheta, and Abelti catchments, respectively. On the other hand, in Figure 6-5, the p-factors were 0.88, 0.73, and 0.79, and the r-factors were 1.10, 0.99, and 1.16 for the Guder, Dedesa, and Wabi catchments, respectively (see Table 6-1). The p-factors and r-factors for every gauged catchment in the OGRB and UBNRB are acceptable, which indicates that the parameter uncertainties were within the desired ranges for the watersheds.

In the OGRB, Gecha and Sheta were two smaller watersheds where calibrated SWAT modelling underperformed and larger watersheds where it worked relatively well (see Table 6-1). The r-factors and p-factors determined for the OGRB watersheds on average were 1.05 and 79%, respectively. In UBNRB watersheds, the p-factors and r-factors were, on average, computed at 83% and 0.98, respectively. The uncertainty analysis showed that SUFI-2 did a worse job of conserving the observations in the OGRB watersheds than in the UBNRB watersheds. It is known that poor measurement of hydroclimatic data can substantially increase hydrological predictive uncertainty. The OGRB scenario may have a high level of uncertainty as a result of the distributed spatial variability of monitoring stations and the quality of hydroclimatic data.

Table 6-1. SWAT model performance metrics in the study watersheds

Watershed	Calibration				Calibration Period	Validation				Validation Period
	NSE	R^2	p-factor	r-factor		NSE	R^2	p-factor	r-factor	
Abelti	0.90	0.90	0.76	0.85	1992-2002	0.88	0.88	0.77	1.04	2003 - 2007
Wabi	0.86	0.86	0.79	1.16	1992-2002	0.85	0.86	0.88	1.08	2003 - 2007
Gojeb	0.79	0.80	0.75	1.00	1992-2002	0.79	0.80	0.73	0.99	2003 - 2007
Gecha	0.60	0.62	0.71	1.00	1996-2009	0.60	0.62	0.72	1.10	2010 - 2012
Sheta	0.77	0.79	0.88	1.15	1998-2006	0.80	0.81	0.88	1.15	2007 - 2012
Dedesa	0.76	0.77	0.73	0.99	1991-2001	0.85	0.86	0.76	0.65	2002 - 2006
Guder	0.90	0.90	0.88	1.10	1992-2002	0.91	0.91	0.93	1.18	2003 - 2007

6.3.2. Assessment of the reliability-weighted strategy

To assess the effectiveness of the reliability-weighted (RB) strategy, a total of seven gauging locations (five from OGRB and two from UBNRB) were chosen. The outcomes of the GM, SP, and PS methods were compared with those of the RB technique at each site (see Table 6-2 and Fig. 6-4).

The GM parameter transfer (poor-man) and PS approaches perform the worst across all test sites, accounting for 22.22% of the total, whereas the novel RB parameter transfer methodology

presented in this work outperforms the other methods by approximately 30%. With a performance rate of approximately 26%, the SP parameter transfer technique falls somewhere in the middle. Despite its lower performance rate, the GM approach outperformed the others during the calibration period at sites with substantially smaller and poorly modelled watersheds (see Table 6-2). This demonstrates how the Poor-man technique produces highly unpredictable model parameter values for the poorly modelled watershed. Generally, the GM approach resulted in NSE values between 0.28 at Sheta and 0.74 at Guder stations in the OGRB and UBNRB, respectively, throughout the calibration period. However, through the validation period, the method has extreme NSE values of 0.32 and 0.80 at Abelti and Gojeb, respectively. In the case of the SP technique, the parameters of the model in the ungauged catchments are being calculated employing the well-known inverse distance weighting (IDW) technique. Performance across the SP method varied from 0.23 in the Sheta watersheds of the OGRB to 0.81 in the Wabi watersheds with respect to the metric NSE (see Table 6-2).

Table 6-2. Performances of regionalization approaches during calibration and validation based on the NSE metric.

Watershed	Regionalization Performances during Calibration				On-site Cali-bration	Regionalization Performances during Validation				On-site Vali-dation
	SP	PS	GM	RB		SP	PS	GM	RB	
Abelti	**0.64**	**0.64**	0.47	**0.64**	0.90	**0.53**	**0.53**	0.32	**0.53**	0.88
Gojeb	**0.61**	**0.61**	0.52	0.59	0.79	0.74	0.74	0.80	**0.84**	0.79
Wabi	0.81	0.69	0.69	**0.82**	0.86	**0.70**	0.63	0.63	0.68	0.85
Guder	**0.74**	**0.74**	**0.74**	**0.74**	0.90	**0.68**	**0.68**	**0.68**	**0.68**	0.91
Gecha	0.34	0.26	**0.40**	0.39	0.61	0.64	0.49	**0.71**	0.69	0.61
Sheta	0.23	0.22	**0.28**	0.22	0.78	**0.55**	**0.55**	0.53	**0.55**	0.82
Dedesa	**0.54**	0.51	**0.54**	0.51	0.75	0.75	**0.77**	0.74	**0.77**	0.85

Note: Values in bold indicate optimum results among the regionalization methods

In the physical similarity approach, the catchment descriptors (see Table 6-3) of the gauged watersheds were grouped into three similar homogeneous groups. The grouping is performed using the most commonly used grouping techniques of k-means and principal component analysis algorithms. In terms of NSE, the PS technique performs between 0.22 and 0.77 in the Sheta and Dedesa watersheds. Both the Sheta and Gecha watersheds have low performance (see Table 6-2). When compared to the other techniques, the RB strategy performed the best overall in 29.63% of the test catchments. The remainder of the procedures examined in the study basins yielded 25.93%, 22.22%, and 22.22%. for the SP, PS, and GM approaches, respectively. As a result, the RB parameter transfer technique showed performance gains of approximately 4% over the second-best parameter transfer strategy for predicting runoff in ungauged catchments (see Table 6-2). The summary of this study's findings in relation to the parameter transfer methodology implies that the RB framework created in this research can be used as a similar best way to precisely estimate runoff in ungauged basins.

Table 6-3. Catchment descriptors statistics (climate descriptors are mean annual value of 32 years)

Watershed	Area (km^2)	Long (E^o)	Lat (N^o)	AGRL (%)	FA (%)	Aridity Index (-)	Mean Elevation (m)	P_{av} (mm)	T_{av} (^oC)
Abelti	15746	37.58	8.23	61	18	0.11	1917	1409.26	19.30
Wabi	1866	37.77	8.25	59	18	0.11	2427	1323.18	20.87
Gojeb	3577	36.38	7.42	30	64	0.08	1909	1861.57	19.67
Gecha	175	36.22	7.28	40	57	0.08	1802	1861.57	19.67
Sheta	190.6	36.23	7.28	36	40	0.08	1971	1861.57	19.67
Dedesa	1806	36.45	8.05	42	38	0.06	2150	2092.66	18.60
Guder	524	37.75	8.95	68	10	0.11	2516	1230.29	19.17

Note: Pav = mean annual rainfall, AI = aridity index, AGRL = agricultural land, FA = forest area, and T_{av} = mean annual temperature

Table 6-2 and Figure 6-6 provide a summary of the calibration and validation period predictions for the regionalized and calibrated models for the research basins. Figure 6-6 presents the boxplot that shows the performance variation in the procedure for transferring parameters based on NSE values in each test catchment. The regionalized model runoff predictive performance in terms of the reliability of the effectiveness of the model that was calibrated on-site in the Wabi watershed of the OGRB with the RB, SP, PS, and GM methods resulted in 95.35%, 94.19%, 80.23%, and 80.23% during the calibration period and 80%, 82.35%, 74.11%, and 74.11% during the validation period, respectively. This shows that the proposed parameter transfer approach, RB, runoff predictive performance at the ungauged catchments during the calibration and validation period provided a very comparable result to that of the optimal at-site calibrated model. The NSE during the calibration period using the at-site calibrated model varied within 0.61 – 0.90 and that using the RB-based regionalized model varied within 0.22 – 0.82. On the other hand, the NSE during the validation period using the at-site calibrated model varies within 0.61 – 0.91, and using the RB-based regionalized model varies within 0.53 – 0.84. The accuracy of meteorological data is a major determinant of the simulation accuracy of hydrological models. The OGRB has few and dispersed weather gauging stations, which makes the findings of hydrologic simulation rather iffy (see Table 6-2 & Figure 6-6).

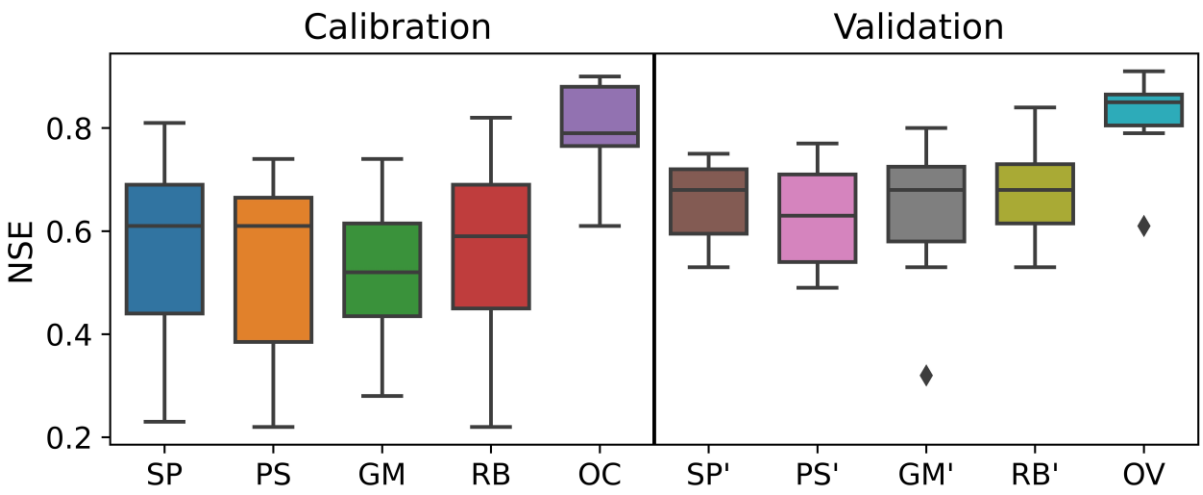

Figure 6.6. Regionalization performances based on NSE metrics during calibration (left) and validation periods (right). (*Note: GM = global mean, PS = physical similarity, RB = reliability-weighted, and SP = spatial proximity*).

As demonstrated above, acceptable model calibration and validation at-site may not guarantee consistent regionalization capabilities to the target ungauged catchment. Even if the models are adequately calibrated and their performance metrics are acceptable, they may not be very transferable (e.g., Gecha and Sheta catchments during calibration, Table 6-2). Following an in-depth examination of the model performance of the Getcha and Sheta catchments, it becomes clear that certain issues must be addressed. The complicated topography of these places, combined with the lack of precipitation gauges, are most likely the key contributors to this unsatisfactory performance. In addition, hydrological modelling can be complicated by various factors such as rough terrain, local climate differences, and differences in land cover within smaller catchments. These factors depend on many variables such as land management activities, vegetation, and anthropogenic environmental change. Anthropogenic activity plays a significant role in regulating the climate effect induced by land use and land cover changes. Different land uses in different catchments can yield significantly different hydrologic outputs, as highlighted by a study

conducted by Lin et al. (2009). This finding is consistent with previous studies by Beck et al. (2016) and Arsenault and Brissette (2016). During the validation period, however, a couple of transferable approaches outperformed the at-site validation, particularly the RB strategy.

The executed RB strategy demonstrated its potential in ungauged catchment regionalization at a test regional scale; however, global and continental levels are not considered in the analysis due to a lack of data and the scope of the study. As a result, more study is needed to prove the model's validity on a larger scale to gain a more comprehensive understanding of the model's capabilities and limitations, resulting in more informed decision-making.

6.3.3. Uncertainty analysis of the proposed method at the ungauged catchments

In the gauged catchment scenario, going from the calibration to the verification period resulted in an increase in median Nash-Sutcliffe model efficiency from 0.79 to 0.85 on average for both periods, showing a 0.06 temporal gain in model efficiency. The minor increase suggests that the model is not overparameterized, which could lead to poor model performance otherwise. When several regionalization strategies are compared, it is discovered that transitioning from gauged to ungauged catchments leads to a spatially larger loss in model performance (see Table 6-2). In comparison to the other regionalization procedures, based on the median efficiency of the Nash-Sutcliffe model, the newly presented strategy closes the gap with the second-best performing option (by approximately 0.01). The newly suggested method also temporarily reduces the loss as of the on-site measurement (by approximately 0.02). It even outperformed the on-site validation at the gauged station in the Gojeb watershed. However, the success of this approach depends on how well the characteristics of the donor catchment align with those of the recipient. The presence of significant similarity across watershed parameters in catchments located in the same climatic and geographic location may result in similar hydrological responses and model prediction

uncertainty, according to different research findings (Arsenault and Brissette, 2016; Sellami et al., 2014). Poor model performances in the ungauged catchment(s) are also anticipated by the proposed reliability-weighted parameter transfer technique, which is associated with poorly modelled hydrographs in the gauged catchment(s), especially in catchments with small catchment sizes. In fact, determining whether poorly modelled gauged catchment(s) parameters should be transferred to ungauged catchment(s) is difficult. Because features transferred from poorly modelled gauged catchment(s) can provide useful variability for ungauged watershed modelling (Oudin et al., 2008), this idea, however, requires further investigation and examination in future work with a larger number of comparable catchments, as it is far from validated in the current study.

6.3.4. Combining the strengths of parameter transfer schemes

The integration of the three parameter transfer schemes (i.e., SP, PS, and RB) performed better than the integration of the three parameter transfer schemes (i.e., SP, PS, and GM) in terms of the reliability of the test catchments. In the case of OGRB, the smaller catchments (Gecha and Sheta), all regionalization techniques, including the combined ones, performed unreliably during the calibration period. Therefore, the outputs of RB, PS, and SP are combined based on their reliability at the test catchments. The combined runoff of the three regionalized models was checked using the test data to estimate the model's effectiveness for entirely unseen data and to confirm the combined regionalized model's actual prediction power. The results reveal that the combination of the three regionalized model outputs significantly improves the NSE of the individual models (PS, SP, and RB) in the majority of test catchments. The combined outputs of the three models did not improve the performance over the best performing individual model, RB, for the Wabi and Gojeb catchments during the calibration and validation periods, respectively. In the OGRB, the combined

regionalized model shows an improvement over the best-performing "RB" strategy with respect to the NSE, which varied from 1.20% in Abelti to 9.10% in Gojeb during the calibration period. In the case of UBNRB, the performance improvement falls within 1.30% to 5.00% in Dedesa. The outcomes of this investigation underline the fact that combining the advantages of parameter transfer systems reduces the degree of uncertainty in runoff prediction in ungauged catchments. This conclusion is consistent with the conclusions of earlier research (Arsenault and Brissette, 2016; Li et al., 2019). Generally, the study recommends the integration of regionalized models based on their reliability.

6.4. Conclusions

Understanding the hydrological processes and the determination of the frequencies and magnitudes of streamflow are crucial for better oversight of available water resources. A significant obstacle to accurately assessing the water resources of the basin is the accessibility of data for hydrologic modelling. For example, nearly 70% of the OGRB area is ungauged. Therefore, the primary goal of this research was to propose a robust approach to accurately estimate the surface water resources in ungauged catchments. This study proposed the RB approach as an alternative strategy to predict runoff in ungauged catchments. The RB was evaluated in view of the three commonly used parameter transfer schemes: (1) global mean, (2) physical similarity, and (3) spatial proximity. The results show that the RB approach outperformed all three regionalization approaches (approximately 30%) for the test catchments. In addition, the RB-based regionalization model across all the test catchments achieved 66.65% and 75.11% regarding the success of the at-site calibrated model for OGRB and UBNRB, respectively, during the calibration period. Similarly, the RB-based regionalization model across all the test catchments achieved 85.34% and 82.65% perception of the calibrated model on-site for OGRB and UBNRB, respectively, during the

validation period. As a result, the parameter transfer technique created for this work could be applicable for similar ungauged basins.

When several regionalization strategies are contrasted, it is discovered that transitioning from gauged to ungauged catchments results in a spatially larger loss in model performance. Based on the median efficiency of the Nash-Sutcliffe model, the newly proposed strategy minimizes the discrepancy (by approximately 0.01) when compared to the second-best performing option. The newly suggested method also temporarily reduces the loss as of the on-site measurement (by approximately 0.02). It even outperformed the on-site validation at the gauged station in the Gojeb watershed. However, the success of the approach depends on how well the characteristics of the donor catchment align with those of the receiver.

Alternatively, the findings of the analysis demonstrated that acceptable at-site model calibration results may not guarantee consistent regionalization capabilities to the target ungauged catchments. This analysis is comparable to the findings of a study by (Arsenault and Brissette, 2016). However, during the validation period, a couple of regionalization strategies, most notably the RB approach, outperformed at-site validation. As a result, more research might be required to improve regionalization efficiency in ungauged catchments.

In conclusion, this study demonstrates how careful selection of desirable catchment areas, whose model parameters have been optimized and are being used to produce streamflow in designated ungauged watersheds, as well as output combining the relative relevance of various catchments based on their reliability, could enhance runoff estimates in ungauged locations. Hence, three key hydrological issues are identified: (1) identifying the most crucial flow parameters; (2) a reliable approach for estimating surface runoff for ungauged catchments; and (3) research that can be used

to develop the idea of combining the strengths of different parameter transfer schemes to reduce the uncertainties of runoff modelling in ungauged catchments.

A novel reliability-weighted approach of regionalization in hydrological modelling is demonstrated in this work using a relatively small number of gauged catchments at the regional scale. Due to a paucity of data and the scope of the study for the Omo-Gibe and Upper Blue Nile basins, which are treated as samples in the analysis, future research may build on this work and evaluate its validity at wider continental and global dimensions.

7. Multi-Objective Cascade Reservoir Operations Under Seasonal Streamflow Variability: A Hydro-Economic Model

Abstract

Our ability to manage river basin systems while meeting competing multisectoral needs in the face of an increasingly uncertain future is strongly reliant on reservoir operations. These issues underscore the need for novel problem-solving methodologies that are effective and efficient in recognizing the multisectoral tradeoffs that underpin diverse reservoir operation strategies. Due to its versatility in incorporating many sources of uncertainty and ability to address numerous objectives, evolutionary many-objective direct policy search (EMODPS) is becoming more significant in this area. The effectiveness of cutting-edge parallel techniques for the autoadaptive Borg multiobjective evolutionary algorithm (MOEA) to support EMODPS is evaluated in this paper. The Omo Gibe River Basin system is the subject of our analysis, which faces competing sectoral needs for hydropower generation, flood management, public and private irrigated farmland, flood recession farming, and environmental flows. The results of the model showed reliable and robust optimal solutions, enabling the evaluation of the tradeoffs between revenue generation, minimum environmental flow provision, and reservoir storage conditions. Under the existing scenario, the hydropower can produce up to 4.6 billion ETB, while the irrigation revenue is 720 million, which is expected to increase faster than hydropower revenue in the near-future scenario, up to 9 billion, whereas hydropower revenue will produce 10 billion, creating more competition, higher water usage, and necessitate better resource management. In addition, the renovated Gibe III Power Station's hydropower production can increase by approximately 65% in 2019 compared to the actual hydropower production. This demonstrates how evolutionary algorithm models can be useful in practical reservoir operations.

Keywords: Borg MOEA, Reservoir Operation Management, Multi-Objective, Trade-off Analysis.

Bahru M. Gebeyehu, Asie K. Jabir, Getachew Tegegne, and Assefa M. Melesse (2023). multiobjective Cascade Reservoir Operations Under Seasonal Streamflow Variability: A Hydro-Economic Model.

7.1. Introduction

Because of the needs of a rising population, climate change-related decisions, and the ongoing discussion over how to maintain natural resources, managing river basin systems is a key global concern. The inherent multisectoral options of reservoir operations remain a prominent focus of research due to the computer requirements and mathematical difficulties they present (Salazar et al., 2017). Emerging computing platforms provide the potential for enhancing reservoir management by reducing the degree of approximation and simplification that has historically made it difficult to employ high-fidelity simulation models (Giuliani et al., 2015a). Recent research in the water resources literature (Alba et al., 2013; Maier et al., 2014; Nicklow et al., 2010) indicates how meta-heuristics and parallel computing platforms are broadening the possibilities for simulation-optimization frameworks in a range of application domains.

Multiobjective evolutionary algorithms (MOEAs) are one of the most quickly growing disciplines in the literature on water resource planning and management. MOEAs are appealing because they provide a clear comprehension of the tradeoffs (Reed et al., 2013) in the systems, which has frequently been an important concern in water management (Cohon and Marks, 1975; Haimes and Hall, 1977). MOEAs employ population-based search to swiftly locate all Pareto-approximate solutions (see discussion in Coello et al. (2007)). Pareto-approximate solutions are those in which improving one goal involves sacrificing success in one or more other goals. MOEAs enable simulation-optimization applications with complex mathematical properties such as nonconvexity, nonlinearity, stochasticity, combinations of continuous and discrete choice variables, multimodality, and stochastic evaluations (Coello et al., 2007; Reed et al., 2013). Monte Carlo

(MC) simulations are increasingly being used to develop dependable operating rules in MOEA applications (Hamarat et al., 2014; Mortazavi-Naeini et al., 2015; Müller and Schütze, 2016; Tsoukalas et al., 2016; Zhang et al., 2017).

Even with its benefits, MOEA simulation-based search requirements can still be computationally expensive. Due to the stochastic nature of MOEAs, it is necessary to run them under numerous random seed trials to take into account potential performance variations for various randomly generated beginning populations or throughout randomized sequences of their search operators. These experiments increase the computational burden, which may restrict the scale or reach of the applications. The increasing use of MC simulations to assess unknown objectives further raises computer requirements and makes the search issues more challenging mathematically (Qu et al., 2018; Reed et al., 2013; Singh and Minsker, 2008).

Numerous study findings demonstrate the limitations of approximation in conventional MC-based evaluations of objectives. However, recent advancements in parallel MOEA strategies have the potential to reduce the computational bottleneck caused by costly MC-based function assessments while also enhancing the effectiveness, efficiency, and dependability of MOEAs when addressing noisy optimization (Alba et al., 2013; Maier et al., 2014; Reed and Hadka, 2014). Efficiency is the practice of achieving solutions using the least amount of computing time. Effectiveness requires Pareto approximation sets of good quality. Across all random trials, algorithmic reliability aims to retain high levels of effectiveness and efficiency. Much work has gone into recent research (Giuliani et al., 2017; Reed and Hadka, 2014) to evaluate the scalability of massively parallel runs that show the promise of MOEAs for widespread water management applications.

In this study, the Borg MOEA optimization method is used to address a reservoir operating problem in the Omo Gibe River basin (OGRB). As a result, the current work aims to analyse the

economic trade-offs between competing water needs using a hydroeconomic model based on this cutting-edge optimization approach. This study also examines the Borg MOEA's ability to provide approximate Pareto policies for the river basin.

Hydropower generation, flood management, public and private irrigated farmland, flood recession farming, and environmental flows are some of the competing water needs that the OGRB system must fulfil. Based on the earlier work of (Salazar et al., 2017), evolutionary multiobjective direct policy search (EMODPS) (Giuliani et al., 2015a) is used to effectively capture the tradeoffs between these conflicting goals. Simulation is utilized in the EMODPS technique to produce Pareto-approximate control plans for multipurpose reservoir operations. To boost its flexibility, EMODPS first parameterizes the control policy structure using global approximators such as artificial neural networks or radial basis functions. Using parallel Borg MOEA, the parameters are then optimized in relation to the aim functions. In this research, we show a decision analytic methodology that integrates reservoir policy formulation with many-objective optimization under uncertainty and visual analytics to investigate Pareto-optimal alternatives to assist water managers in redesigning the operation of their systems.

The research for this chapter is arranged as follows. The Materials and Methods are described in Section 7.2. The research area and data description are introduced in Sections 7.2.1 and 7.2.2, respectively. The methodology used in the study is described in Section 7.2.3. The investigation's results are presented in Section 7.3, and their analysis is covered in Section 7.4. Conclusions are included in Section 7.5.

7.2. Material and Methods

7.2.1. Study area and Data Description

This section has been deleted for brevity and to prevent repetition because Chapter 3 has more details in this regard. As a result, only a small portion of it—which is pertinent to the topic—is included in this section.

The Omo Gibe River basin system (Figure 7-1) serves a number of competing needs common to reservoir systems around the world, including (1) hydropower generation profitability, (2) flood damage mitigation, (3) state and private irrigated farming, and (4) environmental flow standards. These multisectoral needs must be managed while accurately recognizing hydroclimatic variability and changing social values.

Ethiopia is struggling to keep water supply and quality stable while meeting rising demand. In this regard, the country has developed basin-scale Integrated Water Resources Management (IWRM), seeing water as an economic and social good. According to the Ethiopian water resource strategy (MoWIE, 2001), water should be considered as a natural resource with economic value and charges should be levied for services delivered (Hailu et al., 2018). As a result, water is regarded as a critical and finite natural resource, and all charging systems and procedures must be aimed toward water conservation, protection, and efficient usage, while also promoting equity of access. Furthermore, Ethiopia frequently experiences droughts, and its water supplies are erratic, particularly in the Omo-Gibe Basin, underscoring the fact that water is a finite resource that should not be taken for granted. Consequently, water pricing is being addressed in this study because it is considered a critical economic and policy instrument for improving the sustainability of water management, encouraging conservation, and improving the quantitative and/or qualitative status of water.

In the last 20 years, the Omo Gibe River basin has seen the development of three power facilities: Gibe I, II, and III; a fourth, Koysha, is currently under construction. Gibe I is a modest dam with a power plant, but Gibe II is only a power plant connected by an approximately 26-kilometer-long tunnel just downstream from Gibe I. In comparison, Koysha and Gibe III are massive dams and power plants. The development of the Gibe III and Koysha mega dams in the basin has tremendously improved economic growth. Hydropower development in the Omo-Gibe River basin is expected to continue. Ethiopia is moving toward self-sufficiency in power production and 100% access to electricity by 2025, with the ultimate goal of becoming an energy exporter (Asress et al., 2013; Panos et al., 2016; Woodroofe, 1996). As of 2016, 75% of the population, primarily in rural areas such as the Omo Gibe River basin, lacked access to electricity, while Ethiopia's national electrification rate was only 25% (Panos et al., 2016; Zaniolo et al., 2021a). Omo hydropower facilities are being expanded to achieve the nation's ambitious targets. Furthermore, the enormous reservoirs behind the dams enable more consistent energy production in this dry region, where 90% of the annual runoff resides in a mere four months of the year (Sundin, 2017).

Due to storage reservoirs, large irrigated agricultural areas can now be cultivated (Avery and Eng, 2012). FDRE Sugar Corporation and the Ministry of Water, Irrigation, and Electricity have identified 1.5 million hectares of land as ideal for large-scale irrigated sugar development during GTP1(2010). This will enable the construction of 10 additional sugar factories, including Tana Beles (3), Arjo-Didessa (1), Wolkait (1), and Lower Omo Kuraz (5) sugar development projects. A large-scale sugar development proposal in Lower Omo Valley, which uses the Omo River, proposes to establish four sugar factories and cultivate sugarcane fields on net area of 100,000 hectares in order to alleviate the country's present sugar crisis (Ministry of Culture and Tourism of Ethiopia, 2018). The Ethiopian Ministry of Agriculture and Natural Resources has leased the

Kuraz Sugar Development Project to foreign and private investors in the area's south (Horne et al., 2011). According to Carr (2017a), the site will mostly be used for cotton crops. These projects divert water from the main canal, allowing crops to thrive because the area is too dry for rain-fed agriculture (Human-Rights-Watch, 2017).

In the Lower Omo Valley, approximately 200,000 indigenous people employ flood-recession agriculture as a key source of food for their cattle. Because the dry conditions of the Lower Omo cannot support rain-fed agriculture, this approach employs the annual inundations created by the Omo Gibe River's late summer flood pulse as a kind of irrigation (Carr, 2017a). The Omo Gibe River begins to rise in the Omo Valley in July, and it floods in August and September, dumping silt on the floodplain. Once the floodwaters recede, the river's banks can be planted to produce maize and sorghum, which are the local peoples' principal food sources (Carr, 2017a; Jordan et al., 2022). According to some study groups (Carr, 2017a; Human-Rights-Watch, 2017; Jordan et al., 2022), the strengthening of water infrastructure in the basin has slowed the flood wave, increasing the likelihood that there will not be enough land to cultivate crops in any given year, perhaps resulting in food shortages among indigenous people. However, the abnormally extended and widespread rains that began in June 2006 affected over 500,000 people; more than 600 people died as a result of the flash floods. Pastoralists also lost their cattle as a result of floods and other innumerable damages (EEPCO, 2009; Ocha, 2010; Woldegebrael et al., 2022). Finally, in addition to the services already described, the Gibe III reservoir is now offering beneficial recreational services.

Nederveen et al. (2011) reported that the total flood recession area is 11,037 hectares. Millet, maize, and sorghum are grown along the Omo River riverbanks after the flood subsides.

Agropastoral residents in lowlands use traditional hoes to cultivate crops on riverbanks, as per Eyasu et al. (2015). Appendix D contains crop information.

To sustain hydroelectric operations, water supply, and environmental flow requirements, water is frequently available at average flow rates. Low flow conditions, on the other hand, create significant trade-offs for operations while striving to mitigate negative effects. The issues are essentially antagonistic to one another. One aim may have to be set aside to achieve another. To reconcile these competing aims, a sophisticated, cutting-edge multiobjective optimization algorithm is necessary. As a result, in this study, we employ a simulation-optimization model via the Soil & Water Assessment Tool, as well as a sophisticated Multi-Objective Evolutionary Algorithm optimization tool, to find reservoir operating rules that balance all of these competing demands on the Omo Gibe River basin's water resources.

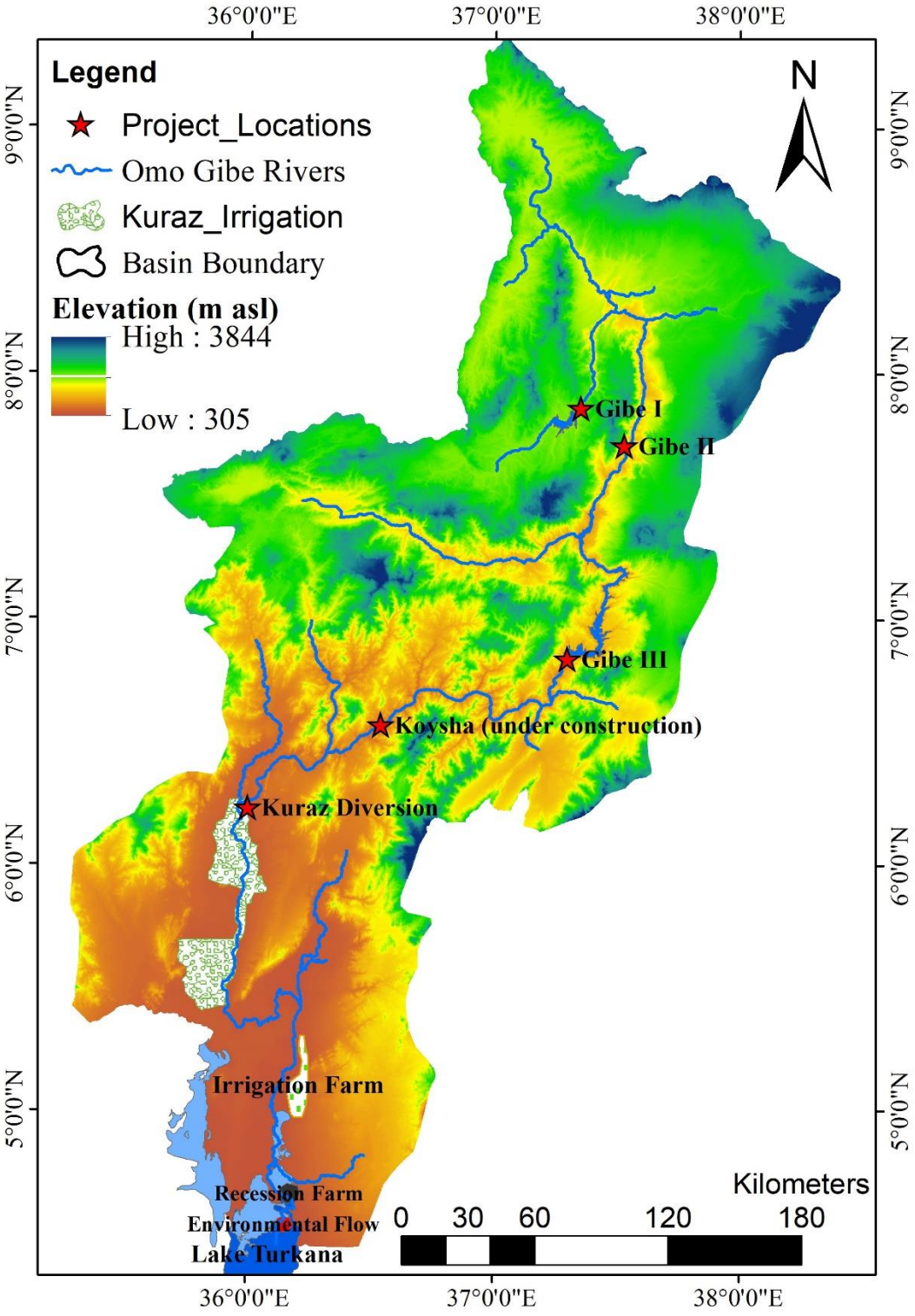

Figure 7.1. Omo Gibe River Basin showing all active hydropower and irrigation projects, as well as approximate locations of flood-recession farm and environmental flow requirements.

7.2.2. Data description

Chapter 3 of this dissertation contains details of the data that were used in this research. Such detail has been left out of this section for the sake of conciseness and to prevent redundancy. The reader is urged to refer to that section of the dissertation for further in-depth information. This part only covers the sections of the study that are relevant to its topic.

Table 7-1 presents the general characteristics of hydropower projects in the Omo Gibe River basin. When it is finished, the Koysha hydropower project will be the hydroelectric plant in the basin with the highest hydropower output capacity. Gibe III, however, wins the top spot in terms of reservoir capacity. When supplies are at their peak, the Gibe III hydropower project's reservoir capacity may be up to two and a quarter time greater than Koysha's (see Table 7-1).

Table 7-1. Highlights of hydroelectric projects in the Omo Gibe River basin (EEPCO, 2016)

Description	Unit	Gibe I	Gibe II	Gibe III	Koysha
Year of Completion	-	2004	2010	2016	Under Completion
Height of Dam	m	40.00	55.00	250.00	178.50
Capacity at FSL	MCM	839.00	1.90	15,245.00	6,540.00
Area at FSL	SKM	0.54	0.21	2.19	1.20
Full supply level (FSL)	m	1,671.00	1,431.50	892.00	680.00
Tail Water Level (TWL)	m	1,430.00	925.50	681.00	526.00
Maximum Flood Level	m	1,675.00	1,432.00	892.50	683.00
Plant Factor (LF)	-	0.45	0.44	0.40	0.34
Number of Turbines	No	3	4	10	8
Plant Installed Capacity	MW	184	420	1,870	2,160
Design Flow (Plant)	m^3/s	102	100	950	1,536
Minimum Release (Monthly)	MCM	89.60	65.88	250.34	505.96
Maximum Release (Monthly)	MCM	268.79	263.52	2,503.44	4,047.67
Minimum (Dead) Storage	MCM	182.00	0.70	2,945.00	483.00
Maximum Storage	MCM	839.00	1.90	15,245.00	6,540.00
Live Storage	MCM	657.00	1.20	12,300.00	6,057.00
Evaporation coefficient (B)	Km^2/ MCM	0.00064	0.11053	0.00014	0.00018
Catchment Area	SKM	4,225.00	4,304.00	34,150.00	44,325.00
Catchment Area Ratio w.r.t d/s Reservoir	%	98.16	12.60	77.04	

7.2.3. Methods

Given the complexity of competing multisector demands and severe hydroclimatic fluctuation that define the river basin system, the Omo Gibe cascade reservoirs are a suitable test example. The Evolutionary Multi-Objective Direct Policy Search (EMODPS) paradigm is utilized in this study to investigate how cascade reservoirs function (Giuliani et al., 2015a). The EMODPS framework provides a general way to identify reservoir control strategies that try to balance conflicts between

competing needs. Water is typically available at regular flow rates to sustain hydroelectric operations, water supply, and environmental flow needs. However, low flow conditions compel operations to make difficult trade-offs while attempting to reduce undesirable consequences. The EMODPS method for identifying potential control policies is simulation-based, as mentioned in the introduction. The operating rules are first parameterized using a mathematical function (such as piecewise linear functions, radial basis functions, neural networks, etc.), and the parameters of those functions are then optimized in relation to the operational goals of the reservoir using MOEAs (Salazar et al., 2017).

Direct policy search performs simulations under various hydro-climatic conditions to assess alternative policies. However, deterministic evaluations based on historical records may underestimate the effects of hydrologic variability and extremes (Cui and Kuczera, 2005). To address this, a stochastic ensemble was generated for the Omo Gibe reservoir system to assess the impact of hydroclimatic uncertainty on reservoir strategies. For further details on how to generate synthetic streamflow data for the study area, please refer to Appendix E.

Within a family of functions, B_θ, the EMODPS framework establishes a reservoir operating policy. Then, rather than optimizing the releases themselves, the parameters of those functions, B_θ, are adjusted in relation to operating goals, $\bar{B}$. The system is simulated once an initial parameter set is specified, and performance is assessed using the operating objectives. Through randomized mating, selection, and mutation processes, the iterative search process of MOEAs is then able to generate and evolve a Pareto-approximate collection of solutions over the competing problem objectives.

The same family of functions can be used to identify the historical operating policy and then refine it from a multiobjective standpoint, investigating the original operation for various trade-offs.

Technically, the following multiobjective problem must be solved to establish the policy parameters B_θ^*:

$$B_\theta^* = \arg min_{B_\theta} (\bar{B}) \tag{7.1}$$

where

$$\bar{B} = \left|-B^{hyd}, -B^{irr}, -B^{rec}, B^{flr}, B^{env}\right| \tag{7.2}$$

Each component of $\bar{B}$ is defined in Section 7.2.3.1, and Section 7.2.3.2 defines the structure of the operational policies B_θ. The Pareto-approximate set, which is the result of the optimization, is a collection of nondominated solutions where no single option outperforms all others in terms of all objectives. The performance of the objectives to be maximized is multiplied by -1 during the optimization process to ensure the correct verse of optimization.

7.2.3.1. Objectives of Operations

To account for the numerous and competing needs of different stakeholders in the basin, we define five operational objectives—hydropower production, irrigation water supply, flood recession farming, and environmental protection—as well as their constraints, calculated across the computing horizon (H).

1. **Hydropower:** To optimize the hydropower objective (to be maximized), the average monthly revenue from hydropower at the four power stations in the Omo River basin is summed up:

$$B^{hyd} = \frac{1}{H}\sum_{t=1}^{H}\sum_{j=1}^{Ny}\left(\rho_t * HP_t^i\right), \quad i = \text{GI, GII, GIII, K} \tag{7.3}$$

where HP_t (MWh) is the average monthly energy production and ρ_t (ETB/KWh) is the energy price (economic value/charge). The hydropower output is given by the equation $HP_t = \eta\gamma\bar{h}_{net}Q_t^{turb} * 10^{-6}$, where η is the turbine efficiency, $\gamma = 9810$ (N/m^3) is the

specific weight of water, $\bar{h}_{net}$(m) is the net hydraulic head, and Q_t^{turb}(m^3/s) is the average monthly turbined flow.

2. **Irrigation Water Supply:** Monthly revenue from irrigation (to be maximized) is defined as:

$$B^{irr} = \frac{1}{H}\sum_{t=1}^{H}((Y_t/D_t) * A_{irr} * \partial_{irr}) \tag{7.4}$$

where Y_t and D_t indicate the monthly delivery and demand, respectively. A_{irr} and ∂_{irr}, respectively, are irrigable area (ha) and economic value/charge (ETB/ha) of the irrigable crop.

3. **Recession Agriculture:** The goal of the recession in agriculture is to maintain the Lower Omo Valley's yearly flood pulse. It is determined as the monthly average squared distance between flow in the Lower Omo Q_t^{LO} and the desired artificial flood Q^{AF}(Jordan et al., 2022). The economic gain of this recession farming can be calculated as:

$$B^{flr} = \frac{1}{H}\sum_{t=1}^{H}\left(\left(\max\left((Q^{AF} - Q_t^{LO}), 0\right)\right)^2 * A_{flr} * \partial_{flr}\right) \tag{7.5}$$

where, A_{flr} and ∂_{flr}, respectively, are area of flood recession (ha) and economic value/charge (ETB/ha) of the flood recession crop.

4. **Environment:** Environmental flow need is defined as the monthly average deficit in relation to the minimum flow requirements (EEPCO, 2016). A quadratic function is used to penalize larger deficits while allowing for smaller, more frequent shortfalls.

$$B^{env} = \frac{1}{H}\sum_{t=1}^{H}\left(\frac{\max\left(Z_t^i - Y_t^i, 0\right)}{Z_t^i}\right)^2 \tag{7.6}$$

where Z_t^i (m^3) represents the required monthly minimum flow (Appendix F: Table F-1 contains detail information) and Y_t^i (m^3) the corresponding monthly release for reservoir *i*.

7.2.3.2. Model Formulation

The reservoir dynamics, which are based on mass balance equations for the storage volume (S_t^i) retained in each reservoir (i), form the fundamental foundation of the system model:

$$S_{t+1}^i = S_t^i + I_{t+1}^i - R_{t+1}^i - L_{t+1}^i \tag{7.7}$$

where L_{t+1}^i is the average loss from reservoir *i* throughout the course of the time period (*t, t+1)* and S_{t+1}^i is the final storage of reservoir *i* at the conclusion of period *t+1*. Inflow and release volume from each reservoir (*i*) in the interval (*t, t+1*) are represented by I_{t+1}^i and R_{t+1}^i, respectively. The released volume is given by $R_t^i = f(S_t^i, I_t^i, u_t^i, L_t^i)$, which depends on the storage S_t^i, the policy-required release decision u_t^i, the inflow I_{t+1}^i, and the loss L_{t+1}^i. The function f(.) describes the relationship between decision u_t and actual release R_{t+1} (Piccardi and Soncini-Sessa, 1991).

In this work, the reservoir level and time index are mapped into release decisions by parameterizing the control policies using Gaussian radial basis functions (RBFs) (Busoniu et al., 2010; Salazar et al., 2017). With RBFs, the k^{th} release policy in the vector $\boldsymbol{u}_t$ (with k = 1, …, N_u) is defined as:

$$u^k = \sum_{i=1}^{N} \omega_i^k \alpha_i \tag{7.8}$$

where n represents the number of RBFs (α_i). The weights are written in such a way that they add up to one (i.e., $\sum_{i=1}^{n} \omega_i = 1$) and are not negative (i.e., $\omega_i \geq 0, \forall i$). Each RBF is described as follows:

$$\alpha_i(\boldsymbol{x}) = \exp\left[-\sum_{j=1}^{m} \frac{(x_j - c_{j,i})^2}{r_{j,i}^2}\right] \tag{7.9}$$

where $\boldsymbol{c}_i$ and $\boldsymbol{r}_i$ are the m-dimensional center and radius vectors of the i^{th} RBF, respectively, and m is the number of input variables for $\mathbf{x}$ (specifically, time and reservoir level). The radii of the RBF must strictly be positive and the centres of the RBF must be contained within the restricted input space (i.e., using normalized variables, $\boldsymbol{c}_i \in [-1, 1]$ and $\boldsymbol{r}_i \in (0, 1)$. As a result, the parameter vector B_θ is defined as $B_\theta = [c_{i,j}, r_{i,j}, w_i^k]$, with i = 1, …., n, j = 1, …, m, and k = 1, …, N_u.

7.2.3.2.1 Storage restrictions in reservoirs

The maximum capacity and minimum (dead) storage of the reservoir limit the volume of storage that can be held there. The minimum storage volume allowed in the reservoir is the dead storage limit, which is formulated as:

$$C_{1,i}(t) = S_{t,i} - S_{min,i} \geq 0;\ \forall\ t \tag{7.10}$$

where $S_{min,i}$ is the minimum volume of reservoir storage i, and $S_{t,i} \geq 0$ is the starting storage of reservoir i at the start of the month t, t = 1, 2, 3, ..., 12.

The maximum storage limit, or capacity, of reservoir i, is denoted by the symbol $C_{2,i}(t)$,

$$C_{2,i}(t) = S_{max,i} - S_{t,i} \geq 0;\ \forall\ t \tag{7.11}$$

where $S_{max,i}$ stands for the maximum normal storage of reservoir i.

7.2.3.2.2 Reservoir release restrictions

Reservoir discharges should be limited between the smallest and largest releases. The lowest volume of water that can be discharged from a reservoir under the minimum release restriction is

$$C_{3,i}(t) = R_{t,i} - R_{min,i} \geq 0;\ \forall\ t \tag{7.12}$$

where $R_{min,i}$ is the minimum release of water from reservoir i, and $R_{t,i} \geq 0$ is the monthly release of water from reservoir i. The maximum volume of water that can be released from a reservoir shouldn't go beyond, for example, a bottom outlet, the capacity of the downstream channel, or the spillway. This can be formulated as:

$$C_{4,i}(t) = R_{max,i} - R_{t,i} \geq 0;\ \forall\ t \tag{7.13}$$

where $R_{max,i}$ stands for the maximum release of water that can be withdrawn from reservoir *i*.

7.2.3.2.3 Restriction on the yearly withdrawal of reservoirs

An extra constraint is introduced to ensure reservoir storage sustainability, ensuring that the starting storage of the first month of the following year is equal to or larger than the starting storage of the previous year. This can be formulated as:

$$C_{5,i}(13) = S_{13,i} - S_{1,i} \geq 0 \tag{7.14}$$

where $S_{1,i}$ indicates the beginning of storage *i* in the first month, and $S_{13,i}$ represents the reservoir storage *i* in the first month of the following year.

7.2.3.3. Multiobjective evolutionary algorithms

A contemporary Borg MOEA is provided by Hadka and Reed (2013) for multiobjective optimization problems. A dominance solution archive, autoadaptive six recombination operators, ε-box techniques for dominance sorting, and an injection approach (Kollat and Reed, 2006) to avoid stagnation are all included. In studies on a range of problems, Hadka et al. (2012), Reed et al. (2013), Woodruff et al. (2015), Salazar et al. (2017), Yan et al. (2017), and Al-Jawad et al. (2019) compared the performance of the Borg MOEA and competing evolutionary algorithms (such as NSGA-II, AMALGAM, -MOEA, SPEA2, etc.). According to Al-Jawad and Tanyimboh (2017), Borg MOEA has recently undergone an examination to address real-world reservoir operation, and the results demonstrate that Borg MOEA considerably enhances the solution.

The Borg MOEA begins with a population of N individuals representing N randomly generated parameter vectors B_θ, according to the DPS approach. To assess each individual's fitness, the program replicates the system while evaluating the objective vector $\overline{\boldsymbol{B}}_\theta$. The best individuals (those with the highest fitness values) are then selected, crossed, and mutated to create a new population

using the Pareto dominance criterion. After a predetermined number of iterations, this procedure is continued until a good approximation of the Pareto front is established.

7.2.3.4. Experimentation with Computation

Mathematical models were created for the Omo Gibe River basin due to the distinct operating goals and restrictions that each river basin has. Decisions about the management of water resources can be related to scales of time and space that span from subdaily to multiyear, and, accordingly, from a single location to the river basin. However, because the purpose of the research is to aid in the development of an efficient seasonal management policy rather than daily operational control, the model incorporates monthly values rather than shorter time scale values (Horne et al., 2016). In this work, we take into account two distinct formulations of the reservoir operating problem for the Omo Gibe River basin based on historical data and a stochastic ensemble of hydroclimatic factors. Equation (7.1) defines the first formulation, also known as the historical formulation, in which the operating objectives (see equations (7.3–7.6)) are assessed against the historical reality of the hydroclimatic variables, namely inflows and evaporation rates.

The Borg MOEA is employed in the proposed many-objective policy formulation technique (see Section 7.2.3) to optimize operating policies via DPS. According to Hadka et al. (2012) and Reed et al. (2013), the Borg MOEA is rather insensitive to parameter selection, with a high probability of success if the algorithm is performed for a sufficient number of iterations. As a result, we employ the default algorithm parametrization with a population of 100 as a starting point (see Hadka and Reed (2013)). Epsilon dominance is utilized to determine the resolution of operational objectives. In this study, we set epsilon values of 0.5 for hydropower revenue, 0.05 for irrigation water supply stability, and 0.001 for the

environmental flow requirement. The optimization was performed using an Ubuntu 20.04-powered computer (Core i7-6700 CPU, 3.4 GHz, 8 GB RAM).

7.3. Results and Discussion

7.3.1. Trade-off Performance Evaluation

Metrics such as the hypervolume metric (Zitzler, 1999), which examines the hypervolume of nondominated solutions, and the generational distance metric (Van Veldhuizen and Lamont, 1998) are widely used to evaluate the success of MOEAs. The majority of the design concepts for these (and other) measures are based on the true Pareto front, which is unknown in actual water resource management systems (Maier et al., 2014). As a result, their findings could be misleading. Hence, both qualitative and quantitative evaluation standards have been developed.

The performed results of the framework assessment are presented in both scenarios of existing and the near future. Figure 7-2 depicts the four-objective Pareto front of the Gibe III optimization findings with the primary axes for hydropower, recession farming, and environmental flow need in 2019. Larger brownish cubes in the upper right corner (see Figure 7-2) reflect the accumulation of optimal values for hydropower and the environmental flow need, whereas the results for recession farming were substantially poorer. The year 2019 was chosen to represent a recent, challenging dry season in which system operators were actively managing the trade-offs for this reservoir under low flow circumstances. Information collected from recorded values kept by the Ethiopian Electric Power Corporation confirmed the situation. For instance, using the enhanced optimization technique, the improved targets predict that Gibe III Power Station's hydropower production can rise by approximately 65% in 2019 compared to the recorded hydropower production (see Figure 7-3). Figure 7-4 also depicts the situation as it was in the Cascade Reservoir's existing power plants according to records kept by the firm.

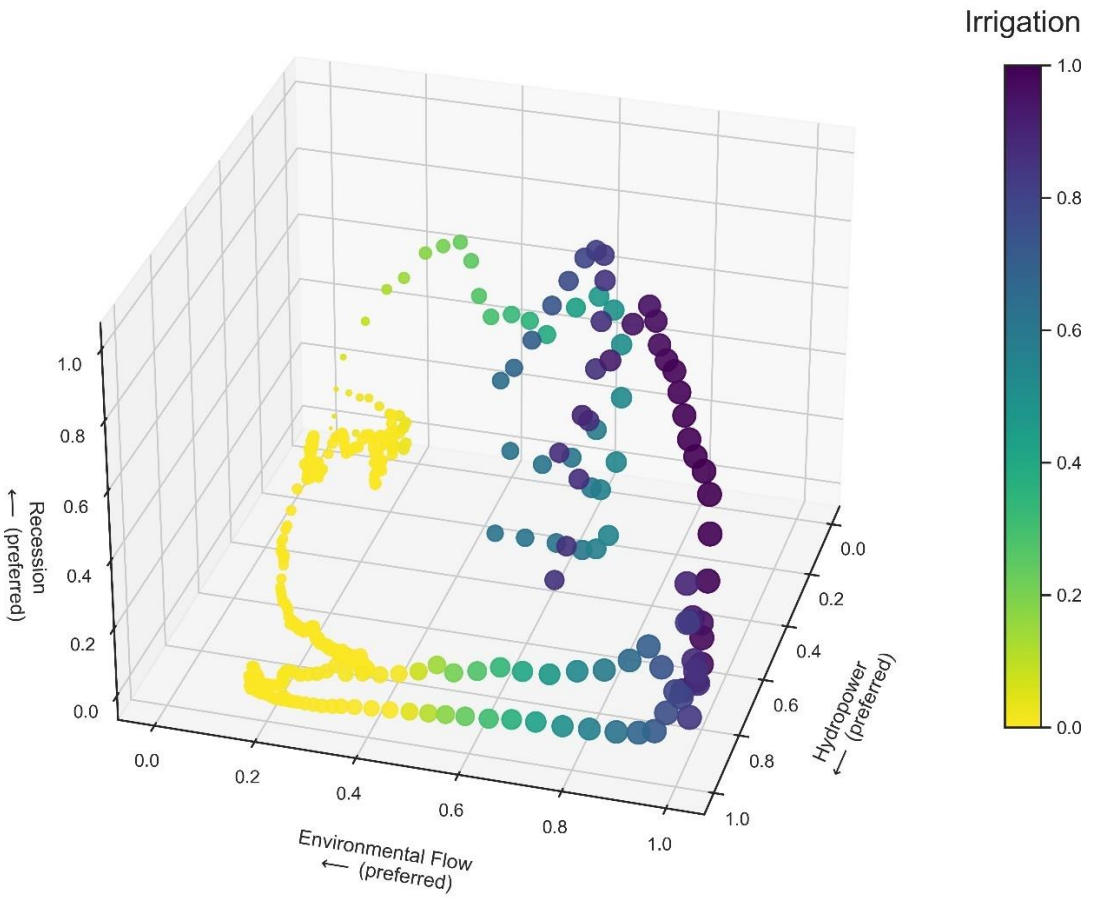

Figure 7.2. Pareto-optimal solution (scaled values) of the competing demands

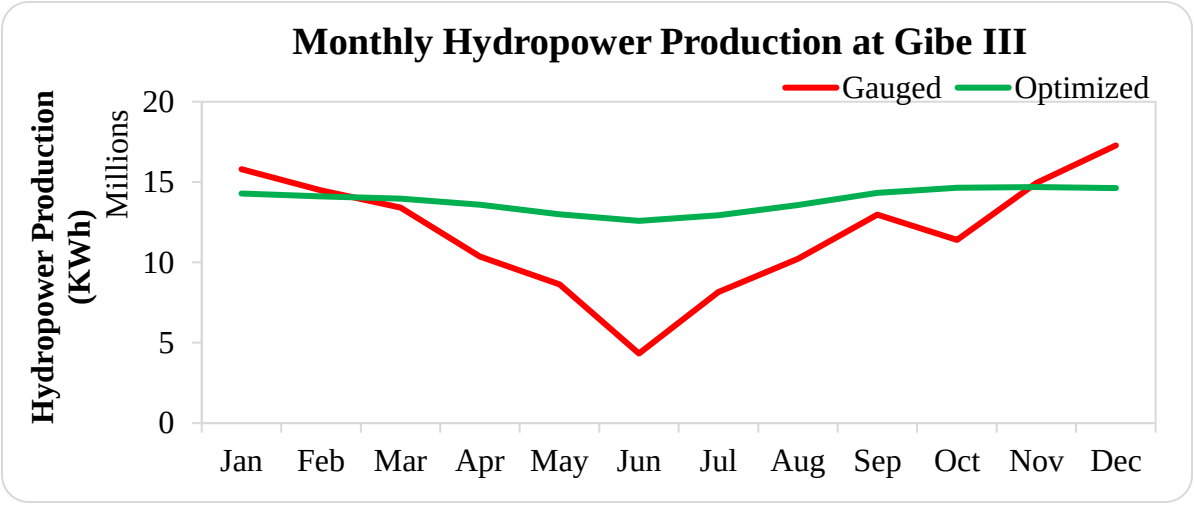

Figure 7.3. Comparison of optimized and gauged monthly hydropower production at the Gibe III power plant for 2019.

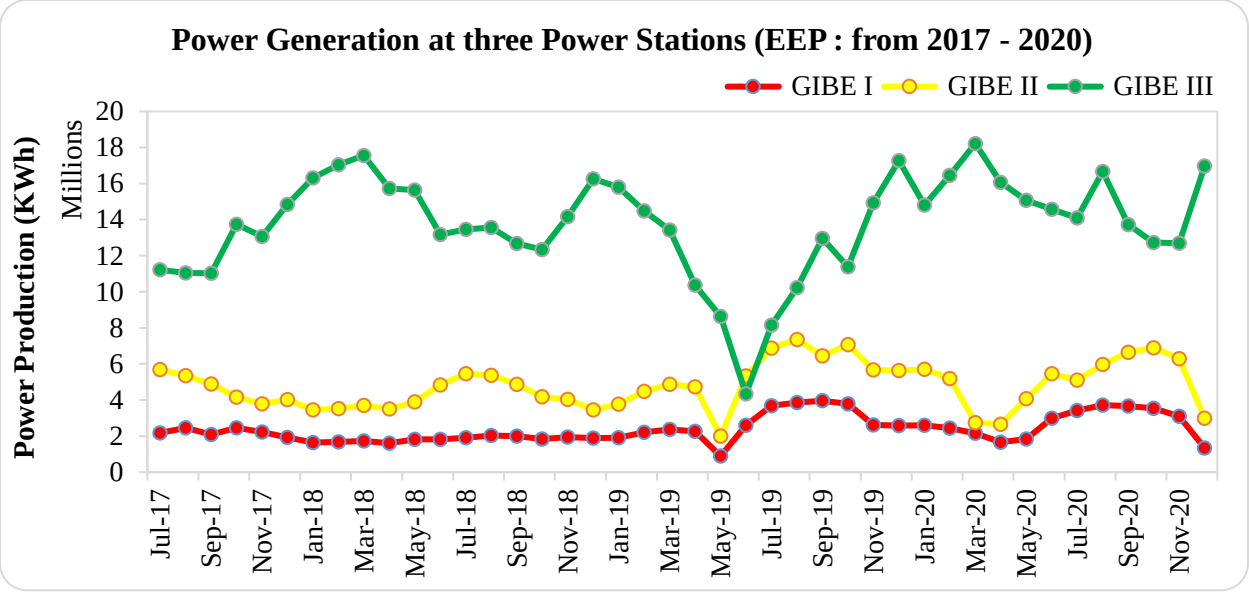

Figure 7.4. Monthly Power Generation at three Power Plants: Gibe I, II, and III showing critical low generation during May and Jun 2019.

A parallel axes figure is shown in Figure 7.5 as an additional visual aid for comprehending the important interacting trade-offs for the Gibe III reservoir. Each optimised solution is represented by a line that crosses the four axes, which correspond to the four objectives, at their respective performance levels in a parallel-coordinate diagram. The axes are set arbitrarily, and the preferred direction is shown with a range of performance for those particular objectives (see Figure 7.5). In addition, the optimal maximum and minimum objective values are displayed at the top and bottom of each axis. Furthermore, a horizontal line following the top of all axes would be the optimal answer. It's important to note that each line unequivocally represents a mead operating policy, which includes a varied range of policy variable combinations. Hence, the lines between two adjacent axes are used to identify the tradeoffs. Particularly when attempting to optimize the revenue generation represented by deep yellow line solutions, Figure 7-6 illustrates evident trade-offs. With an acceptable minimum provision of environmental flow, the revenue generated by irrigation and recession farming is only 720 and 26 million ETB, respectively. On the other hand,

hydropower production can generate a revenue of up to 4.6 billion ETB (see Figure 7.6). There is no doubt that hydropower production generates more revenue than other alternatives, especially under the current conditions.

Figure 7.7 illustrates the Gibe III reservoir storage volume of the optimal solutions for the given objectives. The minimum and maximum permissible reservoir capacity of Gibe III (see Table 7.1) are 2,945 and 15,245 MCM, respectively, hence the optimized values satisfy this basic constraint while operating under the scenario considered. Furthermore, the figure provides a clear visualization that can assist in making informed decisions and taking necessary actions.

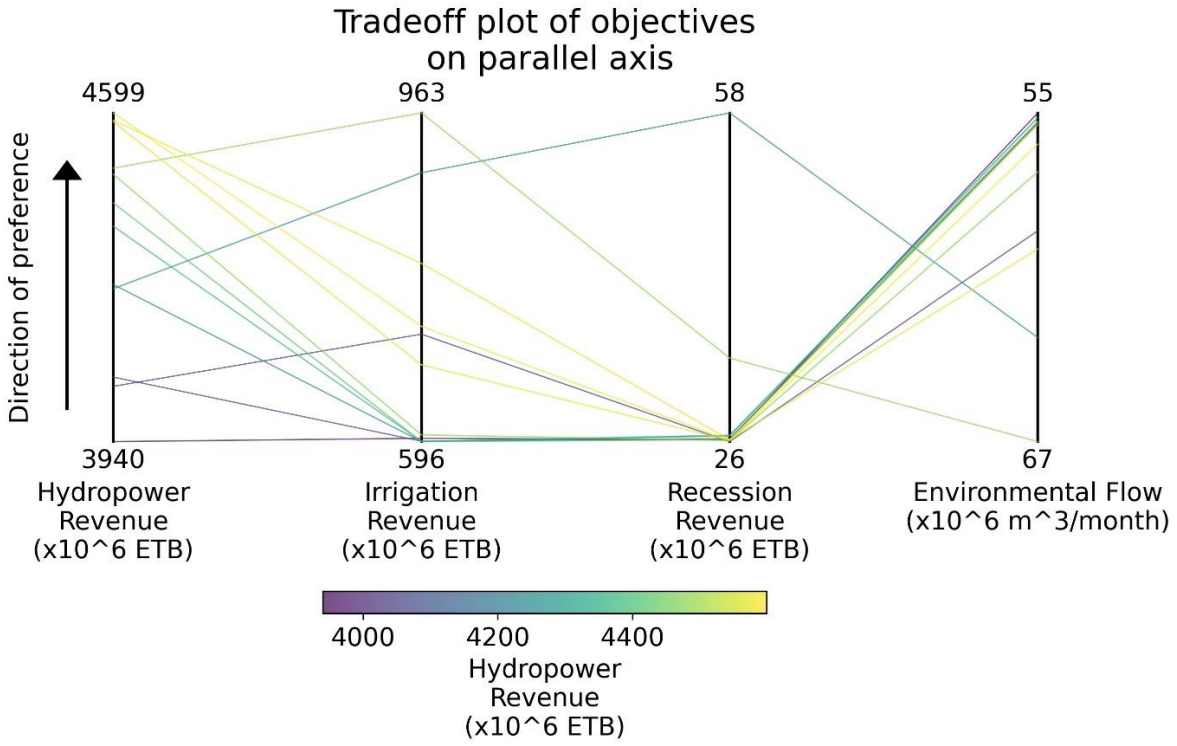

Figure 7.5. Tradeoff performances are contrasted using a parallel-coordinate plot under existing scenario case (Gibe III reservoir) in which the axes are positioned so that the desired direction is always upwards and the optimum objective values are presented for each objective.

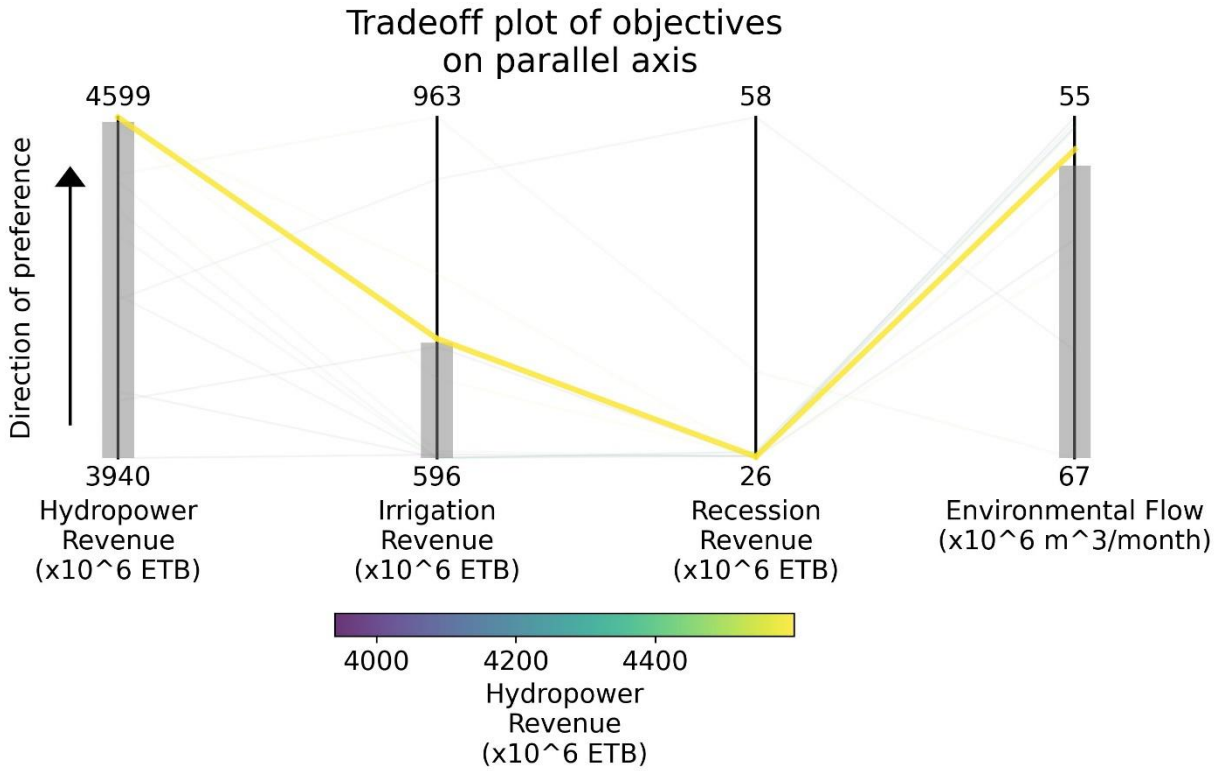

Figure 7.6. Tradeoffs between hydropower, irrigation, and recession revenue vs. environmental flow requirements under existing scenario (Gibe III reservoir).

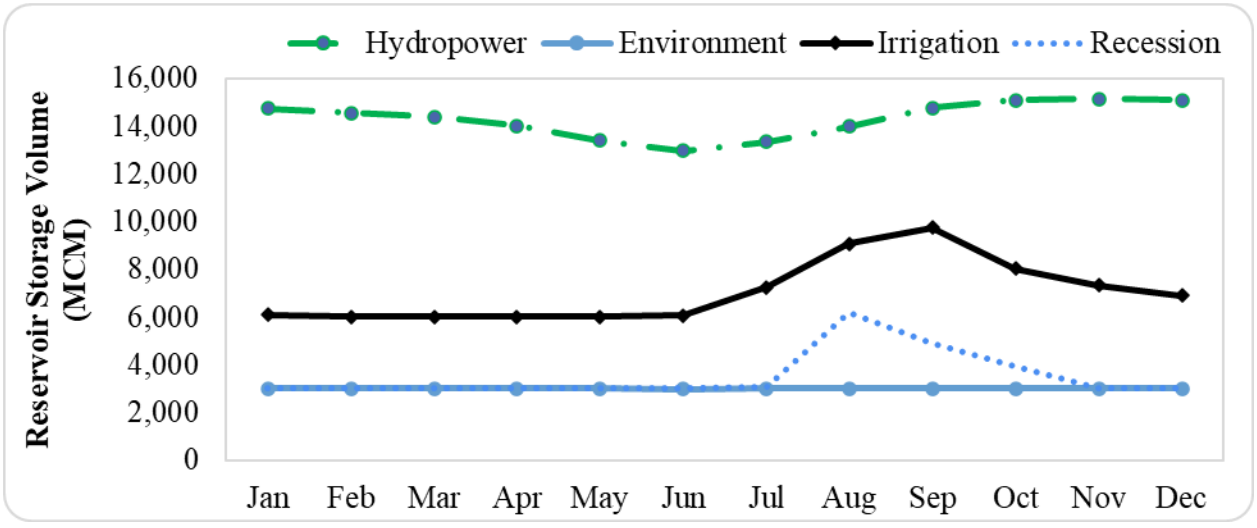

Figure 7.7. Gibe III reservoir storage volume of the optimized competing objectives

Figure 7.8 displays a parallel axes map for the Koysha reservoir under a near future scenario. As expected, in this scenario, the overall revenue generation will be significantly higher due to the expansion of hydropower production through the Koysha dam and the expansion of the irrigation command area. In Figure 7-9, there are clear trade-offs to consider when trying to optimize revenue generation. Two deep yellow line options represent the possible outcomes. When providing an environmental flow of 77 MCM that exceeds the minimum requirement, irrigation and recession farming can generate approximately 8.2 billion ETB and 865 million ETB of revenue, respectively. On the other hand, hydropower production has the potential to earn up to 10 billion ETB in revenue. The second line presents a scenario where both hydropower and irrigation systems are operating at full capacity, resulting in revenue creation of around 10 and 9 billion ETB respectively. In this scenario, the revenue generated during a recession is only 750 million ETB, with a monthly environmental flow provision of approximately 70 (see Figure 7.9). The rate of revenue increase from irrigation is projected to be faster in the near future scenario than in the current situation. It is possible that in the long-term scenario, which is not covered in this analysis, irrigation revenue may surpass hydropower generation revenue due to the availability of a vast irrigation command area. This could lead to increased competition, resulting in a higher demand for water by these competitors. As a result, there may be a need for better resource management to meet the increased demand.

Figure 7.10 illustrates the storage volume of the Koysha reservoir that corresponds to the optimal solutions for the given objectives. The reservoir's minimum and maximum allowable capacities, as indicated in Table 7.1, are 483 and 6,540 MCM, respectively. Thus, the optimized values satisfy this fundamental constraint while operating under the scenario.

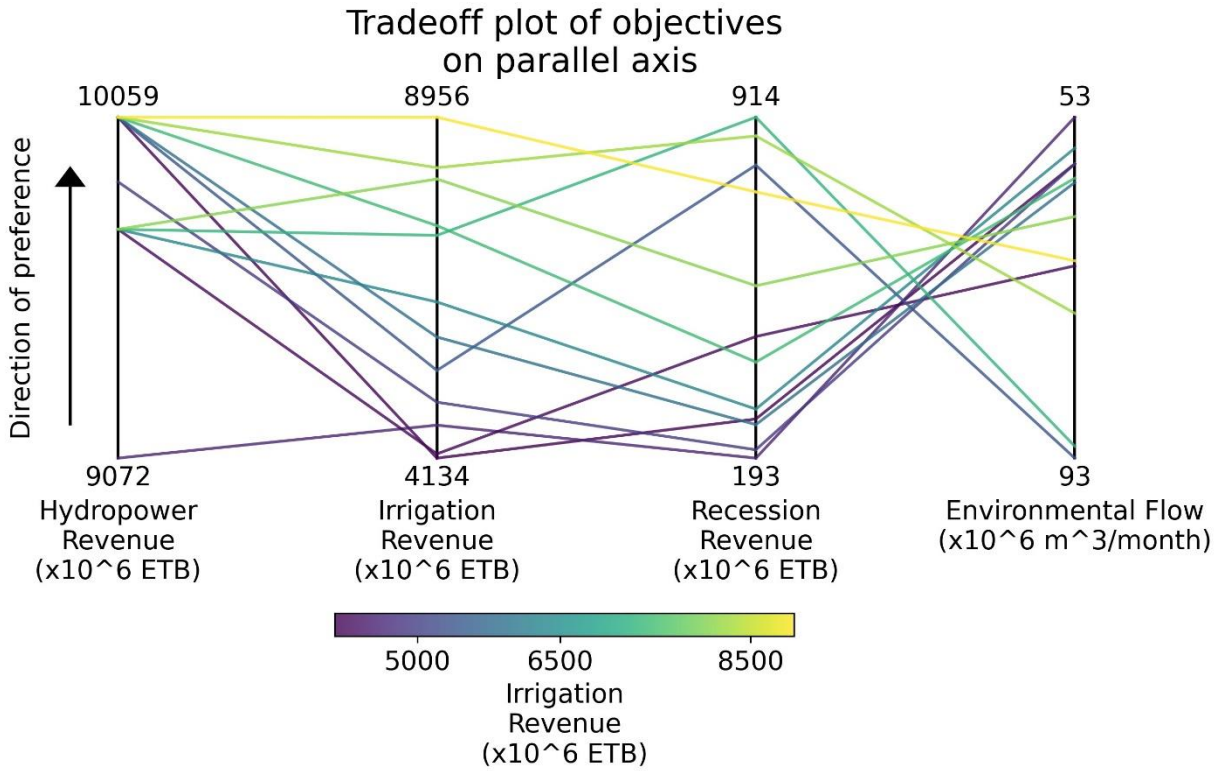

Figure 7.8. Tradeoff performances are contrasted using a parallel-coordinate plot under near future scenario case (Koysha reservoir) in which the axes are positioned so that the desired direction is always upwards and the optimum objective values are presented for each objective.

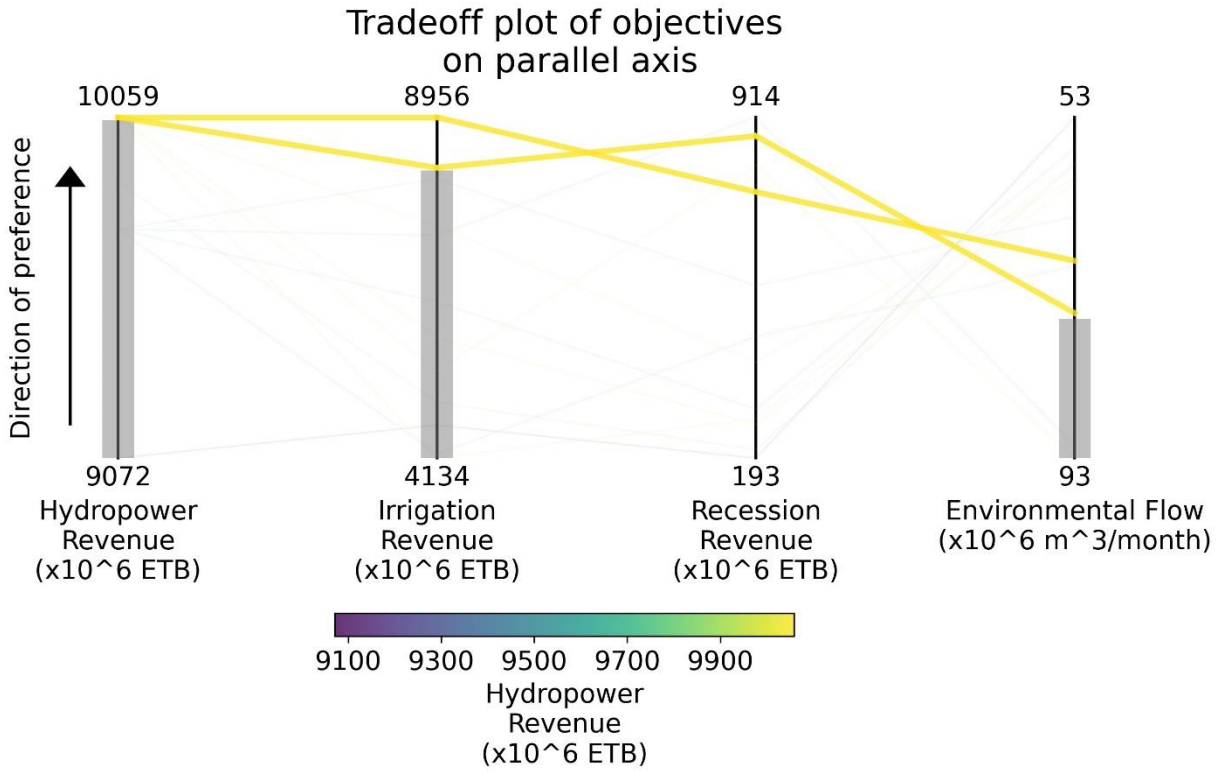

Figure 7.9. Tradeoffs between hydropower, irrigation, and recession revenue vs. environmental flow requirements under near future scenario (Koysha reservoir).

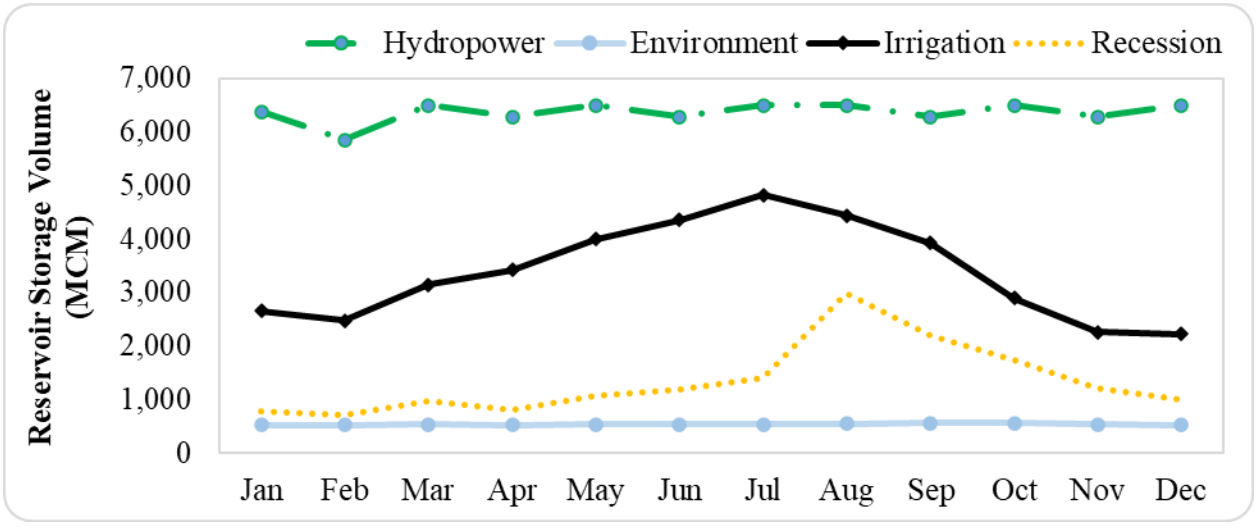

Figure 7.10. Koysha reservoir storage volume of the optimized competing objectives.

Gibe III has a reservoir capacity that is more than twice that of Koysha (see Table 7-1). This means that low reservoir storage at Gibe III could potentially affect the Koysha power plant, especially since they are located near each other. It is also important to keep in mind that Gibe III and Koysha have much flexibility (see Table 7-1); tandem operating rules for the two plants can be effectively adopted to handle demand fluctuation throughout their operating lives, ensuring peak power availability. This is the case with Gibe I and II, which are constructed and run according to a tandem working principle because Gibe II's reservoir is significantly smaller than Gibe I's, aside from the fact that its intake is situated directly beneath Gibe I's outflow. In prior research (EEPCO, 2016), this tandem operating rule between these major reservoirs is also recommended.

The preceding results show that we can use publicly accessible historical streamflow measurements to determine the implicit decision-makers' preferences when evaluating different reservoir operating objectives. The findings also indicate that the operational policy approach prioritizes hydropower profits, water accessibility, and low-flow environmental concerns. This could be because these concerns are easily remedied or because they have a major impact on management decisions (or both). Similar conclusions were also achieved by previous researchers (Giuliani, 2014). As seen in Figure 7-6, substantial policy achievement on one goal often comes at the expense of one or more other goals.

7.4. Conclusions

The goal of this work was to evaluate the applicability of multiobjective evolutionary algorithms to competing water demands in reservoir operations under streamflow variability. Optimization techniques are commonly used by decision-makers to analyse competing water resource management plans. However, earlier studies have demonstrated that an algorithm's optimal result might vary based on the issue at hand. One common mistake is neglecting the quality of the

dependent variables in a project, which could significantly enhance its economic performance. This study tested cutting-edge optimization technology against a realistic water resource strategy. Using objective functions, commonly known as the Pareto front, of particular competitive dependent variables, the Borg MOEA's performance was assessed in relation to the pertinent strategies.

As a result of consistently producing outcomes that were closer to near-optimal solutions, the model's results demonstrated potential optima with advanced reliability and robustness. The pertinent water resources strategic plan was mapped into the complete achievement of the Borg MOEA. The selected case study situation allows for evaluating tradeoffs between revenue generation, minimal environmental flow provision, and reservoir storage conditions. Irrigation and recession farming generate 720 and 26 million Ethiopian birr (ETB) respectively, while hydropower can create up to 4.6 billion ETB under current conditions. However, under near-term conditions, hydropower can generate up to 10 billion ETB, while irrigation and recession farming, with adequate environmental flow, can generate 9 billion and 750 million ETB, respectively. From these two scenarios, it can be observed that irrigation revenue rises at a faster rate than hydropower revenue does. This suggests that irrigation revenue may eventually exceed hydropower generation revenue, which would result in increased competition, higher water use, and the need for better resource management. The outcomes highlight the value of employing evolutionary algorithm models to gain a deeper understanding in a real-world reservoir operation and conduct in-depth analyses of pertinent objectives and factors.

8. Summary, Conclusions and Recommendations

8.1. Summary

Streamflow dictates how reservoirs in a river basin system function. The ability of a river basin to develop water resource infrastructure is mostly dependent on streamflow, which is naturally dependent on the hydrologic system. The ability of a river basin reservoir system to be utilized in the best and most sustainable way is hampered by negligent and disorderly use of these resources. The goal of this dissertation is to assess the long-term performance of a multiobjective cascade reservoir system in the presence of streamflow variability and associated uncertainty.

Hydrologic models are critical instruments for assessing diverse water resources, including hydropower. Hydrologic modelling is regarded as crucial to the current investigation's overall study. The accuracy of hydrologic model projections is crucial when extrapolating model findings for a particular setting. This study offers suggestions for enhancing model performance, resulting in more reliable future forecasts.

The following are the main contributions of the current study:

- systematically evaluated data quality, particularly where there was a scarcity of data (Chapter 4).
- The use of hydrological models to analyse streamflow for a specific flow phase at desired subbasin spatial scale is clearly required (Chapter 5).
- The newly proposed approach proved to be a useful tool for assessing the potential of available water resources in ungauged catchments (Chapter 6).
- evaluated and assessed the influence of the hydrological model parameters' uncertainty (Chapters 5 and 6).

- highlighted the value of employing evolutionary algorithm models to gain a deeper understanding in a real-world reservoir operation and conduct in-depth analyses of competing objectives and factors (Chapter 7).

A compilation of four peer-reviewed publications makes up the thesis. Two of the research studies has already been peer-reviewed and published; the third is a conference paper that was delivered at an international conference; and the fourth is ready for submission.

The main contribution of the current work is proving the value of hydrologic modelling in studies that analyse streamflow. Investigations focused on two crucial areas: the necessity for subbasin spatial scale effects and a novel approach of regionalization for ungauged catchments.

The primary sources of error in hydrologic simulation are closely associated with physical data input, model parameters, and the structure of the model. Moreover, the subbasin spatial scale effects on the SWAT modelling prediction uncertainty were investigated. To replicate various flow phases of the FDC for the Abelti, Gecha, and Wabi watersheds in the Omo-Gibe River Basin, Ethiopia, the uncertainty of the hydrological modelling parameter was assessed. The analysis revealed that the subbasin spatial scale substantially affected the reproduction of various flow phases but only slightly affected the overall flow simulations.

Understanding the hydrological processes and the determination of the frequencies and magnitudes of streamflow are crucial for better oversight of available water resources. A significant obstacle to accurately assessing the water resources of the basin is the accessibility of data for hydrologic modelling. Hence, the newly proposed regionalization strategy, the reliability-weighted (RB) approach outperformed the three commonly used parameter transfer schemes: (1) global mean, (2) physical similarity, and (3) spatial proximity.

Hydrological model uncertainty calculations were performed after performing a data quality check and supplying the appropriate input required to develop a hydrological model using SWAT. Statistical metrics are used to evaluate the model's performance throughout the calibration and validation phases of this modelling technique, where adequate and reliable gauged streamflow is located. However, almost 70% of the Omo Gibe River basin is known to remain ungauged. As a result, using a regionalization strategy is required to adapt the calibrated and validated streamflow to that of the desired site. At this point, the newly proposed regionalization strategy comes to life. Then, using a suitable transfer mechanism, streamflow at the desired site is estimated.

The applicability of advanced multiobjective evolutionary algorithms to competing water needs in reservoir operations of the Omo Gibe cascade reservoir is then examined under conditions of streamflow variability. The successful completion of the Borg MOEA showed the possibility of raising hydropower revenue, reservoir storage, and surface area. In addition, models based on evolutionary algorithms can be used to comprehend objectives and variables that support investment opportunities.

8.2. Conclusions

River basin management has been challenged by competing water demands and environmental regulations, leading to a need to reconsider how freshwater resources are allocated, managed, and exploited. However, it is difficult to implement due to previous agreements and legal limits. Understanding the effects of current reservoir operations is essential to develop alternative policies that balance conflicting goals and performance uncertainties.

To characterize current operations and identify significant trade-offs between alternative policies for balancing competing objectives and system uncertainties, the reservoir operation simulation-optimization strategy used in this study combines reservoir policy identification, many-objective

optimization under uncertainty, and visual analytics. For such an analysis to be relied upon with confidence, solid scientific concepts are needed. Furthermore, credible hydrological inputs are required for better streamflow forecasts. Thus, a good hydrological modelling technique serves as the foundation for bankable streamflow computation over a scenario period.

It may not accurately reflect a hydrologic model's genuine simulation capability to evaluate its performance just in terms of a formal simulation method. This study revealed the importance of subbasin spatial scale implications on SWAT modelling prediction uncertainty, particularly in low-flow estimates. Therefore, it is suggested that more research is necessary to decrease parameter uncertainty in low-flow hydrologic modelling. Furthermore, it suggests an improvement over the existing method of evaluating hydrological models. Thus, it is discovered that accounting for hydrologic model uncertainty is essential for offering a good assessment.

The reliability of a model depends on how well its parameterization is calculated. It is necessary to use an accurate parameter estimation approach. The novel reliability-weighted (RB) strategy outperforms the three regularly used parameter transfer methods of global mean, physical similarity, and spatial proximity. To find parameters that accurately reflect the dominant hydrologic process, such an approach is required in regionalization approaches for ungauged catchments.

The Omo Gibe cascade reservoir operations problem was examined and solved using a cutting-edge evolutionary optimization method (Borg MOEA). By applying radial basis functions to the system dynamics now in place, the implicit policy identification approach captures the current processes. A selection of alternative reservoir policies that are resilient to hydroclimatic uncertainties and are better able to handle the trade-offs across the Omo Gibe cascade reservoirs' multisector services have been successfully identified through a simulation-optimization strategy.

The results of the model showed reliable and robust optimal solutions, enabling the evaluation of the tradeoffs between revenue generation, minimum environmental flow provision, and reservoir storage conditions. Under the existing scenario, the hydropower can produce up to 4.6 billion ETB, while the irrigation revenue is 720 million, which is expected to increase faster than hydropower revenue in the near-future scenario, up to 9 billion, whereas hydropower revenue will produce 10 billion, creating more competition, higher water usage, and necessitate better resource management. In addition, the renovated Gibe III Power Station's hydropower production can increase by approximately 65% in 2019 compared to the actual hydropower production. This demonstrates how evolutionary algorithm models can be useful in practical reservoir operations.

A modelling chain makes up the current methodology. There are issues with the entire assessment procedure. Every step of the modelling process makes the assumption that different parameters are time-invariant, which could be seen as a flaw in the model. The parameters of the hydrological model, the uncertain systems, and the many, competing objectives are these elements of the modelling process. The estimated uncertainty is increased by these parameters' non-stationarity.

8.3. Recommendations

With this dissertation, it cannot be argued that the examination of the ideal distribution of water among conflicting water needs, particularly for the case study rivers, has been resolved. The conducted analysis can be improved or expanded in a number of ways, including:

- The lack of relevant observed data was revealed to be one of many problems that influence the Omo Gibe River basin. The absence of such data has an influence on hydrological modelling and analysis. More research will be required in the future to collect data in a sustainable manner. The current monitoring network and data are not sufficient to calibrate or verify the hydrological models for the Omo Gibe River basin. Upgrades to the

hydrological and climate monitoring systems necessary at the subbasin level are also strongly advocated. This mostly comprises maintaining and expanding monitoring networks for hydroclimatic data.

- The estimated benefits of water use are short-term, but the long-term socioeconomic gains might be different.
- This study has not taken into consideration changes in land use and land cover brought on by socioeconomic growth. Predictions of streamflow in the basin were affected by the assumption that land cover and land use characteristics would not change during the simulation. To quantify streamflow and sediment load in the Omo Gibe cascade reservoirs as well as their impact on subsequent cascade reservoir operations in the river basin employing land use change, additional research is therefore needed.
- Future work will focus on determining the robustness of current policies in the face of extreme uncertainty (Kasprzyk et al., 2013), which will include expanding the range of hydroclimatic variables and taking energy and water pricing into account. Additionally, the addition of hydroclimatic variable ensembles with non-stationarity brought on by the effects of climate change would enable the estimation of the long-term robustness of the various reservoir operating approaches. Finally, it is possible to evaluate whether establishing policies that more accurately represent the actual context of decision-making will ensure their practical value. The implemented cascade reservoir operations constitute a significant step in the development of water reservoir operating policies that can address uncertain systems and various conflicting objectives; nonetheless, more in-depth research encompassing all competing needs is necessary.

Reference

Aalijahan, M., Khosravichenar, A., 2021. A multimethod analysis for average annual precipitation mapping in the Khorasan Razavi Province (Northeastern Iran). Atmosphere, 12(5): 592.

Abbaspour, K.C., 2015. SWAT-CUP: SWAT calibration and uncertainty programs—a user manual. Eawag: Dübendorf, Switzerland: 16-70.

Abbaspour, K.C., Johnson, C., Van Genuchten, M.T., 2004. Estimating uncertain flow and transport parameters using a sequential uncertainty fitting procedure. Vadose zone journal, 3(4): 1340-1352.

Abbaspour, K.C. et al., 2015. A continental-scale hydrology and water quality model for Europe: Calibration and uncertainty of a high-resolution large-scale SWAT model. Journal of hydrology, 524: 733-752.

Abbaspour, K.C., Vaghefi, S.A., Srinivasan, R., 2017. A guideline for successful calibration and uncertainty analysis for soil and water assessment: a review of papers from the 2016 international SWAT conference. Water, 10(1): 6.

Abbaspour, K.C. et al., 2007. Modelling hydrology and water quality in the pre-alpine/alpine Thur watershed using SWAT. Journal of hydrology, 333(2-4): 413-430.

Abdar, M. et al., 2021. A review of uncertainty quantification in deep learning: Techniques, applications and challenges. Information Fusion, 76: 243-297.

Abera, F.F., Asfaw, D.H., Engida, A.N., Melesse, A.M., 2018. Optimal operation of hydropower reservoirs under climate change: The case of Tekeze reservoir, Eastern Nile. Water, 10(3): 273.

Abrahamsson, O., Håkanson, L., 1998. Modelling seasonal flow variability of European rivers. Ecological Modelling, 114(1): 49-58.

Adhikary, S.K., Muttil, N., Yilmaz, A.G., 2016. Genetic programming-based ordinary kriging for spatial interpolation of rainfall. Journal of Hydrologic Engineering, 21(2): 04015062.

Ahmad, A., El-Shafie, A., Razali, S.F.M., Mohamad, Z.S., 2014. Reservoir optimization in water resources: a review. Water resources management, 28: 3391-3405.

Al-Jawad, J.Y., Alsaffar, H.M., Bertram, D., Kalin, R.M., 2019. Optimum socio-environmental flows approach for reservoir operation strategy using many-objectives evolutionary optimization algorithm. Science of the Total Environment, 651: 1877-1891.

Al-Jawad, J.Y., Tanyimboh, T.T., 2017. Reservoir operation using a robust evolutionary optimization algorithm. Journal of environmental management, 197: 275-286.

Alba, E., Luque, G., Nesmachnow, S., 2013. Parallel metaheuristics: recent advances and new trends. International Transactions in Operational Research, 20(1): 1-48.

Annys, S., Ghebreyohannes, T., Nyssen, J., 2020. Impact of hydropower dam operation and management on downstream hydrogeomorphology in semi-arid environments (Tekeze, Northern Ethiopia). Water, 12(8): 2237.

Aravind, P., Ponnuchakkammal, P., Thiyagarajan, G., Kannan, B., 2021. Estimation of Crop Water Requirement for Sugarcane in Coimbatore District using FAO CROPWAT. Madras Agricultural Journal, 108(june (4-6)): 1.

Arnold, J.G. et al., 2012. SWAT: Model use, calibration, and validation. Transactions of the ASABE, 55(4): 1491-1508.

Arnold, J.G., Srinivasan, R., Muttiah, R.S., Williams, J.R., 1998. Large area hydrologic modeling and assessment part I: model development 1. JAWRA Journal of the American Water Resources Association, 34(1): 73-89.

Arsenault, R., Breton-Dufour, M., Poulin, A., Dallaire, G., Romero-Lopez, R., 2019. Streamflow prediction in ungauged basins: analysis of regionalization methods in a hydrologically heterogeneous region of Mexico. Hydrological Sciences Journal, 64(11): 1297-1311.

Arsenault, R., Brissette, F., 2016. Multi-model averaging for continuous streamflow prediction in ungauged basins. Hydrological Sciences Journal, 61(13): 2443-2454.

Arsenault, R., Brissette, F.P., 2014. Continuous streamflow prediction in ungauged basins: The effects of equifinality and parameter set selection on uncertainty in regionalization approaches. Water Resources Research, 50(7): 6135-6153.

Arsenault, R., Gatien, P., Renaud, B., Brissette, F., Martel, J.-L., 2015. A comparative analysis of 9 multi-model averaging approaches in hydrological continuous streamflow simulation. Journal of Hydrology, 529: 754-767.

Ashiq, M.W., Zhao, C., Ni, J., Akhtar, M., 2010. GIS-based high-resolution spatial interpolation of precipitation in mountain–plain areas of Upper Pakistan for regional climate change impact studies. Theoretical and Applied Climatology, 99: 239-253.

Asress, M.B., Simonovic, A., Komarov, D., Stupar, S., 2013. Wind energy resource development in Ethiopia as an alternative energy future beyond the dominant hydropower. Renewable and Sustainable Energy Reviews, 23: 366-378.

Avery, S., Eng, C., 2012. Lake Turkana & the Lower Omo: hydrological impacts of major dam and irrigation developments. African Studies Centre, the University of Oxford.

Awulachew, S.B. et al., 2007. Water resources and irrigation development in Ethiopia, 123. Iwmi.

Azmat, M., Laio, F., Poggi, D., 2015. Estimation of water resources availability and mini-hydro productivity in high-altitude scarcely-gauged watershed. Water Resources Management, 29(14): 5037-5054.

Beck, H.E. et al., 2016. Global-scale regionalization of hydrologic model parameters. Water Resources Research, 52(5): 3599-3622.

Bekele, E.G., Nicklow, J.W., 2007. Multi-objective automatic calibration of SWAT using NSGA-II. Journal of Hydrology, 341(3-4): 165-176.

Beven, K., 1989. Changing ideas in hydrology—the case of physically-based models. Journal of hydrology, 105(1-2): 157-172.

Beven, K., 1993. Prophecy, reality and uncertainty in distributed hydrological modelling. Advances in water resources, 16(1): 41-51.

Beven, K., Binley, A., 1992. The future of distributed models: model calibration and uncertainty prediction. Hydrological processes, 6(3): 279-298.

Bhattacharjee, S., Mitra, P., Ghosh, S.K., 2013. Spatial interpolation to predict missing attributes in GIS using semantic kriging. IEEE Transactions on Geoscience and Remote Sensing, 52(8): 4771-4780.

Bingner, R., Garbrecht, J., G. Arnold, J., Srinivasan, R., 1997. EFFECT OF WATERSHED SUBDIVISION ON SIMULATION RUNOFF AND FINE SEDIMENT YIELD. Transactions of the ASAE, 40(5): 1329-1335. DOI:https://doi.org/10.13031/2013.21391

Blanco, I. et al., 2017. Geographical distribution of COPD prevalence in Europe, estimated by an inverse distance weighting interpolation technique. International journal of chronic obstructive pulmonary disease: 57-67.

Blöschl, G., 2006. Rainfall-runoff modeling of ungauged catchments. Encyclopedia of hydrological sciences.

Blöschl, G., Sivapalan, M., 1995. Scale issues in hydrological modelling: a review. Hydrological processes, 9(3-4): 251-290.

Brouwer, R., Hofkes, M., 2008. Integrated hydro-economic modelling: Approaches, key issues and future research directions. Ecological Economics, 66(1): 16-22.

Busoniu, L., Ernst, D., De Schutter, B., Babuska, R., 2010. Cross-entropy optimization of control policies with adaptive basis functions. IEEE Transactions on Systems, Man, and Cybernetics, Part B (Cybernetics), 41(1): 196-209.

Butts, M.B., Payne, J.T., Kristensen, M., Madsen, H., 2004. An evaluation of the impact of model structure on hydrological modelling uncertainty for streamflow simulation. Journal of hydrology, 298(1-4): 242-266.

Cai, X., McKinney, D.C., Lasdon, L.S., 2003. Integrated hydrologic-agronomic-economic model for river basin management. Journal of water resources planning and management, 129(1): 4-17.

Caldeira, T.L., Mello, C.R., Beskow, S., Timm, L.C., Viola, M.R., 2019. LASH hydrological model: an analysis focused on spatial discretization. Catena, 173: 183-193.

Cannarozzo, M., Noto, L.V., Viola, F., 2006. Spatial distribution of rainfall trends in Sicily (1921–2000). Physics and Chemistry of the Earth, Parts a/b/c, 31(18): 1201-1211.

Carpenter, T.M., Georgakakos, K.P., 2006. Intercomparison of lumped versus distributed hydrologic model ensemble simulations on operational forecast scales. Journal of hydrology, 329(1-2): 174-185.

Carr, C.J., 2017a. River basin development and human rights in Eastern Africa—A policy crossroads. Springer Nature.

Chaemiso, S.E., Abebe, A., Pingale, S.M., 2016. Assessment of the impact of climate change on surface hydrological processes using SWAT: a case study of Omo-Gibe river basin, Ethiopia. Modeling Earth Systems and Environment, 2(4): 1-15.

Chang, K.-T., 2006. Introduction to geographic information systems. McGraw-Hill Higher Education Boston.

Chilkoti, V., Bolisetti, T., Balachandar, R., 2018. Multi-objective autocalibration of SWAT model for improved low flow performance for a small snowfed catchment. Hydrological Sciences Journal, 63(10): 1482-1501.

Choubin, B. et al., 2019. Streamflow regionalization using a similarity approach in ungauged basins: Application of the geo-environmental signatures in the Karkheh River Basin, Iran. Catena, 182: 104128.

Chow, V., 1971. Applied hydrology. McGraw-hill.

Cibin, R., Sudheer, K., Chaubey, I., 2010. Sensitivity and identifiability of stream flow generation parameters of the SWAT model. Hydrological Processes: An International Journal, 24(9): 1133-1148.

Coello, C.A.C., Lamont, G.B., Van Veldhuizen, D.A., 2007. Evolutionary algorithms for solving multi-objective problems, 5. Springer.

Cohon, J.L., Marks, D.H., 1975. A review and evaluation of multiobjective programing techniques. Water resources research, 11(2): 208-220.

Coxon, G. et al., 2015. A novel framework for discharge uncertainty quantification applied to 500 UK gauging stations. Water resources research, 51(7): 5531-5546.

Craig, J.R. et al., 2020. Flexible watershed simulation with the Raven hydrological modelling framework. Environmental Modelling & Software, 129: 104728.

Cui, L., Kuczera, G., 2005. Optimizing water supply headworks operating rules under stochastic inputs: Assessment of genetic algorithm performance. Water Resources Research, 41(5).

da Silva, A.S.A., Stosic, B., Menezes, R.S.C., Singh, V.P., 2019. Comparison of interpolation methods for spatial distribution of monthly precipitation in the state of Pernambuco, Brazil. Journal of Hydrologic Engineering, 24(3): 04018068.

Dai, L. et al., 2017. Multi-objective optimization of cascade reservoirs using NSGA-II: A case study of the Three Gorges-Gezhouba cascade reservoirs in the middle Yangtze River, China. Human and Ecological Risk Assessment: An International Journal, 23(4): 814-835.

Dakhlalla, A.O., Parajuli, P.B., 2019. Assessing model parameters sensitivity and uncertainty of streamflow, sediment, and nutrient transport using SWAT. Information processing in agriculture, 6(1): 61-72.

Dal Molin, M., Schirmer, M., Zappa, M., Fenicia, F., 2020. Understanding dominant controls on streamflow spatial variability to set up a semi-distributed hydrological model: the case study of the Thur catchment. Hydrology and Earth System Sciences, 24(3): 1319-1345.

Dalcin, A.P., Fernandes Marques, G., 2020. Integrating water management instruments to reconcile a hydro-economic water allocation strategy with other water preferences. Water Resources Research, 56(5): e2019WR025558.

Daniel, A., 2011. Water Use and Operation Analysis of Water Resource Systems in Omo Gibe River Basin. Addis Ababa University. Addis Ababa.

Deb, K., 2011. Multi-objective optimisation using evolutionary algorithms: an introduction. Springer.

Deb, K., Agrawal, R.B., 1995. Simulated binary crossover for continuous search space. Complex systems, 9(2): 115-148.

Deb, K., Anand, A., Joshi, D., 2002. A computationally efficient evolutionary algorithm for real-parameter optimization. Evolutionary computation, 10(4): 371-395.

Deutsch, C.V., Journel, A.G., 1992. Geostatistical software library and user's guide. Oxford University Press, 8(91): 0-1.

Devia, G.K., Ganasri, B.P., Dwarakish, G.S., 2015. A review on hydrological models. Aquatic procedia, 4: 1001-1007.

Diks, C.G., Vrugt, J.A., 2010. Comparison of point forecast accuracy of model averaging methods in hydrologic applications. Stochastic Environmental Research and Risk Assessment, 24(6): 809-820.

Ditthakit, P. et al., 2021. Using machine learning methods for supporting GR2M model in runoff estimation in an ungauged basin. Scientific Reports, 11(1): 1-16.

Do, P. et al., 2020. Exploring synergies in the water-food-energy nexus by using an integrated hydro-economic optimization model for the Lancang-Mekong River basin. Science of The Total Environment, 728: 137996.

Dwelle, M.C., Kim, J., Sargsyan, K., Ivanov, V.Y., 2019. Streamflow, stomata, and soil pits: Sources of inference for complex models with fast, robust uncertainty quantification. Advances in Water Resources, 125: 13-31.

Eckhardt, K., Arnold, J., 2001. Automatic calibration of a distributed catchment model. Journal of hydrology, 251(1-2): 103-109.

EEPCO, 2004. Environmental Impact Assessment.

EEPCO, 2009. Gibe III Hydropower Project.

EEPCO, 2016. Koysha Hydroelectric Project. Ethiopian Electric Power Corporation.

Ercan, M.B., Goodall, J.L., 2016. Design and implementation of a general software library for using NSGA-II with SWAT for multi-objective model calibration. Environmental Modelling & Software, 84: 112-120.

Eyasu, Y., Atinkut, M., Tesfa-alem, G., Daniel, T., Ermias, A., 2015. Multi reservoir operation and challenges of the Omo River Basin: Part II: Potential assessment of flood based farming on lower Omo Ghibe Basin. Spate Irrigation Newtwork, Mekele, Ethiopia.

Fan, Y., 2019. Uncertainty quantification in hydrologic predictions: A brief review. Journal of Environmental Informatics Letters, 2(2): 48-56.

Faramarzi, M. et al., 2013. Modeling impacts of climate change on freshwater availability in Africa. Journal of Hydrology, 480: 85-101.

Feng, Z.-k., Niu, W.-j., Cheng, C.-t., Zhou, J.-z., 2017. Peak shaving operation of hydro-thermal-nuclear plants serving multiple power grids by linear programming. Energy, 135: 210-219.

Flatley, A., Rutherfurd, I., 2022. Comparison of Regionalisation Techniques for Peak Streamflow Estimation in Small Catchments in the Pilbara, Australia. Hydrology, 9(10): 165.

Gao, H. et al., 2010. Water budget record from Variable Infiltration Capacity (VIC) model.

Gao, P. et al., 2017. Use of double mass curves in hydrologic benefit evaluations. Hydrological processes, 31(26): 4639-4646.

Gassman, P.W., Reyes, M.R., Green, C.H., Arnold, J.G., 2007. The soil and water assessment tool: historical development, applications, and future research directions. Transactions of the ASABE, 50(4): 1211-1250.

Gebeyehu, B.M., Jabir, A.K., Tegegne, G., Melesse, A.M., 2023. Subbasin Spatial Scale Effects on Hydrological Model Prediction Uncertainty of Extreme Stream Flows in the Omo Gibe River Basin, Ethiopia. Remote Sensing, 15(3): 611.

Gebresenbet, T.S., 2016. Modeling of Cascade Dams and Reservoirs Operation for Optimal Water Use: Application to Omo Gibe River Basin, Ethiopia, 20. kassel university press GmbH.

Giraldo, R., Herrera, L., Leiva, V., 2020. Cokriging prediction using as secondary variable a functional random field with application in environmental pollution. Mathematics, 8(8): 1305.

Giuliani, M., 2014. Agent-based water resources management in complex decision-making contexts.

Giuliani, M., Lamontagne, J., Reed, P., Castelletti, A., 2021. A state-of-the-art review of optimal reservoir control for managing conflicting demands in a changing world. Water Resources Research, 57(12): e2021WR029927.

Giuliani, M., Pianosi, F., Castelletti, A., 2015a. Making the most of data: An information selection and assessment framework to improve water systems operations. Water Resources Research, 51(11): 9073-9093.

Giuliani, M., Quinn, J.D., Herman, J.D., Castelletti, A., Reed, P.M., 2017. Scalable multiobjective control for large-scale water resources systems under uncertainty. IEEE Transactions on Control Systems Technology, 26(4): 1492-1499.

Goovaerts, P., 2000. Geostatistical approaches for incorporating elevation into the spatial interpolation of rainfall. Journal of hydrology, 228(1-2): 113-129.

Guo, J., Su, X., 2019. Parameter sensitivity analysis of SWAT model for streamflow simulation with multisource precipitation datasets. Hydrology Research, 50(3): 861-877.

Guo, Y., Zhang, Y., Zhang, L., Wang, Z., 2021. Regionalization of hydrological modeling for predicting streamflow in ungauged catchments: A comprehensive review. Wiley Interdisciplinary Reviews: Water, 8(1): e1487.

Gupta, H.V., Kling, H., Yilmaz, K.K., Martinez, G.F., 2009. Decomposition of the mean squared error and NSE performance criteria: Implications for improving hydrological modelling. Journal of hydrology, 377(1-2): 80-91.

Hadjimichael, A., Gold, D., Hadka, D., Reed, P., 2020. Rhodium: Python library for many-objective robust decision making and exploratory modeling. Journal of Open Research Software, 8.

Hadka, D., Reed, P., 2013. Borg: An auto-adaptive many-objective evolutionary computing framework. Evolutionary computation, 21(2): 231-259.

Hadka, D., Reed, P.M., Simpson, T.W., 2012. Diagnostic assessment of the Borg MOEA for many-objective product family design problems, 2012 IEEE Congress on Evolutionary Computation. IEEE, pp. 1-10.

Hafi, A., 2006. Conjunctive Water Management: Economic Tools for Evaluating Alternative Policy and Management Options. Australian Bureau of Agricultural and Resource Economics.

Hailu, D. et al., 2018. The Study of Water Use and Treated Wastewater Discharge charge (Irrigation, ...), AAIT.

Haimes, Y.Y., Hall, W.A., 1977. Sensitivity, responsivity, stability and irreversibility as multiple objectives in civil systems. Advances in water resources, 1(2): 71-81.

Hamarat, C., Kwakkel, J.H., Pruyt, E., Loonen, E.T., 2014. An exploratory approach for adaptive policymaking by using multi-objective robust optimization. Simulation Modelling Practice and Theory, 46: 25-39.

Hamby, D.M., 1994. A review of techniques for parameter sensitivity analysis of environmental models. Environmental monitoring and assessment, 32(2): 135-154.

Harou, J.J. et al., 2009. Hydro-economic models: Concepts, design, applications, and future prospects. Journal of Hydrology, 375(3-4): 627-643.

Haverkamp, S., Srinivasan, R., Frede, H., Santhi, C., 2002. Subwatershed spatial analysis tool: Discretization of a distributed hydrologic model by statistical criteria 1. JAWRA Journal of the American Water Resources Association, 38(6): 1723-1733.

Haylock, M. et al., 2008. A European daily high-resolution gridded data set of surface temperature and precipitation for 1950–2006. Journal of Geophysical Research: Atmospheres, 113(D20).

Hengl, T., 2009. A practical guide to geostatistical mapping.

Hodam, S., Sarkar, S., Marak, A.G., Bandyopadhyay, A., Bhadra, A., 2017. Spatial interpolation of reference evapotranspiration in India: Comparison of IDW and Kriging methods. Journal of the Institution of Engineers (india): Series A, 98: 511-524.

Hofstra, N., Haylock, M., New, M., Jones, P., Frei, C., 2008. Comparison of six methods for the interpolation of daily, European climate data. Journal of Geophysical Research: Atmospheres, 113(D21).

Horne, A. et al., 2016. Optimization tools for environmental water decisions: A review of strengths, weaknesses, and opportunities to improve adoption. Environmental modelling & software, 84: 326-338.

Horne, F., Mousseau, F., Metho, O., Mittal, A., Shepard, D., 2011. Understanding land investment deals in Africa. The Oakland Institute, Oakland.

Hosseini, S.H., Khaleghi, M.R., 2020. Application of SWAT model and SWAT-CUP software in simulation and analysis of sediment uncertainty in arid and semi-arid watersheds (case

study: The Zoshk–Abardeh watershed). Modeling Earth Systems and Environment, 6(4): 2003-2013.

Hu, M. et al., 2014. Multi-objective ecological reservoir operation based on water quality response models and improved genetic algorithm: A case study in Three Gorges Reservoir, China. Engineering Applications of Artificial Intelligence, 36: 332-346.

Hu, Q. et al., 2019. Rainfall spatial estimations: A review from spatial interpolation to multi-source data merging. Water, 11(3): 579.

Human-Rights-Watch, 2017. Ethiopia: Dams, Plantations a Threat to Kenyans. Human Right Watch.

Hurford, A.P., Huskova, I., Harou, J.J., 2014. Using many-objective trade-off analysis to help dams promote economic development, protect the poor and enhance ecological health. Environmental Science & Policy, 38: 72-86.

Hussainzada, W., Lee, H.S., 2021. Hydrological modelling for water resource management in a semi-arid mountainous region using the soil and water assessment tool: A case study in northern Afghanistan. Hydrology, 8(1): 16.

İçağa, Y., Emin, T., 2018. Comparative analysis of different interpolation methods in modeling spatial distribution of monthly precipitation. Doğal Afetler ve Çevre Dergisi, 4(2): 89-104.

İmamoğlu, M.Z., Sertel, E., 2016. Analysis of different interpolation methods for soil moisture mapping using field measurements and remotely sensed data. International Journal of Environment and Geoinformatics, 3(3): 11-25.

Jajarmizadeh, M., Harun, S., Salarpour, M., 2012. A review on theoretical consideration and types of models in hydrology. Journal of Environmental Science and Technology, 5(5): 249-261.

Jasperse, J. et al., 2020. Lake Mendocino forecast informed reservoir operations final viability assessment.

Jiang, L. et al., 2021. Identification of Suitable Hydrologic Response Unit Thresholds for Soil and Water Assessment Tool Streamflow Modelling. Chinese Geographical Science, 31(4): 696-710.

Jillo, A.Y., Demissie, S., Viglione, A., Asfaw, D., Sivapalan, M., 2017. Characterization of regional variability of seasonal water balance within Omo-Ghibe River Basin, Ethiopia. Hydrological Sciences Journal, 62(8): 1200-1215.

Johnston, K., Ver Hoef, J.M., Krivoruchko, K., Lucas, N., 2001. Using ArcGIS geostatistical analyst, 380. Esri Redlands.

Jordan, S., Quinn, J., Zaniolo, M., Giuliani, M., Castelletti, A., 2022. Advancing reservoir operations modelling in SWAT to reduce socio-ecological tradeoffs. Environmental Modelling & Software, 157: 105527.

Kanishka, G., Eldho, T., 2020. Streamflow estimation in ungauged basins using watershed classification and regionalization techniques. Journal of Earth System Science, 129(1): 1-18.

Kannan, N., Jeong, J., 2011. An approach for estimating stream health using flow duration curves and indices of hydrologic alteration. EPA region, 6.

Kasprzyk, J.R., Nataraj, S., Reed, P.M., Lempert, R.J., 2013. Many objective robust decision making for complex environmental systems undergoing change. Environmental Modelling & Software, 42: 55-71.

Khalid, K. et al., 2016. Sensitivity analysis in watershed model using SUFI-2 algorithm. Procedia engineering, 162: 441-447.

Kibuye, F.A. et al., 2020. Influence of hydrologic and anthropogenic drivers on emerging organic contaminants in drinking water sources in the Susquehanna River Basin. Chemosphere, 245: 125583.

Kim, W., Lee, J., Kim, J., Kim, S., 2019. Assessment of water supply stability for drought-vulnerable Boryeong multipurpose dam in South Korea using future dry climate change scenarios. Water, 11(11): 2403.

Kita, H., Ono, I., Kobayashi, S., 2000. Multi-parental extension of the unimodal normal distribution crossover for real-coded genetic algorithms. Transactions of the society of Instrument and Control Engineers, 36(10): 875-883.

Kling, H., Gupta, H., 2009. On the development of regionalization relationships for lumped watershed models: The impact of ignoring sub-basin scale variability. Journal of Hydrology, 373(3-4): 337-351. DOI:10.1016/j.jhydrol.2009.04.031

Kollat, J.B., Reed, P.M., 2006. Comparing state-of-the-art evolutionary multi-objective algorithms for long-term groundwater monitoring design. Advances in Water Resources, 29(6): 792-807.

Kumar, S., Merwade, V., 2009. Impact of watershed subdivision and soil data resolution on SWAT model calibration and parameter uncertainty 1. JAWRA Journal of the American Water Resources Association, 45(5): 1179-1196.

Kuriqi, A. et al., 2020. Seasonality shift and streamflow flow variability trends in central India. Acta Geophysica, 68: 1461-1475.

Kurniawan, A., Auladiah, I., Virgianto, R., 2019. DETERMINING THE BEST ANNUAL RAINFALL INTERPOLATION FOR BILA WALANAE WATERSHED.

Labadie, J.W., 2004. Optimal operation of multireservoir systems: State-of-the-art review. Journal of water resources planning and management, 130(2): 93-111.

Li, H., Zhang, Y., 2017. Regionalising rainfall-runoff modelling for predicting daily runoff: Comparing gridded spatial proximity and gridded integrated similarity approaches against their lumped counterparts. Journal of Hydrology, 550: 279-293.

Li, Q. et al., 2019. A combined method for estimating continuous runoff by parameter transfer and drainage area ratio method in ungauged catchments. Water, 11(5): 1104.

Lin, Y.-P., Verburg, P.H., Chang, C.-R., Chen, H.-Y., Chen, M.-H., 2009. Developing and comparing optimal and empirical land-use models for the development of an urbanized watershed forest in Taiwan. Landscape and Urban Planning, 92(3-4): 242-254.

Lund, J.R., Ferreira, I., 1996. Operating rule optimization for Missouri River reservoir system. Journal of Water Resources Planning and Management, 122(4): 287-295.

Ly, S., Charles, C., Degre, A., 2011. Geostatistical interpolation of daily rainfall at catchment scale: the use of several variogram models in the Ourthe and Ambleve catchments, Belgium. Hydrology and Earth System Sciences, 15(7): 2259-2274.

Ly, S., Charles, C., Degré, A., 2013. Different methods for spatial interpolation of rainfall data for operational hydrology and hydrological modeling at watershed scale: a review. Biotechnologie, agronomie, société et environnement, 17(2).

Madsen, H., 2000. Automatic calibration of a conceptual rainfall–runoff model using multiple objectives. Journal of hydrology, 235(3-4): 276-288.

Maier, H.R. et al., 2014. Evolutionary algorithms and other metaheuristics in water resources: Current status, research challenges and future directions. Environmental Modelling & Software, 62: 271-299.

Makhmudova, D., Makhmudov, H., 2021. Analysis and assasment method of the Chirchik river flow for water supply and water use, E3S Web of Conferences. EDP Sciences, pp. 01045.

Malik, M.A., Dar, A.Q., Jain, M.K., 2022. Modelling streamflow using the SWAT model and multi-site calibration utilizing SUFI-2 of SWAT-CUP model for high altitude catchments, NW Himalaya's. Modeling Earth Systems and Environment, 8(1): 1203-1213.

Mamillapalli, S., Srinivasan, R., Arnold, J., Engel, B.A., 1996. Effect of spatial variability on basin scale modeling, Proceedings, Third International Conference/Workshop on Integrating GIS and Environmental Modeling, Santa Fe, New Mexico.

Mannina, G., Viviani, G., 2010. An urban drainage stormwater quality model: Model development and uncertainty quantification. Journal of hydrology, 381(3-4): 248-265.

Matos, J., Liechti, T.C., Portela, M., Schleiss, A., 2014. Pattern-oriented memory interpolation of sparse historical rainfall records. Journal of Hydrology, 510: 493-503.

McMillan, H.K., Westerberg, I.K., Krueger, T., 2018. Hydrological data uncertainty and its implications. Wiley Interdisciplinary Reviews: Water, 5(6): e1319.

Mengistu, D., Bewket, W., Dosio, A., Panitz, H.-J., 2021. Climate change impacts on water resources in the upper blue nile (Abay) river basin, ethiopia. Journal of Hydrology, 592: 125614.

Mengistu, D.T., 2019. Hydrological Modelling of Ethiopian Watersheds: The Application of Hydrological Models for Flow Forecasting and Analysis of Sensitivity to Climate and Landuse Changes.

Meredith, D., Givental, E., 2016. Hydro-politics and hydro-economics: Comparing upstream and downstream challenges for Vietnam and Ethiopia. Yearbook of the Association of Pacific Coast Geographers, 78: 148-167.

Merz, R., Blöschl, G., 2004. Regionalisation of catchment model parameters. Journal of hydrology, 287(1-4): 95-123.

Michalewicz, Z., Logan, T., Swaminathan, S., 1994. Evolutionary operators for continuous convex parameter spaces, Proceedings of the 3rd Annual conference on Evolutionary Programming. World Scientific, pp. 84-97.

Milly, P.C. et al., 2008. Stationarity is dead: Whither water management? Science, 319(5863): 573-574.

Ministry of Culture and Tourism of Ethiopia, G.D., 2018. Progress report on the state of conservation of the Lower Omo Valley heritage property.

Mirchi, A., Watkins, D., Czajkowski, J., Martinez, C., 2015. Hydro-economic model of south Florida's water resources, World Environmental and Water Resources Congress 2015, pp. 2157-2162.

Mitchell, M., 1998. An introduction to genetic algorithms. MIT press.

Moges, E., Demissie, Y., Larsen, L., Yassin, F., 2020. Review: Sources of Hydrological Model Uncertainties and Advances in Their Analysis. Water 2021, 13, 28. s Note: MDPI stays neu-tral with regard to jurisdictional claims in ….

Moges, E., Demissie, Y., Larsen, L., Yassin, F., 2021. Sources of hydrological model uncertainties and advances in their analysis. Water, 13(1): 28.

Mohammed, A.K., 2014. The effect of climate change on water resources potential of Omo Gibe Basin, Ethiopia, München, Univ. der Bundeswehr, Diss., 2013.

Moradkhani, H., Sorooshian, S., 2008. General review of rainfall-runoff modeling: model calibration, data assimilation, and uncertainty analysis. Hydrological modelling and the water cycle: Coupling the atmospheric and hydrological models: 1-24.

Moriasi, D.N. et al., 2007. Model evaluation guidelines for systematic quantification of accuracy in watershed simulations. Transactions of the ASABE, 50(3): 885-900.

Mortazavi-Naeini, M. et al., 2015. Robust optimization to secure urban bulk water supply against extreme drought and uncertain climate change. Environmental Modelling & Software, 69: 437-451.

MoWIE, 2001. The Ethiopian Water Resource Management Policy. Addis Ababa, Ethiopia: Ministry of Water Resources (MoWR).

Mulat, A.G., 2015. WATER RESOURCE SYSTEM MODELING OF EASTERN NILE RIVER BASIN, Addis Ababa University Addis Ababa, Ethiopia.

Müller, R., Schütze, N., 2016. Multi-objective optimization of multi-purpose multi-reservoir systems under high reliability constraints. Environmental Earth Sciences, 75: 1-17.

Murphy, A.H., 1988. Skill scores based on the mean square error and their relationships to the correlation coefficient. Monthly weather review, 116(12): 2417-2424.

Mythili, B., Devi, U.G., Raviteja, A., Kumar, P.S., 2013. Study of optimizing techniques of reservoir operation. International Journal of Engineering Research and General Science, 1(1): 2091-2730.

Nachtergaele, F. et al., 2010. The harmonized world soil database, Proceedings of the 19th World Congress of Soil Science, Soil Solutions for a Changing World, Brisbane, Australia, 1-6 August 2010, pp. 34-37.

Narbondo, S., Gorgoglione, A., Crisci, M., Chreties, C., 2020. Enhancing physical similarity approach to predict runoff in ungauged watersheds in sub-tropical regions. Water, 12(2): 528.

Narsimlu, B., Gosain, A.K., Chahar, B.R., Singh, S.K., Srivastava, P.K., 2015. SWAT model calibration and uncertainty analysis for streamflow prediction in the Kunwari River Basin, India, using sequential uncertainty fitting. Environmental Processes, 2(1): 79-95.

Nash, J.E., Sutcliffe, J.V., 1970. River flow forecasting through conceptual models part I—A discussion of principles. Journal of hydrology, 10(3): 282-290.

Nederveen, S., Mengistu, A., Van Steenbergen, F., Alamirew, T., Geleta, Y., 2011. Flood based farming practices in Ethiopia: Status and potential. Spate Irrigation Network Overview Paper, 3.

Neitsch, S.L., Arnold, J.G., Kiniry, J.R., Williams, J.R., 2011. Soil and water assessment tool theoretical documentation version 2009, Texas Water Resources Institute.

Nesru, M., Shetty, A., Nagaraj, M., 2020. Multi-variable calibration of hydrological model in the upper Omo-Gibe basin, Ethiopia. Acta Geophysica, 68(2): 537-551.

Nester, T., Kirnbauer, R., Gutknecht, D., Blöschl, G., 2011. Climate and catchment controls on the performance of regional flood simulations. Journal of Hydrology, 402(3-4): 340-356.

Nguyen, T.V. et al., 2022. An interactive graphical interface tool for parameter calibration, sensitivity analysis, uncertainty analysis, and visualization for the Soil and Water Assessment Tool. Environmental Modelling & Software, 156: 105497.

Nicklow, J. et al., 2010. State of the art for genetic algorithms and beyond in water resources planning and management. Journal of Water Resources Planning and Management, 136(4): 412-432.

Niu, W.-j., Feng, Z.-k., 2021. Evaluating the performances of several artificial intelligence methods in forecasting daily streamflow time series for sustainable water resources management. Sustainable Cities and Society, 64: 102562.

Niu, W.-j., Feng, Z.-k., Cheng, C.-t., Wu, X.-y., 2018. A parallel multi-objective particle swarm optimization for cascade hydropower reservoir operation in southwest China. Applied Soft Computing, 70: 562-575.

Ocha, 2010. Ethiopia: Floods (Final Report).

Ohmer, M., Liesch, T., Goeppert, N., Goldscheider, N., 2017. On the optimal selection of interpolation methods for groundwater contouring: An example of propagation of uncertainty regarding inter-aquifer exchange. Advances in Water Resources, 109: 121-132.

Oliver, M., Webster, R., 2014. A tutorial guide to geostatistics: Computing and modelling variograms and kriging. Catena, 113: 56-69.

Orkodjo, T.P., Kranjac-Berisavijevic, G., Abagale, F.K., 2022. Impact of climate change on future availability of water for irrigation and hydropower generation in the Omo-Gibe Basin of Ethiopia. Journal of Hydrology: Regional Studies, 44: 101254.

Oudin, L., Andréassian, V., Perrin, C., Michel, C., Le Moine, N., 2008. Spatial proximity, physical similarity, regression and ungaged catchments: A comparison of regionalization approaches based on 913 French catchments. Water Resources Research, 44(3).

Pandi, D., Kothandaraman, S., Kuppusamy, M., 2021. Hydrological models: a review. International Journal of Hydrology Science and Technology, 12(3): 223-242.

Panos, E., Densing, M., Volkart, K., 2016. Access to electricity in the World Energy Council's global energy scenarios: An outlook for developing regions until 2030. Energy Strategy Reviews, 9: 28-49.

Peel, M.C., Blöschl, G., 2011. Hydrological modelling in a changing world. Progress in Physical Geography, 35(2): 249-261.

Pfannerstill, M., Guse, B., Fohrer, N., 2014. Smart low flow signature metrics for an improved overall performance evaluation of hydrological models. Journal of Hydrology, 510: 447-458.

Piccardi, C., Soncini-Sessa, R., 1991. Stochastic dynamic programming for reservoir optimal control: dense discretization and inflow correlation assumption made possible by parallel computing. Water Resources Research, 27(5): 729-741.

Pokhrel, P., Gupta, H., Wagener, T., 2008. A spatial regularization approach to parameter estimation for a distributed watershed model. Water Resources Research, 44(12).

Qi, Y., Bao, L., Ma, X., Miao, Q., Li, X., 2016. Self-adaptive multi-objective evolutionary algorithm based on decomposition for large-scale problems: A case study on reservoir flood control operation. Information Sciences, 367: 529-549.

Qu, B.-Y. et al., 2018. A survey on multi-objective evolutionary algorithms for the solution of the environmental/economic dispatch problems. Swarm and Evolutionary Computation, 38: 1-11.

Quentin Grafton, R., Horne, J., Wheeler, S.A., 2016. On the marketisation of water: Evidence from the Murray-Darling Basin, Australia. Water Resources Management, 30: 913-926.

Rangarajan, H., Hadka, D., Reed, P., Lynch, J.P., 2022. Multi-objective optimization of root phenotypes for nutrient capture using evolutionary algorithms. The Plant Journal, 111(1): 38-53.

Rani, D., Moreira, M.M., 2010. Simulation–optimization modeling: a survey and potential application in reservoir systems operation. Water resources management, 24: 1107-1138.

Razavi, T., Coulibaly, P., 2013. Streamflow prediction in ungauged basins: review of regionalization methods. Journal of hydrologic engineering, 18(8): 958-975.

Razavi, T., Coulibaly, P., 2016. Improving streamflow estimation in ungauged basins using a multi-modelling approach. Hydrological Sciences Journal, 61(15): 2668-2679.

Reed, P.M., Hadka, D., 2014. Evolving many-objective water management to exploit exascale computing. Water Resources Research, 50(10): 8367-8373.

Reed, P.M., Hadka, D., Herman, J.D., Kasprzyk, J.R., Kollat, J.B., 2013. Evolutionary multiobjective optimization in water resources: The past, present, and future. Advances in water resources, 51: 438-456.

Refaeilzadeh, P., Tang, L., Liu, H., 2009. Cross-validation. Encyclopedia of database systems. 2009; 5: 532–538.

Refsgaard, J.C., 1997. Parameterisation, calibration and validation of distributed hydrological models. Journal of hydrology, 198(1-4): 69-97.

Rozos, E., 2019. An assessment of the operational freeware management tools for multi-reservoir systems. Water Supply, 19(4): 995-1007.

Rozos, E., Dimitriadis, P., Bellos, V., 2021. Machine Learning in Assessing the Performance of Hydrological Models. Hydrology, 9(1). DOI:10.3390/hydrology9010005

Salazar, J.Z., Reed, P.M., Quinn, J.D., Giuliani, M., Castelletti, A., 2017. Balancing exploration, uncertainty and computational demands in many objective reservoir optimization. Advances in water resources, 109: 196-210.

Samuel, J., Coulibaly, P., Metcalfe, R.A., 2011. Estimation of continuous streamflow in Ontario ungauged basins: comparison of regionalization methods. Journal of Hydrologic Engineering, 16(5): 447-459.

Satti, S., Zaitchik, B., Siddiqui, S., 2015. The question of Sudan: A hydro-economic optimization model for the Sudanese Blue Nile. Hydrology and Earth System Sciences, 19(5): 2275-2293.

Seibert, J., Staudinger, M., Meerveld, H., 2019. Validation and over-parameterization—experiences from hydrological modeling, Computer simulation validation. Springer, pp. 811-834.

Seleshi, Y., Getahun, A., Teshome, F., Mulatu, D., Germew, S., 2018. The Study of Water Use and Treated Wastewater Discharge charge (Hydropower...).

Sellami, H., La Jeunesse, I., Benabdallah, S., Baghdadi, N., Vanclooster, M., 2014. Uncertainty analysis in model parameters regionalization: a case study involving the SWAT model in Mediterranean catchments (Southern France). Hydrology and Earth System Sciences, 18(6): 2393-2413.

Shafii, M., De Smedt, F., 2009. Multi-objective calibration of a distributed hydrological model (WetSpa) using a genetic algorithm. Hydrology and Earth System Sciences, 13(11): 2137-2149.

Shaw, E.M., Beven, K.J., Chappell, N.A., Lamb, R., 2010. Hydrology in practice. CRC press.

Sheer, D.P., 2010. Dysfunctional water management: Causes and solutions. American Society of Civil Engineers, pp. 1-4.

Singh, A., Jha, S.K., 2021. Identification of sensitive parameters in daily and monthly hydrological simulations in small to large catchments in Central India. Journal of Hydrology, 601: 126632.

Singh, A., Minsker, B.S., 2008. Uncertainty-based multiobjective optimization of groundwater remediation design. Water resources research, 44(2).

Singh, V.P., 1988. Hydrologic systems. Volume I: Rainfall-runoff modeling. Prentice Hall, Englewood Cliffs New Jersey. 1988. 480.

Sivanandam, S., Deepa, S., Sivanandam, S., Deepa, S., 2008. Genetic algorithms. Springer.

Smith, R.C., 2013. Uncertainty quantification: theory, implementation, and applications, 12. Siam.

SOGREAH, 2010. Gibe III Hydropower Project study final report for Europian Investment Bank.

Song, X. et al., 2015. Global sensitivity analysis in hydrological modeling: Review of concepts, methods, theoretical framework, and applications. Journal of hydrology, 523: 739-757.

Sorenson, H.W., Alspach, D.L., 1971. Recursive Bayesian estimation using Gaussian sums. Automatica, 7(4): 465-479.

Spruill, C.A., Workman, S.R., Taraba, J.L., 2000. Simulation of daily and monthly stream discharge from small watersheds using the SWAT model. Transactions of the ASAE, 43(6): 1431.

Storn, R., Price, K., 1997. Differential evolution-a simple and efficient heuristic for global optimization over continuous spaces. Journal of global optimization, 11(4): 341.

Stretch, D., Adeyemo, J., 2018. Review of hybrid evolutionary algorithms for optimizing a reservoir. south african journal of chemical engineering, 25(1): 22-31.

Su, Z. et al., 2020. The effects of pre-season high flows, climate, and the Three Gorges Dam on low flow at the Three Gorges Region, China. Hydrological Processes, 34(9): 2088-2100.

Sun, Y., Kang, S., Li, F., Zhang, L., 2009. Comparison of interpolation methods for depth to groundwater and its temporal and spatial variations in the Minqin oasis of northwest China. Environmental Modelling & Software, 24(10): 1163-1170.

Sundin, C., 2017. Exploring the water-energy nexus in the Omo river basin. KTH, Stockholm.

Swain, J.B., Patra, K.C., 2017. Streamflow estimation in ungauged catchments using regionalization techniques. Journal of Hydrology, 554: 420-433.

Talbot, C.A., Pathak, C.S., 2020. Forecast-Informed Reservoir Operations: An Agency Approach to Testing, Evaluating and Implementing New Water Management Policy, AGU Fall Meeting Abstracts, pp. SY015-0006.

Tan, M.L., Gassman, P.W., Yang, X., Haywood, J., 2020. A review of SWAT applications, performance and future needs for simulation of hydro-climatic extremes. Advances in Water Resources, 143: 103662.

Tedla, E., Gebremichael, M., Hailu, D., Seyoum, S., 2015. River basin scale long-term hydropower operational planning under changing climate. International Journal of Application or Innovation in Engineering & Management (IJAIEM), 4: 2319-4847.

Tegegne, G., Kim, Y.-O., 2018. Modelling ungauged catchments using the catchment runoff response similarity. Journal of hydrology, 564: 452-466.

Tegegne, G., Kim, Y.-O., Seo, S.B., Kim, Y., 2019. Hydrological modelling uncertainty analysis for different flow quantiles: a case study in two hydro-geographically different watersheds. Hydrological Sciences Journal, 64(4): 473-489.

Tegegne, G., Melesse, A.M., Worqlul, A.W., 2020. Development of multi-model ensemble approach for enhanced assessment of impacts of climate change on climate extremes. Science of the Total Environment, 704: 135357.

Tianqi, A., Yoshitani, J., Takeuchi, K., Fukami, K., 2003. Effects of sub-basin scale on runoff simulation in distributed hydrological model: BTOPMC, Weather Radar Information and Distributed Hydrological Modelling: Proceedings of an International Symposium (Symposium HS03) Held During IUGG 2003, the XXIII General Assembly of the

International Union of Geodesy and Geophysics: at Sapporo, Japan, from 30 June to 11 July, 2003. International Assn of Hydrological Sciences, pp. 227.

Tilmant, A., Pinte, D., Goor, Q., 2008. Assessing marginal water values in multipurpose multireservoir systems via stochastic programming. Water Resources Research, 44(12).

Tomlinson, J.E., Arnott, J.H., Harou, J.J., 2020. A water resource simulator in Python. Environmental Modelling & Software, 126: 104635.

Tsoukalas, I., Kossieris, P., Efstratiadis, A., Makropoulos, C., 2016. Surrogate-enhanced evolutionary annealing simplex algorithm for effective and efficient optimization of water resources problems on a budget. Environmental Modelling & Software, 77: 122-142.

Tsutsui, S., Yamamura, M., Higuchi, T., 1999. Multi-parent recombination with simplex crossover in real coded genetic algorithms, Proceedings of the 1st Annual Conference on Genetic and Evolutionary Computation-Volume 1, pp. 657-664.

Ullrich, A., Volk, M., 2009. Application of the Soil and Water Assessment Tool (SWAT) to predict the impact of alternative management practices on water quality and quantity. Agricultural Water Management, 96(8): 1207-1217.

Uniyal, B., Jha, M.K., Verma, A.K., 2015. Parameter identification and uncertainty analysis for simulating streamflow in a river basin of Eastern India. Hydrological Processes, 29(17): 3744-3766.

Upadhyay, P. et al., 2022. Applications of the SWAT model for coastal watersheds: review and recommendations. Journal of the ASABE, 65(2): 453-469.

Valdez, E.S., Anctil, F., Ramos, M.-H., 2022. Choosing between post-processing precipitation forecasts or chaining several uncertainty quantification tools in hydrological forecasting systems. Hydrology and Earth System Sciences, 26(1): 197-220.

van der Vat, M., 2015. Optimizing reservoir operation for flood storage, hydropower and irrigation using a hydro-economic model for the Citarum River, West-Java, Indonesia.

Van Griensven, A., Ndomba, P., Yalew, S., Kilonzo, F., 2012. Critical review of SWAT applications in the upper Nile basin countries. Hydrology and Earth System Sciences, 16(9): 3371-3381.

Van Veldhuizen, D.A., Lamont, G.B., 1998. Evolutionary computation and convergence to a pareto front, Late breaking papers at the genetic programming 1998 conference. Citeseer, pp. 221-228.

Veettil, A.V. et al., 2021. Fully distributed versus semi-distributed process simulation of a highly managed watershed with mixed land use and irrigation return flow. Environmental Modelling & Software, 140: 105000.

Venter, G., 2010. Review of optimization techniques.

Vrugt, J.A., Diks, C.G., Gupta, H.V., Bouten, W., Verstraten, J.M., 2005. Improved treatment of uncertainty in hydrologic modeling: Combining the strengths of global optimization and data assimilation. Water resources research, 41(1).

Vrugt, J.A., Gupta, H.V., Bouten, W., Sorooshian, S., 2003. A Shuffled Complex Evolution Metropolis algorithm for optimization and uncertainty assessment of hydrologic model parameters. Water resources research, 39(8).

Wan, Y. et al., 2021. Performance dependence of multi-model combination methods on hydrological model calibration strategy and ensemble size. Journal of Hydrology, 603: 127065.

Wang, C., Duan, Q., Tong, C.H., Di, Z., Gong, W., 2016. A GUI platform for uncertainty quantification of complex dynamical models. Environmental Modelling & Software, 76: 1-12.

Wang, H., Wang, C., Wang, Y., Gao, X., Yu, C., 2017. Bayesian forecasting and uncertainty quantifying of stream flows using Metropolis–Hastings Markov Chain Monte Carlo algorithm. Journal of hydrology, 549: 476-483.

Wang, S. et al., 2014. Comparison of interpolation methods for estimating spatial distribution of precipitation in Ontario, Canada. International Journal of Climatology, 34(14): 3745-3751.

Wen, S. et al., 2020. Comprehensive evaluation of hydrological models for climate change impact assessment in the Upper Yangtze River Basin, China. Climatic Change, 163: 1207-1226.

Whittington, D., Wu, X., Sadoff, C., 2005. Water resources management in the Nile basin: the economic value of cooperation. Water policy, 7(3): 227-252.

Woldegebrael, S.M., Kidanewold, B.B., Melesse, A.M., 2022. Seasonal Flow Forecasting Using Satellite-Driven Precipitation Data for Awash and Omo-Gibe Basins, Ethiopia. Remote Sensing, 14(18): 4518.

Wood, E.F., Sivapalan, M., Beven, K., Band, L., 1988. Effects of spatial variability and scale with implications to hydrologic modeling. Journal of hydrology, 102(1-4): 29-47.

Woodroofe, R., 1996. Omo-gibe River basin integrated development master plan study final Report Vol. VI Water Resources Surveys and Inventories, Ministry of Water Resources. AA.

Woodruff, M.J., Hadka, D.M., Reed, P.M., Simpson, T.W., 2012. Auto-adaptive search capabilities of the new Borg MOEA: A detailed comparison on alternative product family design problem formulations, 12th AIAA Aviation Technology, Integration, and

Operations (ATIO) Conference and 14th AIAA/ISSMO Multidisciplinary Analysis and Optimization Conference.

Woodruff, M.J., Simpson, T.W., Reed, P.M., 2015. Multi-objective evolutionary algorithms' performance in a support role, International Design Engineering Technical Conferences and Computers and Information in Engineering Conference. American Society of Mechanical Engineers, pp. V02BT03A028.

Worku, F., Werner, M., Wright, N., Van der Zaag, P., Demissie, S., 2014. Flow regime change in an endorheic basin in southern Ethiopia. Hydrology and Earth System Sciences, 18(9): 3837-3853.

Wu, J. et al., 2020. Development of reservoir operation functions in SWAT+ for national environmental assessments. Journal of Hydrology, 583: 124556.

Wu, L., Liu, X., Chen, J., Yu, Y., Ma, X., 2022. Overcoming equifinality: time-varying analysis of sensitivity and identifiability of SWAT runoff and sediment parameters in an arid and semiarid watershed. Environmental Science and Pollution Research, 29(21): 31631-31645.

WWDSE, 2015. Feasibility Study and Detail Design of Omo Valley Farm Irrigation Project.

Xiu, D., Karniadakis, G.E., 2003. Modeling uncertainty in flow simulations via generalized polynomial chaos. Journal of computational physics, 187(1): 137-167.

Y. Al-Jawad, J., M. Kalin, R., 2019. Assessment of water resources management strategy under different evolutionary optimization techniques. Water, 11(10): 2021.

Yan, D., Ludwig, F., Huang, H.Q., Werners, S.E., 2017. Many-objective robust decision making for water allocation under climate change. Science of the Total Environment, 607: 294-303.

Yang, X., Jomaa, S., Rode, M., 2019. Spatiotemporally distributed sensitivity analysis for catchment water quality models, Geophysical Research Abstracts.

Yilmaz, K.K., Gupta, H.V., Wagener, T., 2008. A process-based diagnostic approach to model evaluation: Application to the NWS distributed hydrologic model. Water Resources Research, 44(9).

Yilmaz, M.U., Onoz, B., 2020. A comparative study of statistical methods for daily streamflow estimation at ungauged basins in Turkey. Water, 12(2): 459.

Zamoum, S., Souag-Gamane, D., 2019. Monthly streamflow estimation in ungauged catchments of northern Algeria using regionalization of conceptual model parameters. Arabian Journal of Geosciences, 12(11): 1-14.

Zaniolo, M., Giuliani, M., Bantider, A., Castelletti, A., 2021a. Hydropower development: Economic and environmental benefits and risks, The Omo-Turkana Basin. Routledge, pp. 37-57.

Zaniolo, M., Giuliani, M., Sinclair, S., Burlando, P., Castelletti, A., 2021. When timing matters—misdesigned dam filling impacts hydropower sustainability. Nature Communications, 12(1): 3056.

Zeinivand, H., 2015. Comparison of interpolation methods for precipitation fields using the physically based and spatially distributed model of river runoff on the example of the Gharesou basin, Iran. Russian Meteorology and Hydrology, 40: 480-488.

Zhang, H., Zhou, J., Fang, N., Zhang, R., Zhang, Y., 2013a. Daily hydrothermal scheduling with economic emission using simulated annealing technique based multi-objective cultural differential evolution approach. Energy, 50: 24-37.

Zhang, J. et al., 2017. Assessing the weighted multi-objective adaptive surrogate model optimization to derive large-scale reservoir operating rules with sensitivity analysis. Journal of Hydrology, 544: 613-627.

Zhang, M. et al., 2013b. Extreme drought changes in Southwest China from 1960 to 2009. Journal of Geographical Sciences, 23: 3-16.

Zhang, X. et al., 2018. Impacts of climate change, policy and Water-Energy-Food nexus on hydropower development. Renewable Energy, 116: 827-834.

Zhang, Y., Vaze, J., Chiew, F.H., Li, M., 2015. Comparing flow duration curve and rainfall–runoff modelling for predicting daily runoff in ungauged catchments. Journal of Hydrology, 525: 72-86.

Zhang, Y., Vaze, J., Chiew, F.H., Teng, J., Li, M., 2014. Predicting hydrological signatures in ungauged catchments using spatial interpolation, index model, and rainfall–runoff modelling. Journal of Hydrology, 517: 936-948.

Zheng, F., Zecchin, A., 2014. An efficient decomposition and dual-stage multi-objective optimization method for water distribution systems with multiple supply sources. Environmental Modelling & Software, 55: 143-155.

Zhou, A. et al., 2011. Multiobjective evolutionary algorithms: A survey of the state of the art. Swarm and evolutionary computation, 1(1): 32-49.

Zhu, Y. et al., 2021. Application of the Regression-Augmented Regionalization Approach for BTOP Model in Ungauged Basins. Water, 13(16): 2294.

Zitzler, E., 1999. Evolutionary algorithms for multiobjective optimization: Methods and applications, 63. Shaker Ithaca.

Appendix A

Meteorological data analysis in the study river basin

Table A- 1. Locations and altitudes of the meteorological stations considered in the study.

Station	Data Length	Total (Years)	Latitude (N)	Longitude (E)	Altitude (m)
Abelti	1986 - 2017	32	8.17	37.63	1684
Arba Minch	1985 - 2019	35	6.06	37.56	1207
Areka	1988 - 2019	32	7.06	37.71	1752
Assendabo	1986 - 2021	36	7.75	37.22	1764
Bechi	1988 - 2017	29	7.14	35.34	1261
Billate	1988 - 2019	32	6.82	38.08	1361
Boditi School	1987 - 2019	32	6.95	37.96	2043
Bonga	1985 - 2021	37	7.50	36.50	1779
Bui	1986 - 2019	33	8.35	38.55	2020
Butajira P. Station	1987 - 2019	32	8.15	38.37	2000
Chena	1988 - 2017	29	7.15	35.81	2203
Danna1	1988 - 2018	30	6.63	37.57	1282
Daramalo	1988 - 2018	30	6.32	37.3	1183
Dimeka	1987 - 2019	33	5.17	36.53	1115
Dinke	1988 - 2018	30	6.44	37.42	1596
Ejaji	1989 - 2021	33	8.99	37.32	1732
Erbore	1988 - 2017	29	5.00	36.84	518
Gore	1987 - 2019	32	8.13	35.53	2033
Hossaena	1985 - 2021	37	7.57	37.85	2307
Jimma	1986 - 2021	36	7.67	36.82	1718
Jinka	1985 - 2021	37	5.77	36.55	1373
Kachis	1987 - 2017	31	9.58	37.86	2520
Kako	1988 - 2018	30	5.65	36.65	1409
Key Afer	1986 - 2020	35	5.52	36.73	1597
Konso	1986 - 2019	34	5.33	37.43	1431
Kumbi	1986 - 2018	33	8.12	37.48	1930
Limu Genet	1986 - 2019	34	8.07	36.95	1766
Lote	1988 - 2018	30	6.39	36.99	1254
Masha	1987 - 2018	32	7.75	35.47	2282
Sawula	1985 - 2021	37	6.30	36.84	1348
Sekoru	1986 - 2021	36	7.92	37.42	1928
Shebe	1986 - 2018	33	7.50	36.52	1813
Shishinda	1985 - 2021	37	7.25	35.88	2000
Wolaita Soda	1985 - 2021	37	6.81	37.73	1854
Woliso (Gion)	1986 - 2021	36	8.55	37.98	2058
Wolkite	1986 - 2020	35	8.13	37.45	2000
Zanga	1988 - 2018	30	6.35	36.95	1229

A typical missing data filling using ANN approach of Python-Coded prophet model at the Jima meteorological station

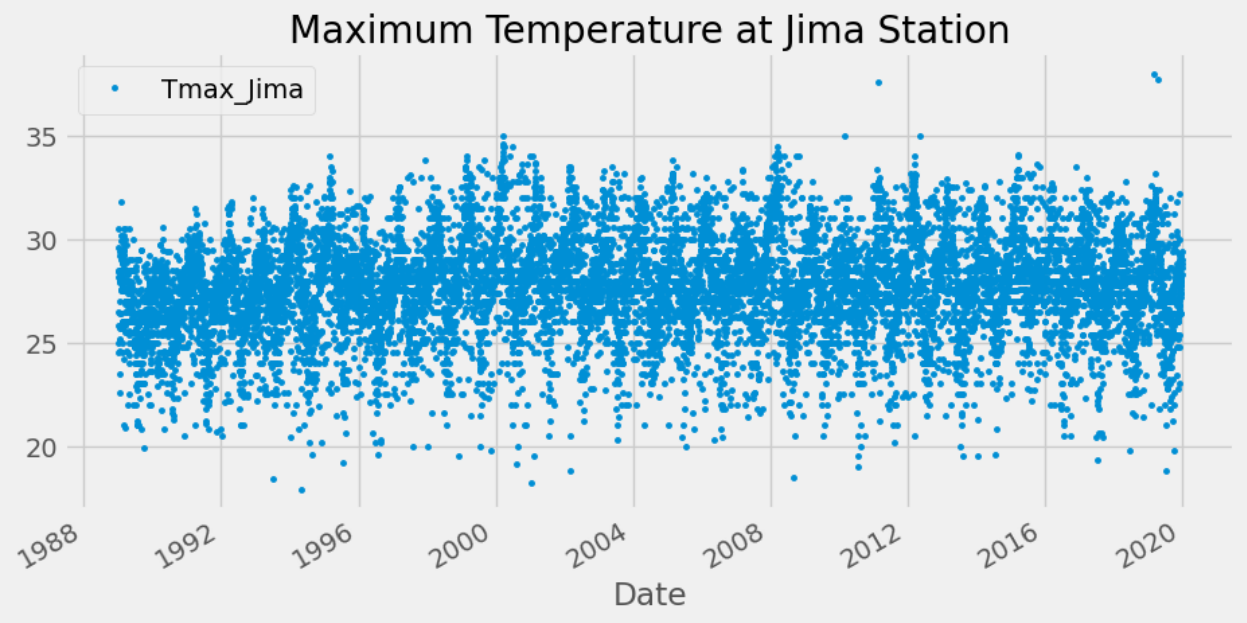

Figure A-1. Plot of raw Temperature timeseries data at Jima meteorological station

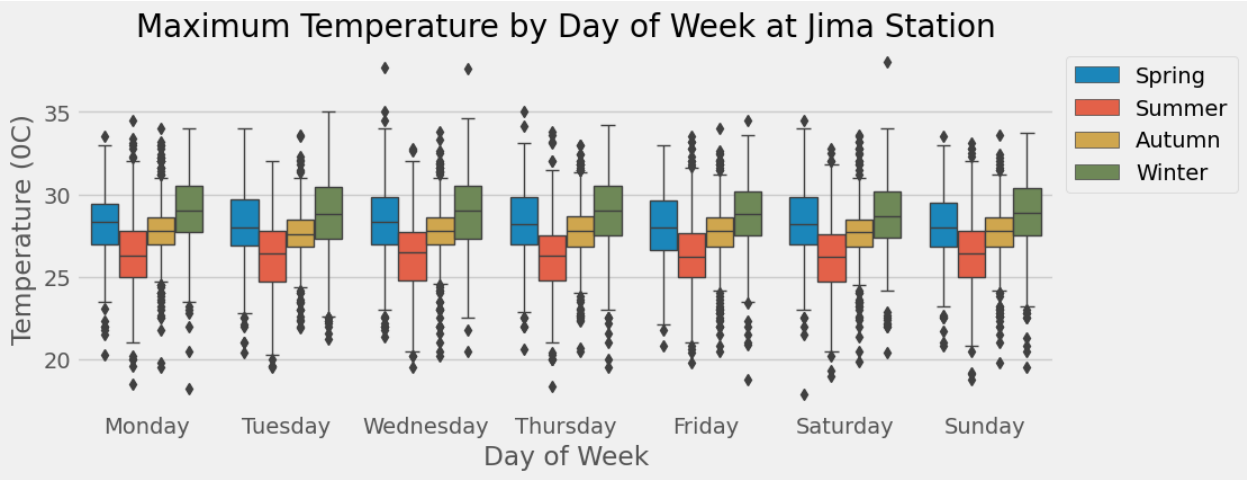

Figure A-2. Seasonal Variation on day of week scale of the Jima meteorological station's maximum temperature timeseries data

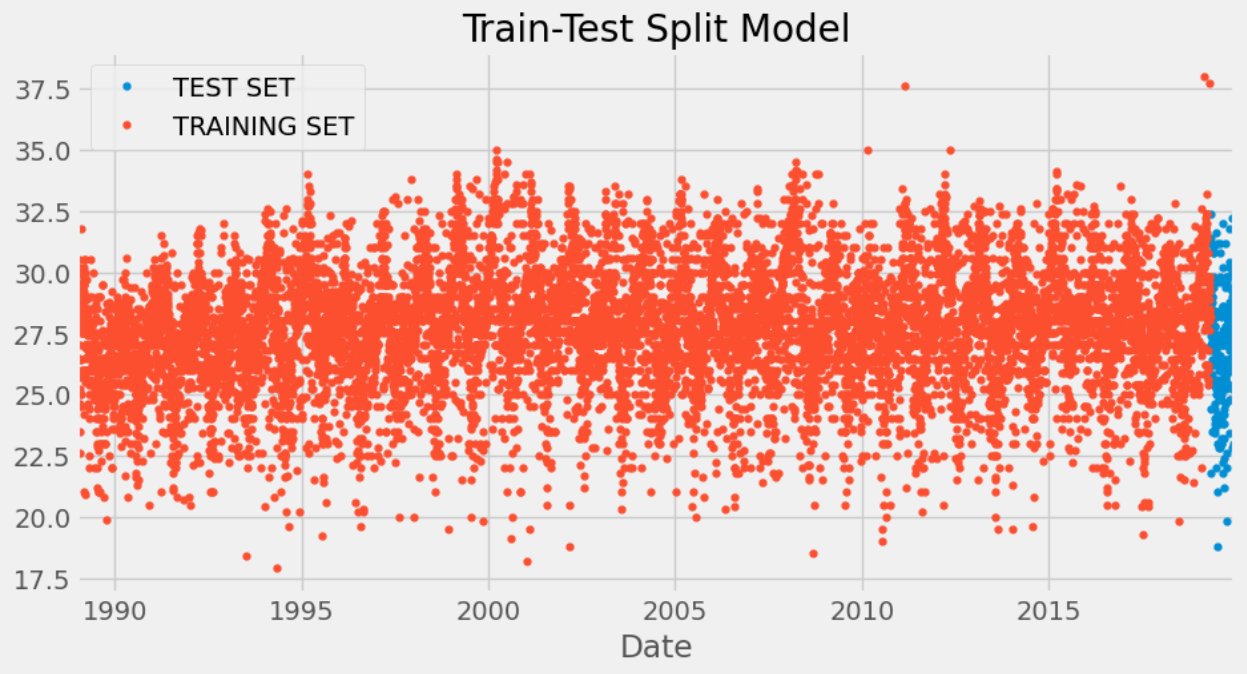

Figure A-3. Plot of Train-Test Split model of maximum temperature at the Jima station

Table A-2. Sample forecasted values including their upper and lower bound estimates

ds	yhat	yhat_lower	yhat_upper
01-05-19	28.26	25.65	30.96
02-05-19	28.21	25.64	30.92
03-05-19	28.14	25.41	30.8
04-05-19	28.09	25.39	30.98
05-05-19	28.09	25.42	30.94

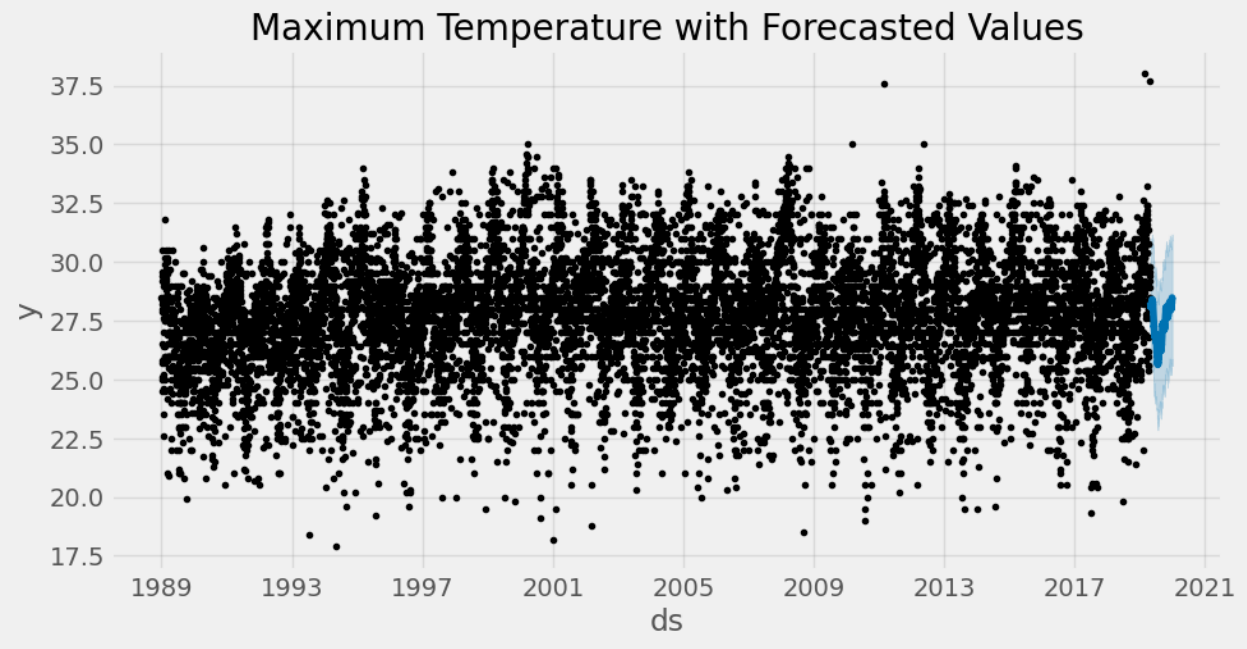

Figure A-4. Plot of the maximum temperature data with forecasted values including their upper and lower bound estimates

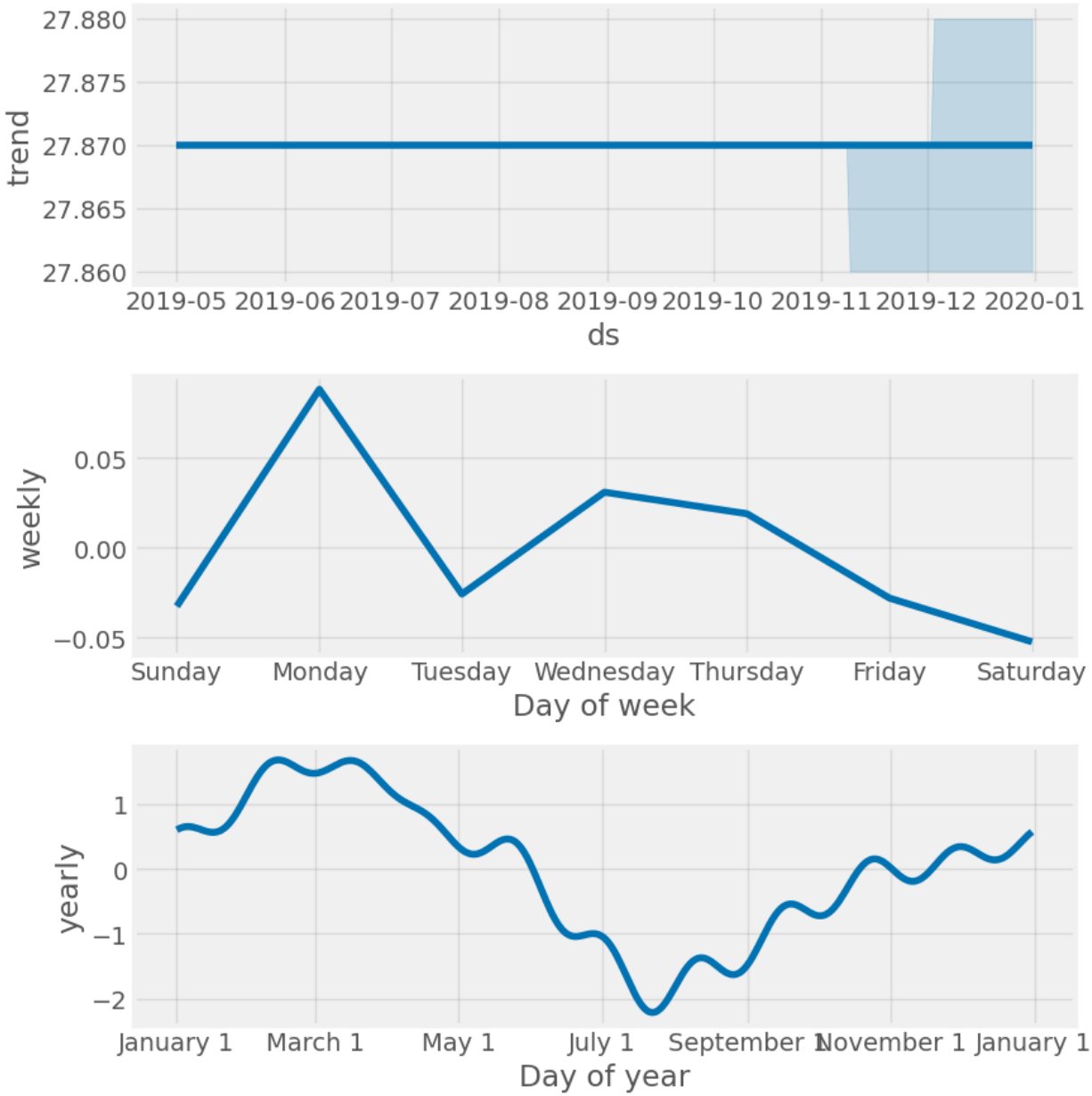

Figure A-5. Model plot components showing trend and seasonal variations of maximum temperature at the Jima meteorological station.

Forecasts can be evaluated using statistical criteria such as mean absolute error (MAE). In this situation, the error is around MAE of 1.51, which is considerably less (better) than a naive approach.

Appendix B

Streamflow data analysis in the study river basin

Table B-1. Locations and catchment areas of the hydrological stations considered in the study.

Station	Data Length	Total (Years)	Latitude (N)	Longitude (E)	Area (Sq.km)
Ajancho Nr. Areka	1990 - 2016	27	7.13	37.72	306
Bidruawana Nr. Sekoru	1990 - 2005	16	7.92	37.40	41
Bulbul Nr. Serbo	1990 - 2005	16	7.57	37.08	526
Demie @ Orota Alem	1990 - 2006	17	6.63	37.52	1119
Dincha @ Bonga	2000 - 2018	19	7.20	36.28	444
G.Gibe @ Abelti	1963 - 2008	45	8.23	37.58	15746
G.Gibe Nr. Asendabo	1998 - 2019	22	7.75	37.18	2966
Gecha Nr. Bonga	1996 - 2012	17	7.28	36.22	175
Gibe Nr. Limugenet	1989 - 2013	25	8.10	36.93	533
Gibe Nr. Seka	1990 - 2006	17	7.60	36.75	280
Gogera Nr. Dana 1	1986 - 2013	28	6.72	37.53	266
Gojeb Nr. Shebe	1989 - 2018	30	7.42	36.38	3577
Guma Nr. Andaracha	1985 - 2012	28	7.15	36.25	231
Kulit Nr. Tedele	1998 - 2014	17	8.45	37.67	350
Mazie Nr. Morka	1990 - 2007	18	6.43	37.20	937
Megech Nr. Gubere	1989 - 2006	18	8.18	37.47	286
Nerie Nr. Jinka	1990 - 2006	17	5.80	36.55	166
Sheta @ Bonga	1998 - 2012	15	7.28	36.23	191
Sokie Nr. Areka	1990 - 2015	26	7.15	36.23	103
Wabi Nr. Wolkite	1991 - 2007	17	8.25	37.77	1866
Walga Nr. Wolkite	1972 - 2005	34	8.33	37.60	1792
Werebesa Nr. Silk Amba	1984 - 2000	17	8.45	37.62	234

Data Quality Analysis

Sample raw data visualization at the Asendabo streamflow station

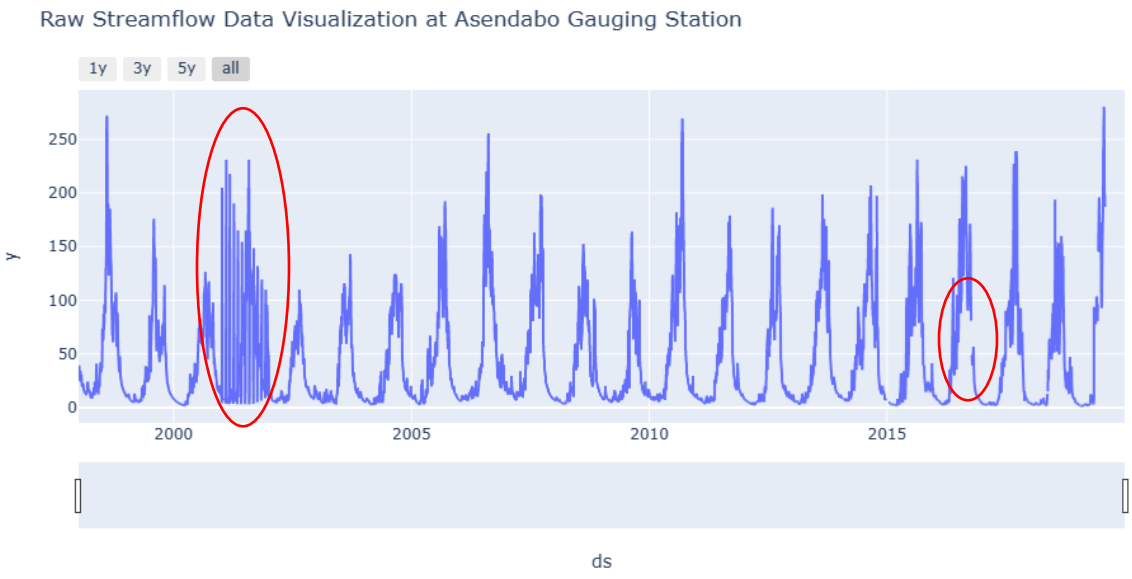

Figure B-1. Sample raw streamflow data visualization: red circles showing data errors

A typical missing data filling using ANN approach of Python-Coded prophet model at the Abelti streamflow station

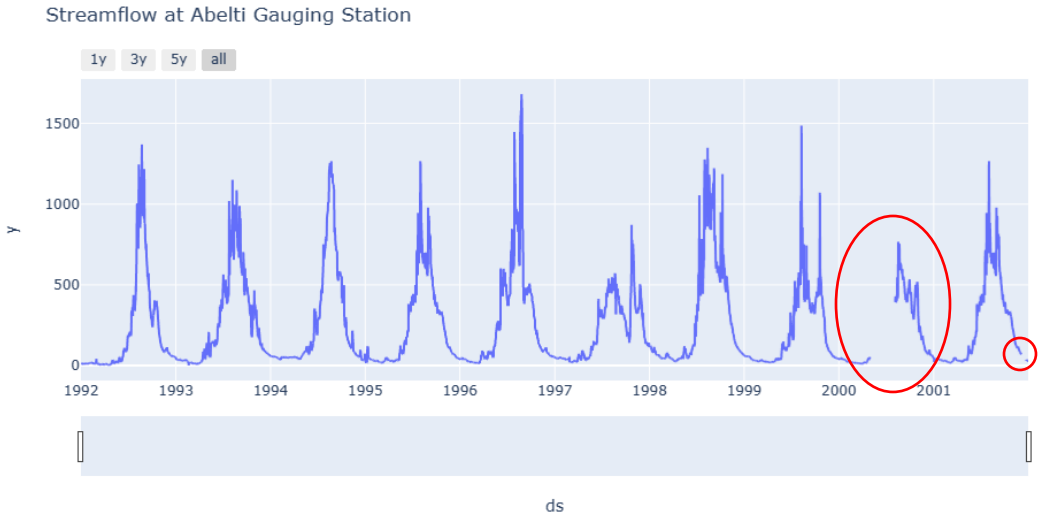

Figure B-2. Typical Streamflow at the Abelti gauging station having missing data multiple places intime.

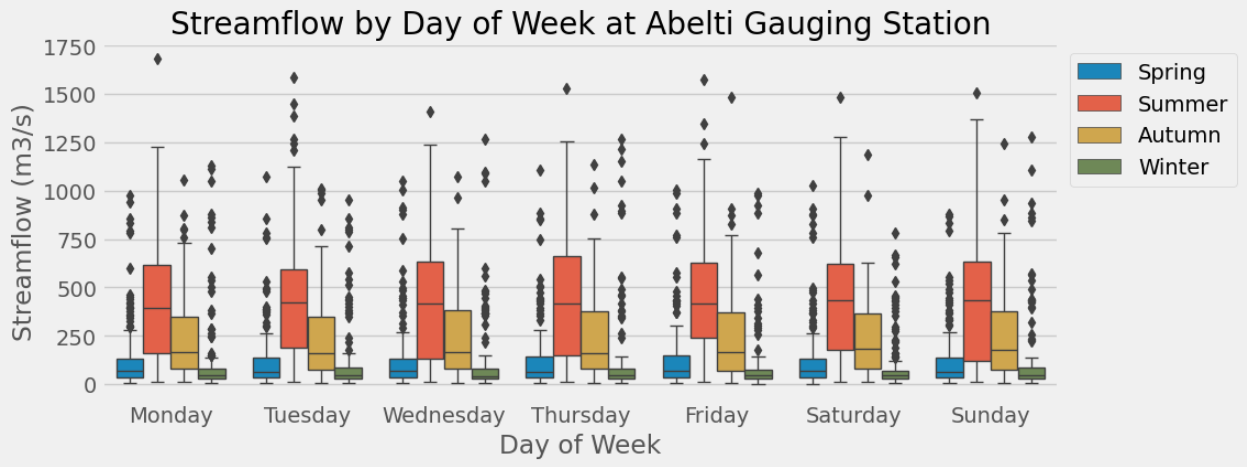

Figure B-3. Streamflow Variation by day of week at the Abelti gauging station

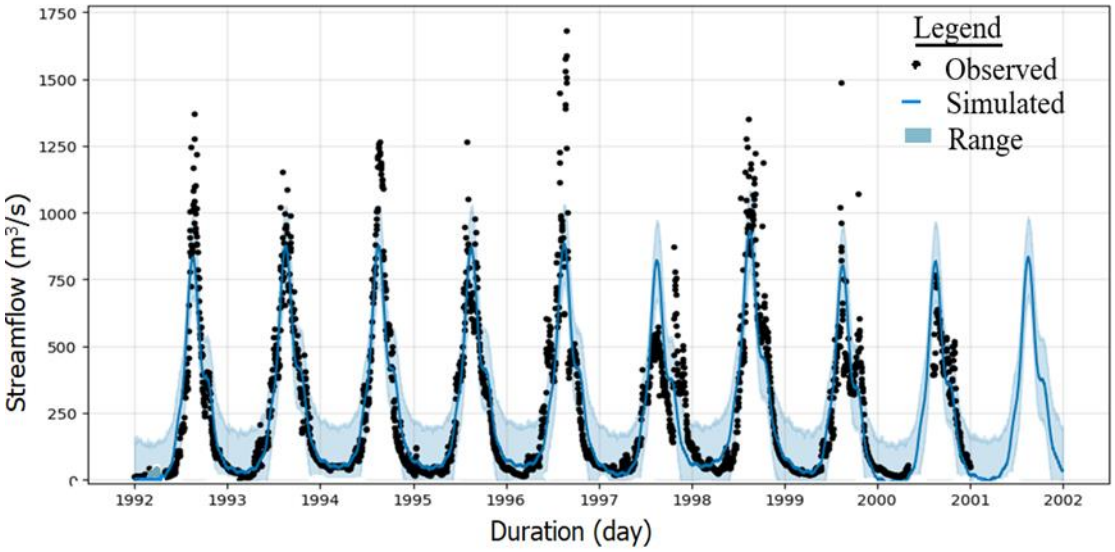

Figure B-4. Raw Streamflow data with forecasted values at the Abelti gauging station

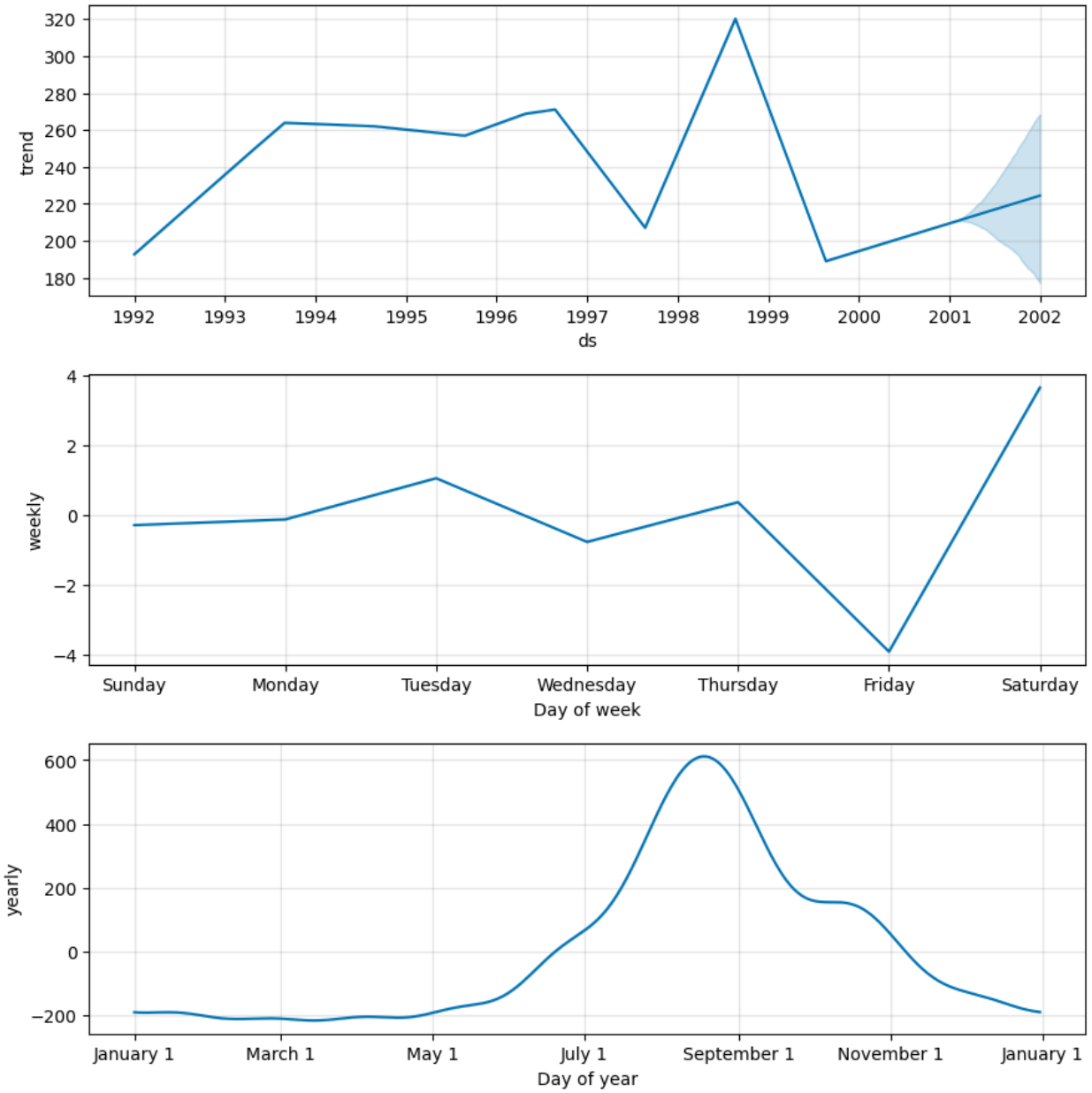

Figure B-5. Model plot components showing trend and seasonal variations of streamflow at the Abelti gauging station.

Appendix C

Calibration and validation plots of sites near or on-site cascade reservoir

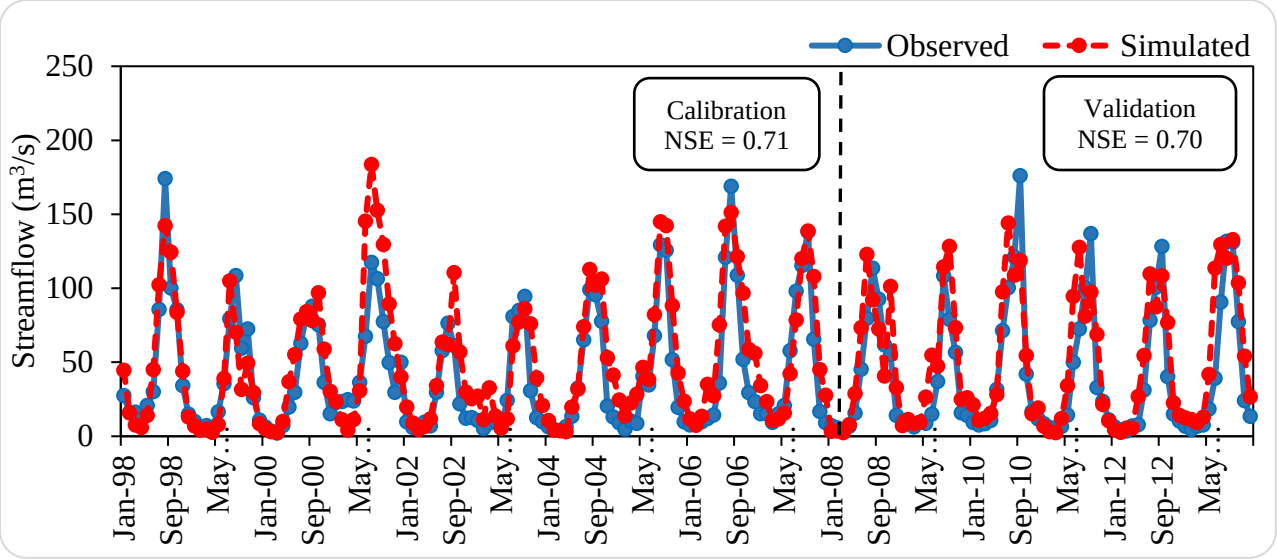

Figure C-1. Calibration and validation plot of observed and simulated streamflow data at the Asendabo station just upstream of Gibe I reservoir.

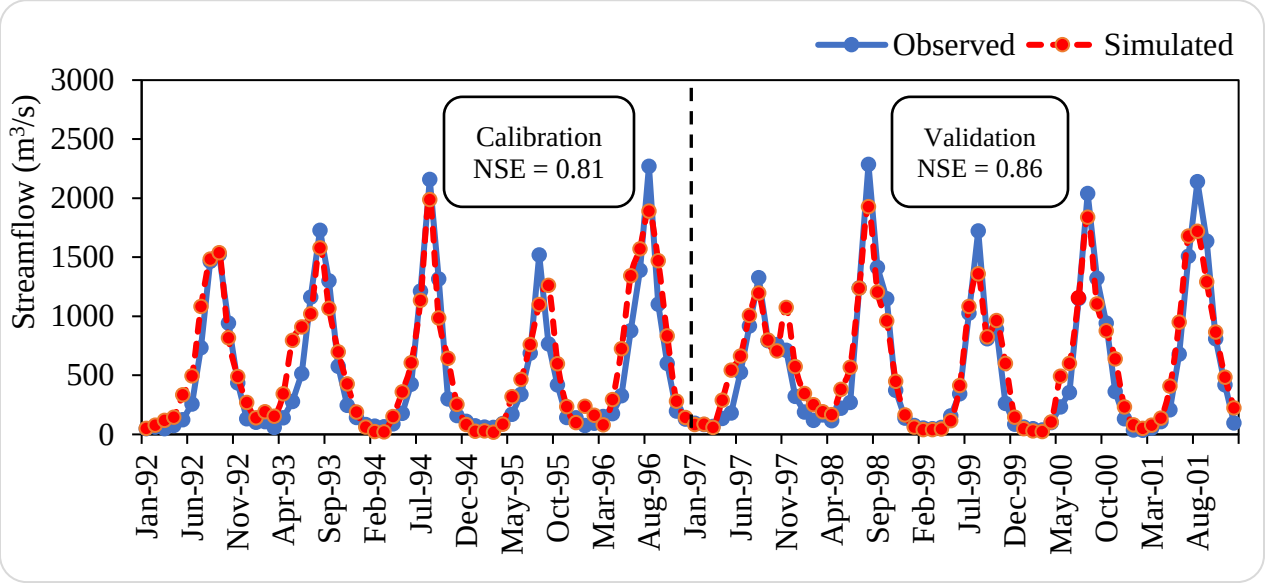

Figure C-2. Calibration and validation plot of observed and simulated streamflow data at the Gibe III Dam.

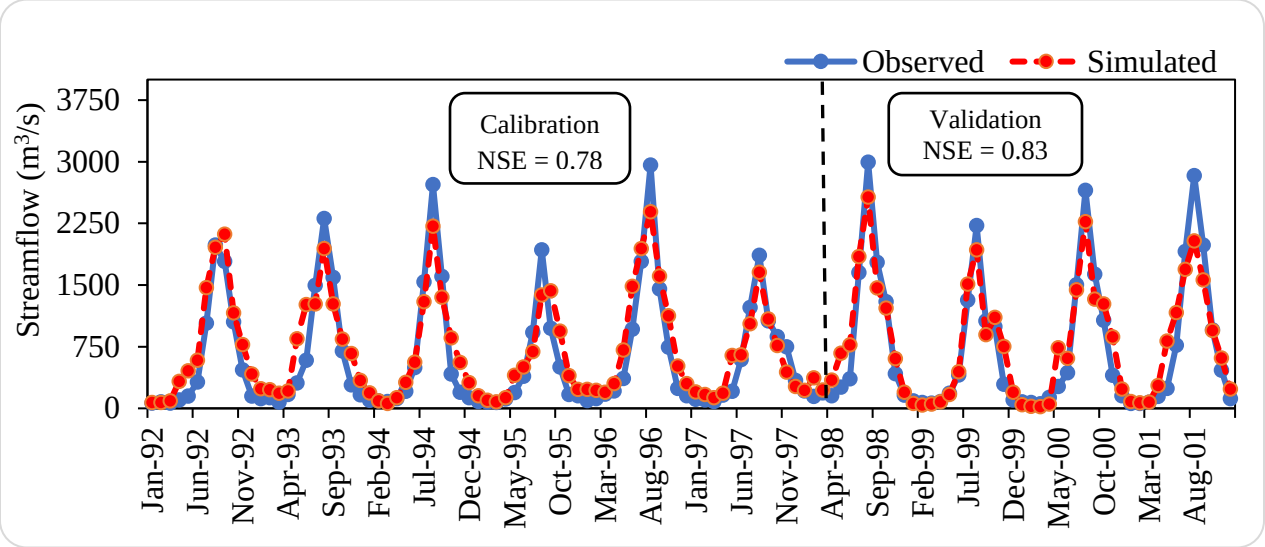

Figure C-3. Calibration and validation plot of observed and simulated streamflow data at the Koysha Dam.

Hydrological Model Performance

The model's success is measured using three statistical indicators: NSE, p-factor, and r-factor. Values closer to 1 are preferred for NSE and p-factor; values closer to 0 are preferred for r-factor (Abbaspour et al., 2015). Table C-1 shows that all metrics indicate that the model's performance is good to very good (Moriasi et al., 2007). A regionalization technique is used to derive the streamflow at Gibe I from the upstream catchment Asendabo station, whose performance is likewise displayed in Table C-1.

Table C- 1*. Calibration and validation metrics of the project locations*

Metrics	Gibe I (Asendabo St.)		Gibe III		Koysha	
	Calibration	Validation	Calibration	Validation	Calibration	Validation
p-factor	0.82	0.81	0.80	0.90	0.74	0.81
r-factor	1.16	1.11	1.12	0.97	1.08	0.87
R^2	0.81	0.77	0.82	0.88	0.79	0.86
NS	0.71	0.70	0.81	0.86	0.78	0.83

Table C- 2*. Actual SWAT flow parameter values at different subbasin spatial scales.*

Spatial Scales	Actual Flow Parameter Values				
	CN2	CH_K	GWQMN	RCHRG_DP	GW_REVAP
A2	65.37	293.94	4788.18	0.05	0.19
A10	70.28	171.39	4545.53	0.05	0.19
A20	72.78	173.91	4518.32	0.05	0.19
G2	70.36	277.58	2996.17	0.05	0.18
G10	75.08	248.97	3158.11	0.05	0.19
G20	74.22	318.83	2986.72	0.05	0.18
W2	67.79	299.91	2737.89	0.05	0.19
W10	64.23	243.74	2698.81	0.05	0.17
W20	72.85	378.24	2440.84	0.05	0.19

Appendix D

Crop type, quantity, and crop water requirements adopted for the study

Table D- 1. Crop type considered in the two scenarios of irrigation optimization (Jillo et al., 2017; Ministry of Culture and Tourism of Ethiopia, 2018; SOGREAH, 2010; WWDSE, 2015)

Owner	Plantation Type	Existing Cropland Area (ha)	Near Future Cropland Area (ha)
Recession Farming	Cereals	11,754	11,754
Private (Fri_el)	Cereals	500	5,000
Government (Kuraz)	Sugarcane	18,000	75,000
Private (Fri_el)	Sugarcane	-	5,000
Private (Fri_el)	Cotton	-	5,000
Private (various)	Cotton	4,000	20,000
Private (Sisay Tesfaye)	Cotton	243	1,200
Private (Omo Valley Farm Cooperation)	Cotton	898	4,702

Table D- 2. Crop water requirement based on FAO CROPWAT Model (Aravind et al., 2021; WWDSE, 2015)

Crop water requirement	Jan	Feb	Mar	Apr	May	Jun	Jul	Aug	Sep	Oct	Nov	Dec
Cotton (Irr.req) (l/s/ha)	0.78	0.65	0.17	0.30	0.40	0.41	0.66	0.71	0.51	0.04	0.10	0.56
Cotton (Irr.req) (m^3/ha)	2089.15	1572.48	455.33	777.60	1071.36	1062.72	1767.74	1901.66	1321.92	107.14	259.20	1499.90
Sugarcane (Irr.req) (l/s/ha)	0.63	0.73	0.85	0.70	0.50	0.42	0.08	0.27	0.46	0.23	0.17	0.43
Sugarcane (Irr.req) (m^3/ha)	1687.39	1766.02	2276.64	1814.40	1339.20	1088.64	214.27	723.17	1192.32	616.03	440.64	1151.71
Maize (Irr.req) (l/s/ha)	0.00	0.00	0.00	0.00	0.00	0.00	0.00	0.00	1.14	1.58	1.71	1.71
Maize (Irr.req) (m^3/ha)	0.00	0.00	0.00	0.00	0.00	0.00	0.00	0.00	2954.88	4231.87	4432.32	4580.06

Table D- 3. Water abstraction and use charge (Hailu et al., 2018; Seleshi et al., 2018)

Project Type	Production	Water use charge
Flood Recession	Cereals	228.4 (ETB/ha)
Mechanised Irrigation	Cereals	228.4 (ETB/ha)
	Sugarcane	1559.58 (ETB/ha)
	Cotton	465.16 (ETB/ha)
Hydropower	Electricity	313.09 (ETB/KWh)

Appendix E

Synthetic Streamflow Generation for Streamflow Variability Study

Generating synthetic streamflow is an essential component of synthetic hydrology, providing a robust platform to test alternative management plans under stochastic scenarios that are different from the ones observed historically.

In this study, we explore four different approaches to solve the multi-objective problem of optimizing multi-reservoir operating strategies in the Omo-Gibe River basin. To ensure a comprehensive analysis of the system's streamflow variability, we conducted optimization on synthetic stream flows that exceed the range recorded in the historical record. This was done in two steps. Firstly, we created artificial stream flows and successfully demonstrated how they augment historical flows while reproducing historical data. Secondly, we describe how run-time diagnostics are utilized to detect several instances of MOEA within the Borg MOEA algorithm for solving optimization issues. All the streamflow data was collected from EEPCO and MWE.

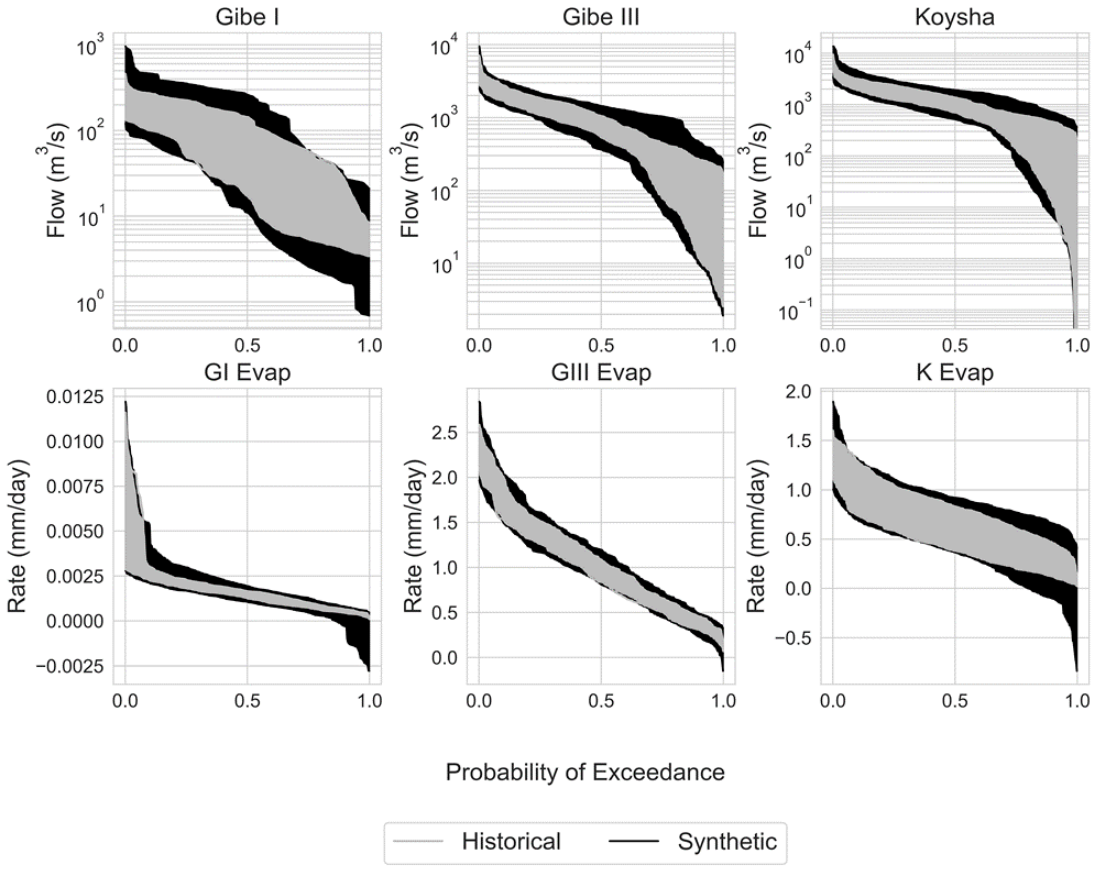

Figure E- 1. Plots of range of flow duration curves from historical record and synthetic generation

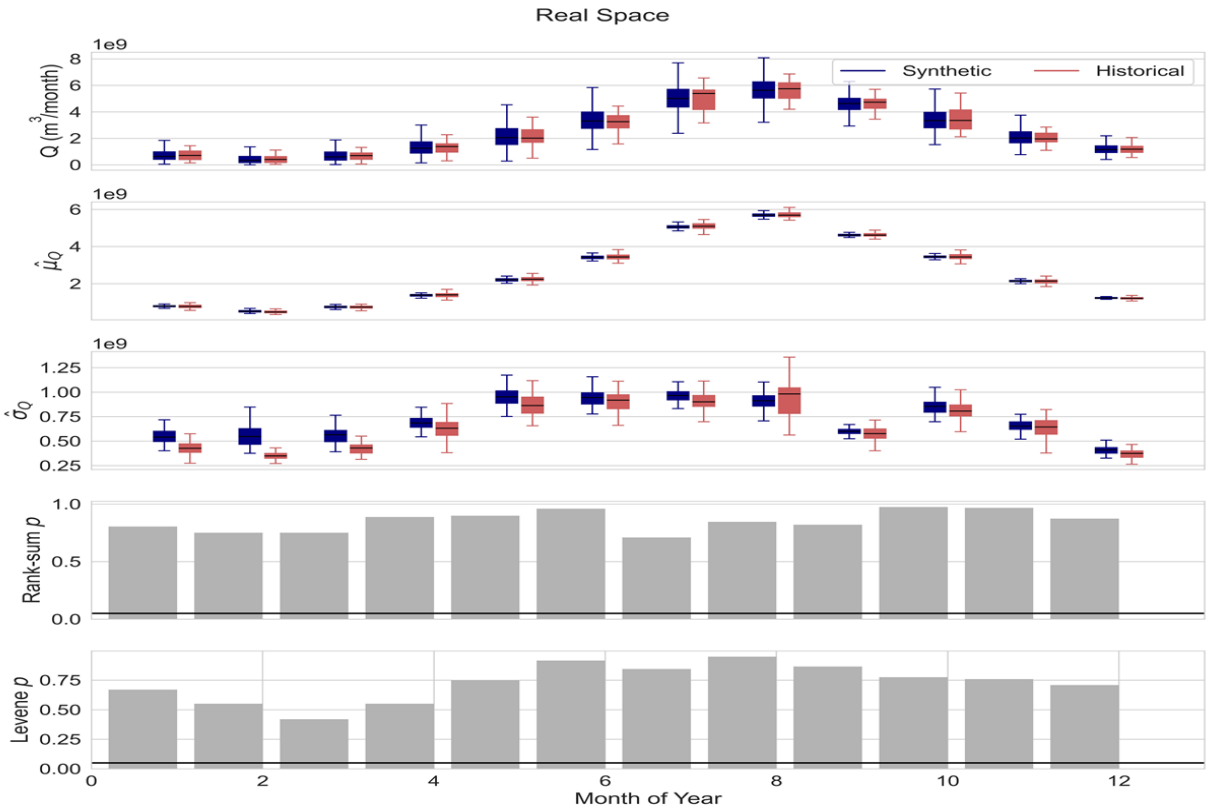

Figure E- 2. Historical monthly flows (pink) and synthetic monthly flows (blue) as well as their means and standard deviations

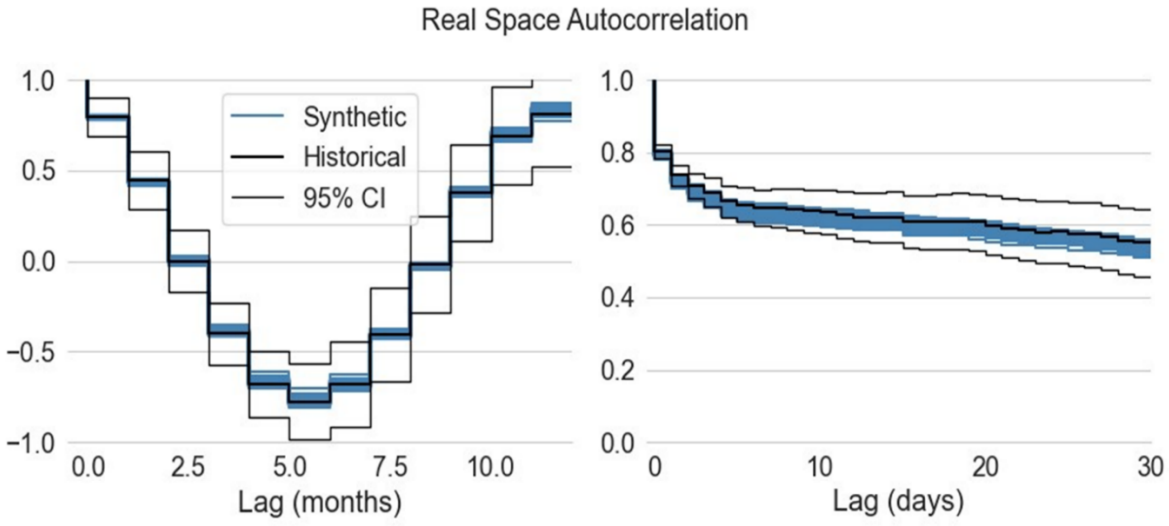

Figure E- 3. Plots the autocorrelation function (acf) and 95% confidence intervals for the historical flows at Marietta (black), as well as the realizations from the synthetic flows (blue).

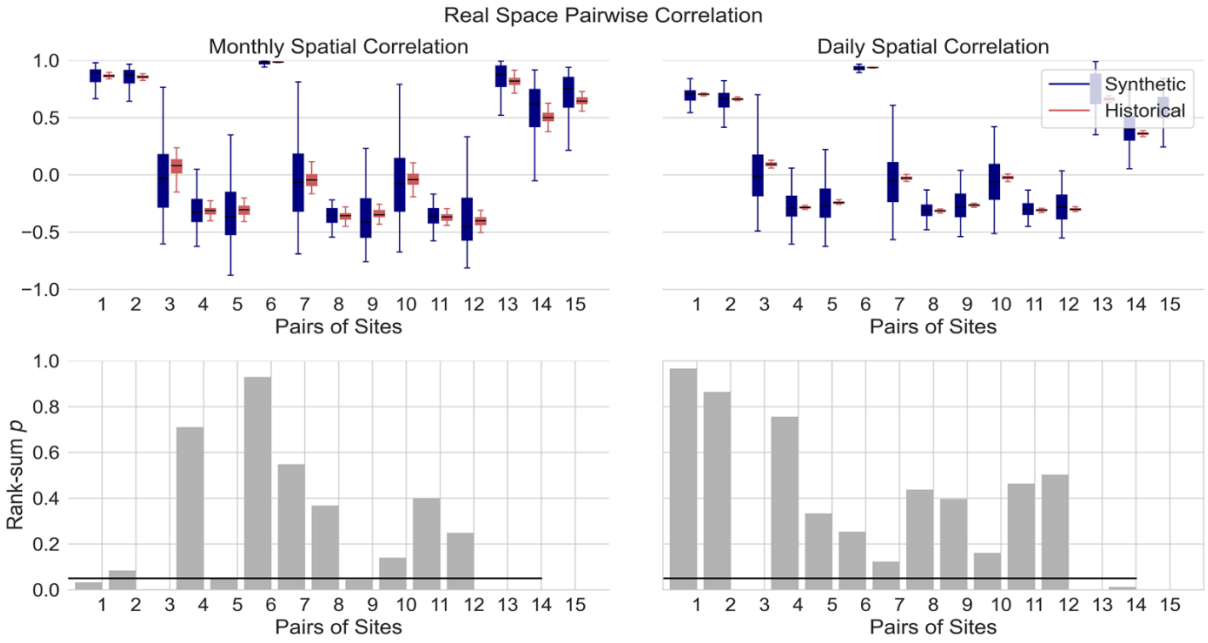

Figure E- 4. Plots of spatial correlations in bootstrapped historical(pink) and synthetic (blue) monthly flows

Appendix F

Minimum environmental flow requirement for the study

Table F- 1. Minimum environmental flow release from existing dams (m^3/s) (EEPCO, 2009, 2016)

Hydropower	Jan	Feb	Mar	Apr	May	Jun	Jul	Aug	Sep	Oct	Nov	Dec
Gibe I & II	2.0	2.0	2.0	2.0	2.0	2.0	2.0	2.0	2.0	2.0	2.0	2.0
Gibe III & Koysha	22.0	21.5	21.5	21.5	21.5	21.5	21.5	22.0	22.0	21.5	21.5	22.0